Stony Brook University

Osteological, Myological, and Phylogenetic Trends of Forelimb Reduction in Nonavian Theropod Dinosaurs

A Dissertation Presented

by

Sara Huntington Burch

to

The Graduate School

in Partial Fulfillment of the

Requirements

for the Degree of

Doctor of Philosophy

in

Department of Anatomical Sciences

Stony Brook University

December 2013

Stony Brook University

The Graduate School

Sara Huntington Burch

We, the dissertation committee for the above candidate for the

Doctor of Philosophy degree, hereby recommend

acceptance of this dissertation.

David W. Krause - Dissertation Co-Advisor
Distinguished Service Professor, Department of Anatomical Sciences

Alan H. Turner - Dissertation Co-Advisor
Assistant Professor, Department of Anatomical Sciences

Brigitte Demes - Chairperson of the Defense
Professor, Department of Anatomical Sciences

Stephen Gatesy
Department of Ecology and Evolutionary Biology, Brown University

This dissertation is accepted by the Graduate School

Charles Taber
Dean of the Graduate School

Abstract of the Dissertation

The Osteological, Myological, and Phylogenetic Trends of Forelimb Reduction in Nonavian Theropod Dinosaurs

by

Sara Huntington Burch

Doctor of Philosophy

in

Anatomical Sciences

Stony Brook University

2013

Limb reduction and vestigialization have occurred multiple times in the evolutionary history of Tetrapoda, most often related to a change in primary mode of locomotion. However, little is known about the functional shifts of reduced limbs or the morphological signals of complete vestigialization. The forelimbs of nonavian theropod dinosaurs, freed from the requirements of terrestrial locomotion, diversified into a wide variety of morphologies including extreme reduction relative to body size. Whether these limbs were functional or merely vestigial is a matter of contention. The primary objective of this dissertation was to provide new insights on the evolution and function of reduced forelimbs in nonavian theropod dinosaurs through analysis of the osteology, myology, and allometric trends of the forelimb.

In the first part of this analysis, the osteology of the pectoral girdle and forelimb of the early theropod *Tawa hallae* and that of the abelisaurid *Majungasaurus crenatissimus* were described to provide a detailed understanding of the extremes in morphology exhibited by the plesiomorphic and highly reduced conditions. The osteological features of the forelimbs of these taxa were used in combination with integrative phylogenetic and comparative techniques to reconstruct the complete musculature of the forelimb and pectoral girdle of *Tawa* and

Majungasaurus. The results of these studies established the plesiomorphic arrangement of the musculature in Theropoda and demonstrated the myological consequences of extreme forelimb reduction in one clade.

Next, shifts in the forelimb musculature were traced along the lineage to another clade exhibiting forelimb reduction, Tyrannosauroidea. The forelimb musculature of *Tyrannosaurus rex* was reconstructed and major changes in the musculature were identified, allowing tests of established functional hypotheses through biomechanical analyses. The results reveal that the forelimb musculature of derived tyrannosaurids was well developed despite the reduced size of the limb, featuring several unique adaptations likely related to prey acquisition and intraspecific interactions.

The final study assessed allometric and evolutionary trends of the pectoral girdle and forelimb across Theropoda using phylogenetic comparative methods, evolutionary model testing, and ancestral state reconstruction. Results of this study show that there is no evidence of negative allometric scaling of the forelimb elements across the entire clade when phylogeny is taken into account, despite long-standing hypotheses that variations in forelimb length of nonavian theropods, whether reduction in tyrannosaurids or elongation in paraves, are directly dependent on overall body size. Instead, clades exhibiting forelimb reduction or elongation underwent active stabilizing selection toward their distinctive proportions. The results also indicate that the relative forelimb length of most theropods and the scapular length across the entire clade exhibit a high degree of conservatism due to strong stabilizing selection, suggesting that biomechanical, developmental, or functional constraints were important in influencing forelimb proportions in most members of this clade. Taken together, these studies indicate that the reduced forelimbs of nonavian theropods were not a result of the process of vestigilization and remained functional even at their small size, likely maintaining roles in prey acquisition, reproduction, or intraspecific display interactions.

Dedication

To my parents, Joe and Janet Burch

Table of Contents

List of Figures

List of Tables

Acknowledgments

Completion of this dissertation was an enormous venture, and one that would not have been possible if not for the help, guidance, and support of many people. First and foremost I must thank my advisors, Dave Krause and Alan Turner. They provided both the intellectual challenges necessary to make me a better scientist as well as the unwavering support needed to meet those challenges. The other members of my committee, Brigitte Demes and Steve Gatesy, also were invaluable contributors to this dissertation and my graduate career as a whole, providing feedback, insights, and thought-provoking queries during this process. As a whole, my dissertation advisors and committee were directly responsible not only for helping me to complete this dissertation but also for my success in securing funding to make it happen.

I must also thank the current and former members of the faculty, graduate students, and friends of the Department of Anatomical Sciences and IDPAS, who created an amazing environment during my time in graduate school and helped to make me a better scientist, teacher, and colleague. There are far to many to list here, but I must draw special attention to Luci Betti-Nash, Matt Borths, Doug Boyer, Matt Carrano, Andy Farke, Justin Georgi, Paul Gignac, Joe Groenke, Simone Hoffmann, Rachel Jacobs, Bill Jungers, Nate Kley, Pat O'Connor, Maureen O'Leary, Matt O'Neill, Stephanie Maiolino, Jonathan Perry, Adam Pritchard, Cornelia and Erik Seiffert, Gina Sorrentino, Jessie Stanton, Jack Stern, Nathan Thompson, and Ian Wallace. I have to specifically thank Chris Johnson and Linda Benson, who make the department run as smoothly as humanly possible, and have always gone out of their way to help me navigate all the nuts and bolts of grad school and grant administration. I would also like to single out Joe Sertich, who was and continues to be a major influence on my life; he is the best "academic big brother" I could ever ask for.

I would like to also thank the people who fostered my early career in paleontology, notably Paul Sereno, Bob Masek, Tyler Keillor, and Carol Abraczinskas of the University of Chicago. From them, I learned a great deal about research, paleontological fieldwork, fossil preparation, and scientific illustration, and gained the foundation that allowed me to succeed in graduate school and with this dissertation.

A huge number of institutions, curators, and collections managers have to be thanked for generously providing access to specimens necessary for this dissertation. They are Ronan Allain (MNHN), Jorge Calvo (MUCPv), Juan Canale (MEB), Matt Carrano (USNM), Sandra Chapman (BMNH), Chinzorig Tsogtbaatar (MPC), Rodolpho Coria (MCF), Mike Getty (UMNH), Mark Goodwin (UCMP), Adam Halamski (ZPAL), Donald Henderson (TMP), Stephen Hutt (MIWG), Randy Irmis (UMNH), Tyler Keillor (University of Chicago), Alex Kramarz (MACN), Carrie Levitt (UMNH), Ricardo Martinez (PVSJ), Carl Mehling (AMNH), Mark Norell (AMNH), Fernando Novas (MACN), Kevin Padian (UCMP), Diego Pol (MPEF), Juan Porfiri (MUCPv), Eduardo Ruigómez (MPEF), Daniela Schwartz-Wings (HMN), Paul Sereno (University of Chicago), Rod Sheetz (BYU), Brandon Strilisky (TMP), Holly Woodward (MOR), Xu Xing (IVPP), and Zheng Fang (IVPP). Additionally, I would like to acknowledge the help of a few researchers, preparators, and collections assistants, without which this dissertation would be a much poorer study, specifically Diego Abelín (PVSJ), Premji Carabajal (MCF), Graeme

Housego (RTMP), Ma Qing-Yu (IVPP), Chris Mejia (UCMP), Cecilia Succar (MCF), and Corwin Sullivan (IVPP).

This dissertation was made possible in part by two field programs. Not only did these projects uncover the fossils used in this study, they also generously invited me to be part of the detailed description and analysis of these animals. First, I must thank Dave Krause and the Mahajanga Basin Project for the opportunity to work on *Majungasaurus* and for providing me with invaluable field experience. I acknowledge the members of the 2005, 2007, 2010, and 2012 field expeditions for the collection of these specimens, and Armand Rasoamiaramanana of the Université d'Antananarivo, the staff and drivers of MICET, and the villagers of Berivotra for logistical support in the field. I also thank Alan Turner, Sterling Nesbitt, Randy Irmis, and Nate Smith for the opportunity to work on the *Tawa* forelimb material, and the members of the Ghost Ranch field crews for the collection of these specimens.

Funding for this dissertation was provided by a National Science Foundation Graduate Research Fellowship, a National Science Foundation Doctoral Dissertation Improvement Grant (DEB 111036), and by the Doris O. and Samuel P. Welles Research Fund of the UCMP.

Finally, I must thank my family, who always gave me the love and support I needed during this process. My parents have encouraged and supported me at every stage of my life, providing me with the courage and confidence to achieve all my goals. Perhaps the greatest amount of thanks are due to Jacob McCartney, who has been there for me unfailingly for the last six years, who stuck through my ups and downs, who dealt with my long absences due to research trips, and who drove me across Long Island to the airport a seemingly innumerable amount of times. I don't know where I'd be without him, and I am so grateful to have shared this time with him.

Chapter I: Introduction and Background

Limb reduction and vestigialization have occurred multiple times in the evolutionary history of Tetrapoda, most often related to a change in primary mode of locomotion (e.g., forelimb reduction after the loss of flight in birds or reduction of all limbs upon elongation of the body and acquisition of concertina locomotion in lepidosaurs). Among extant taxa, limb reduction can be divided into two types depending on the utility and evolutionary trajectory of the limb. In some cases, limb reduction occurs as a transitional state along the evolutionary trajectory of limb loss due to the decay of unused traits, in which a functionless limb is actively or passively selected against as too "costly" to maintain (Fong et al., 1995; Bejder and Hall, 2002; Hall and Colegrave, 2008). Examples of this type of reduction include the hind limbs of cetaceans (Bejder and Hall, 2002; Thewissen et al., 2006) and the forelimbs of some ratites (McGowan, 1982; Maxwell and Larsson, 2007b). However, reduced morphology of a limb is not necessarily a sign of disuse; some animals retain a subset of functions used in ancestral taxa, such as the wings of ostriches, which remain important in display and balance during running (Davies, 2002). In these cases, the relatively small size of a limb may not be transitional but represent a derived, optimal morphology, as suggested by a recent analysis, which found that the so-called "intermediate" body form of reduced-limbed lizards has been selected for and undergone long periods of stability (Brandley et al., 2008). In general, studies of limb reduction have focused on the developmental pathways responsible for reduction (Lande, 1978; Alberch and Gale, 1985; Hamrick, 2002; Shapiro, 2002; Wiens, 2004) and limb length as a passive result of major shifts of bauplan (Presch, 1975; Greer, 1987; Caputo et al., 1995; Greer et al., 1998; Thewissen et al., 2006). Comparatively little is known about the functional shifts of the limbs themselves or the morphological signals distinguishing these two types of limb reduction.

Examples of one or both of these types of reduction may be found among the evolutionary diversity of the forelimbs of nonavian theropod dinosaurs. Nonavian theropods were obligate bipeds and primitively possessed long, well-developed forelimbs, but different evolutionary lineages within the clade diversified into a wide variety of morphologies, including highly reduced forelimbs. Reduced forelimb morphology evolved in multiple independent theropod lineages, even in traditionally long-armed theropod clades such as dromaeosaurids (Turner et al., 2007; Novas et al., 2009). Three clades exhibit an evolutionary trajectory toward forelimb

reduction, with the most derived members exhibiting the greatest reduction: mid-sized abelisaurids, huge tyrannosaurids, and small, birdlike alvarezsaurids.

Which type of limb reduction these forelimbs represent—whether they were functional or merely vestigial—is a matter of contention. Both abelisaurids and tyrannosaurids are often considered to exhibit transitional morphologies on a trajectory toward vestigialization and loss (Horner and Lessem, 1993; Giffin, 1995; Senter and Parrish, 2006), potentially as a result of specialization toward head-based predation or large body size (Vargas, 1999; Bybee et al., 2006; Lockley et al., 2009). Nevertheless, the morphology of the forelimb of tyrannosaurids is robust (Brochu, 2003), eliciting other hypotheses as to its function, including assisting the animal rising from the ground (Newman, 1970), partner clasping during mating (Osborn, 1906), or holding onto struggling prey once it has been brought close to the chest (Brown, 1915). Of the three clades, only alvarezsaurids have never been hypothesized to exhibit forelimb vestigialization, likely because the forelimb, though tiny, exhibits a distinct morphology that has been compared to that of scratch-digging mammals, which use their forelimb to open insect mounds (Perle et al., 1993; Chiappe, 2002; Senter, 2005; Longrich and Currie, 2009). Despite this high level of speculation and controversy, the evolution and function of reduced forelimbs in nonavian theropods has yet to be systematically examined.

The vast majority of studies on the evolution and function of theropod forelimbs have focused on the origin of birds and the evolution of flight, including the evolution of feathers and wing shape (e.g., X. Wang et al., 2011), aerodynamics of early wings (Koehl et al., 2011), developmental identity of the manual digits (Bever et al., 2011; Z. Wang et al., 2011), changes in forelimb proportions relating to flight (Dececchi and Larsson, 2013), evolution of novel morphological features within the avian shoulder (Baier et al., 2007), and assessment of potential ranges of motion in the developing flight stroke (Gishlick, 2001). Those studies that have investigated the other functions of the forelimb, particularly in relation to food acquisition, have been generally limited to range-of-motion descriptions (Carpenter, 2002; Senter, 2005; Senter and Robins, 2005; Senter, 2006) and simple lever analyses of the action of a single muscle (Carpenter and Smith, 2001; Lipkin and Carpenter, 2009; Longrich and Currie, 2009).

Comparatively, much greater progress has been made in the understanding of the evolution and functional role of the theropod hind limb through analyses of major muscular shifts (Gatesy, 1990; Hutchinson, 2001a, 2001b) and the construction of advanced biomechanical models that allow testing of specific functional hypotheses (Hutchinson et al., 2005c; Hutchinson et al., 2007). Although the functional demands on the hind limb are somewhat more straightforward (e.g., the exertion of ground reaction forces during walking versus the myriad and unknown forces that may act on the forelimb) the major limitation of applying these types of methods is a lack of meaningful input data, particularly a complete and phylogenetically rigorous reconstruction of the plesiomorphic morphology of the forelimb musculature and a detailed understanding of the allometric trends present across the clade.

Reconstructing the limb musculature of extinct tetrapods is one of the most fundamental steps in any analysis of functional capability. Complete muscle reconstructions are necessary for understanding the interplay of muscle antagonists and synergists at a joint (e.g., Hutchinson and Gatesy, 2000), and allow for potential functional shifts along an evolutionary lineage to be identified by tracing changes in the morphology of muscle sites and how they relate to each other (e.g., Hutchinson, 2001a; Hutchinson, 2001b). Among the few studies that have reconstructed forelimb musculature in dinosaurs, even fewer have been performed in an explicit phylogenetic context (Nicholls and Russell, 1985; Dilkes, 2000; Jasinoski et al., 2006; Langer et al., 2007; Maidment and Barrett, 2011). Jasinoski et al.'s (2006) reconstruction of the musculature of the dromaeosaurid *Saurornitholestes* represents the most rigorous study of theropod forelimb myology to date. However, it is limited to the shoulder musculature and, for some muscles, features derived, avian morphologies that are not applicable to more basal taxa.

The distal musculature of the forelimb has been generally ignored by most authors, despite the functional significance of many of these muscles on activities such as grasping. The only study that attempted to reconstruct the distal muscles used birds as the primary muscular model (Carpenter and Smith, 2001), and therefore lacks full phylogenetic context and results in difficult interpretations of the distal attachment of many of these muscles. Although homologizing the muscles attaching to the distal antebrachium and manus of birds with those of crocodylians and lepidosaurs presents many challenges, several recent studies on the

development of the avian wrist and hand (Kundrát, 2009; Z. Wang et al., 2011) have made it possible to identify osteological homologs in this region and improved our ability to assess muscular morphology across Archosauria.

The importance of the scaling of limbs relative to body size has received much attention across Tetrapoda, in particular how large animals "solve" the problems of the differential scaling of body mass and the cross-sectional parameters of muscle, tendon, and bone (McMahon, 1975; Alexander, 1981; Schmidt-Nielsen, 1984). Limb proportions, geometry, and posture are limited by the biomechanical requirements of body support and locomotion, which can cause departure from geometric similarity (isometry) in some scaling relationships. These relationships have been investigated in the hind limbs of theropods (Gatesy, 1991; Gatesy and Middleton, 1997b; Carrano, 2001), but a similar understanding is lacking for the forelimb. The allometric scaling of bird wing length exhibits departure from geometric similarity due to the biomechanical demands of wing-based body support during flight (Prange et al., 1979; Olmos et al., 1996; Nudds, 2007). However, what constraints, if any, exist on the forelimb length of flightless bipedal animals is unclear.

The intramembral proportions of the limb segments are relatively conserved in most theropod taxa besides abelisaurids, suggesting that the proportions of the forelimb may undergo selection due to factors such as spatial access, limb folding, or developmental pathways even if the limb is not experiencing constraint through ground reaction forces (Middleton and Gatesy, 2000). It is considered advantageous for a bipedal cursor to have relatively small forelimbs because they are non-propulsive "dead weight" and create problems with balance (Coombs, 1978), but whether forelimb size varies with body size as a result of this is unknown. That reduced forelimbs in nonavian theropods are merely a consequence of large body size has often been hypothesized, but rarely tested. Bybee et al. (2006) found a negative allometric relationship between humeral and ulnar lengths and body size in a sample of adult theropods, and speculated that similar developmental constraints caused large theropods to have relatively small arms. However, a small-bodied tyrannosaur was described recently that possessed forelimb proportions similar to those of large-bodied members of the clade (Sereno et al., 2009), calling into question a simple negatively allometric relationship. At the other end of the spectrum, the forelimb of

maniraptoran theropods is thought to exhibit relative elongation due to functional demands imposed by the evolution of flight (Padian and Chiappe, 1998b; Novas et al., 2009), but recent identification of a trend in body size reduction among this clade (e.g., Turner et al., 2007) has led to the idea that forelimb elongation of this clade is a passive allometric effect of small body size, just as forelimb reduction is a passive allometric effect of large body size (Bybee et al., 2006; Dececchi and Larsson, 2013). In general, the few studies that have investigated forelimb scaling of nonavian theropods have been limited by small sample sizes (Bybee et al., 2006) or no consideration of the effect of phylogeny and sampling bias toward crownward taxa (Dececchi and Larsson, 2013), leaving the true relationship of forelimb length to body size unknown.

This dissertation examines the evolution and function of highly reduced forelimbs in non-avian theropod dinosaurs by analyzing the phylogenetic, scaling, and myological trends across the clade. In the chapters two and three, the osteology of the pectoral girdle and forelimb of the early theropod *Tawa hallae* and that of the abelisaurid *Majungasaurus crenatissimus* is described to provide a detailed understanding of the extremes in morphology exhibited by the plesiomorphic and highly reduced conditions. In the fourth chapter, integrative phylogenetic and comparative techniques are used to reconstruct the complete musculature of the forelimb of *Tawa*, demonstrating the plesiomorphic arrangement of the musculature in Theropoda and providing the basis for muscle reconstructions in other theropod taxa. The results of this reconstruction are used to create a new hypothesis for the forelimb myology of *Majungasaurus* in the fifth chapter, which investigates the myological consequences of extreme forelimb reduction and provides insights into the osteological and myological progression of reduction in abelisaurids. The sixth chapter traces shifts in the forelimb musculature along the lineage to tyrannosaurids. The forelimb musculature of *Tyrannosaurus rex* is reconstructed and major changes in the musculature are identified, allowing tests of established functional hypotheses through biomechanical analyses. Finally, the seventh chapter assesses allometric and evolutionary trends of the pectoral girdle and forelimb across Theropoda. Phylogenetic comparative methods, evolutionary model testing, and ancestral state reconstruction are used to evaluate specific hypotheses of forelimb scaling and selection to determine the driving factors behind forelimb size evolution within the clade.

LITERATURE CITED

Alberch, P., and E. A. Gale. 1985. A developmental analysis of an evolutionary trend: digital reduction in amphibians. Evolution 39:8–23.

Alexander, R. M. 1981. Allometry of the leg muscles of mammals. Journal of Zoology 194:539–552.

Baier, D. B., S. M. Gatesy, and F. A. Jenkins Jr. 2007. A critical ligamentous mechanism in the evolution of avian flight. Nature 445:307–310.

Bejder, L., and B. K. Hall. 2002. Limbs in whales and limblessness in other vertebrates: mechanisms of evolutionary and developmental transformation and loss. Evolution and Development 4:445–458.

Bever, G. S., J. A. Gauthier, and G. P. Wagner. 2011. Finding the frame shift: digit loss, developmental variability, and the origin of the avian hand. Evolution & Development 13:269–279.

Brandley, M. C., J. P. Huelsenbeck, and J. J. Wiens. 2008. Rates and patterns in the evolution of snake-like body form in squamate reptiles: evidence for repeated re-evolution of lost digits and long-term persistence of intermediate bodyforms. Evolution 62:2042–2064.

Brochu, C. A. 2003. Osteology of *Tyrannosaurus rex*: insights from a nearly complete skeleton and high-resolution computed tomographic analysis of the skull. Journal of Vertebrate Paleontology 22:1–138.

Brown, B. 1915. *Tyrannosaurus*, the largest flesh-eating animal that ever lived. The American Museum Journal 15:271–274.

Bybee, P. J., A. H. Lee, and E.-T. Lamm. 2006. Sizing the Jurassic theropod dinosaur *Allosaurus:* assessing growth strategy and evolution of ontogenetic scaling of limbs. Journal of Morphology 267:347–359.

Caputo, V., B. Lanza, and R. Palmieri. 1995. Body elongation and limb reduction in the genus *Chalcides* Laurenti 1768 (Squamata Scincidae): a comparative study. Tropical Zoology 8:95–152.

Carpenter, K. 2002. Forelimb biomechanics of nonavian theropod dinosaurs in predation. Senckenbergiana Lethaea 82:59–76.

Carpenter, K., and M. Smith. 2001. Forelimb osteology and biomechanics of *Tyrannosaurus rex*; pp. 90–116 in D. Tanke and K. Carpenter (eds.), Mesozoic Vertebrate Life. Indiana University Press, Bloomington, IN.

Carrano, M. T. 2001. Implications of limb bone scaling, curvature and eccentricity in mammals and non-avian dinosaurs. Journal of Zoology 254:41–55.

Chiappe, L. M. 2002. The Cretaceous, short-armed Alvarezsauridae, *Mononykus* and its kin; pp. 87–120 in L. M. Chiappe and L. M. Witmer (eds.), Mesozoic Birds: Above the Heads of Dinosaurs. University of California Press.

Coombs, W. P. 1978. Theoretical aspects of cursorial adaptations in dinosaurs. The Quarterly Review of Biology 53:393–418.

Davies, S. J. J. F. 2002. Ratites and Tinamous, Bird Families of the World, Volume 9. Oxford University Press, Oxford, UK, 310 pp.

Dececchi, T. A., and H. C. E. Larsson. 2013. Body and limb size dissociation at the origin of birds: uncoupling allometric constraints across a macroevolutionary transition. Evolution doi:10.1111/evo.12150.

Dilkes, D. W. 2000. Appendicular myology of the hadrosaurian dinosaur *Maiasaura peeblesorum* from the Late Cretaceous (Campanian) of Montana. Transactions of the Royal Society of Edinburgh: Earth Sciences 90:87–125.

Fong, D. W., T. C. Kane, and D. C. Culver. 1995. Vestigialization and loss of nonfunctional characters. Annual Review of Ecology and Systematics 26:249–268.

Gatesy, S. M. 1990. Caudofemoral musculature and the evolution of theropod locomotion. Paleobiology 16:170–186.

Gatesy, S. M. 1991. Hind limb scaling in birds and other theropods: implications for terrestrial locomotion. Journal of Morphology 209:83–96.

Gatesy, S. M., and K. M. Middleton. 1997. Bipedalism, flight, and the evolution of theropod locomotor diversity. Journal of Vertebrate Paleontology 17:308–329.

Giffin, E. B. 1995. Postcranial paleoneurology of the Diapsida. Journal of Zoology 235:389–410.

Gishlick, A. D. 2001. The function of the manus and forelimb of *Deinonychus antirrhopus* and its importance for the origin of avian flight; pp. 301–318 in J. A. Gauthier and L. F. Gall (eds.), New Perspectives on the Origin and Early Evolution of Birds: Proceedings. Peabody Museum of Natural History, Yale University, New Haven, CT.

Greer, A. E. 1987. Limb reduction in the lizard genus *Lerista*. 1. Variation in the number of phalanges and presacral vertebrae. Journal of Herpetology 21:267–276.

Greer, A. E., V. Caputo, B. Lanza, and R. Palmieri. 1998. Observations on limb reduction in the scincid lizard genus *Chalcides*. Journal of Herpetology 32:244–252.

Hall, A. R., and N. Colegrave. 2008. Decay of unused characters by selection and drift. Journal of Evolutionary Biology 21:610–617.

Hamrick, M. W. 2002. Developmental mechanisms of digit reduction. Evolution and Development 4:247–248.

Horner, J. R., and D. Lessem. 1993. The Complete *T. rex*. Simon & Schuster, New York, 239 pp.

Hutchinson, J. R. 2001a. The evolution of pelvic osteology and soft tissues on the line to extant birds (Neornithes). Zoological Journal of the Linnean Society 131:123–168.

Hutchinson, J. R. 2001b. The evolution of femoral osteology and soft tissues on the line to extant birds (Neornithes). Zoological Journal of the Linnean Society 131:169–197.

Hutchinson, J. R., and S. M. Gatesy. 2000. Adductors, abductors, and the evolution of archosaur locomotion. Paleobiology 26:734–751.

Hutchinson, J. R., V. Ng-Thow-Hing, and F. C. Anderson. 2007. A 3D interactive method for estimating body segmental parameters in animals: application to the turning and running performance of *Tyrannosaurus rex*. Journal of Theoretical Biology 246:660–680.

Hutchinson, J. R., F. C. Anderson, S. S. Blemker, and S. L. Delp. 2005. Analysis of hindlimb muscle moment arms in *Tyrannosaurus rex* using a three-dimensional musculoskeletal computer model: implications for stance, gait and speed. Paleobiology 31:676–701.

Jasinoski, S. C., A. P. Russell, and P. J. Currie. 2006. An integrative phylogenetic and extrapolatory approach to the reconstruction of dromaeosaur (Theropoda: Eumaniraptora) shoulder musculature. Zoological Journal of the Linnean Society 146:301–344.

Koehl, M. A. R., D. Evangelista, and K. Yang. 2011. Using physical models to study the gliding performance of extinct animals. Integrative and Comparative Biology 51:1002–1018.

Kundrát, M. 2009. Primary chondrification foci in the wing basipodium of *Struthio camelus* with comments on interpretation of autopodial elements in Crocodilia and Aves. Journal of Experimental Zoology 312B:30–41.

Lande, R. 1978. Evolutionary mechanisms of limb loss in tetrapods. Evolution 32:73–92.

Langer, M. C., M. A. G. Franca, and S. Gabriel. 2007. The pectoral girdle and forelimb anatomy of the stem-sauropodomorph *Saturnalia tupiniquim* (Upper Triassic, Brazil). Special Papers in Palaeontology 77:113–137.

Lipkin, C., and K. Carpenter. 2009. Looking again at the forelimb of *Tyrannosaurus rex*; pp. 167–190 in P. Larson and K. Carpenter (eds.), *Tyrannosaurus rex*: the Tyrant King. Indiana University Press, Bloomington, IN.

Lockley, M., R. Kukihara, and L. Mitchell. 2009. Why *Tyrannosaurus rex* had puny arms: an integral morphodynamic solution to a simple puzzle in theropod paleobiology; pp. 131–164 in P. Larson and K. Carpenter (eds.), *Tyrannosaurus rex*: the Tyrant King. Indiana University Press, Bloomington, IN.

Longrich, N., and P. Currie. 2009. *Albertonykus borealis*, a new alvarezsaur (Dinosauria: Theropoda) from the Early Maastrichtian of Alberta, Canada: implications for the systematics and ecology of the Alvarezsauridae. Cretaceous Research 30:239–252.

Maidment, S. C. R., and P. M. Barrett. 2011. The locomotor musculature of basal ornithischian dinosaurs. Journal of Vertebrate Paleontology 31:1265–1291.

Maxwell, E. E., and H. C. E. Larsson. 2007. Osteology and myology of the wing of the Emu (*Dromaius novaehollandiae*), and its bearing on the evolution of vestigial structures. Journal of Morphology 268:423–441.

McGowan, C. 1982. The wing musculature of the Brown kiwi *Apteryx australis mantelli* and its bearing on ratite affinities. Journal of Zoology 197:173–219.

McMahon, T. A. 1975. Using body size to understand the structural design of animals: quadrupedal locomotion. Journal of Applied Physiology 39:619–627.

Middleton, K. M., and S. M. Gatesy. 2000. Theropod forelimb design and evolution. Zoological Journal of the Linnean Society 128:149–187.

Newman, B. H. 1970. Stance and gait in the flesh-eating dinosaur *Tyrannosaurus*. Biological Journal of the Linnean Society 2:119–123.

Nicholls, E. L., and A. P. Russell. 1985. Structure and function of the pectoral girdle and forelimb of *Struthiomimus altus* (Theropoda: Ornithomimidae). Palaeontology 28:643–677.

Novas, F. E., D. Pol, J. I. Canale, J. D. Porfiri, and J. O. Calvo. 2009. A bizarre Cretaceous theropod dinosaur from Patagonia and the evolution of Gondwanan dromaeosaurids. Proceedings of the Royal Society of London Series B 276:1101–1107.

Nudds, R. L. 2007. Wing-bone length allometry in birds. Journal of Avian Biology 38:515–519.

Olmos, M., A. Casinos, and J. Cubo. 1996. Limb allometry in birds. Annales Des Sciences Naturelles, Zoologie 17:39–49.

Osborn, H. F. 1906. *Tyrannosaurus*, Upper Cretaceous carnivorous dinosaur (second communication). Bulletin of the American Museum of Natural History 22:281–296.

Padian, K., and L. M. Chiappe. 1998. The origin and early evolution of birds. Biological Reviews 73:1–42.

Perle, A., M. A. Norell, L. M. Chiappe, and J. M. Clark. 1993. Flightless bird from the Cretaceous of Mongolia. Nature 362:623–626.

Prange, H. D., J. F. Anderson, and H. Rahn. 1979. Scaling of skeletal mass to body mass in birds and mammals. The American Naturalist 113:103–122.

Presch, W. 1975. The evolution of limb reduction in the teiid lizard genus *Bachia*. Bulletin of the Southern California Academy of Sciences 74:113–121.

Schmidt-Nielsen, K. 1984. Scaling: Why is Animal Size so Important? Cambridge University Press, Cambridge, UK, 256 pp.

Senter, P. 2005. Function in the stunted forelimbs of *Mononykus olecranus* (Theropoda), a dinosaurian anteater. Paleobiology 31:373–381.

Senter, P. 2006. Forelimb function in *Ornitholestes hermanni* Osborn (Dinosauria, Theropoda). Palaeontology 49:1029–1034.

Senter, P., and J. H. Robins. 2005. Range of motion in the forelimb of the theropod dinosaur *Acrocanthosaurus atokensis*, and implications for predatory behavior. Journal of Zoology 266:307–318.

Senter, P., and J. M. Parrish. 2006. Forelimb function in the theropod dinosaur *Carnotaurus sastrei*, and its behavioral implications. PaleoBios 26:7–17.

Sereno, P. C., L. Tan, S. L. Brusatte, H. J. Kriegstein, X. Zhao, and K. Cloward. 2009. Tyrannosaurid skeletal design first evolved at small body size. Science 326:418–422.

Shapiro, M. D. 2002. Developmental morphology of limb reduction in *Hemiergis* (Squamata: Scincidae): chondrogenesis, osteogenesis, and heterochrony. Journal of Morphology 254:211–231.

Thewissen, J. G. M., M. J. Cohn, L. S. Stevens, S. Bajpai, J. Heyning, and W. E. Horton. 2006. Developmental basis for hind-limb loss in dolphins and origin of the cetacean bodyplan. Proceedings of the National Academy of Sciences 103:8414–8418.

Turner, A. H., D. Pol, J. A. Clarke, G. M. Erickson, and M. A. Norell. 2007. A basal dromaeosaurid and size evolution preceding avian flight. Science 317:1378–1380.

Vargas, A. O. 1999. Evolution of arm size in theropod dinosaurs: a developmental hypothesis. Noticiario Mensual 338:16–19.

Wang, X., R. L. Nudds, and G. J. Dyke. 2011. The primary feather lengths of early birds with respect to avian wing shape evolution. Journal of Evolutionary Biology 24:1226–1231.

Wang, Z., R. L. Young, H. Xue, and G. P. Wagner. 2011. Transcriptomic analysis of avian digits reveals conserved and derived digit identities in birds. Nature 477:583–587.

Wiens, J. J. 2004. Development and evolution of body form and limb reduction in squamates: a response to Sanger and Gibson-Brown. Evolution 58:2107–2108.

Chapter II: Osteology of the pectoral girdle and forelimb of *Tawa hallae* from the Late Triassic Hayden Quarry of New Mexico

ABSTRACT

The early theropod *Tawa hallae* from the Late Triassic of New Mexico features a combination of derived and plesiomorphic features in its skull and postcranial skeleton, positioning it as the sister taxon to Neotheropoda. Detailed descriptions of previously known and newly discovered specimens of the pectoral girdle and forelimb of *Tawa* afford new insights into the structure of these elements and the distribution of forelimb characters at the base of Saurischia. The proportions of the forelimb are typically theropod in nature, with a relatively large manus that is more than 40% the length of the rest of the forelimb. The scapula features an elongate, narrow blade that flares distally and the humerus possesses a relatively straight shaft exhibiting a high degree of torsion. The shaft of the radius is sigmoidal in overall shape and articulates loosely with the ulna, which lacks a prominent olecranon process in all specimens. Despite the highly reduced morphology of the fourth digit and complete absence of the fifth, the carpus and manus are relatively plesiomorphic in their morphology, featuring nine carpals and only weakly asymmetrical condyles on the distal metacarpals. The morphology of the carpals and metacarpals shows that several features thought to have been lost by the base of Theropoda were still present in *Tawa*, and a unique, hooked morphology of the lateralmost distal carpal is shared by several early theropods. Overall the forelimb exhibits a large potential range of motion, and its morphology is consistent with an active role in predation.

INTRODUCTION

The Hayden Quarry of the Upper Triassic (Norian) Chinle Formation of northern New Mexico contains an extensive vertebrate fossil record, preserving a wide diversity of archosaurs including basal archosauromorphs, dinosauromorphs, dinosauriforms, and basal saurischian dinosaurs (Irmis et al., 2007; Irmis et al., 2011). Among these, the early theropod *Tawa hallae* has played an important role in understanding basal saurischian relationships and the early evolution of derived theropod traits due to its mosaic skeletal morphology (Nesbitt et al., 2009a). Possessing numerous features of the skull and postcranium found in both basal saurischian taxa

as well as more crownward theropod taxa, material of *Tawa* provides evidence for a more plesiomorphic origin of many characters thought to be synapomorphies of Coelophysoidea. Although many of these derived characters are found in the cranium and the anterior end of the snout (Nesbitt et al., 2009a), the forelimb and manus possess a suite of plesiomorphic characters that potentially have a substantial bearing on the relationships of more basal saurischian taxa.

The forelimb of early dinosaurs, particularly the carpus and manus, has received considerable attention as a phylogenetically important area (e.g., Sereno, 1993; Langer et al., 2007; Martinez et al., 2011) despite the relative paucity of distal forelimb elements in basal saurischian taxa. In particular, key characters supporting the affinities of the Argentinian taxon *Herrerasaurus ischigualastensis* relate to the presence and size of individual carpals (Ezcurra, 2010), a region that is poorly or not at all preserved in many basal saurischian taxa. The phylogenetic importance of other pectoral and forelimb elements is poorly understood, in many cases due to large morphological gaps between the most basal sauropodomorph and neotheropod taxa. The recent discoveries and brief descriptions of the forelimbs of *Tawa* (Nesbitt et al., 2009a) and of the early theropod *Eodromaeus murphi* (see Martinez et al., 2011) have provided important information on the status of these characters, but the detailed morphology of the forelimb has yet to be fully explored for these taxa.

One of the paratype skeletons of *Tawa* (GR 242) preserves a nearly complete and articulated pectoral girdle and forelimb, including an articulated carpus. Although it is the largest of the type specimens, GR 242 still represents an immature individual. The new discovery of a larger specimen referable to *Tawa* provides additional information on the antebrachial morphology of an individual nearer to the adult morphology. These specimens permit a thorough investigation of the pectoral and forelimb morphology in the sister taxon to Neotheropoda. In this paper, I provide a detailed and comprehensive description of these materials, compare the forelimb of *Tawa* with those of other early theropods and saurischians, and discuss the phylogenetic and functional implications of the forelimb in early theropods.

Institutional Abbreviations—AMNH, American Museum of Natural History, New York, NY, U.S.A.; **GR**, Ghost Ranch Ruth Hall Museum of Paleontology, Abiquiu, NM, U.S.A.; **MCZ**, Museum of Comparative Zoology, Cambridge, MA, U.S.A.; **MNA**, Museum of Northern

Arizona, Flagstaff, AZ, U.S.A.; **PVSJ**, Museo de Ciencias Naturales, San Juan, Argentina; **QG**, originally catalogued at the Queen Victoria Museum, Department of Paleontology, Harare (formerly Salisbury), now curated at the National Museum of Natural History, Bulawayo; **SAM**, Iziko South African Museum, Capetown, South Africa; **TMP**, Royal Tyrrell Museum of Paleontology, Drumheller, AB, Canada; **UCMP**, University of California Museum of Paleontology, Berkeley, CA, U.S.A.; **UMNH**, Natural History Museum of Utah, Salt Lake City, UT, U.S.A.

SYSTEMATIC PALEONTOLOGY

DINOSAURIA Owen, 1842

SAURISCHIA Seeley, 1888

THEROPODA Marsh, 1881

TAWA HALLAE Nesbitt, Smith, Irmis, Turner, Downs, and Norell, 2009

Holotype—GR 241, A nearly complete associated but disarticulated skull and postcranial skeleton (Nesbitt et al., 2009a).

Paratypes—GR 155, ilium, pubes, proximal ischium, femora, sacral vertebra, and caudal vertebrae; GR 242, a nearly complete individual; GR 243, cervical vertebrae; GR 244, a complete right femur.

Referred Specimens—See listing in Nesbitt et al. (2009). Additional referred specimens in this publication are: GR 359 – partial left humerus; GR 360 – associated left radius and ulna.

Diagnosis—See Nesbitt et al. (2009).

Age and Distribution—All specimens assigned to *Tawa hallae* were collected from Site 2, Hayden Quarry, Ghost Ranch in Rio Arriba County, New Mexico, USA. The Hayden Quarry is in the lower portion of the Petrified Forest Member of the Upper Triassic Chinle Formation (Irmis et al., 2007) and has been dated to ~212 million years ago (Irmis et al., 2011).

Described Material—This description offers new insights on the previously described forelimb material from the holotype (GR 241), which includes a right scapula, humerus, radius,

and ulna, and one of the paratypes (GR 242), which includes a left scapula, left and right humeri, left radius, ulna, and articulated carpus and manus. In addition, I describe new material of a larger individual, represented by a partial left humerus (GR 359) and complete associated left radius and ulna (GR 360).

Comparative Material—The following specimens were examined to enable the comparisons made in this paper. When published descriptions and illustrations were used, the appropriate reference is given below. *Ceratosaurus nasicornis* (UMNH VP 5278); *Coelophysis bauri* (AMNH nos. 7227, 7228, 7230, 7231, 7238; TMP nos. 84.63.29, 84.63.30, 84.63.32, 84.63.33, 84.63.40, 84.63.50, 84.63.52); *Dilophosaurus wetherelli* (UCMP nos. 37302, 37303, 77270); *Eodromaeus murphi* (PVSJ 560, 562); *Eoraptor lunensis* (PVSJ 512); *Herrerasaurus ischigualastensis* (PVSJ nos. 53, 373, 407; MCZ 7064; Brinkman & Sues, 1987); *Heterodontosaurus tucki* (SAM-K1332; Santa Luca, 1980); *Liliensternus liliensterni* (HMN MB.R. 2175); *Sanjuansaurus gordilloi* (PVSJ 605); *Segisaurus halli* (UCMP 32101); "*Syntarsus*" *kayentakatae* (MNA V2623; Rowe, 1989); "*Syntarsus*" *rhodesiensis* (QG nos. 1, 514, 545, 568, 573, 577; Raath, 1969, 1990).

Position of the Scapulocoracoid and Forelimb for Descriptive Purposes—Due to the lack of a clear neutral position for the forelimb consistent across Theropoda, the positional terminology used in descriptions of forelimb elements vary from publication to publication. Descriptions of the scapulocoracoid vary based on whether the bone is described with the long axis of the scapular blade oriented horizontally (e.g., Madsen, 1976) or vertically (e.g., Brochu, 2003); here we describe the scapulocoracoid in an angled, neutral position that approximates the position it would have occupied in life (Fig. 1), as in Burch & Carrano (2012). The rest of the segments of the forelimb are described in the following orientations: the humerus in a vertical position with the broad surfaces oriented anteriorly and posteriorly such that the internal tuberosity is directed medially and the greater tubercle is positioned directly laterally (e.g., Madsen, 1976; Sereno, 1993); the antebrachium oriented such that the olecranon of the ulna is directed posteriorly and the radial articular surface is positioned either anteriorly or laterally (e.g., Madsen, 1976; Sereno, 1993); and the manus oriented in a horizontal position with digit I medialmost (e.g., Madsen, 1976; Sereno, 1993; Brochu, 2003).

DESCRIPTION

Scapula

In both GR 241 and GR 242 the scapula remains unfused to the coracoid due to their juvenile and subadult status, respectively (Nesbitt et al., 2009a). The scapular blade is long and narrow (Table 1), closer to the proportions of *Sanjuansaurus* (PVSJ 605) and *Herrerasaurus* (PVSJ 53) than those of other early theropods such as *Coelophysis* (AMNH 7227, TMP 84.63.29, TMP 84.63.33) and *Eodromaeus* (PVSJ 562). However, as in the latter taxa the scapular blade of *Tawa* exhibits a distal expansion, gradually flaring to a dorsoventral width just over double the narrowest point (Fig. 2). This expansion is not symmetrically distributed on both sides of the scapula but is instead primarily located along the posteroventral edge, with the anterodorsal margin of the blade appearing slightly convex in lateral view. In other early theropods the condition is nearly inverted; most have a widely flaring anterodorsal edge and a straight to convex posteroventral margin such as in *Segisaurus* (UCMP 32101), *Eodromaeus* (PVSJ 562), *Eoraptor* (PVSJ 512), "*S.*" *rhodesiensis* (see Raath, 1969, 1990), and some specimens of *Coelophysis* (AMNH 7227, 7228), although other specimens of *Coelophysis* (TMP 84.63.29, 84.63.30, 84.63.32; Colbert, 1989) and "*S.*" *kayentakatae* (see Rowe, 1989) exhibit more symmetrical flaring along both margins.

The blade has a flat cross section at its distal end but becomes subtriangular proximally, with a distinct ridge along its medial surface (Fig. 2B). The medial ridge is ventrally shifted from the longitudinal midline of the scapular blade and effectively divides the medial surface into a larger anterodorsal surface and a smaller posteroventral surface. The ridge begins low and rounded from the proximal articular surface for the coracoid and becomes sharper as it extends distally, curving posteroventrally to meet the margin of the scapular blade at its midpoint. Similarly placed medial scapular ridges are present in *Sanjuansaurus* (PVSJ 605) and *Eodromaeus* (PVSJ 562), although the ridge is low and shifted more toward the posteroventral edge in *Liliensternus* (HMN MB.R. 2175) and *Dilophosaurus* (UCMP 37302). Distally, the medial and lateral surfaces of the scapular blade are smooth and unmarked. The anterodorsal and

posteroventral margins of the scapular blade also lack any of the striations, tubercles, or ridges that are developed in more derived taxa such as *Ceratosaurus* (UMNH VP 5278), but are not present in even the largest of the early theropods (e.g., *Dilophosaurus*; *Herrerasaurus*).

The anterodorsal margin of the proximal end of the scapular blade is rounded and tapers to a sharp edge along the acromial expansion. The expansion flares sharply, creating an angle with the scapular blade of approximately 130°, and comes to a narrow, rounded tip bearing a flattened anterior margin (Fig. 2). Equivalent angles for the expansion are found in *Eoraptor* (PVSJ 512), *Coelophysis* (AMNH 7227; TMP 84.63.32, 84.63.33), "*S.*" *rhodesiensis* (see Raath, 1969, 1990), and *Liliensternus* (HMN MB.R. 2175), but the acromial expansion is slightly steeper (i.e., possessing an angle of less than 130°) in *Eodromaeus* (PVSJ 562). The sharpest inclination is present in *Herrerasaurus* (PVSJ 53) and *Sanjuansaurus* (PVSJ 605), where the angle between the edge of the expansion and the scapular blade is 90° or less and, among early theropods, *Segisaurus* (UCMP 32101) exhibits the widest angle, with an acromial expansion that smoothly grades into the anterodorsal edge of the scapular blade. The subacromial depression is large and deep in *Tawa*, occupying most of the surface of the proximal end of the scapula and expanding posteriorly such that the flat surface of the acromial expansion is restricted to a narrow band, differing from the broad, subtriangular surface present posterior to the depression in *Eoraptor* (PVSJ 512), *Coelophysis* (TMP 84.63.32; see Colbert, 1989), "*S.*" *rhodesiensis* (see Raath, 1969, 1990), "*S.*" *kayentakatae* (see Rowe, 1989), *Segisaurus* (UCMP 32101), and *Dilophosaurus* (UCMP 37302).

The scapular portion of the glenoid fossa is slightly concave and subcircular, with a flat anterior margin for articulation with the coracoid. The glenoid does not bear any distinct lips at any point along its edge, and the scapula flares out smoothly from the blade to meet the edge of the glenoid as in *Eoraptor* (PVSJ 512), *Eodromaeus* (PVSJ 562), *Coelophysis* (AMNH 7227, 7238; TMP 84.63.32), "*S.*" *rhodesiensis* (see Raath, 1969, 1990), and "*S.*" *kayentakatae* (see Rowe, 1989). Posterior to the glenoid margin the ventral edge of the scapula bears fine striations marking the attachment of Triceps brachii scapularis (Chapter IV). Development of this scar varies among early theropods; it is completely unmarked in many taxa (e.g., *Eoraptor*, *Coelophysis*, "*S.*" *rhodesiensis*, "*S.*" *kayentakatae*, *Liliensternus*), but a small tubercle is can be

found in *Eodromaeus* (PVSJ 562) and well-developed rugosities are present in *Herrerasaurus* (PVSJ 53) and *Sanjuansaurus* (PVSJ 605). The articular surface for the coracoid is sinuous when viewed laterally, being convex immediately anterodorsal to the glenoid fossa and concave in the area of the subacromial depression.

Humerus

The humerus is long and gracile with a narrow, cylindrical shaft (Fig. 3). The portion of the humerus distal to the tip of the deltopectoral crest is approximately double the length of the part proximal to it, making the humerus relatively long in comparison to those of other early theropods. The shaft is relatively straight as in *Coelophysis* (AMNH 7230; TMP 84.63.30, 84.63.32) and *Herrerasaurus* (PVSJ 407), and it does not exhibit the strong anterior curvature (concave anteriorly) seen in *Dilophosaurus* (UCMP 37302) and *Liliensternus* (HMN MB.R. 2175), nor the medial curvature (concave medially) of "*S.*" *rhodesiensis* (see Raath, 1990). Strong torsion is present in both humeri of GR 242, twisting the distal end externally relative to the proximal end and orienting the long axis of the distal condyles at nearly a 50° angle to the long axis of the humeral head. This degree of torsion is similar to that exhibited by *Dilophosaurus* (UCMP 37302), *Liliensternus* (HMN MB.R. 2175), and *Segisaurus* (UCMP 32101), unlike the relatively untwisted humeral shafts of coelophysids, *Eoraptor* (PVSJ 512), and *Eodromaeus* (PVSJ 562).

The humeral head is cylindrical but appears slightly sinuous in proximal view due to the indistinct medial and lateral boundaries between it and the projections of the internal tuberosity and the greater tubercle, respectively (Fig. 3E). The head is more similar in overall morphology to that of *Herrerasaurus* (PVSJ 373) than to *Dilophosaurus* (UCMP 37302) or *Liliensternus* (HMN MB.R. 2175), but is narrower anteroposteriorly than that of all three. The expansion of the proximal articular surface onto the shaft anteriorly is limited to the medialmost portion of the humeral head, creating a concavity along the lateral part of its anterior edge. A slight overhang is present along the entire anterior border of the proximal articular surface, emphasizing the large, subtriangular depression on the anterior surface of the humerus medial to the deltopectoral crest. The humeral head expands farther posteriorly, exhibiting the bulbous posterior projection found

in other early theropods, although not quite to the extent of that of *Eodromaeus* (PVSJ 562). The posterior edge of the proximal articular surface lacks an overhang and instead grades smoothly into the posterior surface of the humeral shaft, which bears a low ridge extending distally from the apex of the posterior projection.

The internal tuberosity ("medial tuberosity" of Sereno, 1993) is large and projects well beyond the medial border of the humeral head. Proximally, its surface is flat and subtriangular, lacking a distinct lateral boundary from the humeral head. Viewed posteriorly, the proximal surface slopes distally toward its apex at approximately a 50° angle from the humeral head, coming to a rounded point medially and tapering smoothly toward the humeral shaft. This morphology resembles that of *Eodromaeus* (PVSJ 562), *Dilophosaurus* (UCMP 37302), and *Liliensternus* (HMN MB.R. 2175), but the internal tuberosities of coelophysids are typically smaller and set off distally from the humeral head (e.g., Raath, 1990). The posterior surface of the internal tuberosity bears an oval depression containing light striations, and its anterior surface is marked by striations that extend longitudinally along the medial edge.

The greater tubercle of *Tawa* projects laterally at the same level as the humeral head as an extension of the proximal articular surface, curving gently distally into the anterior edge of the deltopectoral crest. This sloping morphology is found in *Coelophysis* (TMP 84.63.30, 84.63.32), but more prominent greater tubercles are present in *Herrerasaurus* (PVSJ 373), *Eodromaeus* (PVSJ 562), "*S.*" *rhodesiensis* (see Raath, 1990), and *Dilophosaurus* (UCMP 37302). Fine striations are present on the posterior surface of the greater tubercle in *Tawa*, covering a roughly ellipsoid area between the posterior projection of the humeral head and a ridge extending distally from the lateral edge of the greater tubercle (Fig. 3D). This ridge defines the posterior border of the deltopectoral crest where it joins the humeral shaft and is developed to varying degrees in other early theropods, ranging from prominent (e.g., *Coelophysis*, *Segisaurus*, *Herrerasaurus*) to low and rounded (e.g., *Liliensternus*, *Dilophosaurus*). Posterior to the lateral ridge is a large furrow, extending from two-thirds along the length of the deltopectoral crest to nearly midshaft. This furrow is longer and deeper in *Tawa* than in other early theropods, of which only *Herrerasaurus* (PVSJ 407) exhibits a similar, though less well developed, morphology.

The deltopectoral crest is prominent, projecting anteriorly and slightly laterally. In lateral view, the entire crest can be divided into thirds, consisting of an evenly sloping proximal section (in some specimens slightly concave; e.g., GR 242, right humerus), a flat middle section with a mediolaterally expanded anterior margin, and a distal section that slopes back toward the humeral shaft at nearly the inverse of the proximal slope. The distinct angle between the proximal and middle sections and sometimes concave proximal margin is also seen in *Dilophosaurus* (UCMP 37302), *Liliensternus* (HMN MB.R. 2175), and *Herrerasaurus* (PVSJ 407), and is taken to an extreme in *Segisaurus* (UCMP 32101), but in other early theropods (e.g., *Coelophysis*, AMNH 7230, Colbert, 1989; *Eodromaeus*, PVSJ 562) these two sections are not distinct and the deltopectoral crest slopes gradually from the edge of the greater tubercle until it comes to a pointed apex near its distal extent. Regardless of overall morphology, in all early theropods the middle third of the deltopectoral crest possesses an anterior margin that is mediolaterally broad and flattened, with a blunt distal end and a proximal end that tapers into the thin margin of the proximal third of the crest. In *Tawa,* this anterior surface extends slightly onto the lateral surface of the deltopectoral crest, where its posterior border is accentuated by a small depression. The entire lateral surface of the deltopectoral crest is slightly concave, causing the margin of the crest to appear sinuous when viewed anteriorly. The degree of this concavity is greater in *Tawa* than in *Eoraptor* (PVSJ 512), *Dilophosaurus* (UCMP 37302), *Liliensternus* (HMN MB.R. 2175), or "*S.*" *rhodesiensis* (see Raath, 1990), but post-depositional crushing in the humeri of other early theropods make it difficult to assess if a concave lateral surface was present more broadly among these taxa.

The distal end of the humeral shaft is marked by several low ridges beginning at approximately midshaft and extending toward the epicondyles. The ectepicondylar ridge extends down the posterolateral side of the shaft and sweeps anteriorly across the lateral surface to the anterolateral side, making a sharp angle before descending straight distally to the radial condyle. This creates a fin-like anterior projection and a flat lateral surface of the ectepicondyle. A similar ridge on the medial side of the humerus descends to the ulnar condyle to join its anteromedial edge, but it does not bear a sharp angle distally and instead is rounded along its edge. The surface of the entepicondyle is more convex and oriented more posteromedially, projecting farther

medially beyond the edge of the condyle than the ectepicondyle projects laterally. It is almost entirely covered by a large, subcircular scar that touches the edge of the distal articular surface. Similar ridges define the anterior edges of both epicondyles in *Herrerasaurus* (PVSJ 373) and the ectepicondyle of *Eodromaeus* (PVSJ 562), but *Tawa* lacks the pits found on the epicondyles of *Herrerasaurus* (PVSJ 373; Sereno, 1993). Although these ridges are less well developed in *Dilophosaurus* (UCMP 37302), *Tawa* shares the flaring, posteromedially facing entepicondyle found in this taxon and in basal tetanurans (e.g., Madsen, 1976), unlike the flat entepicondyles of *Eoraptor* (PVSJ 512), *Herrerasaurus* (PVSJ 373), *Coelophysis* (TMP 84.63.32, 84.63.33), and "*S.*" *rhodesiensis* (see Raath, 1990).

The humerus bears only a slight anterior intercondylar depression proximal to the distal condyles. It is subtriangular and is deepest over the radial condyle. The anterior intercondylar depression is more well developed than that of *Dilophosaurus* (UCMP 37302), but it is shallower than those found in *Herrerasaurus* (PVSJ 373) and "*S.*" *rhodesiensis* (see Raath, 1990). The radial condyle is saddle shaped and its projection onto the anterior surface of the humerus is broad and low. The proximal edge grades smoothly into the anterior surface of the humerus and lacks the distinct lip of *Herrerasaurus* (PVSJ 373) or the bulbous projection of *Eodromaeus* (PVSJ 562) and "*S.*" *rhodesiensis* (see Raath, 1990). In distal view, the articular surface is much wider mediolaterally than it is anteroposteriorly deep and is slightly hourglass shaped, with a narrow waist between expanded medial and lateral ends (Fig. 3F). This overall morphology is more similar to that of *Herrerasaurus* (PVSJ 373) and *Eoraptor* (PVSJ 512)—and likely also *Segisaurus* (UCMP 32101) and *Eodromaeus* (PVSJ 562), although there is incomplete preservation of the distal surfaces in these taxa—than the blocky, anteroposteriorly deep distal articular surfaces of *Dilophosaurus* (UCMP 37302) and *Liliensternus* (HMN MB.R. 2175). As in *Herrerasaurus* (PVSJ 373), in distal view the radial condyle is widest laterally and narrows medially to the junction with the ulnar condyle, although *Tawa* exhibits a greater narrowing between the condyles than does *Herrerasaurus*. The ulnar condyle is large, with a convex anterior edge and concave posterior edge in distal view. Its surface is restricted, extending onto neither the anterior surface of the humerus, as in "*S.*" *rhodesiensis* (see Raath, 1990), or the posterior surface, as in *Herrerasaurus* (PVSJ 373).

Radius

The radius is long and slender, with a total length 92% of the humerus (Table 1). The shaft appears straight in lateral view but exhibits a gentle sigmoidal curvature when viewed anteriorly (Fig. 4). Proximally, the medial surface of the radial shaft is flat but the lateral surface is concave laterally; distally, both surfaces are convex laterally. This sigmoidal shape is present in the radii of *Herrerasaurus* (PVSJ 373) and *Eodromaeus* (PVSJ 562) but is absent among specimens of "*S.*" *rhodesiensis* (see Raath, 1969), *Coelophysis* (TMP 84.63.29, 84.63.32), and *Dilophosaurus* (UCMP 37302, 77270); a slight sigmoidal curvature can be seen in the left radius of *Liliensternus* (HMN MB.R. 2175), but is absent in the right. The proximal articular surface is teardrop-shaped in proximal view, with a wide rounded anterior edge and a point posteriorly (Fig. 4E). Medially, the radial head is flattened for articulation with the ulna, and the ulnar articular facet appears as an inverted triangle proximally on the medial surface of the radius. The lateral edge of the radial head is rounded and projects beyond the lateral surface of the proximal end of the humeral shaft. The proximal articular surface is angled anteriorly in medial view and bears a subcircular concavity bounded anteriorly and posteriorly by slight bulbous projections of the surface. In other early theropods, including *Herrerasaurus* (PVSJ 373), *Eodromaeus* (PVSJ 562), *Dilophosaurus* (UCMP 37302, 77270), and *Liliensternus* (HMN MB.R. 2175), the radial head is elliptical, although all exhibit the flat medial and rounded lateral morphology. A flattened, rugose surface located just distal to the posterior apex of the radial head, found in *Herrerasaurus* (PVSJ 373), *Eodromaeus* (PVSJ 562), and *Dilophosaurus* (PVSJ 37302, 77270), is present in the radius of GR 242 but not in GR 360.

The shaft of the radius is amygdaloid at midshaft, with the long axis running anterolateral to posteromedial. It bears several long, low ridges extending along most of the length of the bone. One begins proximally on the lateral surface of the shaft and wraps around to the anterior surface distally. Similarly, another ridge begins on the medial surface and wraps posteriorly, extending to a posterior distal projection of the radius. A third, shorter ridge extends straight along its posterior surface and is restricted to the proximal half of the bone. These ridges give the shaft the appearance of being twisted counterclockwise about its long axis. Similar twisting

ridges are present in the radius of *Herrerasaurus* (PVSJ 373), and appear to be present in *Eoraptor* (PVSJ 512, right radius), although their distribution across other early theropods is difficult to assess due to post-depositional mediolateral flattening of the radius in many specimens (e.g., *Eodromaeus*, *Coelophysis*). However, the ridges present in the relatively uncrushed left radius of *Dilophosaurus* (UCMP 37302) do not exhibit this twisted morphology.

The radial shaft flares slightly at its distal end and meets the edge of the distal articular surface without a distinct lip or overhang. Just proximal to the articular surface, the radius possesses a posterior projection that is variously developed across the specimens. In GR 242 it is very prominent with a sharp posterior edge forming a distinct wedge on the distal end of the radius. The projection in GR 241 is moderately developed, appearing as a posterior flare in lateral view, whereas in GR 360 the projection is nearly nonexistent and only creates a slight bulging of the distal end posteriorly. Well-developed distal posterior projections are also present in *Herrerasaurus* (PVSJ 373) and *Coelophysis* (TMP 84.63.32), and *Eodromaeus* (PVSJ 562) possesses a similarly placed posterior rugosity on the distal end of the radius. Depending on the development of the posterior projection, the distal articular surface varies from subcircular to elliptical in distal view (Fig. 4F). It is shallowly concave and angled anteriorly in lateral view such that the posterior edge is located more proximal than the anterior edge. This angulation and general morphology is typical among other early theropods.

Ulna

Like the radius, the ulna is long and slender, being 7% longer than the radius (Table 1). In lateral view the anterior and posterior edges of the distal half of the ulna are parallel and begin flaring out toward the proximal articular surface just above midshaft (Fig. 5). Both edges show slight anterior concavities, giving the ulna a slight anterior curvature proximally; the anterior edge curves more strongly than the posterior, accentuating the proximal flare. Viewed anteriorly, the entire shaft is slightly bowed laterally, making the medial surface slightly concave. The proximal shaft is less anteroposteriorly flared in *Tawa* than in other early theropods, and the slight overall anterior curvature is not present among these taxa. A lateral bowing of the shaft is also found in *Sanjuansaurus* (PVSJ 605) and very slightly in

Herrerasaurus (PVSJ 373), whereas the ulna of "*S.*" *rhodesiensis* (see Raath, 1969) appears to bow in the opposite direction (slightly concave laterally), and those of *Dilophosaurus* (UCMP 37302, 77270) and *Liliensternus* (HMN MB.R. 2175) are generally unbowed.

The olecranon process is very poorly developed and is represented by a slight projection of the proximal articular surface posteriorly. In proximal view, the articular surface is subtriangular and is divided unequally by the olecranon into two faces (Fig. 5E). The peak of the olecranon is located posteromedially within the triangle with a ridge that extends from the lateral vertex straight medially to the posterior third of the medial edge. Anterior to this ridge, the slightly concave and gently sloping anterior face of the articular surface is large and forms the main surface for articulation with the humerus. The posterior face is flat and narrow, sloping steeply to the posterior edge of the articular surface. Most early theropods possess large olecranon processes that project far beyond the proximal articular surface, although both *Coelophysis* (TMP 84.63.29, 84.63.32, 84.63.40) and "*S.*" *rhodesiensis* (see Raath, 1969) exhibit both well developed and poorly developed olecranon morphologies, and the olecranon of *Eoraptor* (PVSJ 512) is similar to that of *Tawa*. The development of the olecranon process does not seem to be correlated to the size of the ulna; the olecranon is poorly developed in largest ulna of *Tawa* (GR 360), and both morphologies have been found in ulnae of similar sizes in other coelophysids (Raath, 1990; pers. obs.).

The medial edge of the proximal articular surface bears a slight lip that projects beyond the broad medial surface of the proximal end of the ulnar shaft. The medial surface is slightly concave distal to the articular surface, forming a shallow inverted triangular depression that extends along the proximal third of the shaft. The laterally directed vertex of the proximal articular surface forms a process that marks the posterior border of the radial articular facet, which is smooth and slightly concave. The lateral process is prominent and slightly bulbous, extending distally only a short distance before sharply falling off to the flat lateral surface of the ulna. This morphology is unusual among other early theropods, which typically exhibit a ridge extending from the lateral process distally along the ulna, demarcating the posterior edge of the radial articular facet. At the anterior edge of the radial articular facet a low, round tubercle is present distal to the edge of the proximal articular surface. A tubercle in this position is also

found in *Herrerasaurus* (PVSJ 373) and *Eodromaeus* (PVSJ 562), and likely represents an insertion site for the tendon of Biceps brachii (see Chapter IV).

The cross-section of the ulna is subtriangular at midshaft, defined by strong ridges anteriorly, laterally, and posteromedially. The anterior ridge is sharp and extends distally from the proximal articular surface for nearly the entire length of the ulna. The posteromedial ridge begins at the posteromedial apex of the proximal articular surface and extends along the entire length of the ulna. At the middle third of the ulna it curves slightly more laterally onto the posterior surface of the ulna, but it swings back to the posteromedial corner distally, becoming more rounded as it meets the articular surface. On the lateral surface, two small ridges, beginning at approximately one quarter the total length of the ulna, join form a 'V' from which the distinct lateral ridge descends to the edge of the distal articular surface. The distal shaft of the ulna meets the distal articular surface smoothly without flaring, and the distal end of the ulna is simple and relatively unmarked. The articular surface is convex and subcircular in distal view, with a slight point laterally where the lateral ridge joins its edge. Viewed anteriorly, it is angled slightly medially due to the lateral bowing of the ulnar shaft. The shape of the ulnar shaft does not vary greatly among early theropods, all of which possess major ridges in positions similar to those of *Tawa*. However, the morphology of the distal shaft where it meets the distal articular surface is typically more developed among other early theropods, varying from a simple flare (e.g., *Coelophysis*, TMP 84.63.29, 84.63.32; "*S.*" *rhodesiensis*, see Raath, 1969) to a complex series of tubercles and ridges (e.g., *Herrerasaurus*, PVSJ 373; *Dilophosaurus*, UCMP 37302). The shape of the distal articular surface in distal view is also conserved among early theropods, which exhibit a rounded, convex distal articular surface with a simple circular to elliptical outline in distal view (Fig. 5F).

Carpus

The carpus is composed of nine elements and is preserved in near articulation in the left forelimb of GR 242 (Fig. 6F). As preserved, the radius and ulna are disarticulated slightly toward the ventral surface of the manus, and the shift of the distal articular surfaces also pulled the radiale and ulnare out of anatomical position in relation to the other carpals and the manus. The

radiale was positioned near the proximal end of metacarpal I on its ventral surface, and the ulnare was pulled to the radial side of the carpus, although it maintained a very close association with the distal end of the ulna. The intermedium, which is not present as an independent element in early theropods (e.g., *Herrerasaurus*, *Eodromaeus*) or basal ornithischians (e.g., *Heterodontosaurus*, see Santa Luca, 1980), appears to have been present, although it did not retain its association with the radiale and ulnare as preserved. Six other carpals are also present and appear to have been preserved near anatomical position. Four small carpals forming a row distally and articulating with the metacarpals are identified by their position as distal carpals 1–4. Just proximal to this row, a carpal is present that corresponds to the centralium. The ninth carpal is positioned ventral to the other carpals on the ulnar side of the carpus and is identified as the pisiform.

The presence of nine carpals in *Tawa* is unusual among early theropods; only seven carpals are present in the five-fingered manus of *Eodromaeus* (PVSJ 562) and *Herrerasaurus* (but possibly eight; see Ezcurra, 2010), and coelophysids, which have four digits as in *Tawa*, only possess five to six carpals (Colbert, 1989). Nine carpals are present in the ornithischians *Heterodontosaurus* (see Santa Luca, 1980) and *Camptosaurus* (see Gilmore, 1909). The variation seen among basal taxa is typically the result of fusion or loss of the intermedium, loss of the pisiform, and fusion or loss of the distal carpals. The large number of carpals in *Tawa* may be the result of incomplete ossification of the carpus due to the subadult status of GR 242. Nevertheless, several elements of the carpus exhibit morphologies that are distinct and comparable to those of other early theropods.

The radiale is the largest carpal and is roughly subtriangular with rounded vertices in proximal view (Fig. 6E), similar in overall shape to that of *Herrerasaurus* (PVSJ 373). Its proximal surface is convex along its dorsal edge, with only a small concave divot ventrally. The dorsomedial and ventral surfaces are relatively flat, but the lateral surface is saddle-shaped. This shape is continuous with a concavity on the distal surface of the carpal that takes up the lateral half of the distal surface. The ulnare is wedge shaped, with a proximodistally tall lateral surface that tapers toward a narrow medial surface bearing a flat, slightly concave facet that is directed somewhat distally (Fig. 6B). It is generally similar in shape to that of *Herrerasaurus* (PVSJ 373)

and is distinct from the thin, round ulnare of *Eodromaeus* (PVSJ 562). Shallow concavities cover both the proximal and distal surfaces.

The identity of the bone here identified as the intermedium is not certain given its position as preserved in situ, but its distinct shape limits the possibilities for this bone. It is roughly cylindrical, with flat, proximodistally tall surfaces dorsally, medially, and laterally (Fig. 6). Its proximal and distal surfaces are concave and bear distinct lips along their dorsal and lateral edges. Despite its position in the middle row of carpals, it is unlikely that this bone is a second centralium; not only are two centralia unknown among dinosaurs (Gilmore, 1909; Santa Luca, 1980; Sereno, 1993), these bones are typically rounded with thin edges, as is the unequivocal centralium of *Tawa* (Fig. 6). The row of distal carpals appears complete and articulated in *Tawa* (see below) and the shape does not obviously fit in at any point, making it unlikely that this bone is a displaced distal carpal. The rounded shape of this carpal allows it to articulated in between the facing surfaces of the radiale and ulnare, which are otherwise mismatched (Fig. 6E), and thus it is here indentified as an intermedium. The adjacent distal surfaces of the intermedium and the radiale also form a continuous concave surface that articulates well with the convex proximal surface of the centralium (Fig. 6B). The centralium is round in proximal view and has a slightly concave distal surface for articulation with the distal carpals. The pisiform has an unusual sickle shape when viewed ventrally and bears a large transverse ridge along its dorsal surface, dividing its articular surface for the ulnare and the distal carpals (Fig. 6). It is unlike the rounded, spherical pisiforms of other tetrapods (e.g., Santa Luca, 1980), although its odd shape may be due to incomplete ossification.

The row of distal carpals is composed of four elements, with the second and fourth being the largest (Fig. 6). The first and second distal carpals have a similar shape, being relatively simply round (distal carpal 1) or ellipsoid (distal carpal 2) in distal view with convex proximal and distal surfaces. Distal carpal 3 is subrectangular and tapers ventrally, with a wider surface dorsally. Its proximal and distal articular surfaces are relatively flat, as is its medial surface for articulation with the second distal carpal.

Distal carpal 4 has a distinct, potentially phylogenetically significant shape (see discussion below). It is subtriangular in dorsal view, with a flat dorsal surface. A distally-directed

hooked process is present at its ventrolateral corner (Fig. 6), creating a deep concave distal surface that slightly overlaps the proximal surface of the third distal carpal. This morphology is also found in the lateralmost distal carpals of *Herrerasaurus* (PVSJ 373) and *Eodromaeus* (PVSJ 562), but does not characterize any carpals in ornithischians (Gilmore, 1909; Santa Luca, 1980), or more derived theropods (e.g., *Coelophysis*; see, Colbert, 1989).

Manus

The manus of GR 242 was preserved in near perfect articulation, with only the first phalanx of digit I slightly disarticulated from its metacarpal. The manus is relatively long and is 43% the combined length of the humerus and radius (Table 1, Fig. 1). Although it is composed of four digits, the manus was functionally tridactyl, composed of three large, ungual-bearing digits and a greatly reduced fourth digit (Fig. 7). There is no evidence for a fifth digit as in *Herrerasaurus* (PVSJ 373) or *Eodromaeus* (PVSJ 562). The first three metacarpals are similar in midshaft diameter but have differing lengths, with metacarpal I being the shortest and metacarpal III being the longest (Table 1). This relationship is typical of early theropods, though the length disparity between metacarpals II and III is greater in *Tawa* than in *Herrerasaurus* (PVSJ 373), *Eodromaeus* (PVSJ 562), coelophysids (Colbert, 1989; Raath, 1990), and *Dilophosaurus* (UCMP 37302). Additionally, the diminutive fourth metacarpal is more highly reduced in *Tawa* than in even the more crownward of these taxa, in which it is longer than metacarpal I.

Metacarpal I is over half the length of metacarpal II, giving it proportions more similar to those of *Herrerasaurus* (PVSJ 373) and *Eodromaeus* (PVSJ 562) than of *Coelophysis* (TMP 84.63.33, AMNH 7227), "*S.*" *rhodesiensis* (see Raath, 1990), or *Dilophosaurus* (UCMP 37302). The proximal articular surface is roughly triangular, with each face bearing a curved edge (Fig. 6A). Laterally, the articular edge for metacarpal II is sinuous and directed slightly ventrally. Constrictions at the base of a projecting medial flange give the dorsal and ventral edges a shallow V-shaped outline. The proximal surface is saddle-shaped with the bottom of the depression located slightly lateral to the midpoint in dorsal view. The medial projection is well developed and rounded medially in dorsal view, grading smoothly into the shaft of the metacarpal. Its dorsal surface exhibits some light pitting and striations. Similar medial

projections are found in *Herrerasaurus* (PVSJ 373), *Eodromaeus* (PVSJ 562), and some specimens of *Coelophysis* (TMP 84.63.52), although they are typically poorly developed in the latter taxon (Colbert, 1989). The ventral surface of the shaft is shallowly concave just distal to the edge of the proximal articular surface and bears some light rugosity in this area.

As in other early theropods, the distal end of metacarpal I is asymmetrical, bearing a well-developed lateral condyle and a reduced medial condyle whose axis angles away from the lateral condyle at an approximately 45° angle when viewed distally (Fig. 9). In dorsal view the asymmetry appears weaker and is more similar to the condition in *Herrerasaurus* (PVSJ 373) than that of *Eoraptor* (PVSJ 512), *Eodromaeus* (PVSJ 562), or coelophysids (Colbert, 1989; Raath, 1990), in which the medial condyle appears much shorter in dorsal view. The lateral condyle bears a large, deep collateral pit that fills much of its lateral surface (Fig. 8). A distinct lateral projection, unique among early theropods, is present at the ventral edge of the pit, creating a shallow groove between it and the condyle on its ventral surface. The medial condyle also bears a small, but deep, collateral pit on its medial surface; this pit is variably developed among early theropods and ranges from large and deep (*Eodromaeus*; PVSJ 562) to a shallow depression (*Dilophosaurus*; UCMP 37302). The dorsal surface of the distal end of the metacarpal is shallowly concave between the distal condyles but it lacks a distinct, lipped depression seen in *Herrerasaurus* (PVSJ 373; "extensor depressions" of Sereno, 1993) and *Eodromaeus* (PVSJ 562).

Metacarpal II is long and slender with a narrow proximal end that is only slightly wider mediolaterally than the shaft at its midpoint (Fig. 7). The outline of the proximal end is trapezoidal, having a broad flat base dorsally and sloping, shallowly concave medial and lateral sides. The proximal articular surface is flat and angled toward the dorsal edge, as in *Herrerasaurus* (PVSJ 373) and *Eodromaeus* (PVSJ 562). The dorsomedial corner of the proximal surface projects dorsally and distally into a thin medial flange with a hemispherical profile. A similar, though less developed, projection is found on metacarpal II of *Herrerasaurus* (PVSJ 373), but is absent in *Eodromaeus* (PVSJ 562) and other early theropods. Proximally, the dorsal surface of the shaft is marked by a shallow concavity that is separated from the edge of the proximal articular surface by a narrow, flat band. The ventral surface is slightly convex

proximally and highly striated. The shaft maintains a trapezoidal cross-section proximally, but becomes subrectangular distal to midshaft.

The distal end of metacarpal II is relatively flat in dorsal view, with little distinction between the two condyles. A similar condition is present in *Herrerasaurus* (PVSJ 373) and *Eodromaeus* (PVSJ 562), whereas the distal end of metacarpal II in coelophysids (Colbert, 1989; Raath, 1990) and *Dilophosaurus* (UCMP 37302) exhibit distinctly separated and asymmetrically developed condyles in dorsal view. However, *Eodromaeus* and *Tawa* both show a greater disparity between the development of the condyles than does *Herrerasaurus*. In distal view, the condyles flare away from the midline, with the lateral condyle being wide and rounded ventrally and the medial condyle narrow and pointed. Ventrally, the condyles are only shallowly separated. The lateral surface of the lateral condyle bears a deep, elliptical collateral pit that is shifted toward the dorsal edge of the condyle. The collateral pit on the medial condyle is shallower and tapered at its proximal end, and is located slightly more toward the middle of the condyle. A shallow extensor depression is present on the dorsal surface of the distal end of the metacarpal, but it lacks the distinct lip along its proximal edge as in *Herrerasaurus* (PVSJ 373), *Eodromaeus* (PVSJ 562), and *Dilophosaurus* (UCMP 37302).

Metacarpal III is the longest in the manus and is nearly twice as long as metacarpal I (Table 1). Like metacarpal II, it is long and slender with a narrow proximal end. In proximal view, the proximal articular surface is a nearly equilateral triangle with a flat, medially facing base for articulation with metacarpal II. The surface is slightly concave and slopes toward the ventrolateral vertex, at which point the articular surface extends onto the shaft of the metacarpal in a small lip. This articular surface is the likely point of articulation of the small metacarpal IV, which lacks any other clear point of articulation. This contrasts with the condition of *Herrerasaurus* (PVSJ 373) and *Eodromaeus* (PVSJ 562), in which metacarpal III retains a flat articular facet for metacarpal IV laterally, and that of *Coelophysis* (TMP, 84.63.33, TMP 84.63.40) and *Dilophosaurus* (UCMP 37302), which possesses a distinct notch for metacarpal IV. In *Tawa*, the ventral edge of the articular surface projects beyond the level of the shaft immediately distal to it, creating a shallow depression on the proximal ventral surface of the shaft. The dorsal surface of the shaft of metacarpal III in GR 242 is slightly crushed but appears

to be relatively flat and directed slightly laterally. At its midpoint the shaft is subtriangular with rounded corners.

The shaft of metacarpal III flares distally into a broad, flat distal articular surface (Fig. 7). As in metacarpal II, the condyles are poorly separated and are not distinct in dorsal view. The articular surface is wider ventrally than proximally, which orients the medial and lateral faces of the condyles somewhat dorsally. Like metacarpal II, the medial condyle of metacarpal III is wider and more rounded ventrally, whereas the lateral condyle is narrow and angled laterally to a larger degree. The lateral and medial condylar surfaces both bear narrow, deep collateral pits. These differ in morphology from those of *Herrerasaurus* (PVSJ 373) and *Coelophysis* (Colbert, 1989), in which these pits are subcircular, and from those of *Eodromaeus* (PVSJ 562) and *Dilophosaurus* (UCMP 37302), in which they are shallow and poorly defined. On the dorsal surface of the distal end of the metacarpal the extensor depression is very shallow.

The fourth metacarpal is highly reduced, being only slightly more than half the length and diameter of metacarpal I, and only a third the length of metacarpal III (Table 1, Fig. 7). In other early theropods, including *Herrerasaurus* (PVSJ 373), *Eodromaeus* (PVSJ 562), coelophysids (Colbert, 1989; Raath, 1990), and *Dilophosaurus* (UCMP 37302), this metacarpal is more elongate and is over half the length of metacarpal III. The proximal end of metacarpal IV is somewhat 'comma'-shaped, with a flat dorsal surface and curved medial and lateral surfaces that taper to a rounded end ventrally. The narrow shaft is subcircular and tapers to its minimum width at two-thirds of its length, at which point it flares slightly into very small condyles. They are most easily distinguished when viewed ventrally, where a small depression on the distal end of the metacarpal separates them. A relatively deep collateral ligament pit is present on the medial surface of the medial condyle but is absent laterally.

The phalangeal formula of the manus is 2/3/4/2/X; in digits I–III, the terminal phalanx is a large, laterally compressed, highly recurved ungual. Unusually, *Tawa* retains two phalanges on its fourth digit, whereas other early theropods with a less reduced digit IV (*Herrerasaurus*, PVSJ 373; *Coelophysis*, TMP 84.63.33; "*S.*" *rhodesiensis*, see Raath, 1969; *Dilophosaurus*, UCMP 37302) only possess one phalanx on that digit. *Eodromaeus* is also reported to only bear one phalanx on digit IV (Martinez et al., 2011), but the distal manus is incomplete in both PVSJ 560

and PVSJ 562, so the absence of a second phalanx in this taxon is uncertain. The non-ungual phalanges of digits I–III do not exhibit great variation in overall size, with total lengths within five millimeters of each other.

The first phalanx of digit I is elongate and slender with a gradually flaring proximal end and narrow condyles (Fig. 7). It is the same length as metacarpal I; this proportion is also seen in *Eodromaeus* (PVSJ 562) and is distinct from the elongation of this phalanx relative to the metacarpal seen in coelophysids (Colbert, 1989; Raath, 1990), *Dilophosaurus* (UCMP 37302), and basal tetanurans (e.g., Madsen, 1976). However, unlike *Eodromaeus*, *Herrerasaurus*, and other theropods, the proximal articular surface of this phalanx in *Tawa* is composted of a single concave, semicircular surface and lacks distinct articular facets for the condyles of metacarpal I. The ventral edge is flat and does not extend proximally into a ventral intercondylar process, which is very well developed in *Eodromaeus* (PVSJ 562) and *Herrerasaurus* (PVSJ 373). This surface is a poor match for the distal articular surface of metacarpal I, making articulation of these elements difficult (Fig. 9). The proximal articular surface is slanted dorsally and slightly medially. Ventrally, low ridges extend distally from the medial and lateral corners of the articular surface, creating a shallow depression between them. The distal condyles do not flare much mediolaterally in dorsal view, but are large and round when viewed laterally. Deep, round collateral pits are present on their medial and lateral surfaces, skewed slightly toward the dorsal edge of the condyle. The condylar articular surfaces are symmetrical and separated by a wide, distinct furrow. Between the condyles, the distal end of the phalanx bears a shallow extensor fossa dorsally and a deeper flexor fossa ventrally. Unlike *Eoraptor* (PVSJ 512), *Eodromaeus* (PVSJ 562), and *Herrerasaurus* (PVSJ 373), this phalanx lacks any rotation of the shaft about its long axis, leaving the distal condyles in alignment with the proximal articular surface.

The ungual of digit I is short and highly recurved (Fig. 8). It is strongly laterally compressed and tall dorsoventrally at its base, tapering quickly to a point distally. It appears to have a stronger recurvature than those of *Herrerasaurus* (PVSJ 373) or *Coelophysis* (TMP 84.63.52, TMP 84.63.30). The proximal articular surface bears two symmetrical facets for articulation with the condyles of I-1, but they are shallow and only weakly divided by the low central ridge. The flexor tubercle is massive and rugose, extending distally for over half the

length of the ungual. The extensor process is moderately developed, similar to the condition seen in other early theropods, and possesses slight striations along its dorsal surface. The vascular grooves on the medial and lateral surfaces of the ulna are deep and shifted slightly dorsally, intersecting with the dorsal curvature of the claw before its tip.

Phalanx 1 of digit II is short and features widely flaring proximal and distal ends (Fig. 7). In proximal view the articular surface has a similar shape to that of I-1, with a ventrally flat, single concave surface that is slanted towards its dorsal edge. However, this phalanx articulates well with the flat and indistinct distal condyles of metacarpal II. The ventral surface bears a wide shallow depression proximally, delineated by the low medial and lateral ridges extending distally from the proximal articular surface. Distally, the condyles are asymmetrically developed, with the lateral condyle being much larger than the medial (Fig. 9). The collateral pit of the lateral condyle is also larger and deeper than that of the medial condyle; this morphology of the distal condyles is also seen in *Herrerasaurus* (PVSJ 373), *Eodromaeus* (PVSJ 562), and *Coelophysis* (TMP 84.63.30, TMP 84.63.52). The extensor fossa is very weak dorsally but the flexor fossa is well developed and accentuated by the curvature of the phalanx.

Phalanx 2 of digit II is elongate and more similar in overall proportions to I-1 than to II-1, unlike the condition in *Herrerasaurus* (PVSJ 373), where the two non-ungual phalanges of digit II are subequal in length. The outline of the proximal articular surface is roughly like that of a squashed “D”, having a flat ventral surface and a much more rounded dorsal edge than the subtriangular proximal surface of this phalanx in *Herrerasaurus* (PVSJ 373). The surface is divided into two asymmetrical, concave facets by a low ridge, matching the asymmetrical condyles of II-1 (Fig. 9). The extensor and flexor intercondylar processes are well developed and project proximally well beyond the medial and lateral edges of the articular surface. The ventral surface of the shaft is shallowly concave over the proximal half of the phalanx, with some slight rugosities present at the medial and lateral corners of this surface at its proximal end. Distally, the condyles are slightly dorsoventrally compressed in medial view, giving them an overall ellipsoid shape, and the collateral pits are small but deep and located near the dorsal edge. They are approximately symmetrical and separated by a distinct furrow. The extensor fossa is broad

and relatively deep compared to those of the other phalanges; the flexor fossa appears large but its full morphology is obscured by breakage.

The base of the ungual of digit II is very similar to that of digit I, differing mainly the dorsoventral depth of the flexor tubercle. However, unlike *Herrerasaurus* (PVSJ 373), in which the unguals have a similar curvature, II-3 of *Tawa* is noticeably longer and slightly less highly recurved than I-2 (Fig. 8).

Like I-1 and II-1, the first phalanx of digit III possesses a semicircular proximal articular surface with a flat ventral edge (Fig. 9). It is a single concave surface that is slanted slightly dorsally, although to less of a degree than the other first phalanges. The shaft is short and straight, showing no curvature along its dorsal and ventral surfaces in medial view. Proximally, the ventral surface of the shaft is slightly concave, with low, striated ridges marking the medial and lateral edges. The distal condyles are asymmetrical, with the medial condyle extending farther distally than the lateral. This is reversed from the condition in *Eodromaeus* (PVSJ 562) and *Herrerasaurus* (Sereno, 1993), in which the lateral condyle is larger. Both the medial and lateral condyles bear deep, round collateral pits in the center of the medial and lateral surfaces, respectively. The extensor fossa is small but deep, whereas the flexor fossa is wide and extends proximal to nearly midshaft.

Phalanx 2 of digit III is the shortest in the digit, and in GR 242 the shaft has been mediolaterally crushed (Fig. 7). The proximal end is subtriangular, having a flat ventral base and a narrow peak dorsally at the extensor intercondylar process. As in II-2, the extensor and flexor intercondylar processes are prominent and pointed, and the flexor process is shifted slightly lateral of center due to the asymmetrical condyles of III-1. The distal condyles of this phalanx are also asymmetrical, but opposite the previous phalanx, with the lateral condyle being larger and extending farther distally than the medial. In this case, the morphology matches with the morphology of the distal III-2 of *Herrerasaurus* (PVSJ 373). The lateral collateral pit is larger than the small medial collateral pit, and the dorsal extensor fossa is small, round, and deep.

The third phalanx of digit III is the longest in the digit, in contrast with digit III of *Herrerasaurus* in which the first phalanx is longest (PVSJ 380; Sereno, 1993). The third phalanx is also the longest in *Coelophysis* (TMP 84.63.30, TMP 84.63.40), "*S.*" *rhodesiensis* (Raath,

1969) and, by a narrow margin, in *Eodromaeus* (PVSJ 560; Martinez et al., 2011). In overall morphology it is very similar to III-2, although it is overall more dorsoventrally compressed (Fig. 8). The flexor intercondylar process is relatively longer, projecting well beyond the extensor process, and its apex is located slightly medial of center to account for the asymmetrical distal condyles of III-2. The distal condyles appear asymmetrical but it is unclear how much of this is due to crushing, particularly of the medial condyle; based on the proximal surface of III-4, they seem to have been symmetrical originally. The lateral collateral pit is small and round, located toward the proximal and distal edge of the lateral surface of the condyle. As in the other phalanges of this digit, the dorsal extensor fossa is small but deep.

As in *Herrerasaurus* (PVSJ 373) and *Eodromaeus* (PVSJ 560), *Tawa* retains a large ungual on digit III, in contrast to coelophysids (TMP 84.63.50; Raath, 1969) and *Dilophosaurus* (UCMP 37302), in which the ungual of digit III is relatively smaller than the other phalanges. The base of III-4 is nearly identical to that of II-3, but the former ungual is longer and more shallowly curved than the latter (Fig. 8).

Phalanx 1 of digit IV is tiny but exhibits a distinct phalangeal morphology, including small but distinct distal condyles (Fig. 9). This differs from the small, wedge-shaped IV-1 of *Herrerasaurus* (PVSJ 373), which does not articulate with another phalanx distally. The proximal articular surface is subcircular with a slightly flattened ventral surface. It is flat and slopes toward the dorsal and lateral edges. Proximally, the lateral surface of the shaft flares much more than the medial surface, and it has a distinctly flat, semicircular surface bearing a central divot located just distal to the edge of the proximal articular surface (Fig. 7). The distal end of the phalanx flares slightly at the condyles, which are slightly asymmetrical. They are separated by a slight flexor fossa on the ventral surface of the distal end of the phalanx, but no groove separates them on the articular surface. The medial condyle is slightly larger and possess a relatively large, teardrop-shaped collateral pit on its medial surface; the lateral condyle does not have a collateral pit.

Phalanx 2 of digit IV is extremely reduced and present only as a small, roughly spool-shaped element in GR 242 (Fig. 7). Its proximal surface and distal surfaces are slightly wider than its midpoint, with a narrower ‘waist’ dorsoventrally than mediolaterally.

DISCUSSION

Phylogenetic Implications

The relationships of basal saurischians are controversial, particularly the placement of taxa such as *Herrerasaurus* and *Eoraptor*. Although *Tawa* is relatively consistently recovered as the sister taxon to Neotheropoda (Nesbitt et al., 2009a; Martinez et al., 2011), it features a combination of derived and plesiomorphic characters throughout its skeleton that are informative to the placement of more basal taxa (Nesbitt et al., 2009a). In the pectoral girdle and forelimb, most of the characters that have been argued to support a particular topology are found in the carpus and manus, and many of these have controversial or conflicting codings in different analyses. New data from the carpus and manus of *Tawa*, as well as those of the recently described *Eodromaeus*, provide the opportunity to reassess these characters and their distribution among basal dinosaurs.

(1) *Size of the medialmost distal carpal*. The presence of a small distal carpal I in *Herrerasaurus* has been used to exclude this taxon from Eusaurischia on the basis of an apparently homologous enlarged distal carpal I in Neotheropoda and Sauropodomorpha (Langer and Benton, 2006; Ezcurra, 2010). Nesbitt (2011) argues that the enlarged distal carpal I of neotheropods is not homologous with that of sauropodomorphs because it covers the proximal end of metacarpal II as well as metacarpal I. The medialmost distal carpal in *Coelophysis* and other early neotheropods caps both of these metacarpals because it is the result of the fusion of distal carpals I and II (Colbert, 1989), whereas that of sauropodomorphs is a true distal carpal I that is separate from the distal carpal II that caps metacarpal II (Nesbitt, 2011). Furthermore, both *Tawa* and *Eodromaeus* (PVSJ 560) possess relatively small first distal carpals that have not become fused to the second distal carpal (Fig. 6), indicating that a large medialmost distal carpal is not plesiomorphic for the clade.

(2) *Presence of distal carpal V*. The absence of a distal carpal V has been cited as a eusaurischian synapomorphy (Sereno, 1999; Langer and Benton, 2006). Although *Herrerasaurus* was originally described with only four distal carpals (Sereno, 1993), evidence from an

undescribed herrerasaurid forelimb suggests that PVSJ 373 is missing distal carpal I and that herrerasaurids would have possessed five distal carpals (Ezcurra and Novas, 2007; Ezcurra, 2010), seemingly supporting a placement outside of Eusaurischia. However, the enlarged, ventrally hooked morphology of distal carpal V of herrerasaurids also characterizes the lateralmost metacarpals of *Eodromaeus* (PVSJ 562) and *Tawa*, despite the presence of only four distal carpals in both taxa. In fact, the lateralmost metacarpal of *Eodromaeus* is labeled as "dc5" in the original description, but this identification is presented without comment in the text (Martinez et al., 2011; Fig. 1G). This distinct morphology of the lateralmost metacarpal is not seen in *Heterodontosaurus* (Santa Luca, 1980), basal sauropodomorphs (e.g., *Thecodontosaurus*; Benton et al., 2000), and possibly *Eoraptor* (Martinez et al., 2011; Fig. 1F). This suggests that this carpal morphology may have been acquired at the base of Theropoda and was later lost in neotheropods. Unfortunately the precise homology, identity, and number of the distal carpals in basal saurischians remains difficult to assess based on currently known material.

(3) *Morphology of extensor depressions of metacarpals I–III*. As noted by Nesbitt (2011), this character is imprecise and needs revision. Previously, the presence of deep and asymmetrical extensor pits (depressions) on the distal ends of metacarpals I–III were used to unite *Herrerasaurus* and *Eoraptor* with Theropoda (Sereno, 1993, 1999), although the extensor depression were only scored as present or absent in a more recent analysis assessing the position of *Eoraptor* and *Eodromaeus* (Martinez et al., 2011). The size and shape of the extensor depression varies between metacarpals in these taxa, and assessment of their depth is extremely subjective; although the extensor depressions of *Herrerasaurus* (PVSJ 373) are distinct and bear a strong lip along their proximal edge, I would not consider them deep in comparison to those of more derived theropods such as *Dilophosaurus* (UCMP 37302) or of the basal ornithischian *Heterodontosaurus* (Santa Luca, 1980). In *Eodromaeus* (PVSJ 562), metacarpal I bears a very deep extensor depression whereas that of metacarpal III is barely present and, in *Tawa,* the pits are all relatively shallow. Thus, if this character is to remain in use a more thorough survey of the morphology extensor depressions is necessary among basal dinosaurs.

(4) *Asymmetry of the distal condyles of metacarpal I*. The asymmetry of the distal condyles of metacarpal I is characterized as strong or weak to none. The ambiguity of 'strong'

versus ‘weak’ makes this another character that has been coded differently to support different hypotheses. Ezcurra (2010) codes this morphology in two characters (nos. 228 and 369) and uses it as a synapomorphy of Theropoda + Sauropodomorpha to the exclusion of *Herrerasaurus*. New data from *Tawa* and *Eodromaeus* show that although some asymmetry is present in the distal condyles of metacarpal I in these taxa, it is relatively weak in comparison to the neotheropods used as exemplars in that analysis (*Dilophosaurus* and “*Syntarsus*” *rhodesiensis*). Although some asymmetry in the condyles likely characterizes Saurischia as a whole, strongly asymmetrical condyles were likely independently acquired in neotheropods and sauropodomorphs.

(5) *Ungual shape of digits II and III*. Highly recurved, trenchant unguals of digits II and III have been cited as a potential theropod synapomorphy (Langer and Benton, 2006) and a character shared by *Herrerasaurus* (Sereno, 1993). However, Ezcurra (2010) argues that this character is convergent in herrerasaurids and derived theropods on the basis of poorly recurved manual unguals II and III in *Dilophosaurus* and “*Syntarsus*” *rhodesiensis*. In this case, “strongly curved” is defined as the tip of the ungual projecting “well below” the flexor margin of the proximal articular surface (Ezcurra, 2010; pg. 407). This highly recurved state can be found in the manus of *Coelophysis* (e.g., TMP 84.63.50, TMP 84.63.29) and, arguably, also in the manus of “*Syntarsus*” *rhodesiensis* (see Raath, 1969), but the extremely recurved unguals II and III of *Tawa* clearly indicate that this character is plesiomorphic among Theropoda.

Functional Implications

The orientation of the glenoid fossa, combined with the large posterior excursion of the humeral head, would have given the humerus a posteroventrally directed neutral position and an extensive range of retraction. Although no coracoid is preserved in *Tawa*, the coracoids of other early theropods exhibit a relatively reduced anterior glenoid lip (*Eodromaeus*, PVSJ 562; *Sanjuansaurus*, PVSJ 605), allowing for a large anterior excursion of the humerus despite the posteroventral orientation of the glenoid. The slightly bulbous morphology of the posterior humeral head in *Tawa*, *Eodromaeus*, *Coelophysis*, and “*Syntarsus*” permits a greater range of abduction and adduction at the shoulder than would have been possible in theropods exhibiting a

blockier humeral head, such as *Dilophosaurus*, although these movements would have still been more limited than those of protraction and retraction.

The torsion of the humeral shaft seen in *Tawa* and neotheropods orients the distal condyles of the humerus such that the antebrachium faces somewhat laterally if the internal tuberosity of the humerus is directed medially. Practically, this suggests that rotation of the humerus about its long axis would allow for a larger lateral excursion of the antebrachium and manus and potentially restricted medial excursion, such that the manus may have only been able to meet at the midline and not cross to the opposite side of the body. Lacking a tightly constrained olecranon, *Tawa* had a large degree of extension at the elbow, although the limited excursion of the ulnar condyle anteriorly may have limited the flexion of this joint. As in *Herrerasaurus* (Sereno, 1993), the elliptical radial head of *Tawa* could not rotate on the humeral condyle or against its articular facet on the ulna to accomplish pronation and supination of the manus using the mechanism of the human antebrachium. However, pronation and supination of the antebrachium in tetrapods is not limited to this mechanism and is performed by crocodylians and lepidosaurs with similar radial head morphology to that of basal dinosaurs (Landsmeer, 1983). The expansion of the radial condyle onto the anterior surface of the humerus allows the radius to flex independently of the ulna at the elbow, which in turn causes the distal end of the radius to rotate relative to the ulna; even a small amount of this movement can result in a high degree of pronation of the antebrachium (Landsmeer, 1983).

Pronation of the antebrachium in this manner depends in part on the morphology of the wrist. Articulated wrists of *Eodromaeus* (PVSJ 526) and *Coelophysis* (TMP 84.63.29, TMP 84.63.32) indicate that the radius and ulna would have been nearly or completely separated at their distal ends in early theropods possessing a broad carpus, including *Tawa*. The round, concavo-convex ulnare-ulna joint of *Tawa* would allow a rotary motion similar to that seen during forearm rotation in lepidosaurs (Landsmeer, 1983). The rounded surfaces and loose articulation of the carpals may be a result of incomplete ossification due to the likely subadult status of GR 242 (Nesbitt et al., 2009a), although this morphology is also present to a lesser degree in *Herrerasaurus* (PVSJ 373). This carpal morphology would have allowed a relatively

wide range of motion at the wrist of *Tawa* compared to that of basal dinosaurs with a more close-packed carpus such as *Heterodontosaurus* (see Santa Luca, 1980).

The metacarpals of *Tawa* are notable for their relatively flat distal ends with undifferentiated condyles, which are accompanied by broad, concave proximal articular surfaces in the proximal phalanges, particularly in digits II and III. This condition is also found in digits II and III of *Eodromaeus* (PVSJ 562), *Herrerasaurus* (PVSJ 373), and *Eoraptor* (PVSJ 512) and permits some abduction and adduction of the phalanges at this joint, a movement that is highly restricted in taxa with distinct metacarpal condyles. The lack of intercondylar processes on the proximal phalanges in *Tawa* obviates the need for deep extensor and flexor depressions on the distal end of the metacarpals, while still allowing the manus to retain large flexor and extensor ranges of motion at these joints. These depressions are much larger on the non-ungual phalanges, which possess separated condyles that limit the potential movements to flexion and extension. Even so, the extensor depressions in *Tawa* are shallower than those found in some other early theropods, whereas the flexor depression remains very well developed. The highly recurved unguals of digits I–III bearing large, rugose flexor tubercles further emphasize the importance of digital flexion in the manus of *Tawa*.

SUMMARY AND CONCLUSIONS

The nearly complete and well-preserved pectoral girdle and forelimb material of *Tawa hallae* provides new information on the morphology and function of this system in early theropods and allows for thorough comparisons with other basal dinosaurs. Following other regions of the skeleton, the forelimb exhibits a mosaic of derived and plesiomorphic features that solidify *Tawa*'s position as a transitional taxon among early theropods. *Tawa* shares with herrerasaurids a relatively elongate and narrow scapular blade, yet exhibits the flaring distal end of coelophysoids. Its humerus possesses the high degree of torsion found in more derived theropods, yet retains features of the proximal and distal articular surfaces that characterize those of *Herrerasaurus* and *Eodromaeus*. In particular, the morphology of the carpus and manus permits reassessment of several key characters that have played an important role in determining

the relationships of basal saurischians. *Tawa*'s plesiomorphic nine carpals supply valuable new information on the primitive states among early theropods and provide evidence for a distinct morphology of the lateralmost distal carpal that is currently known for only a few early theropod taxa. Future discoveries of the carpus of other early saurischians will help to clarify the distribution of this morphology.

The function of the forelimb in *Tawa* and other basal dinosaurs is difficult to deduce based on the osteology alone; the reconstruction of the pectoral and forelimb musculature is the subject of another study (Chapter IV). Nevertheless, the arthrology of *Tawa* suggests that each joint of the forelimb likely enjoyed a wide range of motion in several planes, including the ability to pronate and supinate the antebrachium to a limited degree. Joint surfaces in the carpus and manus indicate that early theropods may have possessed degrees of freedom in the movements of the hand and digits that became more limited as early as Neotheropoda, perhaps as the limb became more specialized for particular types of predatory behavior.

ACKNOWLEDGMENTS

I thank D. Krause, A. Turner, B. Demes, and S. Gatesy for their help and support in the development of this study and comments on the early drafts of the manuscript. I also thank A. Turner, S. Nesbitt, R. Irmis, and N. Smith for the opportunity to work on the *Tawa* forelimb material. R. Martinez (PVSJ), D. Henderson (RTMP), B. Strilisky (RTMP), M. Norell (AMNH), C. Mehling (AMNH), K. Padian (UCMP), M. Goodwin (UCMP), M. Getty (UMNH), C. Levitt (UMNH), P. Sereno (University of Chicago), T. Keillor (University of Chicago), and D. Schwartz-Wings (HMN) generously provided access to specimens in their care. I thank J. McCartney for support and feedback during this project. Funding for this project was provided by a National Science Foundation Graduate Research Fellowship, a National Science Foundation Doctoral Dissertation Improvement Grant (DEB 111036), and by the Doris O. and Samuel P. Welles Research Fund of the UCMP.

LITERATURE CITED

Benton, M. J., L. Juul, G. W. Storrs, and P. M. Galton. 2000. Anatomy and systematics of the prosauropod dinosaur *Thecodontosaurus antiquus* from the Upper Triassic of southwest England. Journal of Vertebrate Paleontology 20:77–108.

Brinkman, D. B., and H.-D. Sues. 1987. A staurikosaurid dinosaur from the Upper Triassic Ischigualasto Formation of Argentina and the relationships of the Staurikosauridae. Palaeontology 30:493–503.

Brochu, C. A. 2003. Osteology of *Tyrannosaurus rex*: insights from a nearly complete skeleton and high-resolution computed tomographic analysis of the skull. Journal of Vertebrate Paleontology 22:1–138.

Burch, S. H., and M. T. Carrano. 2012. An articulated pectoral girdle and forelimb of the abelisaurid theropod *Majungasaurus crenatissimus* from the Late Cretaceous of Madagascar. Journal of Vertebrate Paleontology 32:1–16.

Colbert, E. H. 1989. The Triassic dinosaur *Coelophysis*. Bulletin of the Museum of Northern Arizona 57:1–160.

Ezcurra, M. D. 2010. A new early dinosaur (Saurischia: Sauropodomorpha) from the Late Triassic of Argentina: a reassessment of dinosaur origin and phylogeny. Journal of Systematic Palaeontology 8:371–425.

Ezcurra, M. D., and F. Novas. 2007. New dinosaur remains (Saurischia: Herrerasauridae) from the Ischigualasto Formation (Carnian) of NW Argentina. Ameghiniana 44:17R.

Gilmore, C. W. 1909. Osteology of the Jurassic reptile *Camptosaurus*, with a revision of the species of the the genus, and descriptions of two new species. Proceedings of the United States National Museum 36:197–332.

Irmis, R. B., R. Mundil, J. W. Martz, and R. A. Parker. 2011. High resolution U–Pb ages from the Upper Triassic Chinle Formation (New Mexico, USA) support a diachronous rise of dinosaurs. Earth and Planetary Science Letters 309:258–267.

Irmis, R. B., S. J. Nesbitt, K. Padian, N. D. Smith, A. H. Turner, D. Woody, and A. Downs. 2007. A Late Triassic dinosauromorph assemblage from New Mexico and the rise of dinosaurs. Science 317:358–361.

Landsmeer, J. M. F. 1983. Mechanism of forearm rotation in *Varanus exanthematicus*. Journal of Morphology 175:119–130.

Langer, M. C., and M. J. Benton. 2006. Early dinosaurs: a phylogenetic study. Journal of Systematic Palaeontology 4:309–358.

Langer, M. C., M. A. G. Franca, and S. Gabriel. 2007. The pectoral girdle and forelimb anatomy of the stem-sauropodomorph *Saturnalia tupiniquim* (Upper Triassic, Brazil). Special Papers in Palaeontology 77:113–137.

Madsen, J. H. 1976. *Allosaurus fragilis*: a revised osteology. Utah Geological Survey Bulletin 109:1–163.

Marsh, O. C. 1881. Principle characters of American Jurassic dinosaurs. Part V. The American Journal of Science, series 3 21:417–423.

Martinez, R. N., P. C. Sereno, O. A. Alcober, C. E. Colombi, P. R. Renne, I. P. Montañez, and B. S. Currie. 2011. A basal dinosaur from the dawn of the dinosaur era in southwestern Pangaea. Science 331:206–210.

Nesbitt, S. J. 2011. The early evolution of archosaurs: relationships and the origin of major clades. Bulletin of the American Museum of Natural History 352:1–292.

Nesbitt, S. J., N. D. Smith, R. B. Irmis, A. H. Turner, A. Downs, and M. A. Norell. 2009. A complete skeleton of a Late Triassic saurischian and the early evolution of dinosaurs. Science 326:1530–1533.

Owen, R. 1842. Report on British fossil reptiles, part II. Report of the British Association for the Advancement of Science 11:60–104.

Raath, M. A. 1969. A new coelurosaurian dinosaur from the Forest Sandstone of Rhodesia. Arnoldia Series of Miscellaneous Publicatons 4:1–25.

Raath, M. A. 1990. Morphological variation in small theropods and its meaning in systematics: evidence from *Syntarsus rhodesiensis*; pp. 91–105 in K. Carpenter and P. J. Currie (eds.), Dinosaur Systematics. Cambridge University Press, Cambridge, UK.

Rowe, T. A. 1989. A new species of the theropod dinosaur *Syntarsus* from the Early Jurassic Kayenta Formation of Arizona. Journal of Vertebrate Paleontology 9:125–136.

Santa Luca, A. P. 1980. The postcranial skeleton of *Heterodontosaurus tucki* (Reptilia, Ornithischia) from the Stormberg of South Africa. Annals of the South African Museum 79:159–211.

Seeley, H. G. 1888. On the classification of the fossil animals commonly named Dinosauria. Proceedings of the Royal Society of London 43:165–171.

Sereno, P. C. 1993. The pectoral girdle and forelimb of the basal theropod *Herrerasaurus ischigualastensis*. Journal of Vertebrate Paleontology 13:425–450.

Sereno, P. C. 1999. The evolution of dinosaurs. Science 284:2137-2147.

TABLE 2.1. Measurements (in mm) of *Tawa hallae* forelimb and pectoral girdle elements. **Abbreviations**: **AP**, midshaft anteroposterior diameter; **c**, length along the curvature of the ungual; **DAP**, distal anteroposterior diameter; **DML**, distal mediolateral diameter; **GH**, glenoid height; **GW**, glenoid width; **ML**, midshaft mediolateral diameter; **PAP**, proximal anteroposterior diameter; **PML**, proximal mediolateral diameter; **SHD**, scapular height at the distal end; **SHM**, scapular height at the minimum; **SL**, scapular length; **SML**, scapular mediolateral width (measured at mid-scapular length); **TL**, total length. Dashes indicate where measurements could not be taken; plus signs (+) indicate that some length is missing from the element as preserved.

Element	Specimen	SL	SHM	SHD	SML	GW	GH	
Scapula	GR 242 (L)	106	7.1	17.2	3.0	7.6	8.4	
	GR 241 (R)	94.2	6.3	14.1	3.7	7.8	9.0	
Element	Specimen	TL	AP	ML	PAP	PML	DAP	DML
Humerus	GR 242 (R)	102	7.9	7.5	9.2	19.1	7.3	20.5
	GR 242 (L)	98.2	7.9	7.6	9.2	19.2	7.9	19.1
	GR 241 (R)	79.8	5.8	5.7	6.5	14.8	—	—
Radius	GR 242 (R)	83.7	4.7	4.3	8.5	6.1	8.1	5.7
	GR 241 (R)	73.7	3.2	3.3	5.7	4.2	5.7	4.7
	H4-460-11021&22	102	4.2	5.1	9.1	6.0	6.8	7.2
Ulna	GR 242 (R)	88.4	4.9	4.0	10.9	8.7	6.2	6.6
	GR 241 (R)	80.1	4.4	4.3	8.6	4.8	8.9	4.0
	H4-460-11021&22	106	5.2	3.9	11.0	8.1	6.5	5.2
Metacarpal I	GR 242 (R)	17.8	2.2	3.9	4.1	7.1	4.7	6.2
Metacarpal II	GR 242 (R)	27.3	2.4	3.2	5.6	4.8	4.2	6.4
Metacarpal III	GR 242 (R)	33.2	2.7	3.3	5.3	5.4	4.3	6.9
Metacarpal IV	GR 242 (R)	9.9	1.6	1.6	2.1	3.2	1.8	2.2
Phalanx I-1	GR 242 (R)	17.8	2.8	2.7	5.0	5.8	4.6	3.9
Phalanx II-1	GR 242 (R)	16.2	3.4	3.0	5.6	7.0	4.9	5.6

Phalanx II-2	GR 242 (R)	20.0	2.8	3.0	5.8	5.3	4.0	4.1
Phalanx III-1	GR 242 (R)	16.7	3.3	3.6	5.3	6.8	4.7	5.6
Phalanx III-2	GR 242 (R)	15.3	3.1	3.8	5.8	5.0	4.4	5.0
Phalanx III-3	GR 242 (R)	17.5	2.4	4.2	5.5	5.4	4.2	4.7
Phalanx IV-1	GR 242 (R)	5.2	1.3	1.3	2.2	2.3	1.2	1.9
Phalanx IV-2	GR 242 (R)	2.0	1.1	1.1	—	—	—	—
Ungual I	GR 242 (R)	23c+	—	—	7.2	3.8	—	—
Ungual II	GR 242 (R)	25c+	—	—	7.7	4.1	—	—
Ungual III	GR 242 (R)	29c	—	—	8.2	4.1	—	—

FIGURE 2.1. Reconstruction of the articulated right scapula and forelimb of *Tawa hallae* in lateral view. Based on the right scapula, humerus, and manus of GR 242, and the antebrachium of GR 360 (reversed). Hypothetical outline of the coracoid indicated by the dashed line and based on those of other early theropods.

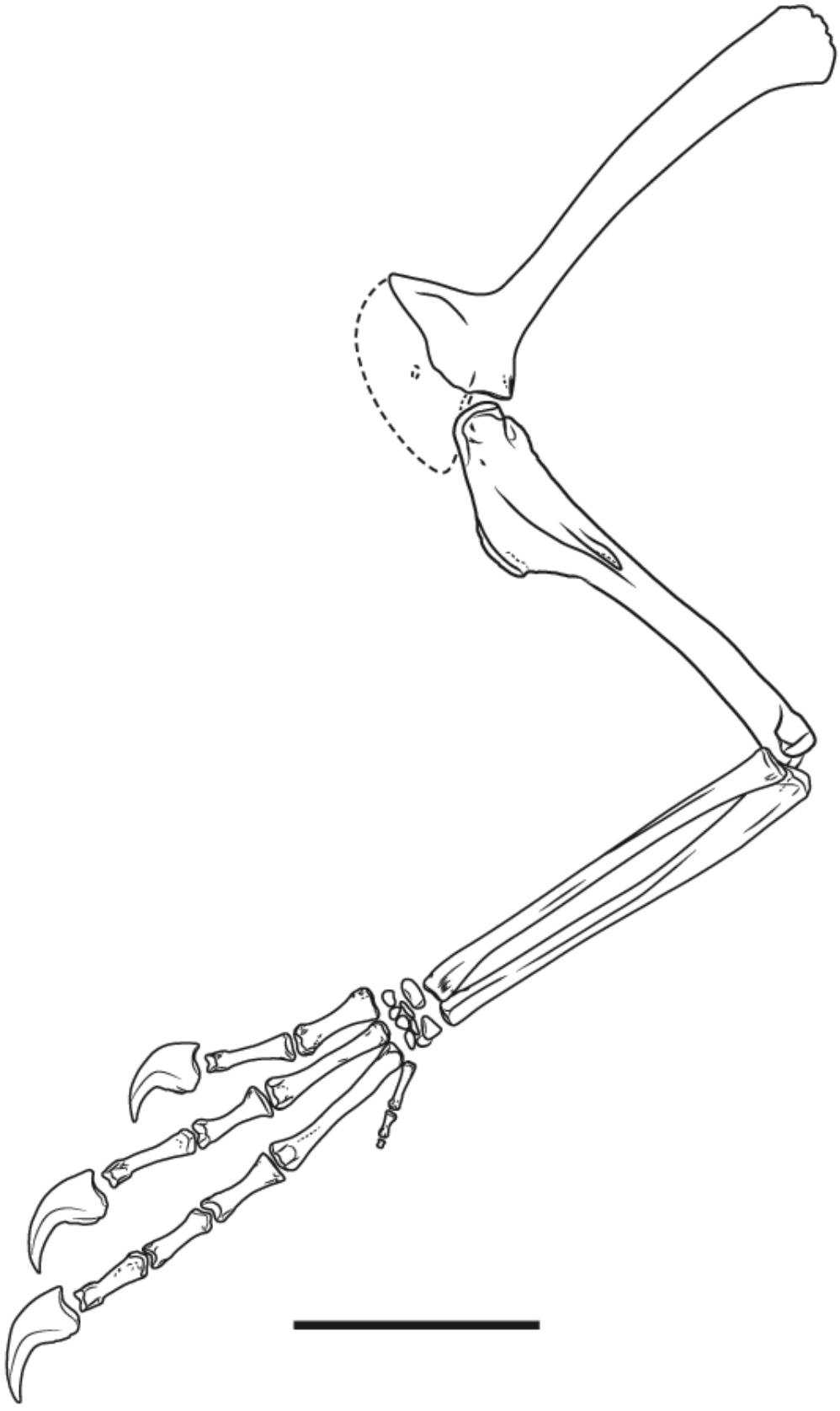

FIGURE 2.2. Right scapula of *Tawa hallae* (GR 242) in lateral (**A**) and medial (**B**) views. **Abbreviations**: **acr**, acromion; **gl**, glenoid; **msr**, medial scapular ridge; **sad**, subacromial depression; **tbs**, scar for Triceps brachii scapularis. Scale bar equals 5 cm.

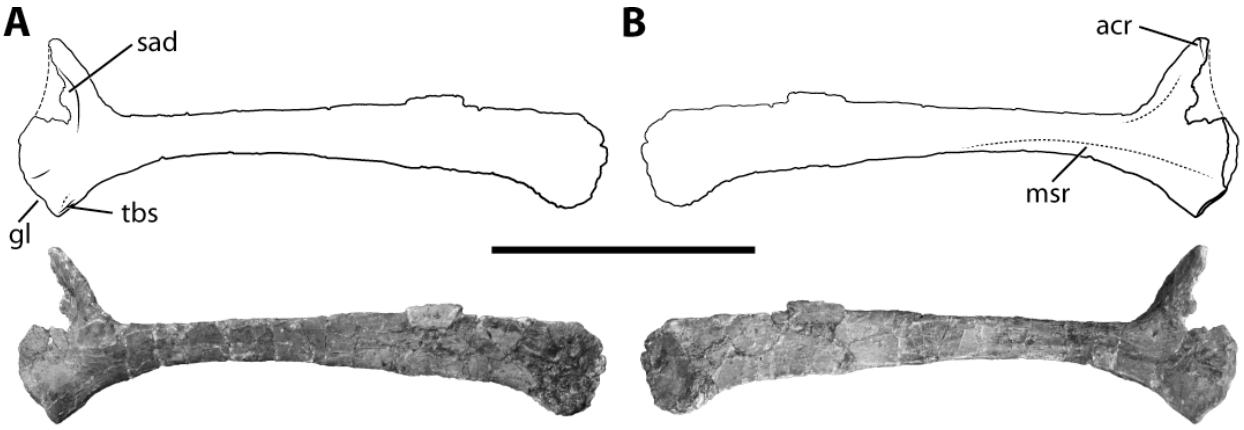
A
sad
tbs
gl
B
acr
msr

FIGURE 2.3. Left humerus of *Tawa hallae* (GR 242) in anterior (**A**), medial (**B**), posterior (**C**), lateral (**D**), proximal (**E**), and distal (**F**) views. **Abbreviations**: **aid**, anterior intercondylar depression; **dpc**, deltopectoral crest; **ect**, ectepicondyle; **ent**, entepicondyle; **gt**, greater tubercle; **hh**, humeral head; **it**, internal tuberosity; **lf**, lateral furrow; **lr**, lateral ridge; **rc**, radial condyle; **uc**, ulnar condyle. Scale bar equals 5 cm.

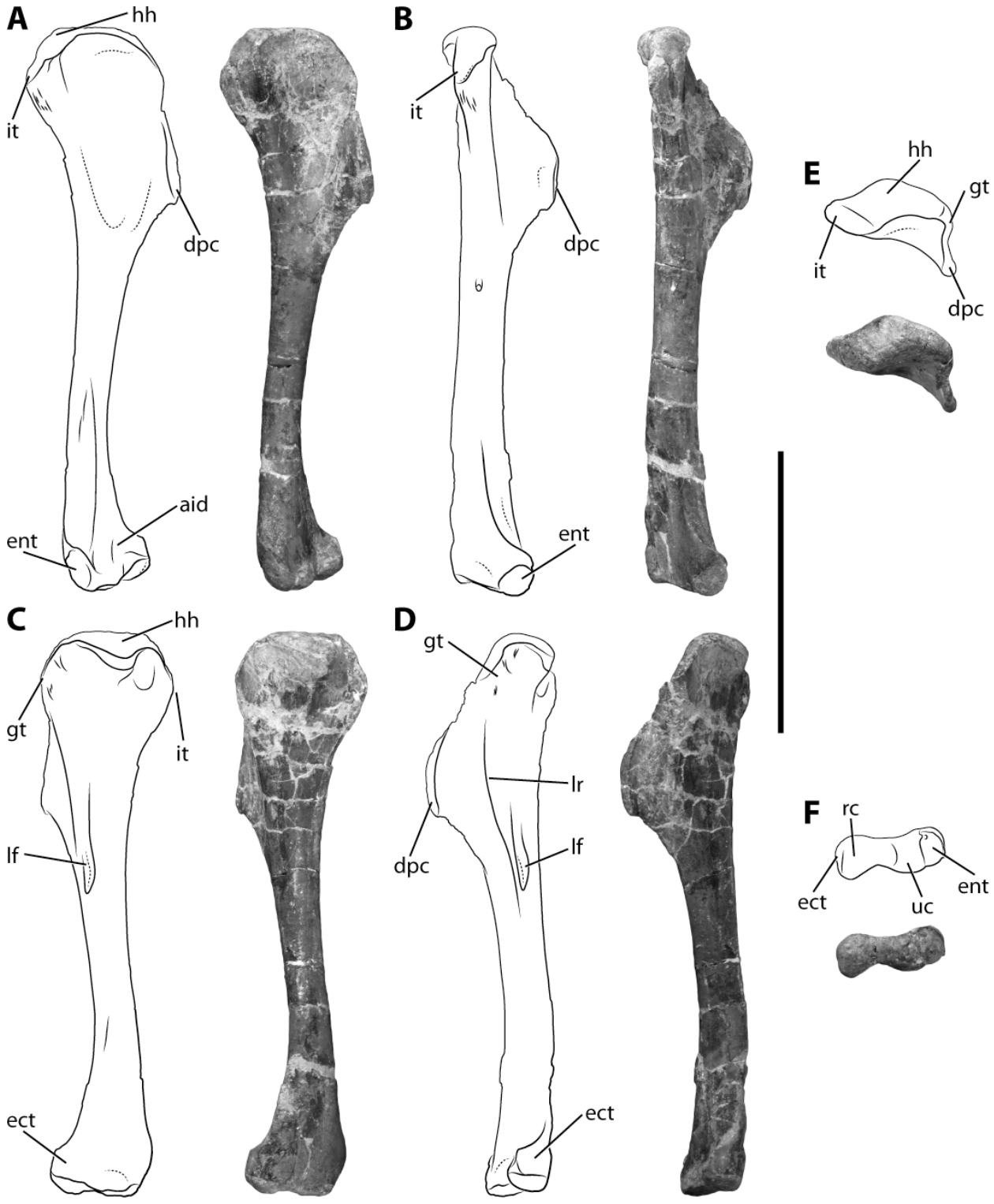
A
hh
it
dpc
aid
ent
B
it
dpc
ent
E
hh
gt
it
dpc
C
hh
gt
it
lf
ect
D
gt
lr
dpc
lf
ect
F
rc
ect
uc
ent

FIGURE 2.4. Left radius of *Tawa hallae* (GR 360) in anterior (**A**); medial (**B**); posterior (**C**); lateral (**D**); proximal (**E**); and distal (**F**) views. Cross-hatching indicates broken bone surface. **Abbreviations**: **pdp**, posterior distal projection; **uaf**, ulnar articular facet. Scale bar equals 5 cm.

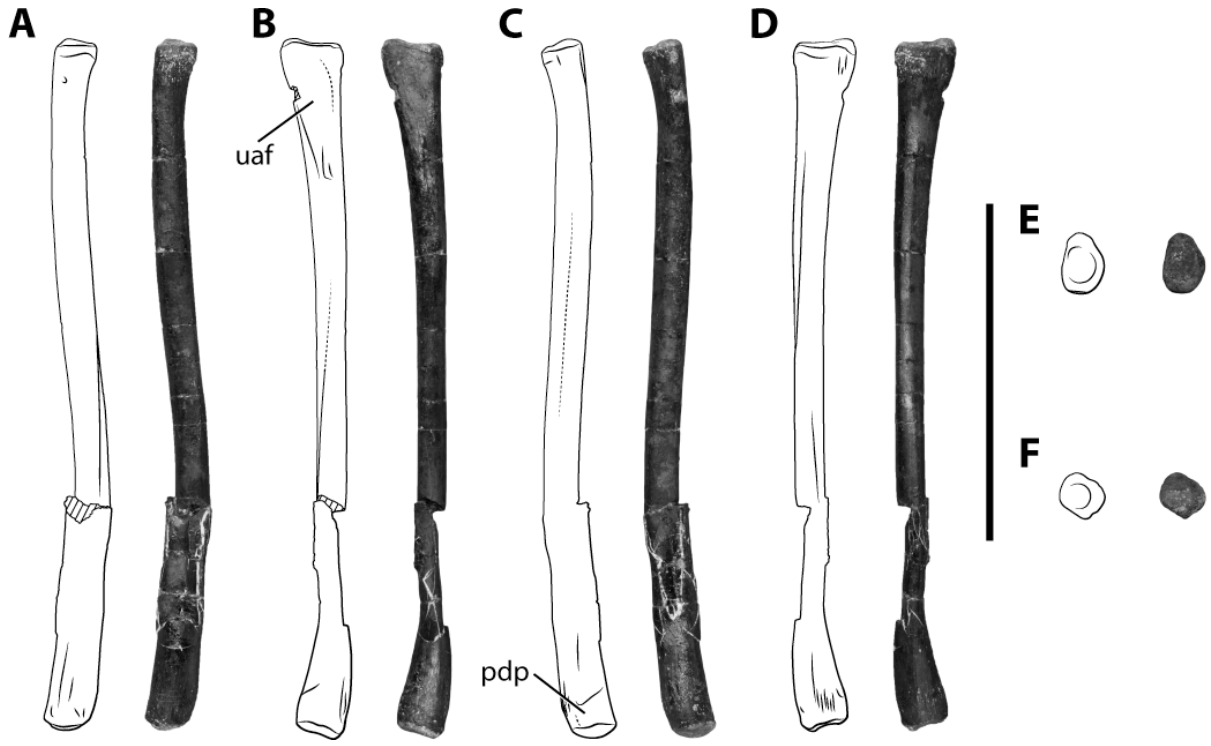
A
B
C
D
E
F
uaf
pdp

FIGURE 2.5. Left ulna of *Tawa hallae* (GR 360) in anterior (**A**); medial (**B**); posterior (**C**); lateral (**D**); proximal (**E**); and distal (**F**) views. Cross-hatching indicates broken bone surface. **Abbreviations**: **at**, anterior tuberosity; **ap**, articular pit; **op**, olecranon process; **raf**, radial articular facet. Scale bar equals 5 cm.

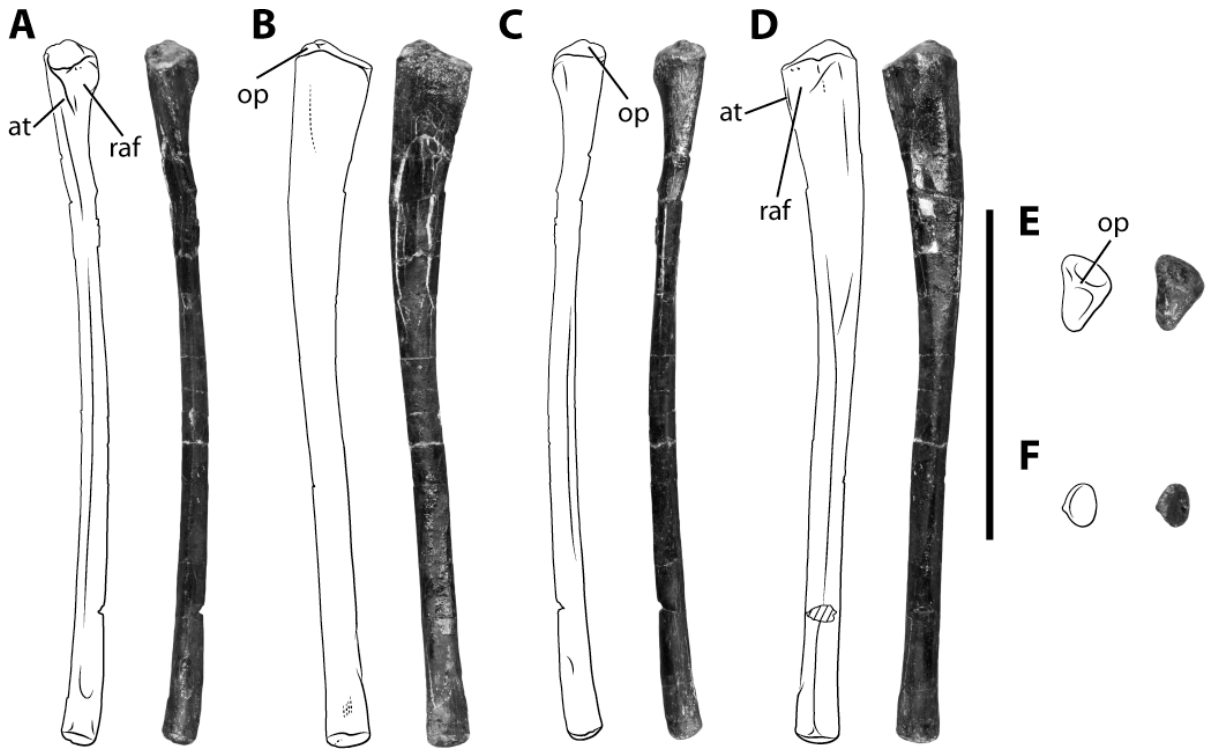
A
at
raf
B
op
C
op
D
at
raf
E
op
F

FIGURE 2.6. Left carpus and proximal metacarpals in articulation of *Tawa hallae* (GR 242). Proximal view of articulated metacarpals (**A**); reconstruction of articulated carpus in dorsal (**B**), ventral (**C**), distal (**D**), and proximal (**E**) views based on CT scans of GR 242. Carpus as preserved in situ, in dorsal view (**F**). Orientation of radius, ulna, and metacarpals indicated in dashed lines. **Abbreviations**: **cen**, centralium; **dc1–4**, distal carpals 1–4; **I–IV**, metacarpals I–IV; **int**, intermedium; **pis**, pisiform; **rad**, radius; **rae**, radiale; **ul**, ulna; **ule**, ulnare. Scale bars equal 1 cm.

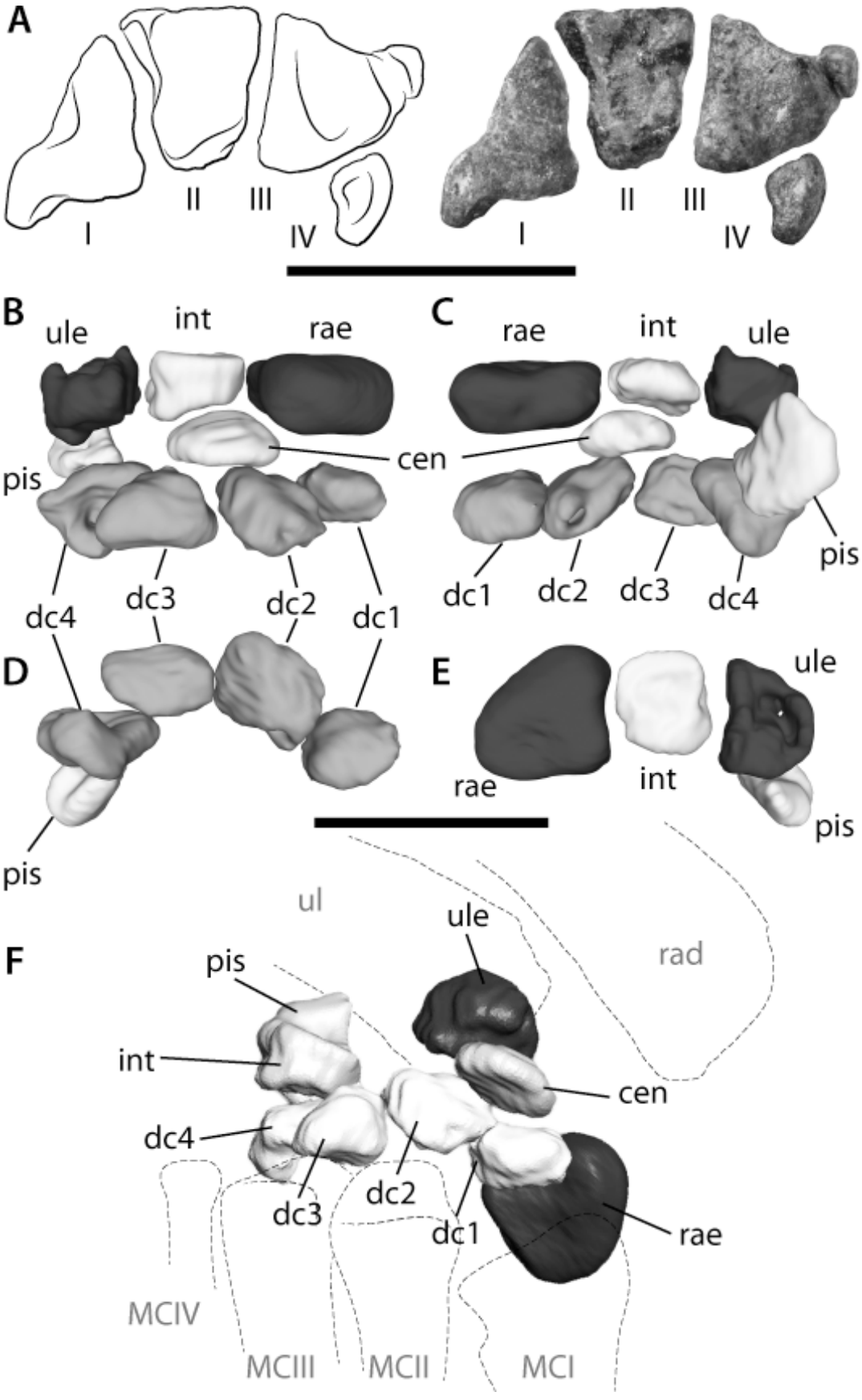
A
I
II
III
IV
I
II
III
IV
B
ule
int
rae
cen
pis
dc4
dc3
dc2
dc1
C
rae
int
ule
pis
dc1
dc2
dc3
dc4
D
pis
E
rae
int
ule
pis
F
ul
rad
ule
pis
int
cen
dc4
dc3
dc2
dc1
rae
MCIV
MCIII
MCII
MCI

FIGURE 2.7. Left manus of *Tawa hallae* (GR 242) in dorsal (**A**) and ventral (**B**) views. Cross-hatching indicates broken bone surface. **Abbreviations**: **I–IV**, digits I–IV; **mp**, medial projection. Scale bar equals 1 cm.

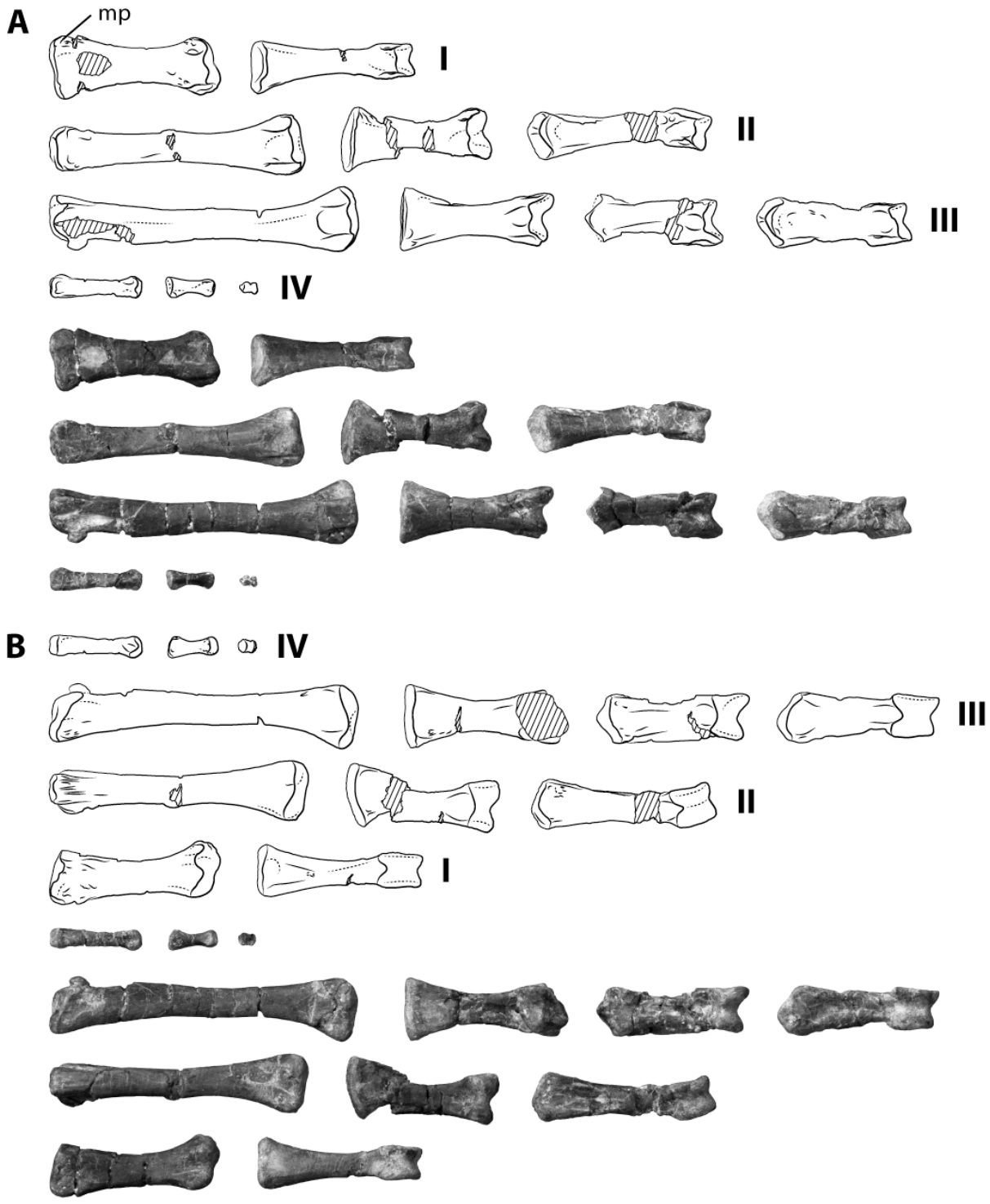
A
mp
I
II
III
IV
B
IV
III
II
I

FIGURE 2.8. Left manus of *Tawa hallae* (GR 242) in lateral (**A**) and medial (**B**) views. Cross-hatching indicates broken bone surface. **Abbreviations**: **I–IV**, digits I–IV; **laf**, lateral articular facets; **mp**, medial projection. Scale bar equals 1 cm.


A
laf
I
II
III
IV

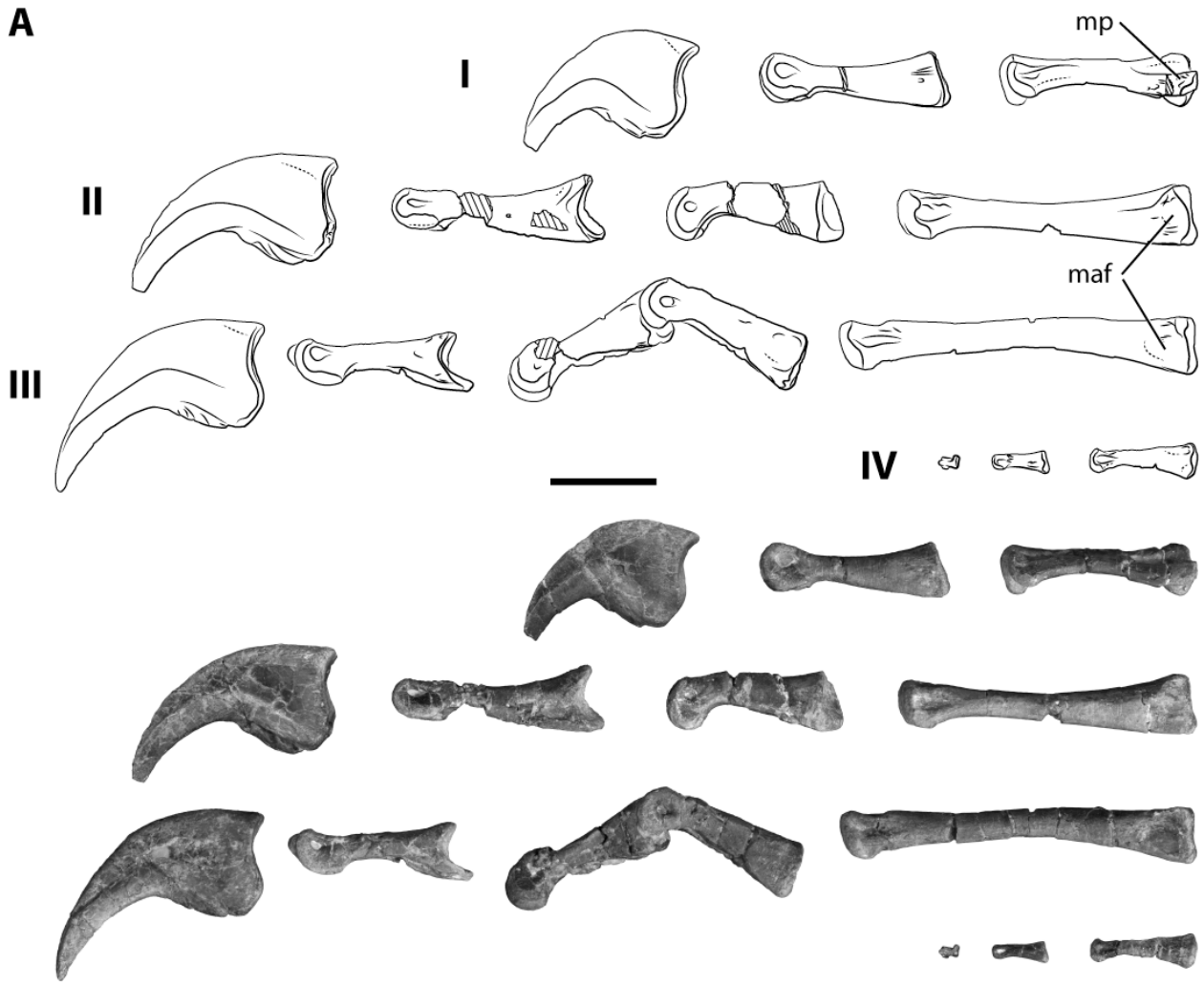
A
I
II
III
IV
mp
maf

FIGURE 2.9. Left manus of *Tawa hallae* (GR 242) in proximal and distal views. Cross-hatching indicates broken bone surface. **Abbreviations**: **1d**, distal view of first phalanx; **1p**, proximal view of first phalanx; **2d**, distal view of second phalanx; **2p**, proximal view of second phalanx; **3d**, distal view of third phalanx; **3p**, proximal view of third phalanx; **4p**, proximal view of fourth phalanx; **I–IV**, digits I–IV; **MCd**, distal view of metacarpal; **MCp**, proximal view of metacarpal. Scale bar equals 1 cm.

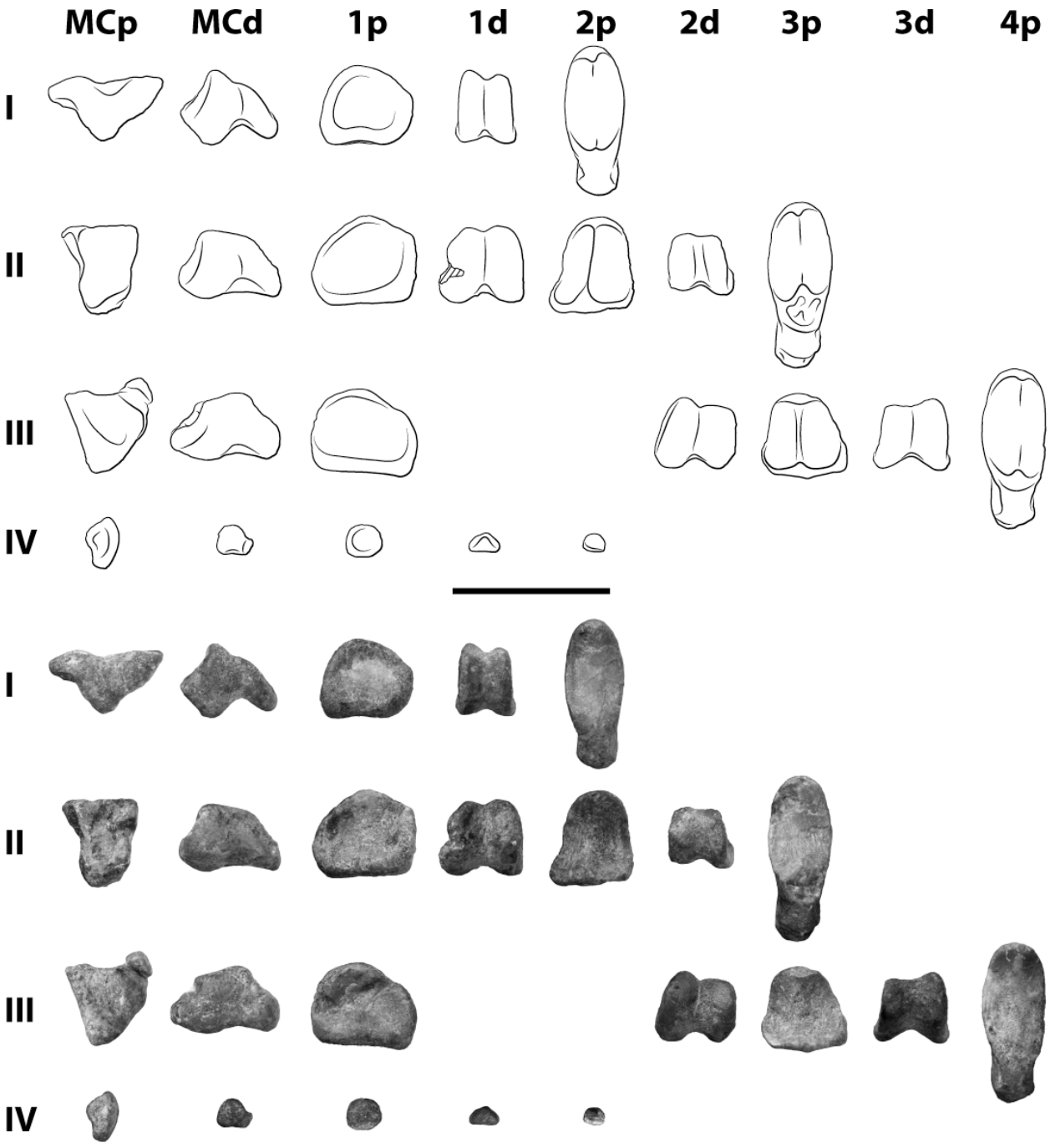
MCp
MCd
1p
1d
2p
2d
3p
3d
4p
I
II
III
IV
I
II
III
IV

Chapter III: Osteology of the pectoral girdle and forelimb of the abelisaurid theropod *Majungasaurus crenatissimus* from the Late Cretaceous of Madagascar

ABSTRACT

Abelisaurid theropods are common members of Cretaceous Gondwanan faunas and are characterized by a bizarre, highly reduced forelimb. Unfortunately, forelimb elements are rarely preserved and thus the basic structure of the abelisaurid forelimb remains poorly understood. Until recently, the Upper Cretaceous Maevarano Formation of northwestern Madagascar has produced numerous exceptional specimens of the abelisaurid theropod *Majungasaurus crenatissimus* but comparatively little forelimb material. A recently discovered articulated skeleton of *Majungasaurus* preserves a virtually complete pectoral girdle and forelimb, which, along with additional isolated forelimb elements, affords important new insights into the structure of these elements.

New specimens of the scapulocoracoid and humerus allow more detailed description of their morphology, and antebrachial and manual elements are described for the first time. The radius and ulna are approximately one-third the length of the humerus and both have expanded proximal and distal articular surfaces relative to their narrow diaphyses. The manus consists of four digits, each composed of a short metacarpal and one (digits I and IV) or two (digits II and III) phalanges. No ossified carpals are present. The proportions of the brachium and antebrachium are stout, more similar to the condition in *Carnotaurus* than in *Aucasaurus*. We reinterpret manual digit identities in *Aucasaurus* and *Carnotaurus* based on new information provided by the manus of *Majungasaurus*. Overall, the morphology of the forelimb in *Majungasaurus* reveals that abelisaurids share an extremely reduced, unique morphology that is dissimilar to the more typical theropod condition seen in other ceratosaurs.

INTRODUCTION

Abelisauridae is a clade of medium- to large-bodied Cretaceous theropod dinosaurs known almost exclusively from Gondwana. First recognized in Patagonia (Bonaparte and Novas, 1985; Bonaparte et al., 1990), numerous representatives of the group are now known from South America (e.g., Coria et al., 2002, 2006; Calvo et al., 2004), Madagascar (e.g., Sampson et al.,

1996; 1998), mainland Africa (e.g., Sereno et al., 2004; Sereno and Brusatte, 2008), and the Indian subcontinent (e.g., Wilson et al., 2003), as well as fragmentary occurrences in southern Europe (e.g., Buffetaut et al., 1988; Allain and Suberbiola, 2003). Among predatory dinosaurs they are unusual for their proportionally shortened but wide skulls and the high degree of cranial sculpturing and elaboration, such as the 'horns' of *Carnotaurus sastrei* (see Bonaparte et al., 1990).

Abelisaurids are also distinguished by a specialized forelimb morphology that is highly reduced, especially in the antebrachium and manus. Despite the improving record of abelisaurids, complete forelimbs are known only from two single-specimen taxa: *Carnotaurus sastrei* (see Bonaparte et al., 1990) and *Aucasaurus garridoi* (see Coria et al., 2002). The forelimb of the holotype of *Carnotaurus* (MACN-CH 894) preserves the humerus, radius, ulna, and several partially articulated metacarpals and phalanges (Bonaparte et al., 1990). The *Aucasaurus* holotype (MCF-PVPH-236) includes a more complete, articulated forelimb that was described only briefly (Coria et al., 2002). An isolated, fragmentary scapulocoracoid and an isolated humerus were also described for the Madagascan abelisaurid *Majungasaurus crenatissimus*, along with a second humeral shaft, but these specimens provided few additional details about the abelisaurid forelimb (Carrano, 2007). New discoveries of *Majungasaurus* now allow a more complete description and comparison of the pectoral girdle and forelimb, the primary subjects of this report.

Majungasaurus is a medium-sized abelisaurid from the Upper Cretaceous (Maastrichtian) Maevarano Formation of northwestern Madagascar. The first specimens representing this dinosaur were described by Depéret (1896a, 1896b), who designated them *Megalosaurus crenatissimus*. Lavocat (1955) later described a partial dentary containing teeth identical to those described by Depéret and assigned the species *M. crenatissimus* to the new genus *Majungasaurus*. The taxon remained poorly known until 1993, when the joint Stony Brook University-Université d'Antananarivo Mahajanga Basin Project collected abundant new and, in some cases, articulated materials from the same general area (for a review, see Krause et al., 2007). Although most of the morphology of *Majungasaurus* has now been thoroughly described (Sampson and Krause, 2007), a few anatomical structures remain poorly known.

A mostly articulated and nearly complete skeleton of *Majungasaurus* was discovered and collected in 2005 (FMNH PR 2836). The specimen includes both scapulocoracoids, a furcula, the right humerus, and the complete left forelimb with all of the preserved elements in articulation or near articulation (Fig. 1). It is remarkable in that it not only contains the first-known elements of the forearm and manus in *Majungasaurus*, but also the first complete, unambiguous furcula known among Abelisauridae. Data on the orientation and nature of the articulations between individual bones were preserved through CT scanning of the specimen and traditional molding prior to complete preparation. In addition, a right radius possibly associated with this specimen and isolated forelimb materials including an ulna, partial radius, metacarpal, phalanx, and humerus were collected during the 2005 and 2007 field seasons in close proximity from the same quarry site. In this paper, we describe these new materials, compare them with materials from related taxa, and discuss their implications for the evolution of the abelisaurid forelimb.

Institutional Abbreviations—FMNH, The Field Museum, Chicago, Illinois, USA; **MACN-CH**, Museo Argentino de Ciencias Naturales, Colección Chubut, Buenos Aires, Argentina; **MCF-PVPH**, Museo Municipal Carmen Fuñes, Paleontología de Vertebrados, Plaza Huincul, Argentina; **MNHN**, Muséum National d'Histoire Naturelle, Paris, France; **UA**, Université d'Antananarivo, Antananarivo, Madagascar.

SYSTEMATIC PALEONTOLOGY

DINOSAURIA Owen, 1842

SAURISCHIA Seeley, 1888

THEROPODA Marsh, 1881

CERATOSAURIA Marsh, 1884

ABELISAUROIDEA (Bonaparte and Novas, 1985)

ABELISAURIDAE Bonaparte and Novas, 1985

MAJUNGASAURUS Lavocat, 1955

MAJUNGASAURUS CRENATISSIMUS (Depéret, 1896) Lavocat, 1955

"Neotype"—MNHN.MAJ 1, nearly complete right dentary of subadult individual (Lavocat, 1955; Carrano et al., 2009; ICZN, 2011).

Referred Specimens—See listing in Krause et al. (2007). Additional referred specimens in this publication are: FMNH PR 2832–partial left radius; FMNH PR 2833–right metacarpal I; FMNH PR 2834–right phalanx III-1; FMNH PR 2835–right radius; FMNH PR 2836–articulated skeleton lacking the hind limbs and the right antebrachium and manus; UA 9856–right humerus; UA 9860–left ulna.

Revised Diagnosis—See Krause et al. (2007).

Age and Distribution—All specimens assigned to *Majungasaurus crenatissimus* were collected from deposits near the village of Berivotra, in the Mahajanga Basin of northwestern Madagascar. Specimens were concentrated in the Anembalemba Member, the uppermost white sandstone unit of the Maevarano Formation, which has been assigned to the Maastrichtian (Rogers et al., 2000, 2007).

Described Material—This description is based primarily on a single articulated pectoral girdle and forelimb (FMNH PR 2836) from locality MAD 05-42. Collected in 2005 as part of a mostly articulated specimen, it includes both scapulocoracoids, a furcula, a complete, articulated left forelimb, and an associated right humerus. In addition, we describe two isolated right humeri, FMNH PR 2423 (previously described by Carrano, 2007) from locality MAD 93-18 and UA 9856 from locality MAD 05-42, an isolated left ulna (UA 9860) from locality MAD 05-04, and an isolated partial left radius (FMNH PR 2832), right radius (FMNH PR 2835), right metacarpal I (FMNH PR 2833), and right phalanx III-1 (FMNH PR 2834), all from locality MAD 05-42.

Neutral Position of the Scapulocoracoid and Forelimb—We reconstructed a possible neutral position of the forelimb of *Majungasaurus* based on positional evidence from this specimen and those of *Aucasaurus* and *Carnotaurus*, as well as a digital, three-dimensional articulation of the forelimb material (Fig. 2). The precise angle of the scapulocoracoid in relation to the body wall is difficult to determine, but the well preserved and expanded acromion limits the horizontality of the scapular blade. This orientation, along with that of the humerus in articulation, is similar to those described for other large theropods. However, the distal elements

of the forelimb articulate such that the interosseous axis of the antebrachial bones extends in an anterolateral-to-posteromedial plane, and the palmar surface of the manus faces slightly anteriorly, placing the first digit anterolaterally and the fourth digit posteromedially.

Position of the Scapulocoracoid and Forelimb for Descriptive Purposes—Due to the lack of a clear neutral position for the forelimb consistent across Theropoda, the positional terminology used in descriptions of forelimb elements vary from publication to publication. Descriptions of the scapulocoracoid vary based on whether the bone is described with the long axis of the scapular blade oriented horizontally (e.g., Madsen, 1976) or vertically (e.g., Brochu, 2003); here we describe the scapulocoracoid in the neutral position described above (Fig. 2), in which the blade is oriented at an angle. The humerus and manus are least variable, and so we describe these elements in the most common manner: the humerus oriented in a vertical position with the broad surfaces oriented anteriorly and posteriorly such that the internal tuberosity is directed medially and the greater tubercle is positioned directly laterally (e.g., Madsen, 1976; Bonaparte et al., 1990; Carrano et al., 2011); and the manus oriented in a horizontal position with digit I medial-most (e.g., Madsen, 1976; Sereno, 1993; Brochu, 2003). The antebrachial elements pose more of a problem due to their highly unusual morphology. In this case, we describe these elements as articulated with the humerus in a vertical position. In this orientation the radial articular surface on the ulna faces laterally and slightly anteriorly, which makes its orientation approximately equivalent to the orientation of the ulna often used in theropod antebrachial descriptions where the olecranon is directed posteriorly and the radial articular surface is positioned either anteriorly or laterally (e.g., Madsen, 1976; Sereno, 1993). This is also essentially equivalent to the orientation of the antebrachium of *Carnotaurus* as described by Bonaparte et al. (1990).

DESCRIPTION

Scapulocoracoid

The scapulocoracoid was previously only known from an incomplete left element (FMNH PR 2278; Carrano, 2007), but both scapulocoracoids of FMNH PR 2836 are complete

and well preserved (Fig. 3), allowing further description. The scapulocoracoid of *Majungasaurus* is expansive anteroventrally, a seemingly incongruous size disparity given the highly reduced condition of its forelimbs. The scapular blade is long and broad anteroposteriorly (Table 1), with parallel margins throughout most of its length. Although it widens slightly just at the distal end, the blade lacks the pronounced expansion seen in coelophysoids and other basal theropods. The cross-section is mediolaterally compressed with parallel surfaces at the distal end but becomes teardrop-shaped near the glenoid fossa, being thickest posteroventrally and thinning to a sharp edge anterodorsally. At the level of the glenoid fossa the dorsal margin of the scapula expands gradually to a well-developed acromion. The acromion has a large, ovoid, anterolaterally facing articular facet for the furcula and is separated from the coracoid by a well-developed notch. On the lateral surface, a narrow groove extends 3 cm ventrally from the notch, further emphasizing the acromion. Immediately posterodorsal to the glenoid fossa, a deep fossa on the posteroventral edge of the blade emphasizes the dorsal lip of the glenoid. Just posterodorsal to this fossa, an elongate tubercle for the origin of M. triceps brachii caput scapulare (Jasinoski et al., 2006) extends 2.5 cm along the posteroventral edge of the scapular blade. The glenoid fossa is large and is oriented slightly laterally, with prominent lips dorsally, ventrally, and medially; laterally there is no substantial lip separating the edge of the glenoid from the lateral surfaces of the scapula and coracoid. A small, teardrop-shaped fossa, its apex pointing posteriorly, interrupts the lateral margin of the glenoid.

The coracoid is large and fused to the scapula, with a rounded anteromedial margin and a prominent posteroventral process. The posteroventral edge of this process is gently curved, and the tip is well rounded but acute. As in FMNH PR 2278 (Carrano, 2007), the scapulocoracoid suture is visible on the lateral surface as it extends anteriorly from the glenoid, and there is a rugosity located on the coracoid just anterior to the suture. Anteroventral to this rugosity, the large coracoid foramen passes obliquely through the bone. The lateral surface of the left coracoid possesses a large, narrow, and subrectangular rugosity (absent on the right side and on FMNH PR 2278) that extends 5 cm along its anteromedial border, 8 cm from the tip of the posteroventral process. Another rugosity, located just ventral to the glenoid and described in FMNH PR 2278 as a “small, faint tubercle” (Carrano, 2007: 165–166), is better defined in both

coracoids of FMNH PR 2836. We identify it as the biceps tubercle, the site of origin for M. biceps brachii (Jasinoski et al., 2006). It is subtriangular with its apex pointing along a prominent subglenoid ridge, which arises from the edge of the coracoid 2 cm from the tip of the posteroventral process. Posterior to the subglenoid ridge is the subglenoid fossa, the origination site for M. coracobracialis brevis (Jasinoski et al., 2006), which is triangular and follows the curvature of the posteroventral process.

The medial surface of the scapulocoracoid is smooth with the exception of the area around the line of fusion between the two elements, which is covered in rugose striations that are oriented perpendicular to the scapulocoracoid suture. These striations are longest near the glenoid and gradually shorten along the line of fusion, covering a triangular area overall. A faint groove, 2 cm from the dorsal edge, extends along the medial surface for 6–8 cm on the middle of the scapular blade, fading out at its dorsal and ventral extents.

Furcula

The furcula of FMNH PR 2836 (Fig. 4) was found slightly out of articulation, lying on the medial surface of the anterior margin on the scapulocoracoid, just below the level of the acromial process. It has a wide V shape, with an interclavicular angle of 140º (measured along the rami from the tips of the epicleideal processes to the symphysis). The apex of the teardrop-shaped cross-section faces ventrally at the symphysis and becomes more triangular at mid-ramus. The symphysis is thicker dorsoventrally than anteroposteriorly (Table 1). The epicleideal processes taper as they extend laterally to rounded points, and each possesses a flattened, rugose surface facing posterodorsally for articulation with the acromion. The articular surfaces are covered in striations that extend mediolaterally along the rami, and the anterior and posterior edges of the surfaces create two highly rugose ridges that extend medially 2.9 cm and 4.0 cm, respectively. The anterior surface of the furcula is smooth, with only faint striations laterally on the epicleideal processes.

Humerus

The humerus of *Majungasaurus* is represented by four specimens: two isolated humeri,

FMNH PR 2423 and UA 9856, and the two humeri of FMNH PR 2836, the left in articulation with its pectoral girdle and forearm, and the right associated with its scapulocoracoid (Fig. 5). The humerus is approximately half the length of the scapular blade and a third the total length of the scapulocoracoid (Fig. 2; Table 1). The humeral shaft is curved in the mediolateral plane, so that it is convex laterally, but relatively straight in the anteroposterior plane. The cross-section of the shaft is elliptical, being compressed anteroposteriorly along its entire length. Viewed from the medial aspect, the distal end flares anteroposteriorly, matching the width of the shaft just distal to the humeral head. At this point the shaft flares abruptly anteroposteriorly as it approaches the articular surface, which is wider than the shaft in this dimension. Posteriorly, the edge of the proximal articular surface curves gently into the shaft, whereas anteriorly the shaft immediately distal to the margin of the humeral head is concave and forms a large depression. The internal tuberosity is well developed and subtriangular proximally, the apex forming a medially hooked lip. The proximal surface of the internal tuberosity is composed of two subtriangular facets, one facing anteromedially and another posteromedially, which meet at the midline of the tuberosity. The anterior edge of the proximal surface displays a weakly developed sinusoidal lip. Just lateral to this, a short but distinct ridge extends proximally to join the articular surface of the humeral head, bounding a shallow depression between it and the lip of the internal tuberosity.

The deltopectoral crest is low but robust and long, extending approximately halfway down the shaft. The muscle scars along the crest are highly rugose and broaden distally. The crest curves around the shaft and ends bluntly in a rounded tubercle on the anterolateral surface. The greater tubercle is highly reduced and located at the proximolateral end of the deltopectoral crest, slightly distal to the level of the internal tuberosity. A shallow groove at the proximal end of the crest extends along its posterior margin from the humeral head to the greater tubercle. A large nutrient foramen is present on the medial surface of the shaft, located near its midpoint. The posterior surface of the humeral shaft bears a tuberosity that varies in size and morphology among the specimens (see below).

The distal articular surface is almost flat and subrectangular, with the radial and ulnar condyles separated only by a shallow, anteroposteriorly oriented groove (Carrano, 2007:fig. 3F). The radial condyle, located in the lateral half of the articular surface, slopes proximally at a 45º

angle relative to the ulnar condyle, which maintains a level surface. On the anterior surface, the shallow, triangular intercondylar depression is defined by two ridges: a faint oblique radial ridge that arises from the posterolateral corner of the radial condyle atop the small ectepicondyle and wraps proximomedially around the humeral shaft, and the more robust medial ridge, which extends proximally and slightly anteriorly from the large entepicondyle. On the posterior face, the shaft is convex distally, with a faint groove present just proximal to the margin of the articular surface.

Substantial variation is evident among the collected humeri. Those of FMNH PR 2836 are proportionally more robust than FMNH PR 2423 (Carrano, 2007), and have a cross-section that is more anteroposteriorly compressed distally (Table 1). UA 9856 represents the largest individual, but its overall proportions are similar to those of the smaller specimens. It is 3 cm longer than either FMNH PR 2836 or FMNH PR 2423, and its midshaft cross-section is more similar to that of FMNH PR 2423 than the more anteroposteriorly compressed FMNH PR 2836. Viewed from medial aspect, the distal end of FMNH PR 2423 flares substantially anteroposteriorly and actually slightly exceeds the width of the humeral head, unlike the narrower distal end in the right humerus of FMNH PR 2836. The distal end of the left humerus of FMNH PR 2836 is very wide but it also exhibits pathological scarring and bone formation on the posterior side of the distal shaft, just above the articular surface. UA 9856 exhibits more postmortem damage than the other specimens, making the articular surfaces somewhat indistinct, so their relative widths cannot be compared.

The humeral head is smaller in FMNH PR 2423 and, when viewed anteriorly, the distal margin is inclined at approximately 60º to the adjacent shaft. The depression on the anterior side of the humerus just distal to the articular surface is well developed in all specimens except UA 9856, where in spite of incomplete preservation it is clearly not as fully developed. The internal tuberosity is not as well preserved in FMNH PR 2423, but the proximal surface appears flatter with less anterior and posterior excursions. The sinusoidal lip on the anterior edge of the proximal surface is not seen in the right humerus of FMNH PR 2836, which possesses a straight margin. The ridge extending distally along the medial side of the shaft from the apex of the internal tuberosity is more prominent than in FMNH PR 2836 and, 4.0 cm distal to the

tuberosity, a shallow groove extends proximally along the anterior side of the ridge. Posteriorly, the edge of the articular surface of the humeral head of FMNH PR 2423 curves more gently into the shaft than in FMNH PR 2836.

The deltopectoral crest and greater tubercle exhibit very similar morphologies among the available humeri. The tuberosity on the posterior surface of the deltopectoral crest is robust in FMNH PR 2423, displaying a wide 'V' morphology similar to that on UA 9856 and the right humerus of FMNH PR 2836. In FMNH PR 2423, the two arms of the 'V' are more distinct and shaped slightly differently; the distal arm is subtriangular with the apex pointing distally, and the proximal arm is amygdaloid. On the left humerus of FMNH PR 2836, the posterior tuberosity is rugose with indistinct boundaries, extending from just below the greater tubercle to near the end of the deltopectoral crest. The right humerus of FMNH PR 2836 also possesses a slightly raised ovoid area on the posterolateral surface of the shaft just below the level of the deltopectoral crest that is not present on any of the other humeri. Also, unlike the condition in the other available specimens, no nutrient foramen is present on the shaft of FMNH PR 2423.

Radius

The radius of *Majungasaurus* is represented in the articulated forelimb specimen (FMNH PR 2836; Fig. 6), by a mostly complete right radius (FMNH PR 2835), and by an isolated, partial left radius (FMNH PR 2832). The radius is only one-quarter the length of the humerus (Table 1). The radius possesses flared proximal and distal ends and prominent 'waisting' of the shaft, with a narrow midshaft diameter relative to the articular surfaces. The surface of the shaft is deeply curved medially, with the distal articular surface forming a small lip, but it is only shallowly curved laterally; the anterior and posterior sides have similarly deep curvatures. The proximal articular surface is ovoid and slopes lateral-to-medial at about 30º to the horizontal in posterior view. The lateral surface of the shaft is covered by a large, low, triangular rugosity (lateral triangular rugosity) with its apex pointing distally, extending the entire length of the shaft. Just posterior to this is another, slightly smaller triangular rugosity pointing proximally (posterolateral triangular rugosity). This rugosity creates a distinct ridge on the posterior aspect of the bone, extending from the posteriormost point of the distal articular surface to midshaft.

The triangular point of this rugosity is separated from the lateral, distally pointing rugosity by a space filled with faint striations that extend anteroproximally to posterodistally between the two rugosities. Also present in this area is a small, semicircular rugosity (lateral semicircular rugosity) that seems to extend out of the edge of the distal articular surface slightly anterior to the apex of the distally pointing rugosity. The proximal edges of this rugosity project very slightly laterally away from the shaft of the radius, forming a small depression just medial to its lip. It extends proximally almost to the tip of the distally pointing rugosity, but they are separated by a few millimeters. The medial surface of the shaft narrows to form a longitudinal ridge, the anterior surface of which possesses a large rugosity that is the attachment line for interosseous ligaments between the radius and ulna. The distal articular surface is not completely preserved on any of the specimens, obscuring its shape and the full extent of its margins. A medially directed surface just distal to the medial ridge forms an articular facet for the ulna and appears to extend smoothly into the articular surface. At its most posterior point, the distal articular surface is rounded when viewed posteriorly. A distinct notch is present in the edge of the distal articular surface; the wide, rounded notch is just anterior to the articular facet for the ulna, separating it from the anterior portion of the distal articular surface. A large rugosity, not seen in the articulated specimen, sits proximal to, or perhaps forms the edge of, the anterior portion of the articular surface and wraps around the notch medially, creating a hook-shaped process. The relationship of this process to the articular surface is not known because of incomplete preservation.

The right radius (FMNH PR 2835) is mostly complete, and very similar to FMNH PR 2836, although the medial surface is poorly preserved. The lateral surface is for the most part undamaged, clearly preserving the two main rugosities and the smaller rugosity that cover the majority of this surface. The shape and development of these rugosities is very similar between FMNH PR 2835 and FMNH PR 2836. Only the medial surface of the isolated left radius (FMNH PR 2832) is preserved, but it displays some differences. Though present as a ridge on the articulated specimen, the medial tubercle for the attachment of the interosseous ligament on this radius is composed of several prominent spikes that may be the result of ossification of fibers within the membrane. A small, low (5 mm) rugosity is present 1 cm anterior to the medial

tuberosity, just distal to the lip of the proximal articular surface.

Ulna

The ulna of *Majungasaurus*, represented in the articulated forelimb specimen (FMNH PR 2836) and by an isolated element (UA 9860; Fig. 7), is short, robust, and mushroom-shaped (Table 1). Both specimens exhibit a wide proximal end that narrows distally before flaring into a cap-like distal articular surface. The proximal articular surface is dished (shallowly concave) and roughly semicircular with the flat base located laterally. At the posteromedial edge of the semicircle the articular surface projects slightly proximally, raising it above the rest of the edges of the surface. Extending approximately 1 cm from the anterolateral corner of the proximal articular surface is a small, wide, ridge-like tuberosity. The posterolateral corner also possesses a ridge extending distally, which connects to a large, highly rugose tuberosity in the middle of the lateral ulnar shaft for the attachment of the interosseous membrane. The 'cap' of the distal articular surface is similar in outline to the proximal articular surface, but it is much more convex. When viewed medially, the posterior edge of the cap is located more proximally than the anterior edge, and both edges continue distally to form a 'V' on the medial surface. On the posterolateral corner at the level of the large lateral interosseous tuberosity and its excursion proximally, the articular surface comes to a prominent point when viewed distally. Additionally, immediately distal to the lateral interosseous tuberosity, the distal articular surface has a proximal excursion that forms an articular facet for the radius, leaving only a narrow channel between its edge and the end of the tuberosity. Also present is a large, round pit located at anterior edge of the distal articular surface.

Although the two available ulnae are similar overall, they differ in a few regards. FMNH PR 2836 possesses a distinct ridge on the anterior side extending nearly the length of the shaft that is lacking in UA 9860. Another, fainter ridge, also lacking in UA 9860, is present on the medial aspect of the shaft, extending at approximately 30º to the larger ridge and meeting it at the shaft midpoint. Whereas most of the original distal articular surface of UA 9860 is not preserved, a portion at the posteromedial corner of the distal articular surface shows a faint groove extending mediolaterally at the edge.

Manus

As preserved, the manus of FMNH PR 2836 (Fig. 1) was partly disarticulated but still provides important information on digit identities and positions. Metacarpals I and II were only slightly dislodged from their positions distal to the radius, whereas metacarpals III and IV had slipped proximally and were preserved near the ulnar side of the elbow. The phalanges of digits I, II, and IV remained articulated with their metacarpals, but those of digit III were found adjacent to digit II, between the distal ends of the radius and ulna. There are no ossified carpals preserved, nor any evidence of additional digits. We interpret the manus as consisting of four digits, each composed of a short metacarpal and minimally one (digits I and IV) or two (digits II and III) phalanges (Fig. 8).

Metacarpal I is short, with a base as wide mediolaterally as it is long (Table 1). It appears subtrapezoidal when viewed dorsally, narrowing distally, and the dorsal surface is shallowly concave. The overall shape of the proximal surface is distorted due to postmortem damage, but it appears flat and slopes slightly ventrodistally. The edge of the proximal articular surface forms a ventral overhang. The distal articular surface sweeps proximally at its ventromedial edge, forming a prominent diagonal lip. A small ridge descends the ventral surface of the shaft to join this lip at its midpoint; two small foramina are located on the shaft at the proximal end of the ridge, and proximal to these foramina is a small rugosity. An isolated right metacarpal I (FMNH PR 2833), collected from the same quarry in 2007, is similar in size but very well preserved excepting a broken lateral edge on the proximal articular surface. The proximal articular surface is subcircular and flat, though it continues onto the ventral surface of the metacarpal for 3 mm. At its edge, it forms two ‘corners’ medially and laterally, creating a medial overhang where the surface of the shaft is deeply concave. The distal articular surface is well rounded and preserves the same sweeping diagonal lip, ridge, and foramina ventrally, as seen in FMNH PR 2836. The lateral edge of the shaft is thin and bears little evidence of a discrete articular surface for metacarpal II (Fig. 9).

The single phalanx of digit I of FMNH PR 2836 resembles a small tetrahedron, although the dorsal surface is damaged. It is not clear from this single preserved element whether the

distal end bears an articular surface or was the terminus of this digit.

Metacarpal II has the most recognizable shape of all the manual elements. It is the longest metacarpal and has a wide, flaring proximal end (Table 1). The proximal articular surface is subrectangular and concave. At its ventrolateral and ventromedial corners, two rounded tubercles extend onto the shaft. The shaft narrows abruptly distally until it meets the distal articular surface, which is well rounded with a faint depression between the two condyles. The lateral condyle is slightly larger, and the medial condyle possesses a very shallow fossa on its medial surface. The medial and lateral edges of the metacarpal are intact and appear to have had large contacts with metacarpals I and III, respectively (Fig. 9).

The first phalanx of digit II has a subrectangular, slightly concave proximal articular surface. Overall, the bone is angled mediolaterally, which is accentuated by a strong lip and tubercle at the ventrolateral edge of the distal articular surface. A shallow groove extends diagonally along the entire length of the medial surface of the shaft from the ventral corner at the proximal articular surface to the dorsal corner of the distal articular surface. The second phalanx is incomplete posteriorly, but it appears subconical. Its ventral surface is flat and a deep groove is present just dorsolateral to the tip of the phalanx.

Metacarpal III suffered some postmortem damage, and the phalanges of digit III are very unusual in their morphology. The metacarpal has a similar shape to that of metacarpal II, though it is not as symmetrical and the rounded distal condyles are not fully preserved. The proximal articular surface is subcircular and concave, with a more extensive ventral projection than is seen in metacarpal II. The lateral surface is not concave like the medial surface, but instead possesses a rugose ridge extending along its length.

It is unclear whether digit III has one or two phalanges, and whether their unusual morphology is the result of pathology. The first phalanx is represented in the articulated hand (FMNH PR 2836) and by an isolated right phalanx (FMNH PR 2834; Fig. 10) collected in 2005 from the same quarry. It is short with a wide base and a slight waist (Table 1). The proximal articular surface is angled downward dorsally, slightly concave, and subcircular; the subrectangular, proximal end of FMNH PR 2836 may be the result of damage at its dorsal and ventral margins. The phalanx bears a slight curvature on its medial and lateral sides, and the

distal articular surface is flat and angled downward dorsally. A medial process is present at the distal ends, although developed to different extents in the two specimens. It is small and triangular in FMNH PR 2834, extending no farther distally than the end of the phalanx itself. This medial process is larger and flatter in FMNH PR 2836, extending laterally around the distal end of the first phalanx. In doing so, it appears to incorporate the proximal end of a second phalanx. The presence of a second phalanx is uncertain, and the distal end of FMNH PR 2834 does not provide definitive evidence of its existence. A small tubercle, present in both specimens, is located directly opposite the process on the distal lateral shaft. A large bony spicule is fused to the medial edge of the proximal articular surface in FMNH PR 2836 and points distally along the medial shaft of the bone. No evidence of this structure appears in FMNH PR 2834, and whether it is related to the increased development of the distomedial process in FMNH PR 2836 is unknown.

Metacarpal IV is rhomboidal when viewed dorsally, and the proximal articular surface is subtriangular, with the apex pointing ventrally (Table 1). Postmortem damage on the proximal surface makes it unclear if the articular surface was concave or flat. Ventrally, the distal articular surface extends proximally midway up the shaft of the bone in a prominent ridge.

The first phalanx of digit IV is fused to the metacarpal at the medial edge of the digit, which may also be the result of a pathology. The distal end of the phalanx of digit IV was broken postmortem, but the preserved portion is subtriangular. The base is as wide as the proximal end of metacarpal IV. It cannot be determined whether this phalanx was terminal or bore an additional element (or elements) distally.

Thus, *Majungasaurus* possessed a minimum phalangeal formula of 1/2/1–2?/1, but we cannot exclude the possibility of additional phalanges on several of the digits.

DISCUSSION

Comparative Anatomy

Scapulocoracoid—The scapulocoracoid of *Majungasaurus* bears numerous general similarities to those of other ceratosaurs, such as *Limusaurus*, *Ceratosaurus*, *Elaphrosaurus*,

Masiakasaurus, *Carnotaurus*, *Rahiolisaurus*, and *Aucasaurus*. As in these forms, the scapular blade is proportionally narrower than in coelophysoids but broader than in tetanurans, and the coracoid is expansive ventrally and bears a large posteroventral process.

The scapulocoracoid of *Majungasaurus* bears the greatest resemblance to those of other abelisaurids. This element is incomplete in *Rahiolisaurus* (Novas et al., 2010) and has not been described for *Aucasaurus* (and was not yet fully prepared during a visit by MTC in August, 2002), so detailed comparisons will only be made with that of *Carnotaurus*. This should not be taken to indicate particular similarity between these forms among abelisaurids, because we cannot specify the phylogenetic level of relevance for many of these features.

Both *Majungasaurus* and *Carnotaurus* (Bonaparte et al., 1990:fig. 27A, B) possess an enlarged tubercle on the ventral edge of the scapula just posterodorsal to the dorsal glenoid labrum for the attachment of M. triceps brachii, a feature absent in other ceratosaurs. The labrum appears strongly offset because the posterior margin of the scapular blade curves inward just before it reaches the glenoid. The posteroventral process of *Majungasaurus* curves gently away from the ventral lip of the glenoid cavity and the dorsal edge of the process is inclined at an angle of approximately 130º from the posteroventral edge of the scapula, whereas this process is more sharply inclined at a 90º angle to the scapular edge in *Carnotaurus* (Bonaparte et al., 1990:fig. 27A, B). The wider angle and more gentle curvature is closer to the condition seen in *Masiakasaurus* (Carrano et al., 2011:fig. 18A) as well as in other theropods such as *Ceratosaurus* (Madsen and Welles, 2000:pl. 20) and *Allosaurus* (Madsen, 1976:fig. 23A, C). The ventral placement of the biceps tubercle, resulting in a small subglenoid fossa, is similar to the condition in *Ceratosaurus* (Madsen and Welles, 2000:pl. 20) and *Masiakasaurus*, whereas in *Carnotaurus* the tubercle is located slightly more dorsally (MTC, pers. obs.), closer to its position in *Tyrannosaurus* (Brochu, 2003:fig. 80) and *Allosaurus*. The anterodorsal border of the scapulocoracoid of *Majungasaurus* retains a distinct notch between the acromion of the scapula and the blade of the coracoid that is seen to some extent in many theropod dinosaurs (e.g., *Allosaurus* [Madsen, 1976:fig. 23A, C]); *Carnotaurus* and *Ceratosaurus* lack this notch, leaving little differentiation between the scapula and coracoid along the anterodorsal border. However, this may vary with ontogeny, as it tends to be present in smaller and (presumably) younger

individuals. The enlarged acromial facet of *Majungasaurus* cannot be observed in *Carnotaurus*, but this region is not well preserved in MACN-CH 894 (MTC, pers. obs.). *Carnotaurus* also appears to be unusual in genuinely lacking any distal expansion of the scapular blade (Bonaparte et al., 1990:fig. 27A, B), a feature weakly present in both *Ceratosaurus* and *Majungasaurus*.

Furcula—The articulated *Majungasaurus* specimen preserves the first complete, unambiguously identified furcula known from Abelisauridae. Bonaparte et al. (1990) identified a small, curved bone associated with the pectoral girdle of *Carnotaurus* as the right clavicle, noting that it may be incomplete. As presently preserved, this element is too fragmentary to identify with certainty because it lacks both ends; it could be part of a gastral segment or a section of a furcula. Given the fully fused furculae of *Majungasaurus* and coelophysoids (Downs, 2000; Tykoski et al., 2002), we consider it unlikely that *Carnotaurus* had unfused clavicles.

The furcula of *Majungasaurus* resembles that of the early tetanurans *Allosaurus* (Chure and Madsen, 1996:fig. 3) and *Suchomimus* (Lipkin et al., 2007:fig. 1) in that it is V-shaped with a wide (140º) interclavicular angle and tapering, rounded epicleideal processes. The cross-section is less circular than in other basal theropods (Nesbitt et al., 2009).

Humerus—The humerus of *Majungasaurus* exhibits several ceratosaur, abelisauroid, and abelisaurid synapomorphies; most of these were reviewed by Carrano (2007). New materials of other ceratosaurs (e.g., *Limusaurus*, *Masiakasaurus*) highlight that the unusually short proportions of the humerus are a characteristic of Abelisauridae within this larger clade.

As noted by Carrano (2007), the humerus of *Majungasaurus* is very similar to those of *Carnotaurus* and *Aucasaurus* in general morphology, being slightly closer to *Aucasaurus* in overall proportions; this remains true even in the largest and most robust specimen (UA 9856). The humerus is slightly more than one-third the maximum length of the scapulocoracoid, making it proportionally slightly longer than the humerus of *Carnotaurus.* The humerus of *Majungasaurus* is not as highly compressed anteroposteriorly as in *Aucasaurus* (MTC, pers. obs.), nor does it possess the distinct lateral ridge at midshaft just below the level of the deltopectoral crest (Coria et al., 2002:fig. 3A), although one humerus (FMNH PR 2836, right humerus) does have a slightly enlarged lump in this location. Posteriorly, the edge of the articular

surface of the humeral head lacks the downturned lip and the associated fossa just distal to it that occurs in *Carnotaurus* (Bonaparte et al., 1990:fig. 28A), instead gently curving into the shaft. Neither *Carnotaurus* nor *Aucasaurus* exhibits the hooked lip seen on the internal tuberosity of FMNH PR 2836; the former two taxa instead share a larger, more globular process (Bonaparte et al., 1990; Coria et al., 2002). The distal articular surface does not flare as widely mediolaterally in *Majungasaurus* as in *Carnotaurus*, instead remaining relatively narrow when viewed anteroposteriorly, as in *Aucasaurus* (Coria et al., 2002:fig. 3A). Finally, *Majungasaurus* and *Aucasaurus* also share a more marked intercondylar depression on the anterior surface of the shaft just proximal to the distal articular surface. This is much weaker in *Carnotaurus*, which lacks the larger entepicondyle and associated ridge seen in *Majungasaurus*. *Carnotaurus* also seems to have a less angled distal end in anteroposterior view, due to the more equable sizes of the condyles (Bonaparte et al., 1990:fig. 28B).

Forearm—The antebrachium in abelisaurids has a distinct, highly derived, and reduced morphology that is demonstrated once again in *Majungasaurus*. This distinguishes the clade from other ceratosaurs (e.g. *Ceratosaurus*, *Limusaurus*), where the forearm tends to be of typical or slightly shortened length but retains an overall morphology similar to that in other basal theropods.

The stout radius and ulna of *Majungasaurus* closely resemble those of *Carnotaurus* and *Aucasaurus*. The preserved forearm of *Majungasaurus* allows us to re-identify the elements previously identified as the radius and ulna of *Aucasaurus* by Coria et al. (2002:fig. 3A) as the ulna and radius, respectively. Relative to the humerus, the radius and ulna of *Majungasaurus* are the same size as those of *Carnotaurus* (Bonaparte et al., 1990); both are proportionally shorter than in *Aucasaurus* (Coria et al., 2002). On the radius, the proximal articulation for the ulna is intermediate in size in *Majungasaurus*, not large and hooked as in *Carnotaurus*, nor flat as in *Aucasaurus* (Coria et al., 2002:fig. 3). However, when viewed posteriorly, the profile of the medial surface of the radius is C-shaped, closer in shape to that of *Carnotaurus*, due in part to the lengthening of the shaft of the radius in *Aucasaurus*. The lateral osseous process on the radii of *Carnotaurus* (Bonaparte et al., 1990:fig. 29A) and *Aucasaurus* (Coria et al., 2002:fig. 3A, visible on the lateral surface of the element labeled 'ulna') is present only as a low triangular rugosity in

Majungasaurus, and is likely the attachment point of M. supinator. This lateral process, described by Coria et al. (2002) as belonging to the radius but figured (Coria et al., 2002:fig. 3A) on the element labeled 'ulna', as well as the overall shape of the elements and their relationship to the humerus as preserved in *Carnotaurus* (Bonaparte et al., 1990:fig. 30) and *Majungasaurus*, indicates that the labels for the radius and ulna of *Aucasaurus* in figure 3A of Coria et al. (2002) are reversed and the radius and ulna of *Carnotaurus* as illustrated in figure 3B are shown from anterior, not posterior ('caudal' of Coria et al., 2002) view (Bonaparte et al., 1990:fig. 29A, C).

Carpus—There are no ossified carpals preserved in the articulated forelimb of *Majungasaurus*, nor have any putative isolated carpals been discovered. An ossified carpus is absent in all other ceratosaurs in which an articulated forelimb is known, including *Limusaurus* (Xu et al., 2009), *Ceratosaurus* (Gilmore, 1920) and *Aucasaurus* (Coria et al., 2002). *Carnotaurus* was described as possessing "a group of carpal bones, of unknown number, below the ulna" (Bonaparte et al., 1990:25). The manus of the holotype (MACN-CH 894) was found in a jumbled state but articulated against the distal ends of the forearm bones. The positions of individual elements (see below) do not appear to retain much original information and, given the nature of definitively identified abelisaurid manual elements, it is likely that these "carpals" represent metacarpals and/or phalanges (Coria et al., 2002). However, the holotype of *Carnotaurus* is a much larger (and presumably ontogenetically older) individual than any of the other ceratosaur specimens with articulated arm skeletons, and so it remains possible that the carpus of ceratosaurs ossified only very late in ontogeny. We note also that the holotype of *Ceratosaurus nasicornis* retains a distinct space between the articulated manus and forearm, suggesting the presence of cartilaginous carpals in this individual (Gilmore, 1920). This differs from the condition in abelisaurids, where articulated manual elements tend to be preserved very close to the distal ends of the radius and ulna.

Manus—All ceratosaurs with well-preserved forelimbs possess four metacarpals, including *Majungasaurus*. Metacarpals II and III are the longest and most similar morphologically, as in *Ceratosaurus* (Gilmore, 1920) and *Limusaurus* (Xu et al., 2009), although the relative size differences between these and the central and outer metacarpals are not as extreme as in *Limusaurus*. (There remains some ambiguity regarding the true size and shape of

metacarpal I in the holotype of *Ceratosaurus*.) Two abelisaurid manus are known from each of the holotype specimens of *Carnotaurus* and *Aucausaurus*. Because we present several reidentifications from the original published descriptions, they are discussed separately below prior to comparison.

The manus of *Aucasaurus* was briefly described (Coria et al., 2002:fig. 3A) but our interpretation of the materials differs somewhat from this description. Due to misidentification of the radius and ulna in figure 3A (Coria et al., 2002; see above), the originally interpreted digital numbering is reversed mediolaterally such that the metacarpal previously interpreted as metacarpal I is actually metacarpal IV, metacarpal II is actually metacarpal III, etc. Both metacarpals I and IV were described as conical, and the phalangeal formula was given as 0/1/2/0. However, there is a distinct phalanx articulated with metacarpal I and, more uncertainly, possibly a rudimentary one fused to the distal end of metacarpal IV. In addition, phalanges II-2 and III-1 have typically rounded distal ends, suggesting that they, too, may have articulated with additional phalanges. We suggest a revised minimum phalangeal formula of 1/2+/1+/1?. This would be consistent with the observed formula in *Majungasaurus*.

In *Carnotaurus*, as noted above, the two manus were articulated with the forearms, but the individual manus bones did not retain their original contacts. As a result, there have been different interpretations of the identities and articulations of the elements (Bonaparte et al., 1990; Ruiz and Novas, 2009). Given the preservation of the manus in this specimen, the present positions of the elements provide only approximate information regarding their identities. The general similarities between abelisaurid metacarpals and phalanges add further difficulty to the sorting process, but the materials of *Aucasaurus* and *Majungasaurus* are helpful.

In each manus of *Carnotaurus*, there is a blocky element lying adjacent to the distolateral corner of the radius. Its proximal end is wider than the distal, which bears two indistinct condyles. It matches well with metacarpal I of *Majungasaurus*. In the left manus it appears to articulate with a fragmentary phalanx, also similar to *Majungasaurus* and *Aucasaurus*. Metacarpal II is the largest in both manus, lies beneath or near the distomedial corner of the radius, and is medially adjacent to the first metacarpal. As in *Majungasaurus*, the proximal end has a squared profile in dorsoventral view, although in *Carnotaurus* it bears distinct collateral

ligament fossae at the distal end. In both manus, a small additional bone lies next to metacarpal II, which we interpret as a phalanx from digit II. Metacarpal III is adjacent to this digit in both manus, beneath the distolateral part of the ulna. It is smaller than metacarpal II but equal in width, and slightly larger than metacarpal I. As in *Majungasaurus*, the distal end is nearly straight, and it articulates with at least one phalanx.

Metacarpal IV is more problematic. The bone originally identified as metacarpal IV, described as "conical-shaped," has a shape that indeed "resembles that of an ungual phalanx" (Ruiz and Novas, 2009:173A). In fact, it is quite possible that this bone is a manual ungual, for in the left manus it also possesses an apparent 'blood groove' along one side. Two other ungual-like elements are visible in the right manus. We consider it unlikely that any of these represent metacarpal IV, especially given the absence of any similar morphology in the reliably identified elements of *Aucasaurus* and *Majungasaurus*. Instead, one of the additional elements in the right manus (a "carpal" of Bonaparte et al., 1990) is positioned at the distomedial edge of the ulna, and is similar in relative size to the small metacarpal IV in other abelisaurids. Therefore, there may have been at least two manual unguals in *Carnotaurus*, most likely associated with digits II and III. This would give a minimum phalangeal formula of 1/2/2/?.

We cannot determine a consistent phalangeal formula for abelisaurs, partly due to uncertainty regarding how complete the available materials are. However, the minimum formula of 1/2/1/1 is probably achieved in all three taxa for which the manus is known. This is the minimum observed formula for *Majungasaurus*, which may not have possessed any unguals, as there are no distal articular surfaces preserved on any of the phalanges in this specimen. Nonetheless, the possibility that portions of this manus exhibit pathologies renders even this conclusion uncertain. In *Aucasaurus*, the distalmost preserved phalanges do bear articular surfaces, raising the possibility that unguals were present in this taxon.

Ceratosaur Forelimb Evolution

The discovery of a complete shoulder girdle and forelimb of *Majungasaurus* allows new insights into the evolution and reduction of the forelimbs in ceratosaurs. The forelimb and manus of *Majungasaurus* exhibit the same, extremely reduced morphology as seen in *Carnotaurus* and

Aucasaurus, being overall more similar to the stout forelimb of *Carnotaurus* (Bonaparte et al., 1990) than to the relatively longer and more gracile limb of *Aucasaurus* (Coria et al., 2002). Generally, although the known abelisaurids do show variations in forelimb and manual morphology, they are much more similar to one another than any is to a non-abelisaurid theropod. Furthermore, the amount and nature of the observed variation points to relatively minor differences in function rather than a wide diversity of forelimb use within Abelisauridae.

When compared to other ceratosaurs, however, more pronounced differences become apparent. The forelimbs of *Ceratosaurus* and *Limusaurus* are reduced in overall size but the arm and forearm bones retain proportions that are similar to those of other primitive theropods, with the radius and ulna being greater than one-third the length of the humerus (Gilmore, 1920; Xu et al., 2009). All abelisaurids have forearm proportions that are one-third or less the length of the humerus but, within Abelisauridae, *Majungasaurus* and *Carnotaurus* are united in possessing antebrachial lengths of one-quarter humeral length, whereas *Aucasaurus* retains a slightly longer forearm with a proportion of one-third (Coria et al., 2002). The unique morphology of the radius and ulna, with their greatly expanded ends and narrow waists, also appears to be an abelisaurid synapomorphy, although the antebrachium remains unknown in noasaurids or basal abelisaurids.

The manus in *Ceratosaurus* and *Limusaurus* are primitive in retaining proximal phalanges that are shorter than their respective metacarpals (Gilmore, 1920; Xu et al., 2009), unlike the condition in abelisaurids where these bones can be subequal in size. In addition, these phalanges are proportionally short relative to their own width and depth, more so than in most other theropods. Isolated manual phalanges of *Masiakasaurus* (Carrano et al., 2011) and *Noasaurus* (Agnolin and Chiarelli, 2010) appear to be short as well, implying that this is an abelisauroid feature. The metacarpus of *Limusaurus* is less than one-third its forearm length (Xu et al., 2009:supp. material, p. 10), a feature it shares with the more derived abelisaurids to the exclusion of *Ceratosaurus*. The overall proportions of the manus in *Limusaurus*, including the extreme reduction of digits I and IV relative to digits II and III, suggest that the forelimb reduction in *Limusaurus* may have occurred independently of the more evenly distributed reduction seen in abelisaurids.

The forelimb is also incompletely known in Noasauridae. In *Masiakasaurus*, the humerus

is long and slender, similar to the condition in *Limusaurus* and *Elaphrosaurus*, although the radius and ulna remain unknown. A number of isolated manual phalanges are shortened and similar in proportions to those in other ceratosaurs (Carrano et al., 2011). These proportions are also present phalanges of *Noasaurus* and *Ligabueino* that were recently reinterpreted as manual (Agnolin and Chiarelli, 2010; Carrano et al., 2011). The forelimb of a new noasaurid from Africa has been only preliminarily described, but has a relatively short forearm, four manual digits (of which digit II is longest), and flattened unguals (Sereno, 2010). Therefore, some distal reduction in forelimb length may have characterized abelisauroids generally, although the trend was only carried through to the proximal element (humerus) in abelisaurids.

A partial metacarpal III and associated phalanx were described with the holotype of *Austrocheiros isasii* and suggested to demonstrate the presence of an abelisauroid with a non-reduced manus (Ezcurra et al., 2010). The fragmentary nature of the specimens, and the uncertainty regarding the phylogenetic position of *Austrocheiros*, make it difficult to comment further on its relevance to ceratosaur forelimb evolution overall. For example, *Austrocheiros* could: (1) lie outside Abelisauroidea but in a more derived position than *Ceratosaurus*, retaining a primitive ceratosaur manual morphology; or (2) be a true abelisauroid but represent an autapomorphic reversal to this condition.

Although the forelimb is highly reduced distally, abelisaurids retain large scapulocoracoids with broad areas for muscle attachment and a robust humeral morphology. The hemispherical humeral head would have allowed an extensive range of motion at the shoulder, potentially less restricted than in typical theropods. The articulation of the flattened humeral distal condyles with the highly dished proximal surfaces of the radius and ulna indicates that there was likely a relatively extensive articular cartilage on the distal humerus that provided the necessary congruence between the joint surfaces. Without ossified carpals and with the bulbous distal surfaces of the radius and ulna, the wrist likely also enjoyed an extensive range of motion, with one extreme (hyperextension) preserved in the articulated manus of the *Aucasaurus* holotype (Coria et al., 2002). The extreme shortness of the manual elements, especially in *Majungasaurus*, makes it unlikely that the individual digits retained much autonomy, and it is possible that the manus was employed as a functional unit. The specific functional capabilities of

the abelisaurid forelimb remain enigmatic, and it is beyond the scope of this paper to address them in detail. A detailed analysis of the evolution of the abelisaurid forelimb musculoskeletal system and its functional implications is the subject of a separate study (Chapter V).

SUMMARY AND CONCLUSIONS

A recently discovered mostly articulated, and nearly complete skeleton of *Majungasaurus crenatissimus* supplies valuable new information on this taxon, particularly on the pectoral girdle and forelimb. The highly reduced abelisaurid forelimb was previously represented by very few specimens, and new material from this region furnishes the opportunity to elucidate its bizarre morphology. This paper provides a description of the first known elements of the *Majungasaurus* forelimb distal to the humerus and further description of the complete pectoral girdle and forelimb, together with a comparative analysis of forelimb evolution in Ceratosauria.

The forelimb of *Majungasaurus* is very similar to those of *Aucasaurus* and *Carnotaurus*, possessing an extremely shortened antebrachium and manus. The morphologies in all three taxa, especially of the distal-most elements, is highly derived and strikingly dissimilar to all other ceratosaurs, providing little clue as to the intervening stages in their evolution. Further materials of basal abelisaurid and noasaurid forelimbs will no doubt allow more detailed analysis of forelimb evolution in Ceratosauria.

ACKNOWLEDGEMENTS

We thank D. Krause for the opportunity to work on the Mahajanga Basin Project and the *Majungasaurus* forelimb materials. We also acknowledge the members of the 2005 and 2007 field expeditions for the collection of these specimens, and A. Rasoamiaramanana of the Université d'Antananarivo, B. Andriamihaja and his staff of the Madagascar Institute pour la Conservation des Ecosystèmes Tropicaux, and the villagers of Berivotra for logistical support in the field. We thank J. Groenke, V. Heisey, and the volunteers of the Science Museum of Minnesota for their skilled preparation of these materials and J. Sertich and W. Simpson for

curation. Assistance with CT-scanning was provided by J. Georgi, J. Groenke, B. Patel, and J. Sertich. D. Schwarz-Wings generously provided access to specimens in her care. We also thank D. Krause and A. Turner for comments on early drafts of this manuscript, and D. Krause, J. McCartney, P. O'Connor, and J. Sertich for helpful discussions. We also thank R. Benson and J. Choiniere for their insightful reviews. Funding for the Mahajanga Basin Project has been provided by the National Science Foundation (DEB-9224396, EAR-9418816, EAR- 9706302, EAR-0106477, EAR-0446488, EAR-1123642), the Dinosaur Society (1995), and the National Geographic Society (1999, 2001, 2004, 2009). Support for SHB was provided by a National Science Foundation Graduate Research Fellowship and a Stony Brook University Graduate Council Fellowship. Support for MTC was provided by the National Science Foundation (DEB-9904045). Translations of Bonaparte and Novas (1985), Buffetaut et al. (1988), Depéret (1896a, 1896b), and Lavocat (1955) are available on the Polyglot Paleontologist website (www.paleoglot.org).

LITERATURE CITED

Agnolin, F. L., and P. Chiarelli. 2010. The position of the claws in Noasauridae (Dinosauria: Abelisauroidea) and its implications for abelisauroid manus evolution. Paläontologische Zeitschrift 85:293–300.

Allain, R., and X. P. Suberbiola. 2003. Dinosaures de France. Comptes Rendus Palevol 2:27–44.

Bonaparte, J. F., and F. E. Novas. 1985. *Abelisaurus comahuensis*, n. g., n. sp., Carnosauria del Cretácio Tardio de Patagonia. Ameghiniana 21:259–265.

Bonaparte, J. F., F. E. Novas, and R. A. Coria. 1990. *Carnotaurus sastrei* Bonaparte, the horned, lightly built carnosaur from the Middle Cretaceous of Patagonia. Natural History Museum of Los Angeles County Contributions in Science 416:1–41.

Brochu, C. A. 2003. Osteology of *Tyrannosaurus rex*: Insights from a nearly complete skeleton and high-resolution computed tomographic analysis of the skull. Journal of Vertebrate Paleontology 22:1–138.

Buffetaut, E., P. Mechin, and A. Mechinsalessy. 1988. Un dinosaure théropode d'affinités gondwaniennes dans le Crétacé supérieur de Provence. Comptes Rendus de l'Académie des Sciences (Paris), Serie II 306:153–158.

Calvo, J. O., D. Rubilar-Rogers, and K. Moreno. 2004. A new Abelisauridae (Dinosauria: Theropoda) from northwest Patagonia. Ameghiniana 41:555–563.

Carrano, M. T. 2007. The appendicular skeleton of *Majungasaurus crenatissimus* (Theropoda: Abelisauridae) from the Late Cretaceous of Madagascar. Society of Vertebrate Paleontology Memoir 8:163–179.

Carrano, M. T., M. A. Loewen, and J. J. W. Sertich. 2011. New materials of *Masiakasaurus knoplferi* Sampson, Carrano, and Forster, 2001, and implications for the morphology of the Noasauridae (Theropoda: Ceratosauria). Smithsonian Contributions to Paleobiology 95:1–53.

Carrano, M. T., D. W. Krause, P. M. O'Connor, and S. D. Sampson. 2009. *Megalosaurus crenatissimus* Depéret, 1896 (currently *Majungasaurus crenatissimus*; Dinosauria, Theropoda): proposed replacement of the holotype by a neotype. Bulletin of Zoological Nomenclature 66:261–264.

Chure, D. J., and J. H. Madsen. 1996. On the presence of furculae in some non-maniraptoran theropods. Journal of Vertebrate Paleontology 16:573–577.

Coria, R. A., L. M. Chiappe, and L. Dingus. 2002. A new close relative of *Carnotaurus sastrei* Bonaparte 1985 (Theropoda: Abelisauridae) from the Late Cretaceous of Patagonia. Journal of Vertebrate Paleontology 22:460–465.

Coria, R. A., P. J. Currie, and A. P. Carabajal. 2006. A new abelisauroid theropod from northwestern Patagonia. Canadian Journal of Earth Sciences 43:1283–1289.

Depéret, C. 1896a. Sur l'existence de Dinosauriens, Sauropodes et Théropodes dans le Crétacé supérieur de Madagascar. Comptes Rendus de l'Académie des Sciences (Paris), Série II 122:483–485.

Depéret, C. 1896b. Note sur les Dinosauriens Sauropodes et Théropodes du Crétacé supérieur de Madagascar. Bulletin de la Société Géologique de France, 3e série 24:176–194.

Downs, A. 2000. *Coelophysis bauri* and *Syntarsus rhodesiensis* compared, with comments on the preparation and preservation of fossils from the Ghost Ranch *Coelophysis* Quarry. New Mexico Museum of Natural History and Science Bulletin 17:33–38.

Ezcurra, M. D., F. L. Agnolin, and F. E. Novas. 2010. An abelisauroid dinosaur with a non-atrophied manus from the Late Cretaceous Pari Aike Formation of southern Patagonia. Zootaxa 2450:1–25.

Gilmore, C. W. 1920. Osteology of the carnivorous Dinosauria in the United States National Museum, with special reference to the genera *Antrodemus* (*Allosaurus*) and *Ceratosaurus*. Bulletin of the United States National Museum 110:1–159.

International Code of Zoological Nomenclature. 2011. Opinion 2269 (Case 3487) *Megalosaurus crenatissimus* Depéret, 1896 (currently *Majungasaurus crenatissimus*; Dinosauria, Theropoda): designation of a neotype. Bulletin of Zoological Nomenclature 68:89–90.

Jasinoski, S. C., A. P. Russell, and P. J. Currie. 2006. An integrative phylogenetic and extrapolatory approach to the reconstruction of dromaeosaur (Theropoda: Eumaniraptora) shoulder musculature. Zoological Journal of the Linnean Society 146:301–344.

Krause, D. W., S. D. Sampson, M. T. Carrano, and P. M. O'Connor. 2007. Overview of the history of discovery, taxonomy, phylogeny, and biogeography of *Majungasaurus crenatissimus* (Theropoda: Abelisauridae) from the Late Cretaceous of Madagascar. Society of Vertebrate Paleontology Memoir 8:1–20.

Lavocat, R. 1955. Sur une portion de mandible de Théropode provenant du Crétacé supérieur de Madagascar. Bulletin du Muséum National d'Histoire Naturelle, 2e série 27:256–259.

Lipkin, C., P. C. Sereno, and J. R. Horner. 2007. The furcula in *Suchomimus tenerensis* and *Tyrannosaurus rex* (Dinosauria: Theropoda: Tetanurae). Journal of Paleontology 81:1523–1527.

Madsen, J. H. 1976. *Allosaurus fragilis*: a revised osteology. Utah Geological Survey Bulletin 109:1–163.

Madsen, J. H., and S. P. Welles. 2000. *Ceratosaurus* (Dinosauria, Theropoda) a revised osteology. Utah Geological Survey Miscellaneous Publications 2:1–80.

Marsh, O. C. 1881. Principle characters of American Jurassic dinosaurs. Part V. The American Journal of Science, series 3 21:417–423.

Marsh, O. C. 1884. Principle characters of American Jurassic dinosaurs. Part VIII. The Order Theropoda. The American Journal of Science, series 3 27:329–340.

Nesbitt, S. J., A. H. Turner, M. Spaulding, J. L. Conrad, and M. A. Norell. 2009. The theropod furcula. Journal of Morphology 270:856–879.

Novas, F. E., S. Chatterjee, D. K. Rudra, and P. M. Datta. 2010. *Rahiolisaurus gujaratensis*, n. gen. n. sp., a new Abelisaurid theropod from the Late Cretaceous of India; pp. 45–62 in S. Bandyopadhyay (ed.), New Aspects of Mesozoic Biodiversity. Springer, Heidelberg.

Owen, R. 1842. Report on British fossil reptiles, part II. Report of the British Association for the Advancement of Science 11:60–104.

Rogers, R. R., J. H. Hartman, and D. W. Krause. 2000. Stratigraphic analysis of Upper Cretaceous rocks in the Mahajanga Basin, northwestern Madagascar: implications for ancient and modern faunas. Journal of Geology 108:275–301.

Rogers, R. R., D. W. Krause, K. C. Rogers, A. H. Rasoamiaramanana, and L. Rahantarisoa. 2007. Paleoenvironment and paleoecology of *Majungasaurus crenatissimus* (Theropoda: Abelisauridae) from the Late Cretaceous of Madagascar. Society of Vertebrate Paleontology Memoir 8:21–31.

Ruiz, J., and F. E. Novas. 2009. New insights about the anatomy of the hand of *Carnotaurus sastrei* (Theropoda: Abelisauridae). Journal of Vertebrate Paleontology 29:173A.

Sampson, S. D., and D. W. Krause, eds. 2007. *Majungasaurus crenatissimus* (Theropoda: Abelisauridae) from the Late Cretaceous of Madagascar. Society of Vertebrate Paleontology Memoir 8, 184 pp.

Sampson, S. D., D. W. Krause, P. Dodson, and C. A. Forster. 1996. The premaxilla of *Majungasaurus* (Dinosauria: Theropoda), with implications for Gondwanan paleobiogeography. Journal of Vertebrate Paleontology 16:601–605.

Sampson, S. D., L. M. Witmer, C. A. Forster, D. W. Krause, P. M. O'Connor, P. Dodson, and F. Ravoavy. 1998. Predatory dinosaurs remains from Madagascar: implications for the Cretaceous biogeography of Gondwana. Science 280:1048–1051.

Seeley, H. G. 1888. On the classification of the fossil animals commonly named Dinosauria. Proceedings of the Royal Society of London 43:165–171.

Sereno, P. C. 1993. The pectoral girdle and forelimb of the basal theropod *Herrerasaurus ischigualastensis*. Journal of Vertebrate Paleontology 13:425–450.

Sereno, P. C. 2010. Noasaurid (Theropoda: Abelisauroidea) skeleton from Africa shows derived skeletal proportions and function. Journal of Vertebrate Paleontology 28:162A.

Sereno, P. C., and S. L. Brusatte. 2008. Basal abelisaurid and carcharodontosaurid theropods from the Lower Cretaceous Elrhaz Formation of Niger. Acta Palaeontologica Polonica 53:15–46.

Sereno, P. C., J. A. Wilson, and J. L. Conrad. 2004. New dinosaurs link southern landmasses in the Mid-Cretaceous. Proceedings of the Royal Society of London Series B 271:1325–1330.

Tykoski, R. S., C. A. Forster, T. Rowe, S. D. Sampson, and D. Munyikwa. 2002. A furcula in the coelophysid theropod *Syntarsus*. Journal of Vertebrate Paleontology 22:728–733.

Wilson, J. A., P. C. Sereno, S. Srivastava, D. K. Bhatt, A. Khosla, and A. Sahni. 2003. A new abelisaurid (Dinosauria, Theropoda) from the Lameta Formation (Cretaceous, Maastrichtian) of India. Contributions from the Museum of Paleontology, University of Michigan 31:1–42.

Xu, X., J. M. Clark, J. Mo, J. Choiniere, C. A. Forster, G. M. Erickson, D. W. E. Hone, C. Sullivan, D. A. Eberth, S. J. Nesbitt, Q. Zhao, R. Hernandez, C. Jia, F.-l. Han, and Y. Guo. 2009. A Jurassic ceratosaur from China helps clarify avian digital homologies. Nature 459:940–944.

TABLE 3.1. Measurements (in cm) of *Majungasaurus crenatissimus* pectoral girdle and forelimb elements. **Abbreviations**: **AP**, midshaft anteroposterior diameter; **DAP**, distal anteroposterior diameter; **DML**, distal mediolateral diameter; **e**, estimated value; **FAP**, furcular anteroposterior width at the symphysis; **FDV**, furcular dorsoventral width at the symphysis; **GH**, glenoid height; **GW**, glenoid width; **ML**, midshaft mediolateral diameter; **PAP**, proximal anteroposterior diameter; **PML**, proximal mediolateral diameter; **SAP**, scapular anteroposterior width (measured at mid-scapular length); **SL**, scapular length; **SML**, scapular mediolateral width (measured at mid-scapular length); **TL**, total length. Dashes indicate where measurements could not be taken; plus signs (+) indicate that some length is missing from the element as preserved.

Element	Specimen	TL	SL	SAP	SML	GW	GH
Scapulocoracoid	FMNH PR 2836 (R)	60.6	45.1	8.2	1.8	4.2	6.7
	FMNH PR 2836 (L)	61.0	45.7	7.9	1.9	4.1	6.4

Element	Specimen	TL	FAP	FDV
Furcula	FMNH PR 2836	11.4	1.4	0.9

Element	Specimen	TL	AP	ML	PAP	PML	DAP	DML
Humerus	FMNH PR 2836 (R)	20.7	2.8	3.9	5.1	5.6	4.2	5.1
	FMNH PR 2836 (L)	20.6e	3.3	4.0	4.5	5.4e	5.9	5.7
	FMNH PR 2423 (R)	20.7	2.7	3.5	4.5	4.6	5.4	4.5
	UA 9856 (R)	24.1	3.6	4.5	—	—	—	—
Radius	FMNH PR 2836 (L)	5.5	2.2	2.9	3.2	5.3	5.1	3.6
	FMNH PR 2835 (R)	5.4	2.1	2.6e	2.9e	—	4.9e	—
Ulna	FMNH PR 2836 (L)	4.8	2.5	1.5	4.1	3.5	4.1	3.1
	UA 9860 (L)	4.8	2.0	1.9	3.8	3.0	4.0	3.3
Metacarpal I	FMNH PR 2836 (L)	1.6	0.7	1.2	1.3	1.6	0.8	1.1
	FMNH PR 2833 (R)	1.8	0.9	1.2	1.5	1.5+	1.1	1.3
Metacarpal II	FMNH PR 2836 (L)	2.2	0.7	1.0	1.5	2.0	1.1	1.3

Metacarpal III	FMNH PR 2836 (L)	1.9	0.8	1.0	1.4	1.6	—	1.1
Metacarpal IV	FMNH PR 2836 (L)	1.3	0.8	1.3	1.2	1.7	1.1	1.5
Phalanx I-1	FMNH PR 2836 (L)	0.9	—	—	0.9e	0.8	0.3	0.4
Phalanx II-1	FMNH PR 2836 (L)	1.4	0.8	0.8	1.2	1.3	0.8	1.0
Phalanx II-2	FMNH PR 2836 (L)	0.6	—	—	0.6	1.0	—	—
Phalanx III-1	FMNH PR 2836 (L)	1.1	0.9	0.9	1.0	1.3	0.8	—
	FMNH PR 2834 (R)	1.2	0.8	0.8	1.3	1.2	0.8	—
Phalanx IV-1	FMNH PR 2836 (L)	0.8+	—	—	0.7	1.5	—	—

FIGURE 3.1. Line drawing of left scapulocoracoid and forelimb of *Majungasaurus crenatissimus*, FMNH PR 2836, as preserved in situ, with detail of the antebrachium and manus in posterolateral view. **Abbreviations**: **H**, humerus; **MC I**, metacarpal I; **MC II**, metacarpal II; **MC III**, metacarpal III; **MC IV**, metacarpal IV; **R**, radius; **U**, ulna.

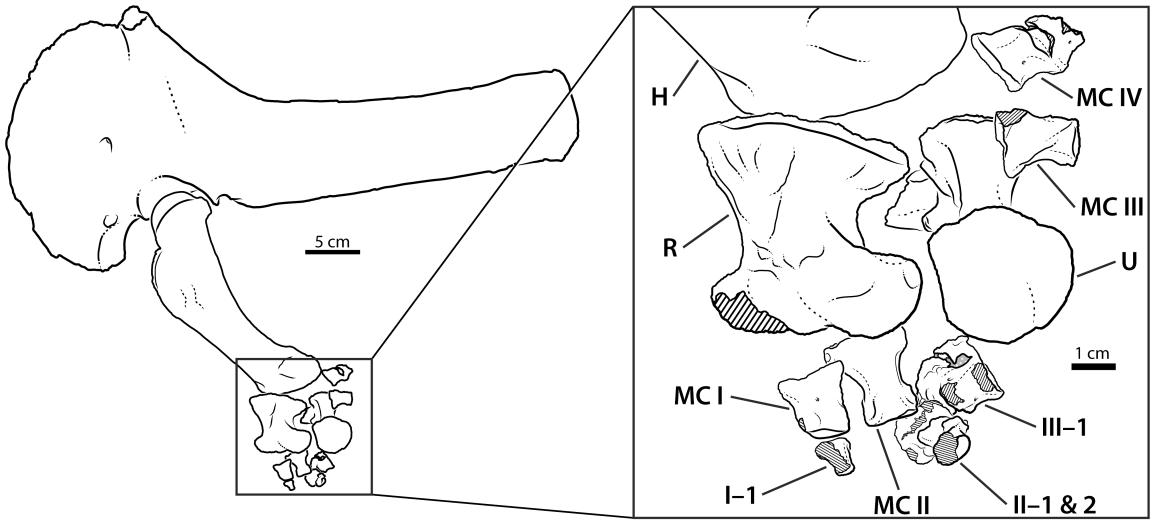
5 cm
H
MC IV
MC III
R
U
1 cm
MC I
III–1
I–1
MC II
II–1 & 2

FIGURE 3.2. Reconstruction of articulated scapulocoracoid and forelimb of *Majungasaurus crenatissimus* in lateral view. Model is composed of CT scans of FMNH PR 2836, right scapulocoracoid and humerus (reversed): UA 9860, left ulna; and FMNH PR 2836, left radius, metacarpals and phalanges. Scale bar equals 5 cm.

FIGURE 3.3. Scapulocoracoid of *Majungasaurus crenatissimus* (FMNH PR 2836). **A**, right scapulocoracoid in lateral view; **B**, left scapulocoracoid in medial view (reversed). **Abbreviations**: **a**, acromion; **bt**, biceps tubercle; **cf**, coracoid foramen; **g**, glenoid; **pag**, pre-acromial groove; **pvp**, posteroventral process; **scs**, scapulocoracoid suture; **sgf**, subglenoid fossa; **sgr**, subglenoid ridge; **tbs**, scar for triceps brachii scapularis. Scale bar equals 5 cm.

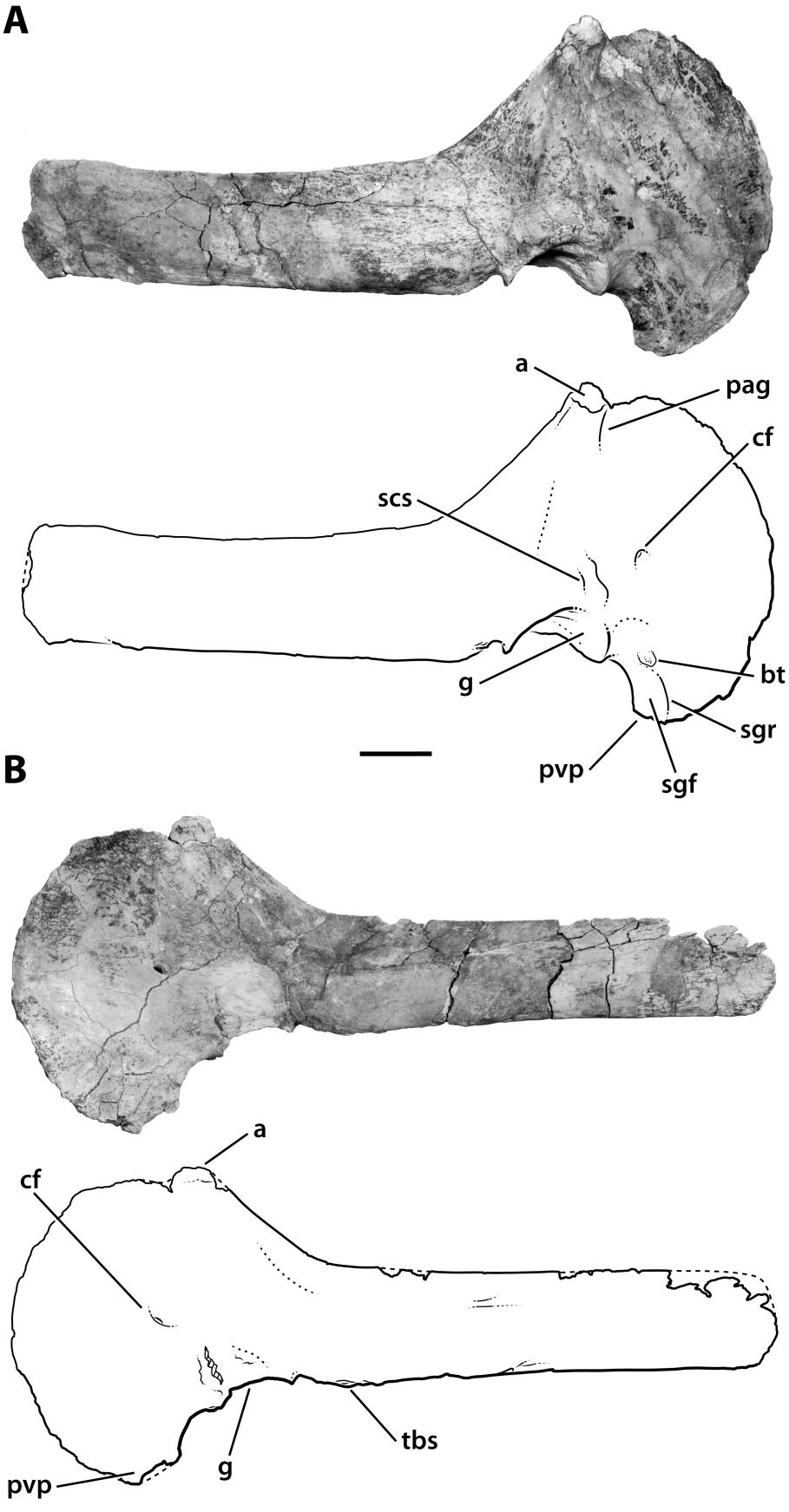
A
a
pag
cf
scs
g
bt
sgr
pvp
sgf
B
a
cf
tbs
g
pvp

FIGURE 3.4. Furcula of *Majungasaurus crenatissimus* (FMNH PR 2836) in anterior (**A**) and posterior (**B**) views. Cross-hatching indicates broken bone surface. Scale bar equals 5 cm.

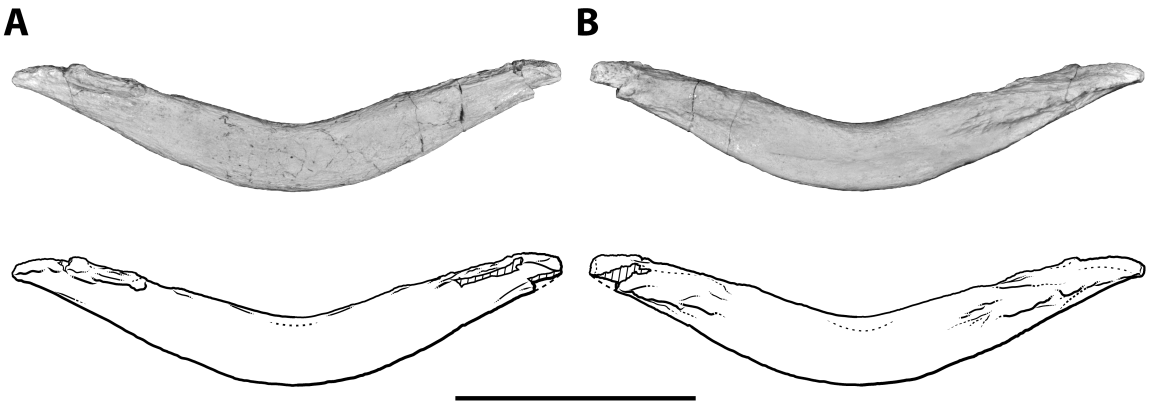
A
B

FIGURE 3.5. Right humerus of *Majungasaurus crenatissimus* (FMNH PR 2836) in anterior (**A)**; medial (**B**); posterior (**C)**; and lateral (**D**) views. Cross-hatching indicates broken bone surface. **Abbreviations**: **aid**, anterior intercondylar depression; **dpc**, deltopectoral crest; **gt**, greater tubercle; **it**, internal tuberosity; **nf**, nutrient foramen; **pt**, posterior tuberosity; **rc**, radial condyle; **uc**, ulnar condyle. Scale bar equals 5 cm.

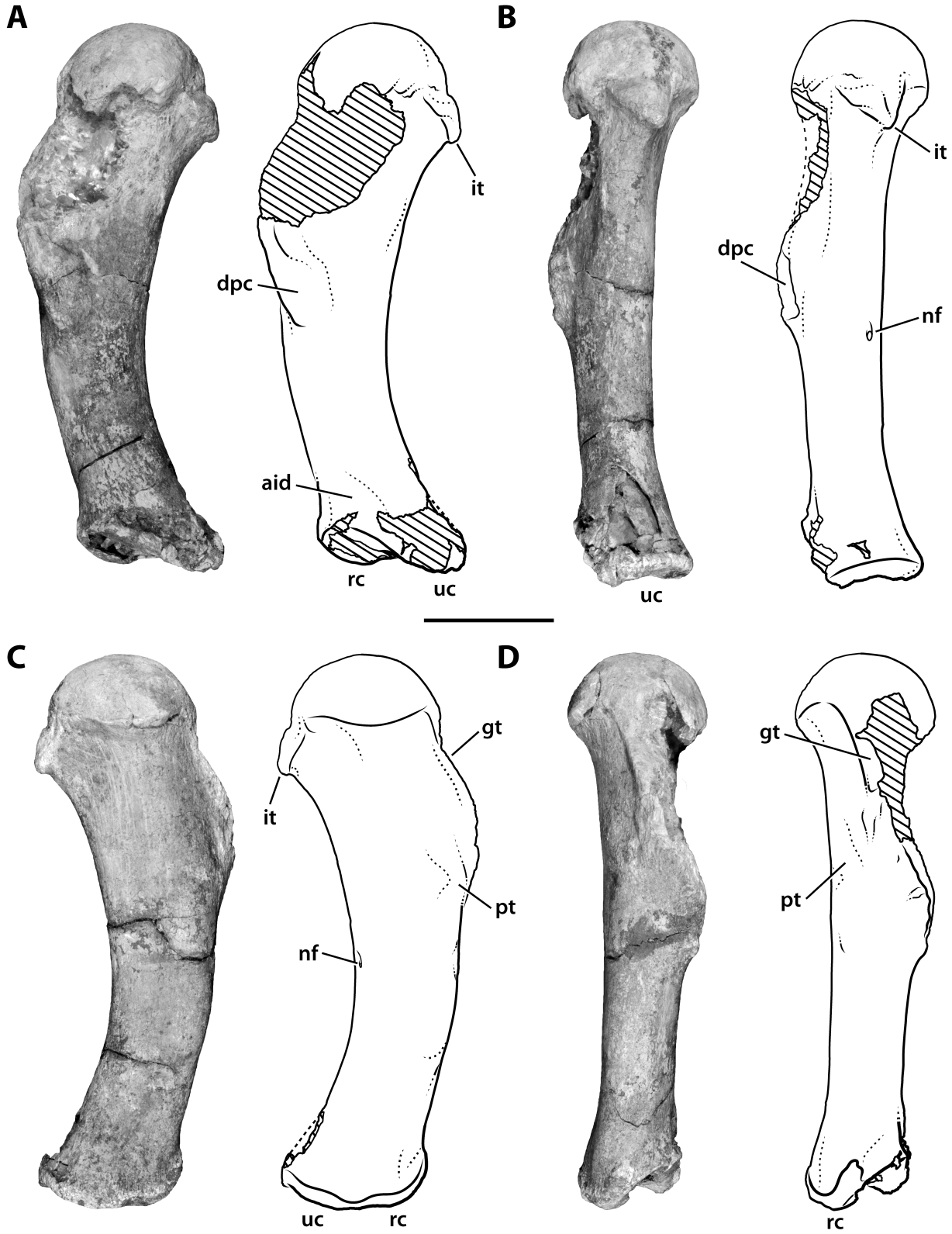
A
it
dpc
aid
rc
uc
B
it
dpc
nf
uc
C
gt
it
pt
nf
uc
rc
D
gt
pt
rc

FIGURE 3.6. Left radius of *Majungasaurus crenatissimus* (FMNH PR 2836) in anterior (**A**); medial (**B**); posterior (**C**); lateral (**D**); proximal (**E**); and distal (**F**) views. Cross-hatching indicates broken bone surface, shaded areas indicate matrix. **Abbreviations**: **dn**, distal notch; **ir**, interosseus ridge; **lsr**, lateral semicircular rugosity; **ltr**, lateral triangular rugosity; **pltr**, posterolateral triangular rugosity; **uf**, ulnar facet. Scale bar equals 5 cm.

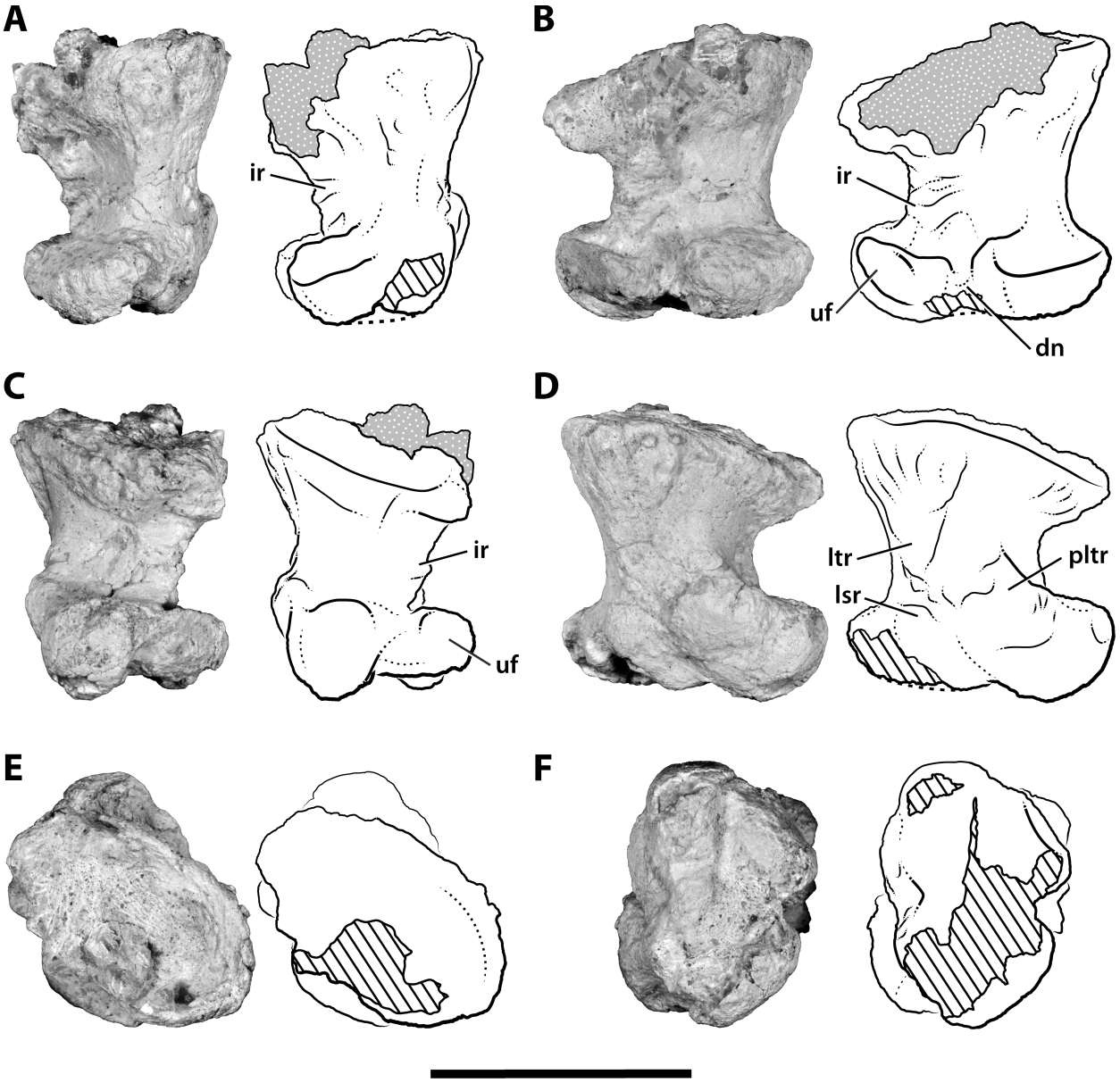
A
ir
B
ir
uf
dn
C
ir
uf
D
ltr
pltr
lsr
E
F

FIGURE 3.7. Left ulna of *Majungasaurus crenatissimus* (UA 9860) in anterior (**A**); medial (**B**); posterior (**C**); lateral (**D**); proximal (**E**); and distal (**F**) views. Cross-hatching indicates broken bone surface. **Abbreviations**: **alr**, anterolateral ridge; **ap**, articular pit; **ir**, interosseus ridge; **rf**, radial facet. Scale bar equals 5 cm.

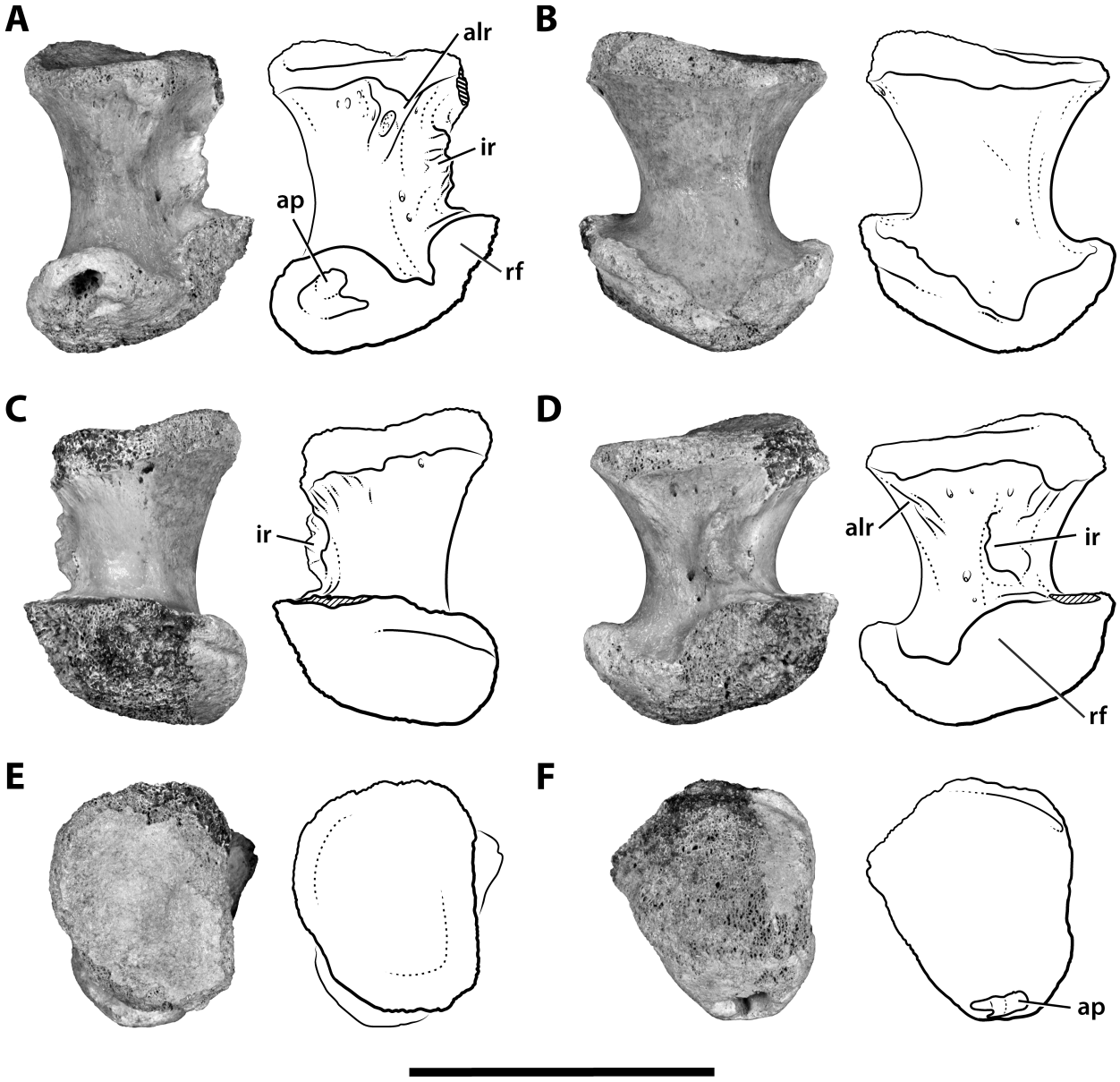
A
alr
ir
ap
rf
B
C
ir
D
alr
ir
rf
E
F
ap

FIGURE 3.8. Left manus of *Majungasaurus crenatissimus* (FMNH PR 2836) in dorsal (**A**, **B**); ventral (**C**, **D**); lateral (**E**, **F**); and medial (**G**, **H**) views. Cross-hatching indicates broken bone surface, shaded areas indicate matrix. **Abbreviations**: **MC I**, metacarpal I; **MC II**, metacarpal II; **MC III**, metacarpal III; **MC IV**, metacarpal IV. Scale bar equals 1 cm.

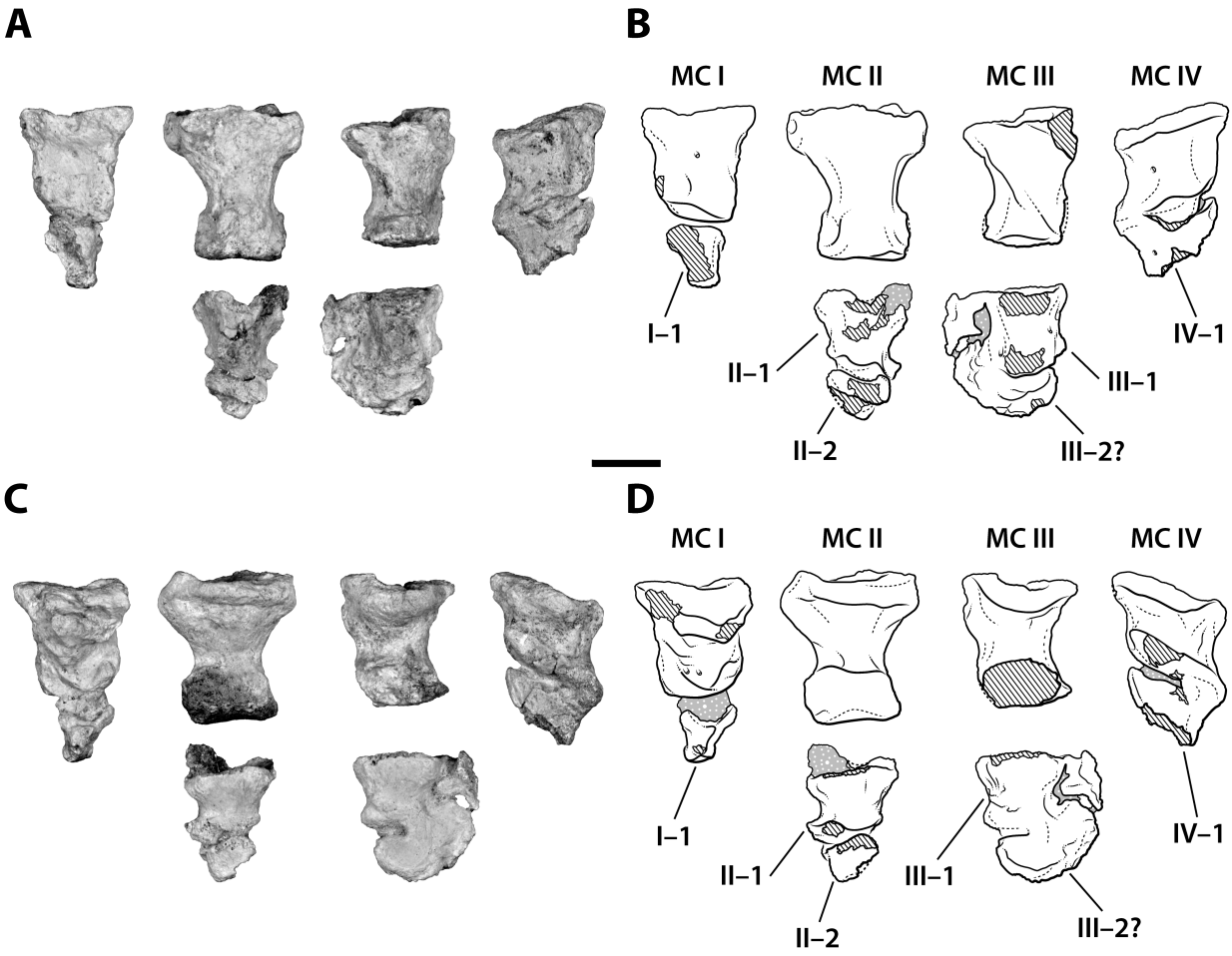
A
B
MC I
MC II
MC III
MC IV
I–1
II–1
II–2
III–1
III–2?
IV–1
C
D
MC I
MC II
MC III
MC IV
I–1
II–1
II–2
III–1
III–2?
IV–1

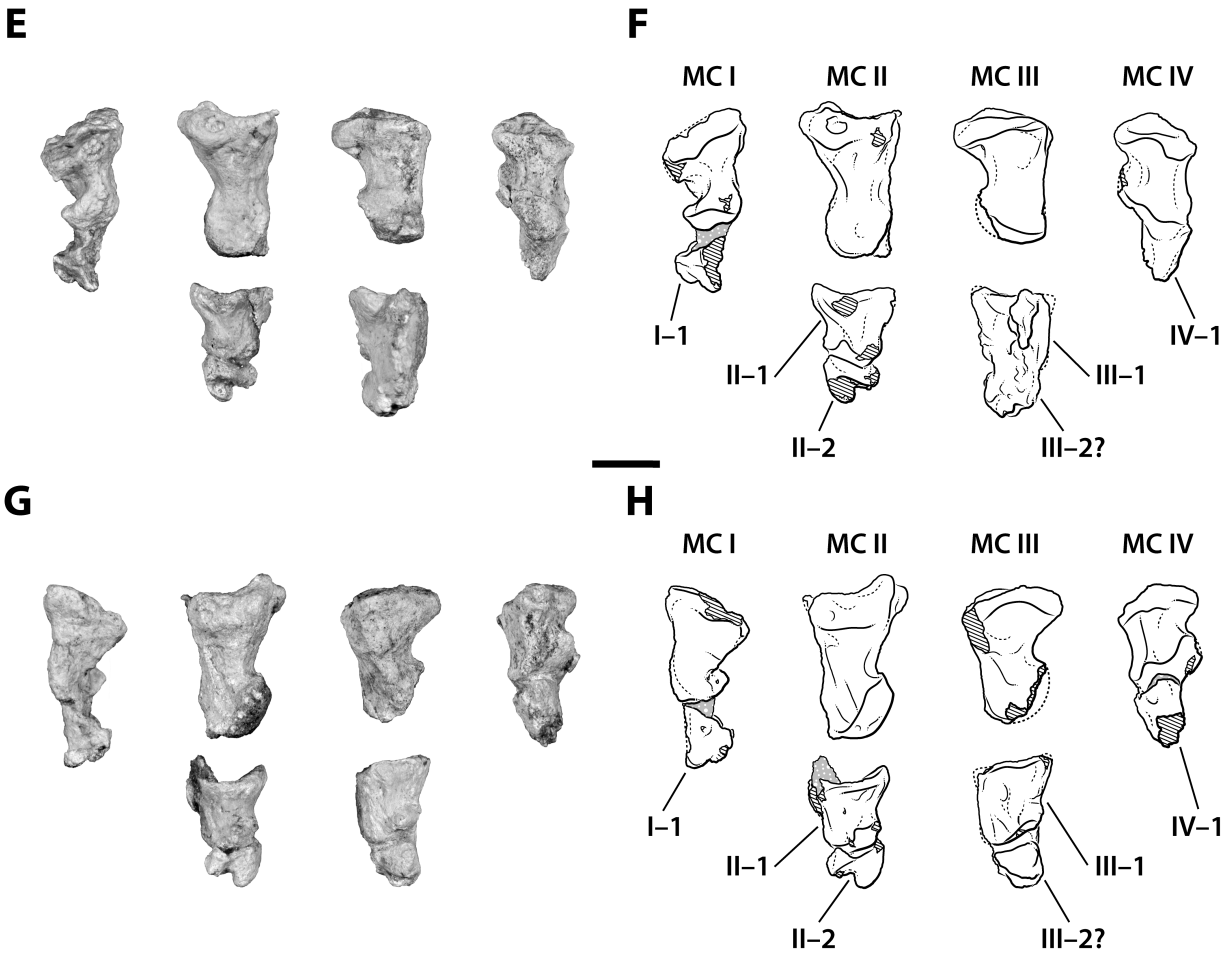
E
F
MC I
MC II
MC III
MC IV
I–1
II–1
II–2
III–1
III–2?
IV–1
G
H
MC I
MC II
MC III
MC IV
I–1
II–1
II–2
III–1
III–2?
IV–1

FIGURE 3.9. Proximal view of articulated left metacarpals of *Majungasaurus crenatissimus* (FMNH PR 2836). **Abbreviations**: **MC I**, metacarpal I; **MC II**, metacarpal II; **MC III**, metacarpal III; **MC IV**, metacarpal IV. Cross-hatching indicates broken bone surface. Scale bar equals 1 cm.

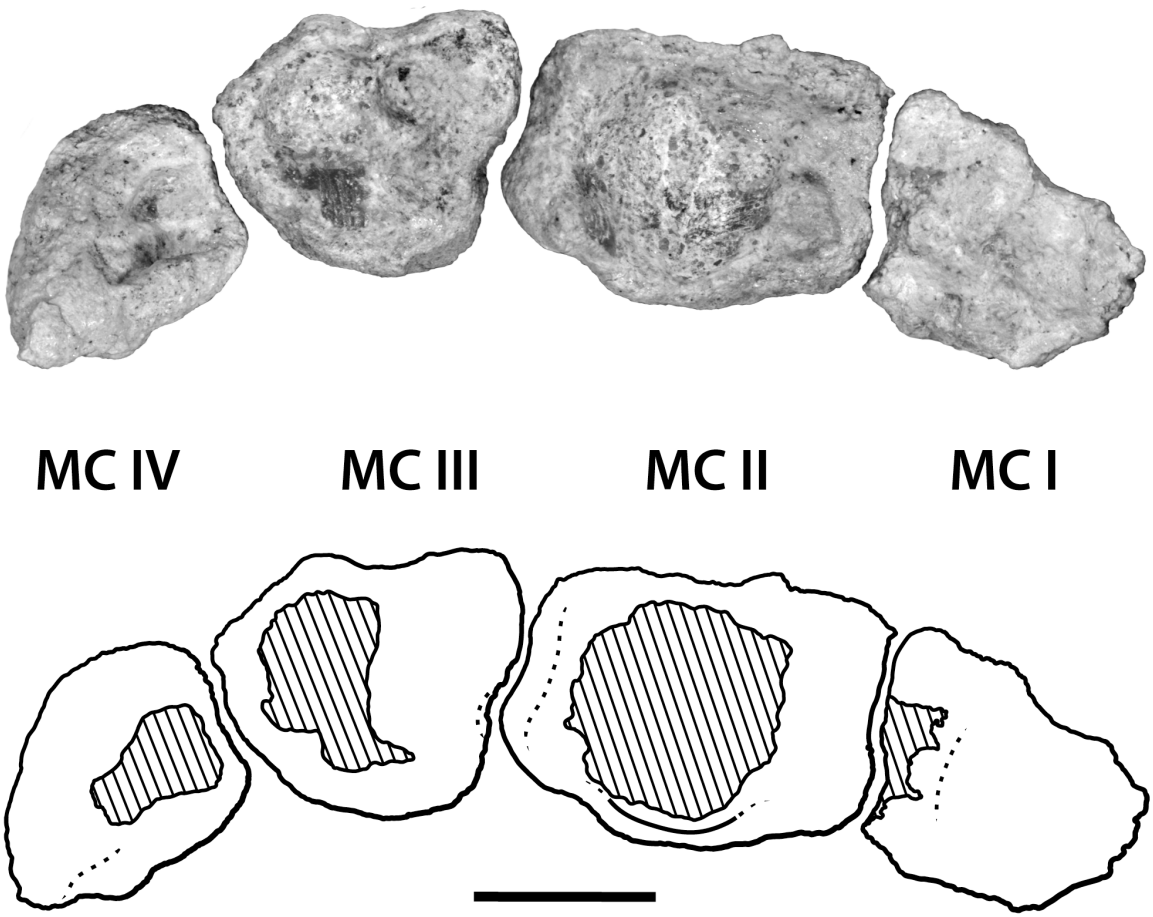
MC IV
MC III
MC II
MC I

FIGURE 3.10. Comparison of manual phalanges (FMNH PR 2836, left, and FMNH PR 2834, right) associated with digit III of *Majungasaurus crenatissimus*. Dorsal views of FMNH PR 2836 (**A**) and FMNH PR 2834 (**B**). Ventral views of FMNH PR 2836 (**C**) and FMNH PR 2834 (**D**). **Abbreviations**: **dp**, distal process. Cross-hatching indicates broken bone surface, shaded areas indicate matrix. Scale bar equals 1 cm.

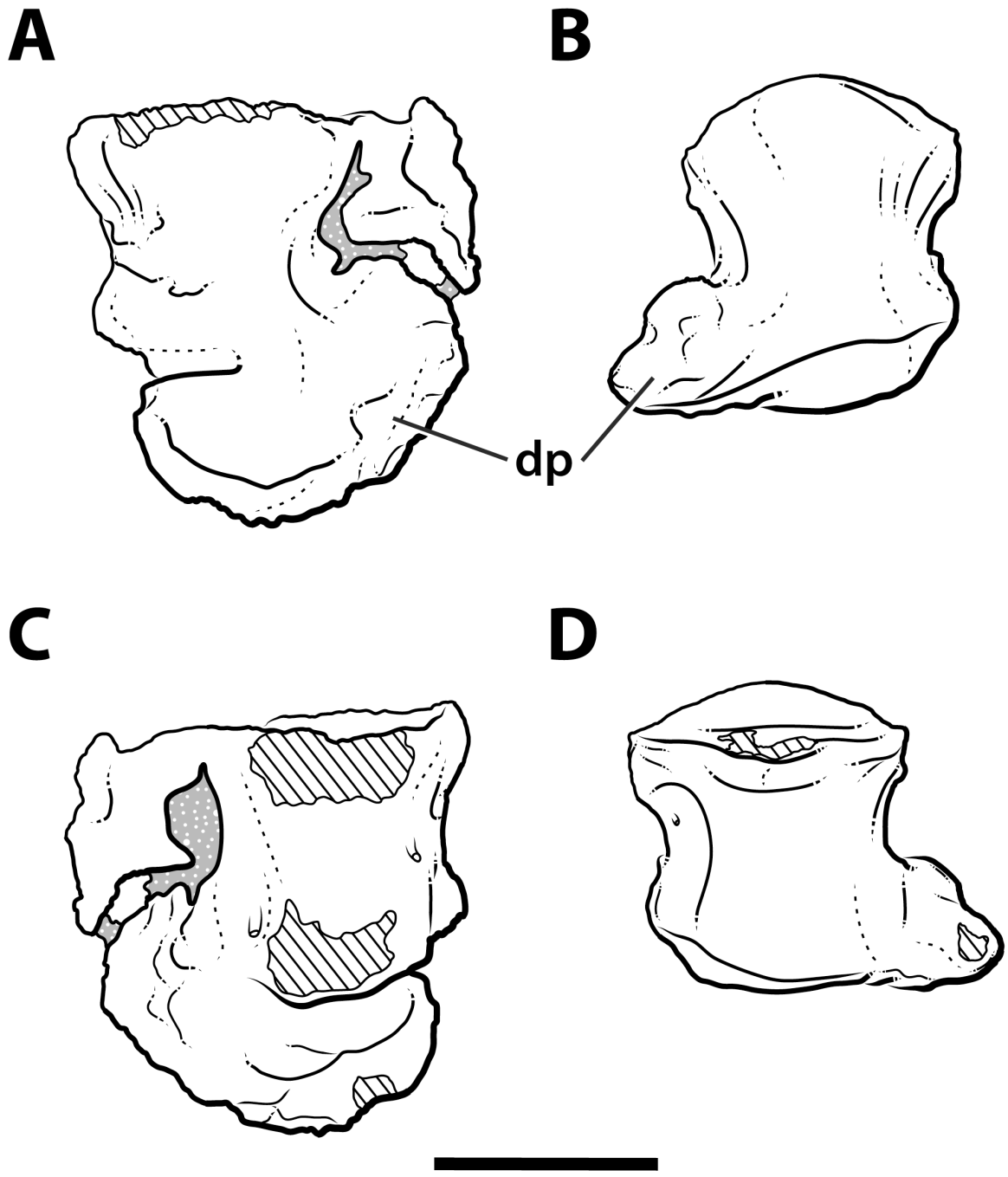
A
B
dp
C
D

Chapter IV: Forelimb musculature of the basal theropod dinosaur *Tawa hallae* from the Late Triassic Hayden Quarry of New Mexico

ABSTRACT

Reconstructing limb musculature provides important information about the function and capability of extinct tetrapod limbs. Previous reconstructions of theropod forelimb myology have focused on the shoulder musculature of derived taxa. This study analyzes the musculature of the forelimb, including the antebrachial and intrinsic manual muscles, using an extant phylogenetic bracket to reconstruct the muscles in the early theropod *Tawa hallae* from the Late Triassic of New Mexico. Data on the forelimb musculature of extant birds, crocodylians, lizards, and turtles were analyzed using ancestral state reconstruction and compared with the osteology of *Tawa* and other early theropods to create the first complete reconstruction of the forelimb musculature in a nonavian theropod dinosaur. The shoulder musculature of early theropods is more similar morphologically to that of basal ornithischians and sauropodomorphs than to that of dromaeosaurids. Basal theropods, however, exhibit several developments of the supracoracoideus and deltoideus musculature that would result in stronger movements of the forelimb at the shoulder than in the other non-avian dinosaurs sampled. New homology hypotheses for the distal musculature of birds enables the unequivocal reconstruction of much of the intrinsic manual musculature, which shows a robust morphology well-suited for powerful digital flexion. The forelimb myology of *Tawa* established here helps infer the ancestral conformation of the forelimb musculature and the osteological correlates of major muscle groups in early theropods. These data are critical for investigations addressing questions relating to the evolution of specialized forelimb function across Theropoda.

INTRODUCTION

The forelimbs of nonavian theropod dinosaurs present complex functional problems to the reconstruction of behavior in extinct taxa. Their closest living relatives, crown-group crocodylians and birds, possess such radically different forelimb morphologies that at first glance they seem to have little in common, and neither has a great similarity to that of nonavian theropods. Most nonavian theropods also lack any extant analogs to forelimb function, as the

only modern animals that do not use their forelimbs for locomotion are humans and terrestrial flightless birds. Nevertheless, the function of theropod forelimbs is a topic of extensive interest and speculation due in large part to the eventual evolution of these forelimbs into instruments of flight. Recent studies on the evolution of theropod forelimbs have focused on the evolution of feathers and wing shape (e.g., X. Wang et al., 2011) including the creation of aerodynamic models (Koehl et al., 2011), the developmental identity of the manual digits (Bever et al., 2011; Z. Wang et al., 2011), changes in forelimb proportions relating to flight (Dececchi and Larsson, 2009), and assessment of potential ranges of motion in the developing flight stroke (Gishlick, 2001). The myology of the forelimb and its importance in testing hypotheses of forelimb function, however, has been largely ignored.

Reconstructing the limb musculature of extinct tetrapods is one of the most fundamental steps in any analysis of the functional capability. The integrative phylogenetic and extrapolatory analysis (Bryant and Russell, 1992) and Extant Phylogenetic Bracket (EPB: Witmer, 1995) methods have become the de facto toolkit for soft tissue reconstructions of extinct taxa (e.g., Carrano and Hutchinson, 2002; Jasinoski et al., 2006) because they analyze soft tissue data of the most closely related extant taxa in an explicit phylogenetic context. Among the few studies that have reconstructed forelimb musculature in dinosaurs, even fewer have been performed in an explicit phylogenetic context (Nicholls and Russell, 1985; Dilkes, 2000; Jasinoski et al., 2006; Langer et al., 2007; Maidment and Barrett, 2011). The musculature of the shoulder in theropods has been thoroughly documented (Jasinoski et al., 2006), but the musculature of the antebrachium and manus in a nonavian theropod has only been reconstructed using birds as the primary muscular model thus lacking full phylogenetic context (Carpenter and Smith, 2001). Two studies have used phylogeny-based methods to reconstruct some antebrachial muscles in non-theropod dinosaurs (Dilkes, 2000; Langer et al., 2007), but both of these studies reconstructed only a few major muscles of the forearm and none of the manus. The muscles controlling the hand and digits in theropods present difficulties in their reconstruction due to the highly divergent manual morphologies of the EPB, yet these muscles are some of the most important in determining the functional capabilities of the theropod forelimb. However, several recent studies on the development of the avian wrist and hand (Kundrát, 2009; Z. Wang et al.,

2011) have made it possible to identify osteological homologs in this region and improved our ability to assess muscular morphology across Archosauria.

An interest in the evolution of flight has resulted in a primary focus on theropod taxa that are phylogenetically close to birds. Most previous reconstructions of theropod forelimb myology of any method have been performed in derived taxa (Nicholls and Russell, 1985; Carpenter and Smith, 2001; Jasinoski et al., 2006), but these animals possess novel osteological features that can complicate muscular reconstruction, particularly in the antebrachium and manus. The reconstruction of the complete forelimb musculature in a phylogenetically early, plesiomorphic taxon establishes a ground state ancestral morphology that can be used in future muscular reconstructions as well as providing a starting point for the analysis of muscular and functional evolution of specialized theropod forelimbs across the entire clade.

The early theropod *Tawa hallae* from the Late Triassic Hayden Quarry of New Mexico (Nesbitt et al., 2009a) provides a nearly complete forelimb and pectoral girdle, allowing a full reconstruction of forelimb musculature. *Tawa* has been identified as the sister taxon to Neotheropoda, possessing a transitional morphology in the skull and postcranium intermediate between Neotheropoda and the most basal theropods (Nesbitt et al., 2009a). The forelimb shares apomorphic features with *Herrerasaurus ischigualastensis* and early neotheropods such as *Coelophysis bauri* and *Dilophosaurus wetherelli*, while retaining a plesiomorphically larger number of carpals (nine) than other theropods. This suite of features makes *Tawa* an ideal model for the reconstruction of the forelimb musculature in an early theropod.

Institutional Abbreviations—AMNH, American Museum of Natural History, New York, NY, U.S.A.; **GR**, Ghost Ranch Ruth Hall Museum of Paleontology, Abiquiu, NM, U.S.A.; **MPC**, Mongolian Paleontological Collection, Ulaanbaatar, Mongolia; **OUVC**, Ohio University Vertebrate Collections, Athens, OH, U.S.A.; **PVSJ**, Museo de Ciencias Naturales, San Juan, Argentina; **TMP**, Royal Tyrrell Museum of Paleontology, Drumheller, AB, Canada.

MATERIALS AND METHODS

Data on muscle attachment sites in extant taxa were primarily obtained from published

myological reports and supplemented with dissections of key taxa that are not represented in the literature. In total, data from the literature were collected for 41 avian species representing 26 family-level clades, four crocodylian species, six lepidosaurian species, and six testudine species (for a complete list of taxa and sources, see Supplemental Table 1). Three additional avian taxa from the collection of Ohio University were dissected: *Bubo virginianis* (OUVC 10641), *Caprimulgus carolinensis* (OUVC 10642), and *Megaceryle alcyon* (OUVC 10643). Muscle data were also collected from two forelimbs of adult ostriches (*Struthio camelus*) obtained frozen from O.K. Corral Ostrich Farms (Oro Grande, CA, USA). Osteological features on the forelimb of *Tawa hallae* were assessed on all known forelimb material, which includes two previously described individuals (GR 241 and 242; Nesbitt et al., 2009a) and elements from larger individuals including a partial humerus (GR 359) and complete associated antebrachium (GR 360). Additionally, data collected on osteological features of other basal theropods such as *Herrerasaurus* (PVSJ 407, 373, 53), *Sanjuansaurus* (PVSJ 605), and *Coelophysis* (AMNH 7227, 7228, 7230, 7231, 7238; TMP 84.63.29, 84.63.30, 84.63.32, 84.63.33, 84.63.40, 84.63.50, 84.63.52) were used to create hypothetical reconstructions of coracoid attachment sites (not preserved in *Tawa*), and in cases where they provided osteological evidence for an otherwise equivocal origin or insertion.

Homologies of the muscles of the antebrachium and manus in archosaurs and other reptiles are not straightforward, and they are often not reported in the literature. A recent survey of reptile limb homologies with a broad taxonomic scope (Diogo and Abdala, 2010) provides a useful basis for many muscles but does not focus on archosaurs or the special problems presented by the bird manus. To address this, previous hypotheses of homology were concatenated from available sources including previous muscle reconstructions (Miner, 1925; Holmes, 1977; Dilkes, 2000), comparative anatomical reports (Howell, 1936; Haines, 1939; Straus, 1942; Haines, 1950; Meers, 2003), and developmental analyses (Sullivan, 1962). These hypotheses were critically appraised in light of the overall muscle morphology and novel dissections of the antebrachium and manus of the ostrich. Developmental studies of the carpus and metacarpus in birds (Kundrát, 2009) and crocodylians (Müller and Alberch, 1990; Buscalioni et al., 1997) were employed to assess muscle attachment site homologies in this highly modified region (Table 1).

Homology hypotheses novel to this analysis are discussed below. In particular, the explicit homologies of the avian intrinsic manual musculature have not previously been proposed, and are summarized in Table 2. Terminology of muscles in this region is not standardized and contributes to the confusion about homology, although an attempt to rectify this was made recently by Diogo and Abdala (2010). Their terminology is fortunately congruent with that of Jasinoski et al. (2006), and has been adopted in this study in most cases.

Independent characters with discrete states were created for the positions of the origin and insertion for each muscle of the antebrachium and manus (for a complete list of characters and codings, see supplemental information). Each taxon was coded for these characters and ancestral states at each node were reconstructed using maximum likelihood in the program Mesquite (Maddison and Maddison, 2010) employing a consensus phylogeny (Figure 1) built from recent morphological (Livezey and Zusi, 2007) and molecular (Jetz et al., 2012; Hackett backbone) avian phylogenies in combination with a recent lepidosaurian tree (Conrad, 2008) and a recent total-evidence testudine tree (Sterli, 2010). Reconstructions were also tested on the independent molecular and morphological trees to assess their robustness to varying phylogenies. Proportional probabilities of the possible character states at the nodes surrounding Dinosauria (Supplemental Table 2) were combined with observations of osteological correlates of muscle attachment sites in *Tawa* and used to create a map of the origin and insertion sites for each muscle. Reconstruction of the muscles crossing the shoulder utilized the results of Jasinoski et al. (2006) combined with observations of the osteological features of the scapula and humerus of *Tawa*. Because a coracoid is unknown for *Tawa*, major muscles originating on the coracoid were reconstructed primarily based on *Coelophysis* coracoid morphology with consideration of the morphology of other early theropods (*Eodromaeus*, *Sanjuansaurus*, *Herrerasaurus*, *Segisaurus*, and *Dilophosaurus*).

The designation of levels of inference are as follows: Level I inference is assigned if the proportional probability of a particular character state is greater than 0.50 for both of the nodes immediately above and below Dinosauria (Aves and Archosauria, respectively). A Level II inference is assigned if only one of these nodes possesses a proportional probability greater than 0.50 for a character state. If neither node shows a proportional probability of greater than 0.50,

this is designated as a Level III inference. In all cases, the "prime" level (i.e., Level I′, II′, and III ′) is assigned if osteological evidence that supports the character state is not present. Prime levels are ranked below non-primes of the same level, but are preferred over non-primes of a lower level (i.e., Level I′ is preferred over Level II). In this analysis, Level II′ inferences are minimally required to reconstruct a feature. One-sided phylogenetic inferences without osteological evidence are accepted here due to the limitations of reconstructing the intrinsic manual musculature in dinosaurs. In the highly derived avian manus, several muscles have become highly modified or completely lost. In these cases, if the majority of the outgroup taxa share identical morphologies for these muscles, this morphology is accepted as most parsimonious to reconstruct in dinosaurian taxa.

RESULTS

The following reconstruction is divided into two sections. The first contains a description of the morphology of the muscles of the shoulder and brachium based predominantly on the shoulder reconstruction of Jasinoski et al. (2006), applied to the forelimb of *Tawa*. The second part is a novel reconstruction of the antebrachial and manual musculature in *Tawa* based on new data and analyses. In this section the proportional probabilities of the relevant nodes are given and levels of inference are cited. Comparisons to other muscular reconstructions are presented elsewhere (see Discussion).

Pectoral and Brachial Musculature

Serratus superficialis (SS)—Serratus superficialis is phylogenetically unequivocally present in theropods. The exact extent of origin of Serratus superficialis from the body wall, however, is phylogenetically equivocal and difficult to reconstruct due to a lack of osteological correlates (Jasinoski et al., 2006). In both crocodylians and birds this broad, sheet-like muscle takes origin from the lateral surfaces of the anterior dorsal ribs, extending to the cervical ribs in birds and some of the thoracic musculature in crocodylians (Jasinoski et al., 2006). In *Tawa* the

origin is tentatively and conservatively reconstructed as arising from the lateral surfaces of the posteriormost cervical and anteriormost two to three dorsal ribs.

Based on a tubercle present in neognath birds and the oviraptorosaur *Ingenia yanshini*, Jasinoski et al. (2006) reconstructed this muscle as being composed of two separated divisions at its insertion, which they refer to as pars cranialis and pars caudalis. This tuberosity, located on the posteroventral surface of the scapular blade approximately one-third the way along the scapula from the proximal end, is the point of insertion of the cranial portion of this muscle. A scar in this area, varying in development from a simple tubercle to an elongate, rugose groove, is present in many coelurosaurian theropod taxa besides *Ingenia* but is absent in all non-tetanuran theropod taxa, including *Herrerasaurus*, *Coelophysis*, *Sanjuansaurus*, and *Tawa*. This lack of differentiation may indicate the retention of a single, elongate insertion along the posteroventral edge of the distal two-thirds of the scapular blade, as in crocodylians (Meers, 2003) and lepidosaurs (Russell and Bauer, 2008), and this morphology is reconstructed in *Tawa* (Figure 2). In this position, the Serratus superficialis would have acted to retract and depress the scapula.

Serratus profundus (SP)—As with Serratus superficialis, Serratus profundus is phylogenetically unequivocally present in theropods, although its origin is equivocal. It also originates from the anteriormost dorsal ribs in both birds and crocodylians but unlike Serratus superficialis it attaches close to the dorsal vertebrae and also takes origin from the cervical and dorsal vertebrae in birds (Jasinoski et al., 2006). A likely origin for this muscle in *Tawa* would have been from the anteriormost dorsal ribs close to their articulation with the dorsal vertebrae.

The insertion of Serratus profundus is found on the medial surface of the distal end of the scapular blade in both crocodylians and birds (Jasinoski et al., 2006). There are no osteological signs on the scapula of *Tawa* that indicate the extent of the insertion of this muscle, but it is likely to have inserted over most of the distal half to one-third of the scapular blade (Figure 2). In this position, Serratus profundus would have acted to protract the scapula.

Rhomboideus (RH)—The division of Rhomboideus into superficialis and profundus divisions is equivocal in theropods. A profundus division is only found in birds, and is reconstructed in dromaeosaurids by Jasinoski et al. (2006) on the basis of a likely subhorizontal position of the scapular blade in that clade. Ancestrally in theropods the position of the scapular

blade was more sharply angled so, in the absence of any other osteological evidence, the profundus division is not reconstructed in *Tawa*. Like Serratus muscles, Rhomboideus has an equivocal origin on the body wall, which is dependent on the orientation of the scapular blade. Because *Tawa* likely possessed a scapular orientation somewhere in between that of birds (subhorizontal) and crocodylians (subvertical), it is possible that the origin of Rhomboideus was also intermediately located, attaching to both the fascia of the dorsal cervico-thoracic region and several neural spines of the posteriormost cervical and anteriormost dorsal vertebrae (Jasinoski et al., 2006).

Based on scapular orientation, the insertion of Rhomboideus in *Tawa* is reconstructed as attaching in a somewhat intermediate position on the anterior half of the distalmost portion of the medial scapular blade (Figure 2). This differs from a more bird-like reconstruction along the anterior edge of the scapula provided by Jasinoski et al. (2006) in dromaeosaurids based on a subhorizontal orientation of the scapula. In this position Rhomboideus would have acted to protract the scapula.

Levator scapulae (LS)—This muscle is not present in birds, and Jasinoski et al. (2006) did not reconstruct it as present in dromaeosaurids but noted that some non-coelurosaurian theropods possess muscle scars on the scapula that may correspond to the superficial part of this muscle. In crocodylians the superficial Levator scapulae inserts on the anterior edge of the scapular blade along most of its length posterior to the acromial expansion and sometimes leaves a scar in this region (Meers, 2003). An elongate sulcus or rugosity along the anterodorsal part of the scapular blade is not common among nonavian theropods but it can be found not only in ceratosaurs and tetanurans (Jasinoski et al., 2006), but also tyrannosaurids such as *Tarbosaurus* (MPC-D 107/2). This scar is not known from any early theropod, but its presence in more derived taxa provides a phylogenetic bracket to reconstruct this muscle (Figure 2). The origin of Levator scapulae in nonavian theropods would most likely be from the cranial cervical ribs, as in crocodylians (Meers, 2003). In this position it would have acted as a rotator of the scapular blade, as well as a lateral flexor of the neck.

Trapezius (TR)—The presence of Trapezius in nonavian theropods follows the same pattern as Levator scapulae, although this muscle lacks any osteological correlates. If Levator

scapulae and Trapezius are hypothesized to have been lost due to the reorientation of the scapular blade into a subhorizontal position in birds (following Jasinoski et al., 2006), they may be reconstructed in theropods that lack this scapular orientation (i.e., most non-maniraptorans). Given osteological evidence for the presence of Levator scapulae in nonavian theropods, the Trapezius is also reconstructed as present in these taxa.

The Trapezius is a broad, fan-shaped muscle and would have taken its origin from the median parts of the cervical and thoracodorsal fascia covering the axial musculature, as in crocodylians and lepidosaurs (Meers, 2003; Russell and Bauer, 2008). These taxa also share a common area of insertion on the anterior edge of the acromion and acromial expansion of the scapula. In crocodylians the insertion of this muscle is often intermingled with the insertion of Levator scapulae such that it is difficult to determine the exact boundaries of the insertion sites between these two muscles (Meers, 2003). Because of this, Trapezius and Levator scapulae are reconstructed as inserting together in *Tawa*, but would primarily have been restricted to the proximal part of this insertion site (Figure 2). In this position the trapezius would have acted to rotate the scapular blade, likely assisting in protraction of the forelimb, as in chameleons (Peterson, 1984).

Latissimus dorsi (LD)—This superficial muscle is composed of a broad, thin sheet in crocodylians and lepidosaurs with a long, linear origin arising from the neural spines of the last cervical vertebra to the sixth or seventh dorsal vertebra and/or the thoracodorsal fascia near the vertebral column in that area (Meers, 2003; Russell and Bauer, 2008). In birds, however, this muscle is divided into two parts, but they are variably present across the clade and sometimes form an almost continuous sheet of muscle (George and Berger, 1966). As such, Latissimus dorsi is reconstructed as a single muscle in theropods (Jasinoski et al., 2006). Although the exact extent of the origin in theropods is equivocal, the muscle arises from the same general area in all taxa studied, and thus can be reconstructed as most likely originating from the neural spines or thoracodorsal fascia in the region of the first to fifth dorsal vertebrae.

A muscle scar for the insertion of Latissimus dorsi on the lateral side of the humerus posterior to the deltopectoral crest is present in crocodylians, birds, and lepidosaurs, and may be expressed as a rugose tubercle, crest, pit, or linear sulcus (Meers, 2003; Jasinoski et al., 2006).

The linear sulcus reported to be present in this region by Jasinoski et al. (2006) in dromaeosaurids and troodontids can be found in many theropods, including *Tawa*, and likely represents the insertion site of Latissimus dorsi in these taxa (Figure 3). In this position Latissimus dorsi would have acted to retract the humerus.

Pectoralis (P)—Pectoralis has a broad origin involving a variety of elements of the pectoral girdle in archosaurs and lepidosaurs, but they share a common area of origin on the ventral surface of the sternum. There are currently no sternal plates known for basal theropods, although it is presumed that the elements were present but cartilaginous in these taxa (Padian, 2004). Reconstructing additional areas of origin from the sternal ribs (as in crocodylians) or the coracoid (as in *Struthio*) requires a Level II′ inference although unlike Jasinoski et al. (2006), this analysis does not eliminate an origin from the coracoid based on the presence of Coracobrachialis longus in this position (see below). Due to a lack of ossified and preserved elements in this area of the pectoral girdle, it is difficult to assign the exact boundaries of origin with any certainty.

The insertion of Pectoralis is unequivocally located on the medial surface of the deltopectoral crest. Unlike the condition in dromaeosaurids (Jasinoski et al., 2006), however, there is an osteological correlate for this insertion found in *Tawa* expressed as a small, oblong depression on the medial surface of the deltopectoral crest near its tip (Figure 3). This limited insertion area is similar to the insertion in crocodylians (Meers, 2003) and is less extensive than the insertion in birds, which extends over much of the medial surface of the deltopectoral crest (Jasinoski et al., 2006). The action of Pectoralis would have been to adduct and protract the humerus.

Subscapularis (SBS)—The origin of Subscapularis is unequivocally located on the medial surface of the scapular blade. As in dromaeosaurids (Jasinoski et al., 2006) and many other theropods, *Tawa* possesses a distinct ridge on the medial surface of the scapula that extends along the proximal half to two-thirds of the scapula. Jasinoski et al. (2006) noted that a ridge in a similar position defining the dorsal edge of the origin of Subscapularis is also present in *Meleagris* and uses this as evidence for an origin ventral to this ridge in dromaeosaurids. However, this ridge is also present in crocodylians (Meers, 2003) and the ventral fossa it creates

is instead part of the site of origin of Scapulohumeralis posterior (see below). In *Tawa* this ridge is ventrally shifted from the midline and curves distally to meet the posteroventral edge of the scapula less than half-way along the scapular blade, resulting in an extremely reduced potential area of origin, whereas the flaring blade of the scapula provides an extensive surface for an origin more similar to that in crocodylians. It is possible that the origin of this muscle migrated ventrally to the medial ridge as the scapular orientation became more subhorizontal and bird-like in theropods (e.g., dromaeosaurids), but in *Tawa* it is reconstructed in a more dorsal position based on the reduced attachment area ventrally for this typically large muscle (Figure 2).

The insertion site of this muscle is unequivocally located on the internal tuberosity of the humerus (Figure 3), sharing an insertion tendon with Subcoracoideus (Jasinoski et al., 2006). Regardless of the exact location of the origin of Subscapularis, the primary action of this muscle would have been to retract and rotate the humerus.

Subcoracoideus (SBC)—Subcoracoideus is not an independent muscle in crocodylians, and is instead fused to Subscapularis. In birds and lepidosaurs, however, it possesses a separate insertion on the medial surface of the coracoid, and thus it can be unequivocally reconstructed as distinct in theropods (Jasinoski et al., 2006). It is unknown how extensive the origin would have been in theropods, but in the absence of contrary evidence it is here reconstructed as in Jasinoski et al. (2006) as a small area covering the coracoid foramen (Figure 2).

As mentioned above, Subcoracoideus shares a tendon of insertion with Subscapularis, which inserts on the internal tuberosity of the humerus (Figure 3). In this position Subcoracoideus would have adducted and laterally rotated the humerus.

Supracoracoideus (SC)—The origin of Supracoracoideus exhibits a variable morphology in the study taxa, primarily arising from the coracoid but with attachments to the scapula in crocodylians and to the sternum in neognathous birds. Minimally it originated from the coracoid in theropods, potentially in the anterodorsal quadrant (Jasinoski et al., 2006). It is also possible that the subacromial depression of the scapula of nonavian theropods represents the extension of the Supracoracoideus origin onto the scapula. This depression is usually continuous with the adjacent lateral surface of the coracoid, providing a broad, flat area for the origin of this muscle from both bones, as in crocodylians (Meers, 2003). Reconstruction of the

Supracoracoideus accessorius muscle (see below) indicates that the subacromial depression may have housed the supracoracoideus complex of muscles, and it is reconstructed this way in *Tawa* (Figure 2).

The area of insertion of Supracoracoideus is phylogenetically equivocal, inserting on the tip and nearby portion of the lateral surface of the deltopectoral crest in crocodylians, and on the posterior surface of the greater tubercle in birds. Jasinoski et al. (2006) reconstructed the insertion as in that of birds based on the presence of a rugose depression on the anterior surface of the greater tubercle in *Velociraptor*, but an insertion in this position is unlikely at least in earlier theropods. In neognathous birds Supracoracoideus is highly modified to provide elevation and rotation of the wing during upstroke (Poore et al., 1997), using an osteological structure of the scapulocoracoid called the triosseal canal that is not found in nonavian theropods. Without this specialized osteology, an insertion of Supracoracoideus on the greater tubercle in theropods would result in a very poor mechanical advantage for this muscle. With an insertion on the tip of the deltopectoral crest, however, Supracoracoideus would retain its capabilities as a strong protractor of the humerus, as in crocodylians (Meers, 2003). Furthermore the humerus of *Tawa* possesses a small oblong depression, located on the lateral surface of the deltopectoral crest immediately adjacent to its tip, that is consistent with this site of insertion and indicates the extent of the lateral excursion of the insertion (Figure 3). In this position Supracoracoideus would have acted as a protractor and slight abductor of the humerus.

Supracoracoideus accessorius (SCA)—Reconstruction of this muscle is based on a new hypothesis of homology presented here. The homology of the avian Deltoideus minor in crocodylians is controversial; typically it is regarded as a novel muscle in birds and thus lacking a homolog in crocodylians (Dilkes, 2000; Jasinoski et al., 2006), or homologized with the Deltoideus clavicularis (Diogo and Abdala, 2010). This confusion stems primarily from a problem of nomenclature: the Deltoideus minor is not a member of the deltoid group embryologically, although it arises from a similar area to the Deltoideus major in birds (Sullivan, 1962; see below). Sullivan (1962) attempted to rectify the misnomer by changing the name of this muscle to Coracobrachialis anterior, but he was widely ignored. The avian Deltoideus minor is actually a derivative of the Supracoracoideus muscle mass, which is also closely related to the

Coracobrachialis muscle mass in all reptiles (Romer, 1944; Sullivan, 1962). In birds the Deltoideus minor typically arises from the lateral surface of the acromion of the scapula, sometimes including the adjacent lateral coracoid, and inserts just distal to the proximal articular surface of the humerus, often along the proximal edge of the deltopectoral crest (Hudson and Lanzillotti, 1955; George and Berger, 1966; Jasinoski et al., 2006). This pattern of attachment and development almost exactly matches that of a small, semi-independent muscle in crocodylians. It is sometimes described as part of the Supracoracoideus; Dilkes (2000) labeled it as Supracoracoideus pars scapularis, and although Jasinoski et al. (2006) designate the Supracoracoideus complex as a single muscle, they describe a separate "M. supracoracoideus" that does not share an origin or insertion with the other parts of Supracoracoideus (longus and intermedius) on the tip of the deltopectoral crest. Meers (2003) separated this muscle from the Supracoracoideus complex completely and called it the M. coracobrachialis brevis dorsalis. Here it is referred to as Supracoracoideus accessorius based on its derivation from the Supracoracoideus group developmentally, but it is distinct from the other muscles of this group.

In nonavian theropods, the reconstruction of both the origin and insertion of this muscle are unequivocal. It would have originated from the subacromial depression of the scapula, possibly sharing this area with the Supracoracoideus (Figure 2), and inserted on the proximal edge of the deltopectoral crest between the greater tubercle and the tip of the crest (Figure 3). In this position the Supracoracoideus accessorius would have acted with the Supracoracoideus to protract and abduct the humerus.

Coracobrachialis (CB)—The origin of this muscle can be unequivocally reconstructed based on an origin from the posteroventral portion of the lateral surface of the coracoid in crocodylians and paleognathous birds and its position posterior to the origin of Biceps brachii in neognaths. As noted by Jasinoski et al. (2006), the posteroventral process of the coracoid in many theropods possesses a distinct subglenoid fossa that is the likely location for the origin of this muscle (Figure 2).

The insertion site of this muscle is also phylogenetically unequivocal, located on the anterior surface of the humerus distal to the proximal articular surface and extending onto the medial surface of the deltopectoral crest. In many theropods, including *Tawa*, there is a broad,

subtriangular depression in this area that covers most of the anterior surface of the humerus with a distally pointing apex that extends just distal to the end of the deltopectoral crest. This depression likely served as the insertion site of Coracobrachialis (Figure 3). In this position, the primary action of this muscle would have been protraction of the humerus.

Coracobrachialis longus (CBL)—The presence of this muscle is phylogenetically equivocal, as it is not present in crocodylians. Although Jasinoski et al. (2006) reconstructed this muscle as unequivocally present based on the report of its presence in crocodylians by Nicholls and Russell (1985), they themselves did not find the muscle in any of their dissections, nor has the muscle or anything fitting its description been reported in any other discussion of crocodylian musculature (Romer, 1944; Holmes, 1977; Cong et al., 1998; Dilkes, 2000; Meers, 2003). In the face of this evidence, I regard the Coracobrachialis longus to be not typically present in crocodyliforms. Furthermore, the homology of the Coracobrachialis posterior of neognathous birds and the Coracobrachialis longus of lepidosaurs is uncertain. The muscle known as Coracobrachialis posterior in birds is a derivative of the Subcoracoideus muscle and part of the dorsal muscle mass (Sullivan, 1962), whereas the Coracobrachialis longus of lepidosaurs is related to the Biceps brachii and Supracoracoideus and is part of the ventral muscle mass (Romer, 1944). Thus these two muscles are not regarded as homologous, and reconstruction of Coracobrachialis longus in theropods becomes a Level II′ inference based on its status as a novel muscle in neognathous birds.

Scapulohumeralis posterior (SHP)—Scapulohumeralis posterior originates from the posteroventral part of the lateral surface of the scapular blade in both crocodylians and birds. The origin in birds is typically much more extensive distally than that of crocodylians, but in *Struthio* the origin is restricted to a narrow area along the posteroventral edge near the glenoid that closely matches the condition in crocodylians (Jasinoski et al., 2006). In crocodylians the origin of Scapulohumeralis posterior also wraps around the posteroventral edge of the scapula near the glenoid and inserts in the area ventral to the medial ridge of the scapula (Meers, 2003). *Tawa* possesses a similarly small area ventral to the medial ridge (see above), so the origin may have extended onto the medial surface in basal theropods as well (Figure 2).

The insertion of Scapulohumeralis posterior is unequivocally on the posterior surface of the proximal humerus. Although it can be extensive in some crocodylians (Meers, 2003), a more restricted insertion on the posterior surface of the internal tuberosity, similar to the insertion area in birds, has also been reported (Jasinoski et al., 2006). Similar to that of some dromaeosaurids, the humeri of *Tawa* all have an oval depression on the posterior surface of the internal tuberosity that may correspond to the insertion site of this muscle (Figure 3). In this position Scapulohumeralis posterior would have acted to retract the humerus.

Scapulohumeralis anterior (SHA)—Scapulohumeralis anterior is reconstructed in nonavian theropods based on its presence in birds (including tinamous) and lepidosaurs, although it has been lost in extant crocodylians and ratites (Jasinoski et al., 2006). In most lepidosaurs this muscle is composed of two parts, and the origin of this muscle in birds on the scapular blade near the glenoid cavity most closely matches with the short-fibered part of this muscle in lepidosaurs. The absence of the long-fibered part of this muscle in chameleons is related to increased humeral mobility relative to terrestrial forms (Jasinoski et al., 2006), and it is likely that this is also the case in nonavian theropods. Jasinoski et al. (2006) assigned the origin of Scapulohumeralis anterior in dromaeosaurids to a small oval rugosity on the posteroventral portion of the scapular blade. No such scar exists among early theropods, but both *Herrerasaurus* (PVSJ 53) and *Sanjuansaurus* (PVSJ 605) possess a weak fossa on the posteroventral part of the scapular blade dorsal to the insertion area of Triceps brachii scapularis (see below) that may represent the area of origin for this muscle (Figure 2).

The insertion of Scapulohumeralis anterior in both birds and lepidosaurs is tendinous in a relatively small area on the posterior surface of the proximal end of the humerus, although it inserts farther laterally in lepidosaurs than in birds (Jasinoski et al., 2006). Unfortunately there is no osteological correlate for the insertion of this muscle in nonavian theropods as there is in birds (pneumatic fossa). In this study it is reconstructed as inserting just distal and lateral to the insertion of Scapulohumeralis posterior and medial to a ridge that extends down the posterior side of the proximal end of the humerus from the middle of the posteriorly projecting humeral head (Figure 3). The action of Scapulohumeralis anterior would have primarily been to retract the humerus.

Deltoideus clavicularis (DC)—The reconstruction of Deltoideus clavicularis is not straightforward due to the morphology of its homolog in birds, Propatagialis. This homology is supported by the embryological origin of Propatagialis from the Deltoideus group musculature (Howell, 1937; Sullivan, 1962). Deltoideus clavicularis is not homologous with the avian Deltoideus minor as suggested by Diogo and Abdala (2010) (who erroneously ascribed this homology hypothesis to Dilkes (2000)) because Deltoideus minor is developmentally part of the ventral muscle mass, as opposed to the rest of the Deltoideus musculature, which is part of the dorsal muscle mass (Sullivan, 1962). Meers (2003) suggested that Propatagialis is homologous to the crocodylian Humeroradialis, but there is no other published evidence for this hypothesis. Propatagialis is a highly modified muscle relating to the propatagium of the avian wing, and may consist of more than one belly or tendon of insertion (George and Berger, 1966). Crocodylians and some birds share a common area of origin on the scapula on or near the anterior edge of the acromion process, so I reconstruct the Deltoideus clavicularis as taking origin from the anterior edge of the acromion process and acromial expansion in early theropods. This differs from the reconstruction of Jasinoski et al. (2006) who placed the origin in the subacromial depression. The origin of Deltoideus clavicularis is nearly linear and restricted to the anterodorsal edge of the acromion process in all of the extant taxa studied, and I have found no evidence for the extension of this attachment site onto the lateral surface of the scapula ventral to the acromion process. Instead, the dorsal edge that bounds this depression likely represents the ventral extent of this muscle onto the scapula (Figure 2). In birds, this muscle also originates from the dorsal surface of the furcula (clavicle), and this area of origin is also present in lepidosaurs (Jasinoski et al., 2006), suggesting that it has been independently lost in modern crocodylians. Although there is no furcula preserved in *Tawa*, furculae are known for many theropods including *Coelophysis* (Rinehart et al., 2007; Nesbitt et al., 2009b), and so the origin of Deltoideus clavicularis is reconstructed as extending onto the hypothetical furcula in this taxon.

The avian Propatagialis has a primary insertion in the region of the carpus in birds, which is highly modified from the state exhibited by its homolog in crocodylians and lepidosaurs. However, the fleshy belly itself extends only to the distal end of the deltopectoral crest in most birds, the rest of the length being composed of a long tendon (George and Berger, 1966). The

insertion of Deltoideus clavicularis in crocodylians is broadly on the lateral surface of the deltopectoral crest, a position that is filled by the homolog of Deltoideus scapularis in birds (see below). In *Iguana*, as in most lepidosaurs, Deltoideus clavicularis and Deltoideus scapularis share a small area of insertion on the lateral surface of the deltopectoral crest, but the insertion morphology of the more basal *Sphenodon* closely resembles that of crocodylians (Dilkes, 2000). Thus, the insertion of Deltoideus clavicularis is here reconstructed as occupying a relatively large area on the lateral surface of the deltopectoral crest, posterior to the insertion of the Supracoracoideus musculature. In many theropods, including *Tawa*, this area is set off from the humeral shaft by a low ridge, indicating the posterior extent of this muscle in these taxa (Figure 3). In this position, Deltoideus clavicularis would have acted to abduct and slightly protract the humerus.

Deltoideus scapularis (DS)—As with Deltoideus clavicularis, the avian homolog of Deltoideus scapularis is modified relative to its morphology in crocodylians and lepidosaurs. Its origin has shifted proximally from the primitive location of a broad area on the lateral surface of the distal half of the scapula to a position on the acromion process, near the origin of the Deltoideus clavicularis homolog (Jasinoski et al., 2006). Due to the specialized attachment of the Deltoideus clavicularis homolog on the carpus, Deltoideus scapularis assumes its functional role in birds. As a result, its actions as an abductor of the humerus are diminished, but this is compensated by the development of Supracoracoideus. In basal nonavian theropods, where the primitive attachments of Deltoideus clavicularis are retained and Supracoracoideus is not modified to provide strong humeral abduction (see above), it is unlikely that the origin of Deltoideus scapularis would take the proximal position seen in birds. Furthermore, the broad, distally flaring scapula provides a large potential area of attachment for this muscle. Thus, this muscle is reconstructed as originating on the lateral surface of the distal end of the scapula (Figure 2).

In crocodylians and *Sphenodon,* Deltoideus scapularis inserts in a small area on the posterior surface of the proximal end of the humerus, just distal to the greater tubercle (Dilkes, 2000). The insertion in birds is shifted distally, covering most of the lateral surface of the deltopectoral crest and in some cases extending down the humeral shaft to the ectepicondylar

process (George and Berger, 1966). Following the reconstruction of the origin of this muscle as in crocodylians, the insertion is also reconstructed in the more primitive position. In *Tawa* there is a small, oval depression containing striations in this location that likely represents a scar for this muscle (Figure 3). Deltoideus scapularis would have acted to abduct and retract the humerus.

Triceps brachii (TB)—Although Triceps brachii can be unambiguously reconstructed, the number of heads that it possessed is equivocal phylogenetically. Birds and crocodylians both have the scapular and medial heads, but the coracoid head is vestigial in birds and the lateral head has been completely lost.

The origin of Triceps brachii caput scapulare (TBS) is conserved across archosaurs and lepidosaurs. It has a tendinous origin from a small area just posterodorsal to the scapular lip of the glenoid fossa, often associated with a scar in the form of a rugose tubercle (Jasinoski et al., 2006). A rugosity in this area is variably developed across Theropoda and, although no distinct tubercle appears in this position in *Tawa*, the area is lightly striated (Figure 2).

Although Triceps brachii caput coracoideum (TBC) can be found in some neognathous birds, the muscle belly is extremely reduced and thought to possibly function as a mechanoreceptor in the wing (Vanden Berge and Zweers, 1993). The tendon of origin of this muscle originates from a ligamentous band, called the sternoscapular ligament in birds, which connects the scapula, sternum, and sometimes the coracoid (George and Berger, 1966). Much larger in crocodylians, this muscle has a similar origin from the section of the medial scapulosternal ligament that connects the coracoid and scapula (Jasinoski et al., 2006). This origin is also found among lepidosaurs, although development of the muscle is variable (Russell and Bauer, 2008). As has been suggested for dromaeosaurids, Triceps brachii caput coracoideum may have already been vestigial or absent in basal theropods based on evidence from chameleons, in which this muscle has been lost to improve humeral mobility (Jasinoski et al., 2006).

Triceps brachii caput mediale (TBM) has a wide, fleshy origin on the posteromedial surface of the shaft of the humerus in both birds and crocodylians, although the exact boundaries of the origin are slightly variable. In both taxa the medial head of the triceps is bifid proximally, extending on either side of the insertion of Scapulohumeralis posterior (in crocodylians) and

anterior (in birds; Jasinoski et al., 2006). It extends distally until the humeral shaft begins to flare and almost completely covers the humeral shaft except at its anterolateral margin (Figure 3). There are no muscle scars associated with the origin of Triceps brachii caput mediale in theropods.

Jasinoski et al. (2006) did not reconstruct Triceps brachii caput laterale (TBL) as present in dromaeosaurids based on the lack of a clear lateral triceps ridge as is seen in crocodylians (Meers, 2003). However, a ridge in this area, used to define the posterior border of Deltoideus clavicularis (see above) is found in many other theropods, including *Tawa*, and likely represents the linear area of origin for this head of triceps (Figure 3).

All three heads of Triceps brachii coalesce into a single tendon that inserts on the olecranon process of the ulna. Although *Tawa*'s olecranon is short, it does have faint striations on its posterior surface, indicating the point of insertion of this muscle (Figure 4). Triceps brachii would have acted as the primary extensor of the antebrachium, as well as contributing to the extension of the humerus.

Biceps brachii (BB)—The primary head of Biceps brachii, originating from the coracoid, was unequivocally present in nonavian theropods, but the presence of a secondary head originating from the humerus is ambiguous phylogenetically. Of the study taxa, only neognathous birds possess a humeral head of biceps; in reptiles that do have two heads, both heads typically arise from the coracoid, one tendinously and the other fleshily (Diogo and Abdala, 2010). The tendinous origin of biceps from the coracoid is typically located on a tubercle anterior to the glenoid fossa in both crocodylians and birds, and the coracoid tubercle of theropod dinosaurs has generally been accepted as the site of origin for this muscle. Although there is some debate, it seems likely that the assignment of this tubercle as the origin of Biceps brachii is correct (for a review see Jasinoski et al., 2006). Further evidence is provided by tracing evolutionary changes in the morphology of the coracohumeral/acrocoracohumeral ligament, which attaches very near the origin of Biceps brachii in both crocodylians and birds (Baier et al., 2007). Typically, early theropods do not have prominent or even distinct coracoid tubercles (e.g., *Coelophysis*, *Syntarsus*) but the attachment site in these taxa would likely have been located anterior to the glenoid and just dorsal to the subglenoid fossa (Figure 2). The humeral head of

biceps in birds takes its origin from a round area on the anterior surface of the internal tuberosity (Jasinoski et al., 2006), and the presence of the secondary attachment is supported in nonavian theropods by an oval, striated depression in this area in *Tawa*, as well as similar rugosities and depressions in many other theropods (Figure 3).

Biceps brachii inserts on the proximal ends of the radius and ulna in birds and in lepidosaurs, where the pattern is highly consistent across taxa (Russell and Bauer, 2008). In crocodylians, it is typically described as only possessing a radial insertion (Cong et al., 1998; Meers, 2003; Jasinoski et al., 2006), although a secondary attachment to the ulna has been reported (Reese, 1915). Based on the outgroup bracket provided by lepidosaurs, an ulnar insertion for biceps is reconstructed in nonavian theropods. These insertions do not typically leave a distinct scar on either bone in the extant taxa, but in *Tawa* there is a slight bulge on the anterior edge of the ulna just distal to the articular surface that likely corresponds to this attachment (Figure 4). The primary action of Biceps brachii would have been to flex the antebrachium.

Humeroradialis (HR)—The homology of the crocodylian Humeroradialis is uncertain and controversial. It is sometimes considered to be a neomorphic archosaurian muscle (Meers, 2003; Diogo and Abdala, 2010), but it has also been homologized with the muscle of the same name in *Sphenodon* (Romer, 1944). Both of these muscles appear to be embryological derivatives of the deltoid muscle mass, although Humeroradialis in *Sphenodon* may have a compound origin as evidenced by the dual innervation pattern of this muscle (Russell and Bauer, 2008). Its potential origin from the deltoideus musculature is likely the reason it has been homologized to Propatagialis (tensor propatagialis) in birds (Meers, 2003), but because these muscles share neither a common origin nor insertion, here Propatagialis is considered to be the homolog of Deltoideus clavicularis (see above). Sullivan (1962) identified a distal portion of the developing deltoid lobe in an early stage chicken embryo as possibly a transitory vestige of Humeroradialis, but this portion is not retained in the adult.

The presence of Humeroradialis in nonavian theropods was inferred by Jasinoski et al. (2006) based on the presence of a rugose tuberosity distal to the deltopectoral crest on the lateral surface of the humeral shaft in maniraptorans, which corresponds to scars for this muscle found

on the humeral shafts of crocodylians in this position. Unfortunately a scar, in this area is rare in more basal taxa, although a small rugosity anterior to the furrow for Latissimus dorsi is present in one specimen of *Herrerasaurus* (PVSJ 407), and may represent an origin scar for Humeroradialis (Figure 3). The insertion of this muscle in crocodylians is marked by a distinct tubercle (Meers, 2003), and some nonavian theropods (e.g., *Herrerasaurus*, PVSJ 373) exhibit a small tubercle on the anterior surface of the radius near its proximal end. This likely represents the insertion of this muscle (Figure 4). Because the theropod Humeroradialis is reconstructed here following the morphology seen in crocodylians, the ligamentous sling on the proximal radius that redirects the insertion tendon of this muscle at the elbow (Meers, 2003) is also reconstructed. The action of Humeroradialis would have been to flex the antebrachium, although the presence of the ligamentous sling displaces the line of action distally, resulting in a primary role as a fast flexor of the forearm.

Brachialis (BR)—In all birds, Brachialis originates from the Fossa musculus brachialis, an impression on the cranial surface of the distal end of the humerus just proximal to the condyles (Baumel et al., 1979). This contrasts with its elongate origin from the distal part of the deltopectoral crest extending along much of the anterolateral surface of the humeral shaft in crocodylians (Meers, 2003), lepidosaurs (Russell and Bauer, 2008), and turtles (Walker, 1973). The anterior intercondylar depression, present in many theropod dinosaurs, may be evidence for the distal migration of this muscle in nonavian theropods. However, this feature is absent or poorly developed in basal theropods such as *Tawa* and *Herrerasaurus*, indicating that they retain the more proximal origin of Brachialis (Figure 3).

Brachialis inserts in common with Biceps brachii on the proximal ends of the radius and ulna in crocodylians and lepidosaurs, whereas it is restricted to the proximal end of the ulna in birds, leaving a distinct Impressio brachialis in most taxa. There is no evidence of an anterior ulnar depression in theropods, so the Brachialis is reconstructed as inserting as in crocodylians (Figure 4). In this position its action would have been to flex the forearm.

Antebrachial Musculature

Anconeus (AN)—This muscle of the dorsal division originates on the ectepicondyle of the humerus and inserts on the anterolateral surface of the ulna. Its presence in nonavian theropods is phylogenetically unequivocal. In birds it is known as Ectepicondylo-ulnaris (Vanden Berge and Zweers, 1993), and Meers (2003) refers to it as Flexor ulnaris (Table 1). Developmentally, it is closely connected to Extensor carpi ulnaris, which it is fused to for all or part of its length in some taxa (Haines, 1939; Sullivan, 1962). It is present in *Sphenodon* (Miner, 1925; Haines, 1939), but has been lost in other squamates (Russell and Bauer, 2008).

The origin of Anconeus is the most distal on the ectepicondyle in all taxa studied, with the exception of those in which it shares a tendon of origin with Extensor carpi ulnaris. The fusion of the tendon with Extensor carpi ulnaris is ancestral for Aves, with a 0.820 proportional likelihood at the node at the base of the clade. Unfortunately, there is little resolution on this point on the other side of the tree because crocodylians lack Extensor carpi ulnaris, Anconeus is absent in Squamates, it is almost entirely fused to Extensor carpi ulnaris in turtles (Haines, 1939; Walker, 1973; Abdala et al., 2008), and both states have been reported in *Sphenodon* (Miner, 1925; Haines, 1939), leaving the proportional likelihoods at exactly 0.50 at the base of the archosaur clade. Based on these likelihoods, I tentatively reconstruct the muscle as arising from the ectepicondyle along with ECU in basal theropods (Figure 3). Regardless, the muscle possesses a very distally located origin that is closely associated with that of ECU.

Anconeus can be reconstructed unequivocally as inserting fleshily on the lateral surface of the ulna starting just distal to the proximal articular surface and extending for most of its length, with a proportional probability of near 1.0 for both nodes. In *Tawa*, a prominent ridge on the lateral surface of the ulna beginning at midshaft and extending to the distal end provides a distinct surface for the distal extent of Anconeus and separates its insertion from the origin of Extensor carpi radialis brevis (Figure 4). The action of Anconeus would have been to flex the forearm.

Extensor carpi ulnaris (ECU)—This muscle is one of the only antebrachial muscles that is nearly always referred to by the same name, although its homologies in archosaurs are not straightforward due to the general uncertainty of the homology of some crocodylian extensor

musculature. Crocodylians possess a dorsal division muscle that arises from the middle of the ectepicondyle and inserts on the base of metacarpal II, with variable extensions to the bases of metacarpals I, III, IV and the radiale (Ribbing, 1907; Haines, 1939; Cong et al., 1998; Meers, 2003). Although Meers (2003) identified this muscle as Extensor carpi ulnaris, other authors have homologized this muscle with Extensor digitorum longus [communis] (Ribbing, 1907; Haines, 1939; Cong et al., 1998), which inserts on the bases of the metacarpals in most tetrapods. Adding to the confusion, the insertion of Extensor carpi ulnaris in many neognathous birds has shifted to a process at the base of metacarpal II, hinting that this may be a derived feature among archosaurs if the crocodylian muscle is indeed ECU. However, in paleognaths the ECU inserts on the base of the lateralmost metacarpal (III), which is also one of the major insertions in lepidosaurs (see below). This distribution of states suggests that insertion on the lateralmost metacarpal, not metacarpal II, is the plesiomorphic state. In the absence of a developmental study on the forelimb musculature in crocodylians that could shed light on the affinities of the crocodylian muscle in question, I adopt the homology of earlier authors in assigning it to Extensor digitorum longus and coding ECU as absent in crocodylians.

As discussed above, the separation of the origins of Anconeus and Extensor carpi ulnaris is somewhat equivocal in theropods, though their close proximity even when separate does not allow for much variability in the reconstruction of their origins as the most distal muscles on the humeral ectepicondyle (Figure 3). A secondary tendon of origin from the proximal ulna, as seen in some birds (George and Berger, 1966), is very unlikely (proportional probability of presence of 0.040). Extensor carpi ulnaris tends to insert to multiple areas around the carpus; in lepidosaurs, its insertion tendon attaches to both the pisiform and lateral edge of the lateralmost metacarpal (Russell and Bauer, 2008), although *Varanus* also has an attachment to the ulnare (Haines, 1939). In turtles, ECU inserts on the pisiform and the ulnare, but not on the lateral-most metacarpal (Haines, 1939; Walker, 1973). Birds lack a pisiform and the ulnare of birds is not homologous to the ulnare of other tetrapods because it is a de novo ossification (Kundrát, 2009), so ECU in birds does not share any of these insertion points. As mentioned above, although ECU inserts at the base of metacarpal II in many neognaths, it inserts at the base of metacarpal III in paleognaths (Parker, 1891; pers. obs.; Hudson et al., 1972) and there appears to be a reversal to

insertion on metacarpal III in Passeriformes (proportional probability of 0.934; Hudson and Lanzillotti, 1955; Berger, 1956; George and Berger, 1966; Raikow, 1977; McKitrick, 1985). The proportional likelihoods at the base of Aves provide moderate support for insertion on metacarpal III, the lateralmost metacarpal (proportional probability of 0.650). Thus, insertion on the lateralmost metacarpal is unequivocal, but insertion on any carpals is phylogenetically equivocal. Because *Tawa* retains a full complement of carpals including a pisiform, I infer ECU to also insert on the pisiform as well as the lateralmost metacarpal, as in lepidosaurs (Figure 5). Upon the loss of the pisiform in the theropod wrist, ECU likely lost that insertion but retained the insertion on the base of the lateralmost metacarpal, as seen in some birds. With these attachment points, the action of ECU would have been extension and abduction of the wrist, along with slight extension of the forearm.

Supinator (SU)—Sometimes called Tractor radii in the older literature (Table 1), Supinator is a muscle of the dorsal division that originates on the ectepicondyle of the humerus and inserts on the shaft of the radius. In turtles, lepidosaurs, and crocodylians its origin is consistently the most proximal of the dorsal division muscles, often extending beyond the boundary of the ectepicondyle onto the shaft of the humerus (Haines, 1939). Alternately, in birds, Supinator has a much more distally located origin near that of Extensor digitorum longus, whereas the Extensor carpi radialis takes its place proximally, an arrangement that is consistently found across all of the bird taxa in this study. This leaves the proportional probabilities of the two states exactly opposite at the nodes surrounding Dinosauria. The avian conformation of these muscles is an adaptation for the specialized automating musculoskeletal mechanisms of the wing (see below; Vazquez, 1994), so I tentatively reconstruct the origin of Supinator as the most proximal on the ectepicondyle in basal theropods (Figure 3). In this case, a more proximal origin would have improved the function of Supinator as a flexor by lengthening its lever arm.

The insertion area of Supinator is located on the anterolateral surface of the radius for most of its length in all turtles, lepidosaurs, and crocodylians, and in all but a handful of derived avian species. Therefore, the insertion of Supinator in theropods can be unequivocally reconstructed on the anterolateral surface of the radius for greater than half its length (proportional probability of 0.999). The degree to which the insertion is oriented anteriorly or

laterally on the shaft of the radius varies slightly and depends on the anatomical position of the bones, but both birds and crocodylians typically possess an almost entirely anteriorly located supinator insertion (George and Berger, 1966; Meers, 2003). Reconstruction of this position in basal theropods is supported by the flat anterior surface of the radius, bounded by low ridges running the length of the bone, seen in *Tawa* (Figure 4). The action of Supinator in basal theropods would have been be to flex and supinate the forearm.

Extensor carpi radialis (ECR)—The origin of Extensor carpi radialis longus and its relationship to those of other dorsal division muscles is exactly the inverse of Supinator: in turtles, lepidosaurs, and crocodylians the origin is located between that of Supinator and Extensor digitorum longus, whereas in birds the origin is more proximally located than the other muscles arising from the ectepicondyle. This is taken to the extreme in some birds, which possess an anteriorly projecting Processus supracondylaris dorsalis onto which the ECR attaches (Baumel et al., 1979). The ECR is an important part of the automatic musculoskeletal mechanism for flexion and extension of the wrist and elbow in the avian wing, and the proximally shifted attachment of this muscle allows for slight extension of the elbow to fully extend the manus (Vazquez, 1994). As such, it is likely that this conformation of the origin evolved alongside the modification of the avian wrist and, as such, was not present in basal theropods. It is reconstructed here in a position similar to that of crocodylians, lepidosaurs, and turtles on the ectepicondyle (Figure 3). In some birds, a second fleshy head of origin is present arising just distal to the main tendon (George and Berger, 1966); this may represent the remnant of the Abductor radialis muscle, which has been lost in birds (see below).

The insertion of ECR is phylogenetically equivocal because an insertion on the radiale as in lepidosaurs and crocodylians is not retained in birds, where it inserts on the carpometacarpus in the vicinity of the base of metacarpal I, no doubt due to the highly derived state of the avian wrist. The wrists of basal theropod dinosaurs such as *Tawa* possessed a plesiomorphic morphology that is more similar to those of lepidosaurs than either crocodylians or birds, so retention of the plesiomorphic insertion of ECR on the radiale is inferred here (Figure 5). The action of the ECR in basal theropods would have been to extend and adduct the wrist as well as contribute to flexion of the forearm.

Abductor radialis (AR)—The nomenclature of this muscle is confusing and varied due to its developmental origin in the extensor group of muscles but its lack of function as an extensor. It originates on the humeral ectepicondyle in close proximity to the origin of Extensor carpi radialis and its affinity with this muscle has led to its designation in many publications as Extensor carpi radialis intermedius and/or profundus (e.g., Russell and Bauer, 2008), despite the fact that it has no action on the carpus. It also has been referred to as Extensor antebrachii radialis (Diogo and Abdala, 2010), but this is misleading because it implies that the muscle is an extensor of the antebrachium. I adopt the terminology of Meers (2003), who describes the action of the muscle for most tetrapods in which it is present. Although this muscle possesses two parts in lepidosaurs and some turtles (Haines, 1939; Walker, 1973; Russell and Bauer, 2008), it has only one belly in crocodylians (Meers, 2003). In birds, ECR sometimes possesses a second head at its origin that joins the main belly not long after origin (George and Berger, 1966); although it does not attach to the radius, it is likely that this head represents a remnant of Abductor radialis, which has itself been referred to as a division of ECR in other taxa. This, along with the presence of only a single belly in crocodylians, indicates a general reduction of this muscle in archosaurs, and results in a phylogenetically unequivocal origin of a single belly in close proximity to ECR on the ectepicondyle (Figure 3). The insertion of Abductor radialis remains equivocal due to its fusion distally to ECR in birds. Functionally, the robust forelimb morphology of basal theropods would have been best served by insertion on the proximal half of the lateral surface of the radius (Figure 4), where it would have a stabilizing function similar to that in crocodylians (Meers, 2003). The action of Abductor radialis would have been to abduct and slightly flex the forearm.

Abductor pollicis longus (APL)—This muscle is another that has been given many very different names in the literature (Table 1); for theropods I have adopted one of the more common designations, which describes one of the primary actions of this muscle. The origin of APL is phylogenetically unequivocal and is synapomorphic for Archosauria. In lepidosaurs and turtles the muscle arises only from the shaft of the ulna (Haines, 1939; Russell and Bauer, 2008), but crocodylians and birds both possess a second head of origin from the shaft of the radius, making the muscle bipennate (George and Berger, 1966; Meers, 2003). This has been reversed in Passeriformes (Swinebroad, 1954; Hudson and Lanzillotti, 1955; Berger, 1956; George and

Berger, 1966; Raikow, 1977), but the radial head is present in all other birds studied. The proportional probability of presence of the radial head at the Archosaur node is 0.955, thus the APL unequivocally originated from the facing surfaces of the radius and ulna in *Tawa* (Figure 4).

Although birds possess the derived origin of APL, they retain the plesiomorphic insertion site on the medial side of the base of metacarpal I, as in lepidosaurs and turtles (Walker, 1973; Russell and Bauer, 2008). Abductor pollicis longus (Extensor longus alulae) in birds inserts on the extensor process of the carpometacarpus, which is developmentally part of metacarpal I (Kundrát, 2009). This insertion is not shared by crocodylians, in which the insertion tendon attaches to the radiale (Haines, 1939; Meers, 2003). Phylogenetic inference strongly suggests that this is a derived state within the clade, with a proportional likelihood of 0.980 at the base of Archosauria in favor of insertion on metacarpal I. Additionally, metacarpal I of *Tawa*, *Herrerasaurus*, and other basal theropods possesses a medial flange at the base that likely represents an insertion site similar to the extensor process in birds (Figure 5). With these attachments, the action of APL in basal theropods would have been extension and abduction of the wrist, and abduction of the first digit.

Extensor digitorum longus (EDL)—The origin of Extensor digitorum longus exhibits little variation in relation to the other muscles originating on the ectepicondyle of the humerus. In almost all taxa studied, it originates from approximately the middle of the ectepicondyle, between the origins of Extensor carpi ulnaris and Extensor carpi radialis or Supinator (proportional probability of near 1.0 at all nodes), and so it can unequivocally be reconstructed in this position in basal theropods (Figure 3). Its insertion, however, is less straightforward. Possibly representing the basal tetrapod condition (Haines, 1939), EDL inserts on the base of all five metacarpals in all of the turtle taxa studied with the exception of *Lissemys* (Shah and Patel, 1964), but insertion on the fifth digit is lost in all lepidosaurs and archosaurs (proportional probability of 0.995). All lepidosaurs and turtles possess insertion tendons for metacarpal IV, and attachment to this digit has also been reported in *Alligator mississippiensis* (see Reese, 1915; Haines, 1939). A similar pattern exists for attachment to digit III, except in this case an insertion on metacarpal III has also been reported for *Crocodylus acutus* (see Ribbing, 1907). An insertion at the base of metacarpal II is invariably present in all turtles, lepidosaurs, and crocodylians,

whereas insertion on the base of metacarpal I is only present in turtles (except *Lissemys*; Shah and Patel, 1964), *Sphenodon* (Miner, 1925; Haines, 1939), and *Crocodylus acutus* (see Meers, 2003). In the highly modified manus of birds, EDL inserts on both digits I and II, but on the base of phalanx I of these digits rather than the metacarpal. Phylogenetically, insertion on digits I and II is unequivocally supported, but other attachments remain equivocal. The manus of *Tawa* contains three functional digits and a highly reduced digit IV, thus functional inference supports insertion on metacarpal III as in lepidosaurs and some crocodylians (Figure 5). Because of the small size of digit IV, it is likely that the insertion on metacarpal IV was already lost in basal theropods. The action of EDL would have been to extend the wrist.

Pronator teres (PT)—Arising from the humeral entepicondyle and inserting on the radius, Pronator teres is present in all taxa used in this study. Its origin is consistently the most proximally located of all the ventral division muscles. In some neognaths such as Charadriiformes and Anatidae, the origin has migrated proximal to the borders of the entepicondyle (Hudson et al., 1969; Zusi and Bentz, 1978; Livezey, 1990), although the ancestral state slightly favors this reconstruction at the base of Neognathae (posterior probability of 0.528). Pronator teres arises from the entepicondyle itself in paleognaths, dropping the posterior probability of the proximal insertion to 0.082 at the base of Aves. Thus, phylogenetically its origin is unequivocally located on the entepicondyle in theropod dinosaurs; the ridge and small anterior projection at the proximal extent of the entepicondyle in *Tawa* probably represent the anteroproximal border of the origin (Figure 3).

Pronator teres has an elongate, narrow insertion on the anteromedial surface of the radius to varying extents in the taxa surveyed here. In turtles and most lepidosaurs, it inserts on less than half of the radius distally, though it has been reported to insert on the radius for most of its length in a variety of squamate taxa including *Varanus* and *Ctenosaura* (Straus, 1942; Haines, 1950; Russell and Bauer, 2008). This long insertion is also present in all of the crocodylians and paleognathous birds studied, as well as a seemingly random smattering of neognaths. A derived insertion on less than half of the radius proximally is present in many neognaths and is reconstructed as the most likely ancestral state in this clade (posterior probability of 0.677), although there is no clear pattern to its evolution. Phylogenetically, the insertion of Pronator teres

is unequivocally reconstructed in a line along the anteromedial shaft of the radius for greater than half of its overall length (posterior probability at both Aves and Archosauria nodes of 0.815). This is supported by the morphology of the radius in *Tawa*, which features a distinct anteromedial surface defined by ridges running the length of the radius (Figure 4). The action of Pronator teres would have been to flex the forearm and pronate the manus.

Pronator Accessorius (PA)—Attaching to the humeral entepicondyle and the anteromedial surface of the radius, Pronator accessorius serves a very similar function as Pronator teres. It is absent in crocodylians, *Sphenodon*, and paleognaths except for tinamous (Hudson et al., 1972), but present in squamates, turtles, and all neognaths studied. Its origin is consistently located more distally than that of Pronator teres, at the distal end of the entepicondyle near the origin of Flexor digitorum longus superficialis, and it is reconstructed with this morphology in *Tawa* (Figure 3).

The narrow insertion along the medial side of the radius is variable across the tree, however. In turtles it is consistently located distally for less than half of the length of the radius, and this state is present in some squamates such as *Varanus* and *Tetradactylus* (Haines, 1950; Berger-Dell'mour, 1983) where it is hypothesized to be primitive (Russell and Bauer, 2008). An insertion on the proximal end of the radius for less than half its length is present in some other lepidosaurs, including *Iguana* and *Liolaemus*, and a few neognaths (George and Berger, 1966; Abdala and Moro, 2006; Russell and Bauer, 2008), but the majority of birds have an insertion that extends for the most of the length of the radius. This distribution of character states causes the long insertion to be reconstructed at the base of Aves (posterior probability of 0.950), and the restricted distal insertion to be reconstructed at the lepidosaur + archosaur node (posterior probability of 0.878). There are unfortunately no osteological signals on the radius of *Tawa* to indicate the extent of the insertion of this muscle in basal theropods. To account for this uncertainty, I tentatively reconstruct the insertion on the distal end of the radius for slightly over half its length (Figure 4). In this position Pronator accessorius would have acted to flex and pronate the antebrachium.

Pronator quadratus (PQ)—Pronator quadratus of crocodylians, lepidosaurs, and turtles is likely homologous to the Ulnimetacarpalis ventralis of birds (Sullivan, 1962), although this is

not obvious due to the derived insertion site of Ulnimetacarpalis ventralis on the base of the carpometacarpus. This muscle originates from a line along the ventral/medial surface of the ulna in all taxa studied, but the proximal extent of its origin is variable. In crocodylians, lepidosaurs, and most turtles, Pronator quadratus arises from more than half of the length of the ulna (Walker, 1973; Meers, 2003; Russell and Bauer, 2008), whereas in birds it is typically restricted to the distal half or less (George and Berger, 1966). An elongate origin is found in the clade containing passeriforms and raptors as well as a few other birds, leaving a reduced distal origin in birds at a 0.834 posterior probability. The posterior probability of an elongate origin at the Archosauria node is 0.756, making the reconstruction of the proximal extent of this muscle a Level II′ inference. Given the distally displaced insertion of this muscle in birds, a distally shifted origin is not unexpected. It is unlikely that basal theropods possessed the derived avian morphology of the insertion (see below), so this muscle is reconstructed in *Tawa* with a proximally extensive origin covering most of the length of the ulna (Figure 4).

The insertion of this muscle in taxa other than birds is consistently on the ulnar-facing side of the ventral radius (Meers, 2003; Russell and Bauer, 2008). However, in some lepidosaurs and all turtles this insertion extends to the ventral surface of the carpals (Straus, 1942; Haines, 1950; Walker, 1973; Berger-Dell'mour, 1983), which is consistent with the insertion of this muscle onto the base of the carpometacarpus in birds. This attachment can be unambiguously reconstructed in basal theropods (posterior probability of its presence at the base of Archosauria of 0.783), having been secondarily lost in modern crocodylians. The retention of the radial attachment of Pronator quadratus in nonavian theropods is equivocal phylogenetically, but it was likely present because its absence in birds is a derived state relating to the evolution of the avian wing. Dissections of *Struthio* also revealed a double insertion of this muscle onto the distal end of the radius and the base of the carpometacarpus. Although this does not affect the equivocal results from the ancestral state reconstruction, it provides some further evidence that Pronator quadratus in nonavian theropods retained the radial insertion (Figures 4 and 5). In this position the primary action of Pronator quadratus would have been to pronate the antebrachium and manus.

Epitrochleoanconeus (EA)—This muscle, known as Entepicondylo-ulnaris in birds, is only present in turtles, lepidosaurs, galloanseriform birds, *Apteryx,* and tinamous. It is the mirror in the flexor compartment of Anconeus, arising from the entepicondyle of the humerus and inserting on the ventral surface of the ulna. In *Apteryx* it is largely fused to Flexor carpi ulnaris, and often cannot be distinguished from this muscle (McGowan, 1982). This is also true of most turtles, in which Epitrochleoanconeus is usually described as the deep or medial part of Flexor carpi ulnaris (Shah and Patel, 1964; Walker, 1973; Abdala et al., 2008). Reconstruction of its presence in nonavian theropods is phylogenetically unequivocal (posterior probability of presence at the Archosauria node of 0.863, presence at the base of Aves of 0.903), although the morphology of its origin is not. In turtles and lepidosaurs, this muscle has a close proximity with the origin of Flexor carpi ulnaris, sometimes arising from the same tendon, although an origin just proximal to that of Flexor carpi ulnaris is typical in lepidosaurs (Russell and Bauer, 2008). In birds this muscle typically takes origin from the tendon of Pronator accessorius, except in *Apteryx* where the muscle is not differentiated from Flexor carpi ulnaris (George and Berger, 1966). The posterior probability slightly favors the derived state at the base of Aves (0.527), so reconstructing the origin in either state is a Level II′ inference. I tentatively reconstruct the origin in *Tawa* to be located between the origins of Flexor carpi ulnaris and Pronator accessorius on the entepicondyle, similar to the morphology in lepidosaurs, which may represent an intermediate morphology between the two alternate states (Figure 3).

The extent of the insertion of Epitrochleoanconeus on the ventral/medial surface of the ulna is unequivocally restricted to its proximal half. In birds (except *Apteryx*) and most lepidosaurs, it inserts on only the proximal one-quarter to one-half of the ulna, whereas in turtles and *Apteryx* it inserts upon the majority of the length of the ulna; in *Sphenodon* and *Tetradactylus* it inserts only on the distal half (Miner, 1925). The proportional probabilities moderately favor the proximally restricted insertion (0.876 at the base of Aves, 0.698 at the Archosauria + Lepidosauria node), so it is reconstructed in this position in basal theropods as well (Figure 4). Epitrochleoanconeus would have acted to flex the antebrachium.

Flexor carpi ulnaris (FCU)—This muscle is found in every study taxon and has a relatively consistent morphology. Its tendon of origin is always the most distally located on the

humeral entepicondyle, arising from its posterior aspect just above the distal articular surface. It is sometimes comprised of multiple parts with separate origins in lepidosaurs (Straus, 1942; Abdala and Moro, 2006), but these do not seem to be related to the smaller second belly present in many birds, which possesses a novel attachment to the base of the secondary flight feathers (George and Berger, 1966). Thus, FCU in *Tawa* is reconstructed as arising from a single tendon on the posterodistal aspect of the entepicondyle (Figure 3).

The insertion of FCU is phylogenetically equivocal due to the modified avian wrist. In crocodylians and most lepidosaurs, FCU has a single tendinous insertion on the pisiform, which is joined by a secondary tendon inserting on the ulnare in most turtles and *Varanus* (Haines, 1950; Shah and Patel, 1964; Walker, 1973). The insertion in birds is also on the ulnare but, as mentioned above, this bone is neomorphic in birds and not homologous to the tetrapod ulnare, which disappears during development (Kundrát, 2009). With the loss of the two primary attachment areas, the insertion of this muscle would have shifted to the neomorphic avian 'pseudoulnare' to maintain its functional role. Because *Tawa* retains a full complement of carpals, including an ossified pisiform, I reconstruct FCU as attaching primarily to the pisiform, with a possible additional attachment to the (true) ulnare (Figure 5). It is unknown when the 'pseudoulnare' replaced the ulnare in the theropod wrist; Kundrát (2009) interpreted the ulnare of *Archaeopteryx* to be the avian pseudoulnare. Regardless, pseudoulnare is the functional analog of the ulnare and, as such, the shift in its identity does not change the functional role of FCU. The primary actions of this muscle would have been to flex and adduct the wrist.

Flexor digitorum longus (FDL)—Flexor digitorum longus is composed of two main parts, Flexor digitorum longus superficialis (FDLS), which originates on the humerus, and profundus (FDLP), which originates from the antebrachium. Both of these parts coalesce into a single set of tendons for insertion in the manus, so they are treated under one heading here.

Although the superficial head of FDL is absent in ratites (McGowan, 1982; dissections), it is present in all other birds including tinamous (Hudson et al., 1972), as well as in crocodylians. Thus, it is unambiguously reconstructed as present in nonavian theropods. It arises from a single tendinous origin on the entepicondyle of the humerus, sandwiched between the origins of Flexor carpi ulnaris and Pronator teres, in nearly all taxa studied; it is therefore

reconstructed in this position in *Tawa* (Figure 3). A second head of origin from the entepicondyle, as in some squamates (Straus, 1942; Russell and Bauer, 2008), or the ulna, as in a few bird taxa (Fisher and Goodman, 1955; Fitzgerald, 1969), are rare occurrences and are not likely to have been present in nonavian theropods (posterior probabilities of their absences of nearly 1.0 at both nodes).

An origin of FDLP from the ulna is present in all study taxa and thus phylogenetically unequivocal. FDLP arises from the ventral/medial surface of the ulna along most of its length; in crocodylians and lepidosaurs its extent is roughly equivalent with that of the origin of Pronator quadratus (Cong et al., 1998; Meers, 2003; Russell and Bauer, 2008), whereas in birds the two origins do not overlap and the distal extent of FDLP is limited by the proximal extent of PQ (George and Berger, 1966). The limited origin in birds may be related to the reduction of the FDL musculature as a result of the reduction of the digits in extant birds. *Tawa* retains a four-fingered hand, so the FDLP is reconstructed here with a full insertion, as is seen in crocodylians and lepidosaurs (Figure 4).

As mentioned before, the tendons of insertion of FDLS fuse with those of FDLP in all outgroup taxa and a somewhat random selection of neognathous birds. Although this state is present in less than half of the bird taxa sampled, the distribution is such that it is reconstructed as the most likely state at the base of Aves (posterior probability of 0.885). The joined tendons insert on the ventral surface of the terminal phalanx of all digits in lepidosaurs and turtles (Walker, 1973; Russell and Bauer, 2008). In crocodylians, which have somewhat reduced, non-ungual-bearing manual digits IV and V, the tendinous slips to these digits are typically lost (Ribbing, 1907; Meers, 2003) and a slip to digit IV has only been reported once (Cong et al., 1998). In the modified avian manus, the tendon of FDL typically inserts only onto the major digit, which is identified as digit II (Bever et al., 2011), although there are several notable exceptions. A tendinous slip to digit I, the alula, is found in tinamous (Hudson et al., 1972), *Struthio* (dissections), *Opisthocomus* (Hudson and Lanzillotti, 1964), *Balaeniceps* (Vanden Berge, 1970), *Coturnix* (Fitzgerald, 1969), and *Bubo* (dissections). Although this may represent a retention of the plesiomorphic state in paleognaths, its presence in some of these species is possibly functionally linked. The young of *Opisthocomus*, the Hoatzin, retain a functional,

clawed first digit that is used in climbing trees prior to fledging, potentially requiring flexor capacity in the first digit beyond that of most birds (Young, 1888; Beddard, 1889; Shufeldt, 1918). Despite the low number of avian taxa exhibiting this character, a slip to the first digit most likely occurs at the base of Aves (posterior probability of 0.882). An insertion slip to the third digit is found in all outgroup taxa but is not found in birds, with the exception of *Struthio*, where a small tendon to digit III was found in one dissected specimen. This does not appreciably affect the posterior probability of the presence of this slip at the base of Aves (0.043), making the reconstruction of it in basal theropods phylogenetically equivocal. However, the manus of *Tawa* possesses a well-developed, functional third digit that likely would have retained its insertion slip from FDL. The fourth digit of *Tawa* is very reduced, so this digit probably lacked a tendinous slip, as in crocodylians (Figure 5). FDL would have acted to flex the digits and the wrist in basal theropods.

Intrinsic Manual Musculature

The homologies of the muscles of the manus in birds are difficult and somewhat speculative **(e.g., Diogo and Abdala, 2010)**. The highly modified avian manus has undergone extensive fusion of metacarpal elements and reduction in number and size of phalanges, resulting in the reduction and loss of much of the intrinsic manual musculature. Nevertheless, these muscles control the independent movements of the manual digits, and reconstructing these muscles in nonavian theropods, even tentatively, is an important step in assessing the functional capabilities of their forelimbs. The hypotheses of homology used in this study are summarized in Table 2.

Extensores digitores breves (EDB)—Tetrapods have two layers of intrinsic extensor musculature, Extensor digitores breves superficiales (EDBS) and profundi (EDBP). Crocodylians, lepidosaurs and turtles all have EDB musculature that arises by way of separate muscle bellies from the proximal carpals (EDBS) and the metacarpals (EDBP). The superficialis and profundus bellies for each digit coalesce into a single tendon of insertion that attaches to the dorsal surface of the proximal end of each terminal phalanx in crocodylians and lepidosaurs (Meers, 2003; Russell and Bauer, 2008), although it only extends to more proximal phalanges in

most turtles (Shah and Patel, 1964; Walker, 1973). Crocodylians have a somewhat unusual arrangement of the EDBS origin sites, in which they are spread across the proximal carpals instead of being confined to the ulnare, intermedium, and/or distal ulna as in turtles and lepidosaurs (Haines, 1939). Thus although the origins of the lateralmost divisions are relatively conserved in the outgroup taxa, the medial divisions do not have consistent sites of origin.

In birds, the digital extensors attach to the first and second digits and consist of Extensor brevis alulae and Extensor longus digit majorus, which has both proximal and distal parts (Vanden Berge and Zweers, 1993). Additionally, the robust Ulnimetacarpalis dorsalis is likely a short extensor and not a homolog of Abductor digiti minimi (see below). Extensor brevis alulae originates from the dorsal surface of the extensor process of the avian carpometacarpus, which corresponds embryologically to the base of the first metacarpal (Kundrát, 2009). This is consistent with the origin of EDBP of digit I in all other taxa; a secondary origin from the adjacent surface of metacarpal II, seen primarily in 'gruiform' birds (e.g., Fisher and Goodman, 1955), has been reported in *Alligator* and *Sphenodon* (Haines, 1939), but is not likely to have been present in basal theropods (posterior probabilities of its absence are nearly 1 at both Aves and Archosauria nodes). There is little evidence for a superficial division of EDB to digit I in birds, however a second, more proximal belly arising from the radiale has been reported in *Geococcyx* (Berger, 1954) and a similar belly arising from the distal end of the radius and radiale has also been found in *Struthio* (dissections). Although the radial attachment of these bellies may have been secondarily gained in birds, they may also indicate that the arrangement of the EDBS musculature in crocodylians may be a shared derived feature for Archosauria.

Extensor longus digit majorus likely corresponds to the EDB divisions of digit II despite its proximally shifted origins. This muscle contains both proximal (superficialis) and distal (profundus) portions that join to form a single tendon that inserts on the dorsal surface of the distal phalanx of digit II. The proximal belly arises from the ulnar surface of the radius in all birds, although the length of the belly varies from nearly the entire length of the radius to being restricted to the distal third (George and Berger, 1966). This creates an entirely ambiguous character reconstruction at the archosaurian node, but the origin is still most closely aligned with that of crocodylians, from the radiale (Meers, 2003), than with an origin from the ulnare,

intermedium, or distal ulna as in lepidosaurs and turtles. When present, the distal belly of this muscle arises from various structures near the radiale in birds, but it is restricted to the dorsal surface of metacarpal II in some neognaths and in all paleognaths (Hudson et al., 1972; dissections). As with Extensor brevis alulae, this morphology is congruent with that of the EDBP belly of the corresponding digit in crocodylians and lepidosaurs. In these taxa the origin often extends onto the base of metacarpal I as well (Haines, 1939; Meers, 2003), and this may also be the case in birds when it arises from the base of the carpometacarpus, where it is impossible to delineate the borders of the metacarpals in most taxa.

Ulnimetacarpalis dorsalis has been suggested to be either a homolog for Abductor digiti minimi or a member of the short manual extensors (Diogo and Abdala, 2010), and I consider the latter hypothesis to be more strongly supported. This muscle is embryologically derived from the dorsal division of the manual muscles and is thus closely related to the extensor musculature of the manus (Sullivan, 1962), whereas Abductor digiti minimi is usually described as being in close association with the flexor musculature (Russell and Bauer, 2008; see below). Its proximally displaced origin from the distal end of the ulna suggests that it pertains to the EDBS musculature but, unlike other EDB musculature, it only extends to insert on the lateral surface of metacarpal III (George and Berger, 1966). Although it would seem to correspond to EDB of digit III, embryologically it is associated with the primordium of digit IV, which is resorbed later in development (Sullivan, 1962; Kundrát, 2009). EDBS of digit IV has been reported as arising from the distal end of the ulna in crocodylians (Ribbing, 1907), and EDBS of digit V arises from the distal end of the ulna in all crocodylians (Ribbing, 1907; Haines, 1939; Meers, 2003). Although EDBS of digits IV and V both retain a distally located insertion on the terminal phalanges, the insertion of EDBP in digit V is shifted to metacarpal V in crocodylians, in which this digit is reduced (Meers, 2003). Whether this muscle pertains to the EDB slips of digit III, IV, or V, its proximal insertion on the shaft of metacarpal III may be a result of the reduction and/or loss of these three digits in birds.

The general similarities of the extensor musculature of the first two to three digits in birds to the organization of the crocodylian musculature suggests that the morphology of the EDB musculature in basal theropods was similar to that of the crocodylian manus. It is unlikely that

Tawa lacked EDB divisions to either the large third digit or the reduced fourth digit, because small bellies of EDB are still found in the reduced fifth digit of modern crocodylians as well as in the reduced digits of some lepidosaurs (Berger-Dell'mour, 1983; Meers, 2003). However, the EDBP belly to digit IV may have exhibited an insertion on the metacarpal rather than the terminal phalanx, as in crocodylians and possibly birds (Meers, 2003). The areas of origin of EDBS in early theropods are somewhat equivocal but based on evidence from the avian manus, I reconstruct the divisions for digits I and II as arising from the dorsal surface of the radiale and the divisions for digits III and IV as arising from the dorsal surface of the ulnare in *Tawa* (Figure 5). Origins for the EDBP divisions are more conserved; in all taxa the bellies associated with each digit arise from their metacarpals, and extend onto the base of the metacarpal medial to it in most crocodylians, lepidosaurs and possibly in some birds. Thus, this morphology is reconstructed for EDBP for all digits in *Tawa* (Figure 5). The insertion of this musculature can unequivocally be reconstructed as on the dorsal surface of the proximal end of the distal phalanges (unguals). In *Tawa*, an oval, lightly striated area on the dorsal surface of all three manual unguals likely represents the insertion area (Figure 5). In *Tawa*, EDB would have acted to extend the metacarpophalangeal and interphalangeal joints of the digits.

Flexores digitores breves (FDB)—Like the extensors, the short flexor musculature of the hand is divided into superficialis and profundus layers but, unlike the extensors, these two layers maintain separate insertions on the phalanges. Additionally, many tetrapods possess an assortment of smaller muscles related to FDB that vary between and sometimes within clades. These muscles are sometimes called Flexor digitorum brevis intermedius or Contrahentes digitorum and typically originate on the medial side of the carpus and insert on the fourth and/or fifth digits. Due to their variable nature, the reconstruction of these muscles would be highly speculative in extinct taxa. Furthermore, these muscles may have been lost in the manus of *Tawa*, which lacks a fifth digit and has a highly reduced fourth digit, as they have in lizards that exhibit a similar morphology (Berger-Dell'mour, 1983). Thus, in this reconstruction I will focus on the two major layers of this muscle group, FDBS and FDBP.

The only likely avian homolog for FDBS is Flexor alulae, which arises from the base of the carpometacarpus and the tendon of FDL. This is nearly identical to the origin of these

muscles in crocodylians, where they arise from the distal carpals and the tendon of FDL (Meers, 2003). In lepidosaurs and turtles, these muscles take their origin entirely from the annular ligament covering the carpals, but this ligament is absent in extant birds and crocodylians due to the modified wrists in both taxa. The wrist of *Tawa* was more similar in morphology to that of a lepidosaur than to those of either modern birds or crocodylians, and it is likely that the annular ligament was retained in it and other basal theropods with unmodified wrists. This would allow the origin of the FDBS divisions to originate on this ligament in the basal taxa, shifting to an origin from the distal carpals upon later modification of the theropod wrist. Although *Tawa* possessed a very primitive carpus, I have reconstructed origins for the FDBS muscles on the distal carpals, which may also be an archosaurian synapomorphy (Figure 5).

The distal tendons of the FDBS muscles bifurcate to allow passage of the tendons of FDL and then either rejoin to form a single tendon of insertion (lepidosaurs; Russell and Bauer, 2008) or insert separately on either side of the flexor processes of the first phalanx of digits I and II, and the second phalanx of digit III, as in crocodylians and turtles (Walker, 1973; Meers, 2003). The exception to this trend is FDBS of digit I, which does not have a bifid tendon in lepidosaurs or birds, and inserts simply on the ventromedial side of the base of the first phalanx of digit I. The reconstruction of this morphology is favored at the base of Archosauria (posterior probability of 0.786), so it is reconstructed that way in *Tawa* (Figure 5).

The bellies of FDBP variously arise from the distal carpals and the ventral surfaces of the metacarpals and insert near FDBP on the flexor process of the first phalanx in crocodylians, lepidosaurs, and turtles. In birds, each digit of the manus has retained its division of FDBP: Adductor alulae, lying just deep to Flexor alulae, is the probable homolog of FDBP to digit I; Abductor digiti majoris is the probable homolog of FDBP to digit II; and Flexor digiti minoris is the probable homolog of FDBP to digit III. Adductor alulae has a very similar origin and insertion to that of Flexor alulae, and in some birds they are difficult to distinguish, but its insertion is slightly medial and distal to that of the Flexor alulae on the carpometacarpus. Abductor digiti majoris has its origin on the base of the carpometacarpus and the ventral surface of the shaft of metacarpal II, and it inserts on the base of the proximal phalanx of digit II. Flexor digiti minoris is variably developed and is only weakly present in some birds, but it has a large

fleshy belly in *Struthio*. It takes its origin from the distal half of metacarpal III and inserts tendinously on the base of the proximal phalanx of digit III. In lizards and turtles the origins of the FDBP divisions are typically restricted to the distal carpal row (Walker, 1973; Russell and Bauer, 2008), whereas crocodylians exhibit origins involving both the distal carpals and the metacarpals of each digit (Meers, 2003). An origin from the metacarpals may be an archosaurian synapomorphy, but it also may be convergent due to the modified wrists of modern archosaurs, as in the origin of FDBS. In this case it is most parsimonious to reconstruct the origin of these muscles from both the distal carpals and the metacarpals, as in crocodylians, which is an intermediate state between that of lepidosaurs and that of birds (Figure 5). The insertion of FDBP is highly conserved, with a single attachment to the ventral surface of the flexor process of the first phalanx of each digit in nearly every taxon studied. Thus it is reconstructed to have retained this attachment in the manus of *Tawa*, where it would have inserted between the two distal tendons of FDBS (Figure 5). This group of muscles would have been primarily responsible for flexing the metacarpophalangeal joints of each digit.

Abductor pollicis brevis (APB)—The likely homolog of APB in the avian manus is Abductor alulae, which is located on the anteroventral side of the manus. The origin of this muscle is from the area of the carpus on the radial side, but the exact points of origin exhibit a high degree of variability. It arises from the ventral surface of the radiale in all crocodylians, most lepidosaurs, and one turtle (*Lissemys*; Shah and Patel, 1964). Other reported origins have been from the distal carpals in *Trachemys* (Walker, 1973) and *Tetradactylus* (Berger-Dell'mour, 1983), from the distal radius in *Podocnemis* and *Trachemys* (Abdala et al., 2008), from the base of the carpometacarpus in some birds (e.g., Fisher and Goodman, 1955), and from the tendon of ECR in most birds (George and Berger, 1966). An accessory attachment to the distal radius has been found to be variably present in *Struthio*. Because it is present in most lepidosaurs as well as in crocodylians, origin from the radiale is likely the plesiomorphic condition, retained in crocodylians despite their modified wrists, and is the most likely character state at the base of Archosauria (posterior probability of 0.881). Although it remains phylogenetically equivocal, this morphology is reconstructed in *Tawa* because it is unlikely that basal theropods exhibited the derived avian morphology (Figure 5).

The insertion of APB is unequivocally located on the medial surface of the first phalanx of digit I near its base (posterior probability of 0.837 at Archosauria and 0.993 at Aves). This muscle has a more proximal attachment in crocodylians (Meers, 2003), *Sphenodon* (Miner, 1925), and *Liolaemus* (Abdala and Moro, 2006), inserting on the lateral aspect of the first metacarpal, but the distal attachment is found in turtles, other lepidosaurs, and all birds. Thus, this insertion site is reconstructed in *Tawa* as well (Figure 5). APB would have acted to abduct the first digit.

Abductor digiti minimi (ADM)—Abductor digiti minimi of crocodylians, lizards, and turtles originates from the distal edge of the pisiform and inserts on the lateral surface of the lateralmost metacarpal (in crocodylians; Meers, 2003) or the ventrolateral surface of the first phalanx (in lepidosaurs and turtles; Russell and Bauer, 2008). It has been suggested that the avian homolog of this muscle is Ulnimetacarpalis dorsalis (Diogo and Abdala, 2010), but this hypothesis was rejected based on the embryological differences between the two muscles (see above, in Extensores Digitores Breves). ADM is ventrally located in the hand, and in some cases has been described as part of Flexor carpi ulnaris, or arising from its tendon of insertion (Günther, 1867; Russell and Bauer, 2008). No similar muscle has ever been previously described in the avian manus, but a muscle fitting this description was found in both specimens of *Struthio* that I dissected. This muscle is well developed, originating from the ventral surface of the (pseudo)ulnare and the insertion tendon of Flexor carpi ulnaris and inserting on the ventrolateral surface of metacarpal III. In birds, muscles attaching to the pisiform have shifted their attachments to the pseudoulnare (see above, in Flexor carpi ulnaris), so in this case an origin from the pseudoulnare is considered homologous to the origin from the pisiform in other taxa. The insertion on the lateralmost metacarpal is similar to the condition in crocodylians and may be related to reduction of the lateral digits in both of these taxa. In *Tawa*, this muscle would have originated from the pisiform, which was still present, and likely inserted on the metacarpal of the reduced digit IV (Figure 5). In this position it would have acted to abduct the fourth digit and the manus.

Lumbricales (L)—Although there seem to be no homologs of these muscles present in the avian manus, lumbricals to at least digits II through IV are present in all other taxa studied.

However, the number and exact insertion of the slips of this muscle are extremely variable. In all cases they arise from the tendons of Flexor digitorum longus in the manus and/or the palmar aponeurosis, although they may insert on all digits (Haines, 1950; Walker, 1973; Abdala and Moro, 2006), or only digits II through IV (Meers, 2003; Russell and Bauer, 2008), and on either the metacarpophalangeal joint (Meers, 2003; Abdala and Moro, 2006), or the proximal interphalangeal joint (Haines, 1950; Russell and Bauer, 2008). Thus, although it is likely that these muscles were present in the manus of *Tawa* given their presence in all taxa with 'normal' manual morphology, reconstruction of their exact morphology is considered too speculative in the present study. The lumbricals would have acted to extend the metacarpophalangeal and possibly the proximal interphalangeal joints of the digits.

Interossei (IO)—All birds possess two muscles that bear the name of 'interosseus', but their homology to the Interossei of other tetrapods is uncertain based on their attachments and development (Sullivan, 1962). Even among tetrapods, the homology of the muscles variously called Interossei, Intermetacarpales, Dorsometacarpales, and Contrahentes digitorum is not clear (Howell, 1936). As with Lumbricales, these muscles were almost certainly present in the manus of *Tawa* given their presence in some form in the manus of all other tetrapods, but there is no consistency in their number or morphology across the studied taxa, making them impossible to reconstruct with any confidence. Furthermore, there are no osteological correlates that correspond to the possible attachment locations in the metacarpals of *Tawa*. However, the crocodylian arrangement of these muscles would potentially have provided the greatest utility in the hands of theropod dinosaurs. In crocodylians, each digit is served by an abductor (dorsal) and adductor (ventral) that originate from the proximal end of the adjacent metacarpal and insert on the distal metacarpal, joint capsule, and/or proximal phalanx of that digit (Cong et al., 1998; Meers, 2003). This arrangement is not unlike that of the human hand, allowing for independent adduction and abduction of each digit. Unlike the condition in most other tetrapods, the manual interossei of theropods were not constrained by the demands of locomotion, and a crocodylian-type morphology would have provided more control over the movements of the individual manual digits.

DISCUSSION

Comparisons With Previous Reconstructions

Among the few studies that have reconstructed the forelimb musculature in extinct archosaurs, the majority focuses on a small subset of large muscles crossing the glenohumeral joint and do not assess the smaller muscles of the forelimb, including those of the antebrachium and manus. The major deviations of the shoulder musculature of this reconstruction from that of Jasinoski et al. (2006) have been detailed above, but mostly concern the origins of the supracoracoideus musculature, the presence of Coracobrachialis longus, and the origins and insertions of the deltoideus musculature (Figure 6). The configuration of the deltoid musculature proposed here is consistently displayed in other recent reconstructions (Dilkes, 2000; Langer et al., 2007; Maidment and Barrett, 2011) and, although Langer et al. (2007) also reconstruct the Coracobrachialis longus as present, most other workers agree with Romer (1944) that its absence is plesiomorphic among archosaurs (Dilkes, 2000; Meers, 2003; Maidment and Barrett, 2011). A broad origin of Supracoracoideus from the anterolateral surface of the coracoid extending onto the scapula in the subacromial depression is reconstructed by both Dilkes (2000) and Langer et al. (2007), and an origin crossing the scapulocoracoid suture is also hypothesized by Maidment and Barrett (2011), although with a much more dorsally restricted attachment (Figure 6).

The humeral origin(s) of Triceps brachii is more controversial. The presence of two humeral heads (TBM and TBL) as reconstructed here is equivocal phylogenetically, and most authors choose to reconstruct only one humeral head in dinosaurs (Dilkes, 2000; Jasinoski et al., 2006; Langer et al., 2007; Maidment and Barrett, 2011). However, reconstructions for both heads are Level II inferences and thus equally parsimonious, and a distinct ridge on the posterior surface of the humerus in basal theropods provides osteological evidence of a separate origin of TBL (see above). Whether or not the humeral heads of triceps were fused in dinosaurs or not, both crocodylians and birds exhibit a wide fleshy origin of the humeral head(s) of triceps, and thus it is likely that the origin in dinosaurs was not restricted to a small area, as some authors have proposed (Fig. 6; Langer et al., 2007; Maidment and Barrett, 2011). Langer et al. (2007) reconstruct Brachialis as originating distally from the anterior intercondylar depression, and this

feature may correspond to the Impresso brachialis of birds (Baumel et al., 1979), but it is typically not present as a distinct impression in basal theropods or basal ornithiscians (Maidment and Barrett, 2011). Although the extent of the distal excursion of the origin of Brachialis is equivocal and a more distally placed origin is possible (Maidment and Barrett, 2011), a more proximally placed origin, as in crocodylians (Meers, 2003) and as reconstructed by Jasinoski et al. (2006) and this study, would result in a longer moment arm for this muscle and thus a greater mechanical advantage.

Distally on the humerus, the origins of the muscles attaching to the entepicondyle and the ectepicondyle have only been reconstructed individually in two studies (Carpenter and Smith, 2001; Langer et al., 2007), neither of which reconstruct all possible muscles. Though consisting of only four muscles, the arrangement in Carpenter and Smith's (2001) avian-based reconstruction is generally congruent with the current study, as is the arrangement of the extensor (ectepicondylar) muscles of Langer et al. (2007). Although a joined origin of Extensor carpi ulnaris and Supinator is not supported phylogenetically, it is possible that these two muscles originated in close proximity to each other, given the phylogenetic uncertainty in their proximodistal arrangement. Additionally, it is unlikely that the origin of Flexor carpi ulnaris was located proximal to the origin of Flexor digitorum longus, as has been proposed by Langer et al. (2007), because this muscle consistently has the most distal origin on the entepicondyle in all extant taxa studied.

Of the muscle attachment sites on the antebrachium, the insertion of Biceps brachii is one of the few that is typically reconstructed. Most authors agree on a dual insertion on both the radius and ulna (Dilkes, 2000; Jasinoski et al., 2006; Langer et al., 2007) and in some cases small rugosities and tubercles have been identified on both bones that may correspond to the insertion site in this area (Carpenter and Smith, 2001; Langer et al., 2007). A more distally located tubercle on the anterior surface of the radius, as exhibited in *Herrerasaurus* (Sereno, 1993), likely does not represent the insertion of Biceps brachii or Brachialis but instead that of Humeroradialis, which possesses an insertion site marked by a large tubercle and located distal to those of Biceps brachii and Brachialis in crocodylians (Meers, 2003).

Langer et al.'s (2007) reconstruction of 'Flexor ulnaris' (here Anconeus) and Pronator quadratus are congruent with those of this study, but an insertion of Flexor carpi ulnaris onto the medial surface of the proximal ulna is not supported. An accessory ulnar origin of Flexor carpi ulnaris has been reported for some lepidosaurs (Russell and Bauer, 2008), but it is not commonly nor consistently present within a single genus. Carpenter and Smith (2001), who based their reconstruction primarily on birds, also reconstructed an attachment to the ulna, but there is little evidence for this as well. In neognathous birds, this muscle passes through a ligamentous structure called the humeroulnar pulley, which attaches to the proximal end of the ulna, but it does not take origin from the ulna nor the humeroulnar pulley and thus has no attachment to the proximal end of the ulna (George and Berger, 1966). The insertion extends onto the distal end of the ulna in *Apteryx* (McGowan, 1982), but not in *Struthio* or in tinamous (Hudson et al., 1972; pers. obs.). Most differences in the reconstruction of the antebrachial musculature of this study and that of Dilkes (2000) are related to presence of the radiale and ulnare, which have been lost in *Maiasaura* but retained in *Tawa*, and the derived morphology of the manus in the former taxon.

Evolutionary and Functional Implications

Reconstruction of the shoulder musculature in a basal theropod allows for direct comparison with recent muscular reconstructions of the basal members of other dinosaurian clades as well as with more derived theropods. Although many ornithischians and sauropodomorphs reevolved quadrupedality, the most basal members of both clades were bipedal and retained a similar forelimb morphology to that of basal theropods (Maidment and Barrett, 2011). As such, the overall arrangement of the shoulder musculature in basal ornithiscians (Maidment and Barrett, 2011) and basal sauropodomorphs (Langer et al., 2007) is remarkably similar to that of basal theropods in both the relative development of various muscle groups and their potential actions (Figure 6). In each clade the scapulocoracoid and proximal end of the humerus exhibit large, well-developed attachment sites for all major muscle groups of the shoulder. The humeri of basal saurischians generally exhibit larger, more anteriorly protruding deltopectoral crests than those of basal ornithischians. This provides a longer moment arm for the

Supracoracoideus musculature, increasing its mechanical advantage for protracting the humerus and resulting in stronger flexion of the shoulder in basal saurischians. An expanded deltopectoral crest also enlarges the potential area for the insertion of Deltoideus clavicularis, indicating a potentially greater capacity for abduction in basal saurischians.

Basal theropods differ from basal sauropodomorphs and basal ornithiscians in possessing relatively longer scapular blades, placing the origin of Deltoideus scapularis farther from the glenohumeral joint and thus slightly increasing the torque provided by the muscle for extension of the humerus. The more distal insertion of Latissimus dorsi on the humerus, lengthening its lever arm, reinforces the emphasis on extension of the humerus in early theropods. The accentuation of humeral extension in early theropods over the morphology seen in early sauropodomorphs and ornithiscians may reflect the role of the forelimb in predation. A large struggling prey item would exert a flexor moment on the shoulder, which would need to be counteracted by powerful extension. Although this would have been important for a carnivorous early theropod like *Tawa*, basal ornithischians and sauropodomorphs are usually inferred to be herbivorous to omnivorous (Barrett, 2000; Barrett et al., 2011), and likely would not have been hunting large prey. The similarities of the rest of the forelimb musculature between the basal taxa indicate that they likely shared many other possible functions, such as manipulation of small prey items, grooming, or intraspecific interactions.

Reorientation of the scapulocoracoid in derived maniraptorans to a more bird-like position (Jasinoski et al., 2006) caused many functional changes in the shoulder musculature relative to the basal condition. The large, sheet-like muscles attaching to the scapular blade are responsible for scapular protraction, retraction, and overall rotation and have an important role in increasing the anteroposterior excursion of the entire forelimb in crocodylians (Meers, 2003) and especially in arboreal lizards like chameleons and anoles (Peterson, 1973). Levator scapulae and Serratus profundus are active during retraction of the forelimb, pulling the distal end of the scapula anteriorly and thus moving the coracoid posteriorly, whereas Serratus superficialis, acting on the distal end of the scapula in the opposite direction, is active during protraction of the forelimb (Peterson, 1973). Trapezius also assists in protraction of the forelimb through its fibers that insert near the acromion of the scapula, thus pulling the proximal end of the scapula

anteriorly (Meers, 2003). This mechanism was likely also in place in basal theropods, allowing a greater anterior reach of the forelimb than has been previously described when considering only the range of motion of the glenohumeral joint (e.g., Carpenter, 2002). However, both Trapezius and Levator scapulae have been lost in birds, and the horizontal orientation of the scapula has altered the functions of Serratus muscles to assist in respiration (superficialis) and stabilization of the scapula and movements related to gliding (profundus) (Fisher, 1946). A subhorizontal scapular orientation in dromaeosaurids, as interpreted by Jasinoski et al. (2006), would result in a similar reduction of the rotational capability of the scapula and subsequent reduction in the anterior excursion of the forelimb in these taxa.

Despite extreme modification of the distal segments of the forelimb in birds, there is a large amount of conservation in the muscles attaching to the antebrachium among archosaurs. Birds retain a full complement of pronator and supinator muscles, and their development is potentially related to the amount of nonsteady flight in which a bird engages (Dial, 1992b). In this capacity, these muscles possess some ability to pronate and supinate the distal segments of the wing (Dial, 1992a), although the specifics of their function and mechanism are not well understood. It has been proposed that the morphology of the radius of theropods limits the degree of pronation and/or supination of the forearm (e.g., Carpenter, 2002), but rotation of the forearm on its long axis to some degree also occurs in lepidosaurs by methods other than that seen in mammals (Landsmeer, 1983), so it is likely that the pronators and supinator of the forearm in basal theropods possessed some pronatory and supinatory capabilities along with their roles as flexors of the forearm.

The carpus of basal dinosaurs exhibits the morphology of neither extant birds nor extant crocodylians, instead bearing a closer overall resemblance with that of lepidosaurs, but it quickly became modified in the theropod lineage. In particular, the loss of the pisiform early in theropod evolution necessitated the shift of the attachments of several antebrachial muscles to other elements. In birds, the insertion of FCU and the origin of ADM have both shifted from the pisiform to the neomorphic ‘pseudoulnare’ (not homologous to the ulnare of other tetrapods; Kundrát, 2009); it is unknown when this structure evolved, but these muscles probably attached to the ulnare in theropods that lack a pisiform, regardless of homology. These new attachments to

a very nearby bone do not change the function of these muscles, both of which are active during ulnar deviation of the manus. Although the osteology of the avian manus is highly modified, many of the intrinsic manual muscles can be considered to retain their plesiomorphic attachments when the development of the carpometacarpus is considered (Kundrát, 2009). Additionally, the newly dissected, well-developed manual musculature of the ostrich, which revealed the presence of Abductor digiti minimi, further elucidates the plesiomorphic morphology of these muscles. Evidence for well-developed Abductor pollicis longus muscles in basal theropods indicate that digit I had some independence from the other digits of the hand, but close articulation of the metacarpals likely precluded any true opposition of the theropod thumb. The manual unguals of basal theropods typically exhibit a very large flexor tubercle but no distinct extensor tubercle or process, indicating that, while digital flexion was important in these taxa, extension and especially hyperextension of the phalanges and unguals was less so.

CONCLUSIONS

This study provides the first full reconstruction of the forelimb musculature in a dinosaur, resulting in a more complete picture of each muscle and how these muscles work together. The inclusion of a phylogenetically broad sample of extant taxa and a phylogenetic ancestral state reconstruction in this analysis allowed for the unequivocal reconstruction of many distal forelimb muscles that have been previously deemed too uncertain to reconstruct. Although these muscles have been dismissed as secondary in investigations of locomotor function (e.g., Maidment and Barrett, 2011), they have great importance when considering function of the forelimbs in bipedal theropods, including hypotheses of grasping and predatory behavior. Furthermore, some antebrachial muscles have an important role in the automating musculoskeletal mechanism of avian flight (Vazquez, 1994), and an analysis of the changes in their distal attachments may elucidate when this mechanism evolved in the avian lineage. Hypotheses of theropod forelimb function have previously been tested primarily through range of motion studies (Carpenter, 2002; Senter and Robins, 2005) that do not consider the potential contribution by the musculature and the potential restrictions that it may impose on forelimb movement. The myology provided by

this reconstruction allows for further testing of functional hypotheses using techniques such as three-dimensional modeling of muscle moment arms (e.g., Hutchinson et al., 2005c).

Nonavian theropods exhibit a diverse range of forelimb morphologies from highly reduced to extremely elongate but we still understand very little about their evolution and function. This study provides the basis for future investigations of forelimb function in these derived theropod taxa by providing a foundation for muscle reconstructions in individual taxa and enabling analysis of the sequential changes in the forelimb musculature along their evolutionary trajectories.

ACKNOWLEDGMENTS

I thank D. Krause, A. Turner, B. Demes, and S. Gatesy for their help and support in the development of this study and for comments on early drafts of the manuscript. I also thank A. Turner, S. Nesbitt, R. Irmis, and N. Smith for the opportunity to work on the *Tawa* forelimb material. R. Martinez (PVSJ), D. Henderson (RTMP), B. Strilisky (RTMP), M. Norell (AMNH), and C. Mehling (AMNH) generously provided access to specimens in their care. Thanks to P. O'Connor for providing the forelimbs of OUVC avian specimens for dissection, and to A. Pritchard for assistance with ostrich dissections. I thank J. McCartney for support and feedback during this project. Funding for this project was provided by a National Science Foundation Graduate Research Fellowship, a National Science Foundation Doctoral Dissertation Improvement Grant (DEB 111036), and by the Doris O. and Samuel P. Welles Research Fund of the UCMP.

LITERATURE CITED

Abdala, V., A. S. Manzano, and A. Herrel. 2008. The distal forelimb musculature in aquatic and terrestrial turtles: phylogeny or environmental constraints? Journal of Anatomy 213:159–172.

Abdala, V., and S. Moro. 2006. Comparative myology of the forelimb of *Liolaemus* sand lizards (Liolaemidae). Acta Zoologica 87:1–12.

Baier, D. B., S. M. Gatesy, and F. A. Jenkins. 2007. A critical ligamentous mechanism in the evolution of avian flight. Nature 445:307–310.

Barrett, P. M. 2000. Prosauropods and iguanas: speculation on the diets of extinct reptiles; pp. 42–78 in H.-D. Sues (ed.), Evolution of Herbivory in Terrestrial Vertebrates: Perspectives from the Fossil Record. Cambridge University Press, Cambridge, UK.

Barrett, P. M., R. J. Butler, and S. J. Nesbitt. 2011. The roles of herbivory and omnivory in early dinosaur evolution. Earth and Environmental Science Transactions of the Royal Society of Edinburgh 101:383–396.

Baumel, J. J., A. S. King, A. M. Lucas, J. E. Breazile, and H. E. Evans eds. 1979. Nomina Anatomica Avium. Academic Press, New York, NY, 637 pp.

Beddard, F. E. 1889. Contributions to the anatomy of the Hoatzin (*Opisthocomus cristatus*), with particular reference to the structure of the wing in the young. Ibis 31:283–293.

Berger, A. J. 1954. The myology of the pectoral appendage of three genera of American cuckoos. Miscellaneous Publications Museum of Zoology, University of Michigan 85:1–35.

Berger, A. J. 1956. On the anatomy of the Red Bird of Paradise, with comparative remarks on the Corvidae. The Auk 73:427–446.

Berger-Dell'mour. 1983. Der übergang von echse zu schleiche in der gattung *Tetradactylus* Merrem. Zoologische Jahrbücher. Abteilung für Anatomie und Ontogenie der Tiere 110:1–152.

Bever, G. S., J. A. Gauthier, and G. P. Wagner. 2011. Finding the frame shift: digit loss, developmental variability, and the origin of the avian hand. Evolution & Development 13:269–279.

Bryant, H. N., and A. P. Russell. 1992. The role of phylogenetic analysis in the inference of unpreserved attributes of extinct taxa. Philosophical Transactions: Biological Sciences 337:405–418.

Buscalioni, A. D., F. Ortega, D. Rasskin-Gutman, and B. P. Pérez-Moreno. 1997. Loss of carpal elements in crocodilian limb evolution: morphogenetic model corroborated by palaeobiological data. Biological Journal of the Linnean Society 62:133–144.

Carpenter, K. 2002. Forelimb biomechanics of nonavian theropod dinosaurs in predation. Senckenbergiana Lethaea 82:59–76.

Carpenter, K., and M. Smith. 2001. Forelimb osteology and biomechanics of *Tyrannosaurus rex*; pp. 90–116 in D. Tanke and K. Carpenter (eds.), Mesozoic Vertebrate Life. Indiana University Press, Bloomington, IN.

Carrano, M. T., and J. R. Hutchinson. 2002. Pelvic and hindlimb musculature of *Tyrannosaurus rex* (Dinosauria: Theropoda). Journal of Morphology 253:207–228.

Cong, L., L. Hou, X.-C. Wu, and J. Hou. 1998. The Gross Anatomy of *Alligator sinensis* Fauvel. Science Press, Beijing, 388 pp.

Conrad, J. L. 2008. Phylogeny and systematics of Squamata (Reptilia) based on morphology. Bulletin of the American Museum of Natural History 310:1–182.

Dececchi, T. A., and H. C. E. Larsson. 2009. Patristic evolutionary rates suggest a punctuated pattern in forelimb evolution before and after the origin of birds. Paleobiology 35:1–12.

Dial, K. P. 1992a. Activity patterns of the wing muscles of the pigeon (*Columba livia*) during different modes of flight. Journal of Experimental Zoology 262:357–373.

Dial, K. P. 1992b. Avian forelimb muscles and nonsteady flight: can birds fly without using the muscles in their wings? The Auk 109:874–885.

Dilkes, D. W. 2000. Appendicular myology of the hadrosaurian dinosaur *Maiasaura peeblesorum* from the Late Cretaceous (Campanian) of Montana. Transactions of the Royal Society of Edinburgh: Earth Sciences 90:87–125.

Diogo, R., and V. Abdala. 2010. Muscles of Vertebrates: Comparative Anatomy, Evolution, Homologies and Development. Science Publishers, New Hampshire, 482 pp.

Fisher, H. I. 1946. Adaptation and comparative anatomy of the locomotor apparatus of New World vultures. American Midland Naturalist 35:545–727.

Fisher, H. I., and D. C. Goodman. 1955. The myology of the Whooping Crane, *Grus americana*. Illinois Biological Monograph 24:1–127.

Fitzgerald, T. C. 1969. The Coturnix Quail: Anatomy and Histology. The Iowa State University Press, Des Moines, IA, 306 pp.

George, J. C., and A. J. Berger. 1966. Avian Myology. Academic Press, New York, 500 pp.

Gishlick, A. D. 2001. The function of the manus and forelimb of *Deinonychus antirrhopus* and its importance for the origin of avian flight; pp. 301–318 in J. A. Gauthier and L. F. Gall (eds.), New Perspectives on the Origin and Early Evolution of Birds: Proceedings. Peabody Museum of Natural History, Yale University, New Haven, CT.

Günther, A. 1867. Contribution to the anatomy of *Hatteria* (*Rhynchocephalus*, Owen). Philosophical Transactions of the Royal Society of London 157:595–629.

Haines, R. W. 1950. The flexor muscles of the forearm and hand in lizards and mammals. Journal of Anatomy 84:13–29.

Haines, R. W. 1939. A revision of the extensor muscles of the forearm in tetrapods. Journal of Anatomy 73:211–233.

Holmes, R. 1977. The osteology and musculature of the pectoral limb of small captorhinids. Journal of Morphology 152:101–140.

Howell, A. B. 1936. Phylogeny of the distal musculature of the pectoral appendage. Journal of Morphology 60:287–315.

Howell, A. B. 1937. Morphogenesis of the shoulder architecture: Aves. The Auk 54:364–375.

Hudson, G. E., K. M. Hoff, J. C. Vanden Berge, and E. C. Trivette. 1969. A numerical study of the wing and leg muscles of Lari and Alcae. Ibis 111:459–524.

Hudson, G. E., and P. J. Lanzillotti. 1955. Gross anatomy of the wing muscles in the Family Corvidae. American Midland Naturalist 53:1–44.

Hudson, G. E., and P. J. Lanzillotti. 1964. Muscles of the pectoral limb in galliform birds. American Midland Naturalist 71:1–113.

Hudson, G. E., D. O. Schreiweis, S. Y. C. Wang, and D. A. Lancaster. 1972. A numerical study of the wing and leg muscles of Tinamous (Tinamidae). Northwest Science 46:207–255.

Hutchinson, J. R., F. C. Anderson, S. S. Blemker, and S. L. Delp. 2005. Analysis of hindlimb muscle moment arms in *Tyrannosaurus rex* using a three-dimensional musculoskeletal computer model: implications for stance, gait and speed. Paleobiology 31:676–701.

Jasinoski, S. C., A. P. Russell, and P. J. Currie. 2006. An integrative phylogenetic and extrapolatory approach to the reconstruction of dromaeosaur (Theropoda: Eumaniraptora) shoulder musculature. Zoological Journal of the Linnean Society 146:301–344.

Jetz, W., G. H. Thomas, J. B. Joy, K. Hartmann, and A. O. Mooers. 2012. The global diversity of birds in space and time. Nature 491:444–448.

Koehl, M. A. R., D. Evangelista, and K. Yang. 2011. Using physical models to study the gliding performance of extinct animals. Integrative and Comparative Biology 51:1002–1018.

Kundrát, M. 2009. Primary chondrification foci in the wing basipodium of *Struthio camelus* with comments on interpretation of autopodial elements in Crocodilia and Aves. Journal of Experimental Zoology 312B:30–41.

Landsmeer, J. M. F. 1983. Mechanism of forearm rotation in *Varanus exanthematicus*. Journal of Morphology 175:119–130.

Langer, M. C., M. A. G. Franca, and S. Gabriel. 2007. The pectoral girdle and forelimb anatomy of the stem-sauropodomorph *Saturnalia tupiniquim* (Upper Triassic, Brazil). Special Papers in Palaeontology 77:113–137.

Livezey, B. C. 1990. Evolutionary morphology of flightlessness in the Aukland Islands Teal. The Condor 92:693–673.

Livezey, B. C., and R. L. Zusi. 2007. Higher-order phylogeny of modern birds (Theropoda, Aves: Neornithes) based on comparative anatomy. II. Analysis and discussion. Zoological Journal of the Linnean Society 149:1–95.

Maddison, W. P., and D. R. Maddison. 2010. Mesquite: a modular system for evolutionary analysis. 2.73. http://mesquiteproject.org.

Maidment, S. C. R., and P. M. Barrett. 2011. The locomotor musculature of basal ornithischian dinosaurs. Journal of Vertebrate Paleontology 31:1265–1291.

McGowan, C. 1982. The wing musculature of the Brown kiwi *Apteryx australis mantelli* and its bearing on ratite affinities. Journal of Zoology 197:173–219.

McKitrick, M. C. 1985. Myology of the pectoral appendage in kingbirds (*Tyrannus*) and their allies. The Condor 87:402–417.

Meers, M. B. 2003. Crocodylian forelimb musculature and its relevance to Archosauria. The Anatomical Record Part A 274A:891–916.

Miner, R. W. 1925. The pectoral limb of *Eryops* and other primitive tetrapods. Bulletin of the American Museum of Natural History 51:145–312.

Müller, G. B., and P. Alberch. 1990. Ontogeny of the limb skeleton in *Alligator mississippiensis*: developmental invariance and change in the evolution of archosaur limbs. Journal of Morphology 203:151–164.

Nesbitt, S. J., N. D. Smith, R. B. Irmis, A. H. Turner, A. Downs, and M. A. Norell. 2009a. A complete skeleton of a Late Triassic saurischian and the early evolution of dinosaurs. Science 326:1530–1533.

Nesbitt, S. J., A. H. Turner, M. Spaulding, J. L. Conrad, and M. A. Norell. 2009b. The theropod furcula. Journal of Morphology 270:856–879.

Nicholls, E. L., and A. P. Russell. 1985. Structure and function of the pectoral girdle and forelimb of *Struthiomimus altus* (Theropoda: Ornithomimidae). Palaeontology 28:643–677.

Padian, K. 2004. Basal Avialae; pp. 210–231 in D. B. Weishampel, P. Dodson, and H. Osmolska (eds.), The Dinosauria, Second Edition. University of California Press, Berkeley, CA.

Parker, T. J. 1891. Observations on the anatomy and development of *Apteryx*. Philosophical Transactions of the Royal Society B 182:25–134.

Peterson, J. A. 1984. The locomotion of *Chamaeleo* (Reptilia: Sauria) with particular reference to the forelimb. Journal of Zoology 202:1–42.

Peterson, J. A. 1973. Adaptation for arboreal locomotion in the shoulder region of lizards. Doctoral thesis/dissertation, Anatomy, University of Chicago, Chicago, IL, 603 pp.

Poore, S. O., A. Sanchez-Haiman, and G. E. Goslow. 1997. Wing upstroke and the evolution of flapping flight. Nature 387:799–802.

Raikow, R. J. 1977. Pectoral appendage myology of the Hawaiian honeycreepers (Drepanididae). The Auk 94:331–342.

Reese, A. M. 1915. The Alligator and Its Allies. The Knickerbocker Press, New York, NY, 358 pp.

Ribbing, L. 1907. Die distale armmuskulatur der Amphibien, Reptilien und Säugetiere. Zoologische Jahrbücher 23:587–682.

Rinehart, L. F., S. G. Lucas, and A. P. Hunt. 2007. Furculae in the Late Triassic theropod dinosaur *Coelophysis bauri*. Paläontologische Zeitschrift 81:174–180.

Romer, A. S. 1944. The development of tetrapod limb musculature — the shoulder region of *Lacerta*. Journal of Morphology 74:1–41.

Russell, A. P., and A. M. Bauer. 2008. The appendicular locomotor apparatus of *Sphenodon* and normal-limbed squamates; pp. 1–466 in C. Gans, A. S. Gaunt, and K. Adler (eds.), Biology of the Reptilia 24, Morphology 1. Society for the Study of Amphibians and Reptiles, Ithaca, NY.

Senter, P., and J. H. Robins. 2005. Range of motion in the forelimb of the theropod dinosaur *Acrocanthosaurus atokensis*, and implications for predatory behavior. Journal of Zoology 266:307–318.

Sereno, P. C. 1993. The pectoral girdle and forelimb of the basal theropod *Herrerasaurus ischigualastensis*. Journal of Vertebrate Paleontology 13:425–450.

Shah, R. V., and V. B. Patel. 1964. Myology of the chelonian pectoral appendage. Journal of Animal Morphology and Physiology 11:58–84.

Shufeldt, R. W. 1918. Notes on the osteology of the young of the Hoatzin (*Opisthocomus cristatus*) and other points on its morphology. Journal of Morphology 31:599–606.

Sterli, J. 2010. Phylogenetic relationships among extinct and extant turtles: the position of Pleurodira and the effects of fossils on rooting crown-group turtles. Contributions to Zoology 79:93–106.

Straus, W. L. 1942. The homologies of the forearm flexors: urodeles, lizards, mammals. American Journal of Anatomy 70:281–316.

Sullivan, G. E. 1962. Anatomy and embryology of the wing musculature of the domestic fowl (*Gallus*). Australian Journal of Zoology 10:458–518.

Swinebroad, J. 1954. A comparative study of the wing myology of certain passerines. American Midland Naturalist 51:488–514.

Vanden Berge, J. C. 1970. A comparative study of the appendicular musculature of the Order Ciconiiformes. American Midland Naturalist 84:289–364.

Vanden Berge, J. C., and G. A. Zweers. 1993. Myologia; pp. 189–247 in J. J. Baumel, A. S. King, J. E. Breazile, H. E. Evans, and J. C. Vanden Berge (eds.), Handbook of Avian Anatomy: Nomina Anatomica Avium. Nuttall Ornithological Club, Cambridge, UK.

Vazquez, R. J. 1994. The automating skeletal and muscular mechanisms of the avian wing (Aves). Zoomorphology 114:59–71.

Walker, J. W. F. 1973. The locomotor apparatus of testudines; pp. 1–100 in C. Gans and T. S. Parsons (eds.), Biology of the Reptilia 4. Academic Press, New York.

Wang, X., R. L. Nudds, and G. J. Dyke. 2011. The primary feather lengths of early birds with respect to avian wing shape evolution. Journal of Evolutionary Biology 24:1226–1231.

Wang, Z., R. L. Young, H. Xue, and G. P. Wagner. 2011. Transcriptomic analysis of avian digits reveals conserved and derived digit identities in birds. Nature 477:583–587.

Witmer, L. M. 1995. The extant phylogenetic bracket and the importance of reconstructing soft tissues in fossils; pp. 9–33 in J. J. Thomason (ed.), Functional Morphology in Vertebrate Paleontology. Cambridge University Press, Cambridge, UK.

Young, C. G. 1888. On the habits and anatomy of *Opisthocomus cristatus*, Illig. Notes from the Leyden Museum 10:169–175.

Zusi, R. L., and G. D. Bentz. 1978. The appendicular myology of the Labrador Duck (*Camptorhynchus labradorius*). The Condor 80:407–418.

TABLE 4.1. Homologies of the antebrachial musculature of archosaurs, lepidosaurs, and testudines.

Muscle	Aves (Baumel et al., 1979)	Crocodylia (Meers, 2003)	Lepidosauria (Russell & Bauer, 2008)	Testudines (Walker, 1973)
Anconeus	Ectepicondylo-ulnaris	Flexor Ulnaris	Anconeus quartus	Extensor carpi ulnaris (part)
Extensor carpi ulnaris	Extensor carpi ulnaris	absent	Extensor carpi ulnaris	Extensor carpi ulnaris (part)
Supinator	Supinator	Supinator	Supinator longus	Tractor radii
Extensor carpi radalis	Extensor carpi radialis	Extensor carpi radialis longus	Extensor carpi radialis superficialis	Extensor carpi radialis superficialis
Abductor radialis	absent	Abductor radialis	Extensor carpi radialis intermedius and profundus	Extensor carpi radialis intermedius and profundus
Abductor pollicis longus	Extensor longus alulae	Extensor carpi radialis brevis	Supinator manus	Supinator manus
Extensor digitorum longus	Extensor digitorum communis	Extensor carpi ulnaris longus	Extensor digitorum longus	Extensor digitorum communis
Pronator teres	Pronator superficialis	Pronator teres	Pronator teres	Pronator teres
Pronator accessorius	Pronator profundus	absent	Pronator accessorius	absent
Pronator quadratus	Ulnometacarpalis ventralis	Pronator quadratus	Pronator profundus	Pronator profundus
Epitrochelo-anconeus	Entepicondylo-ulnaris	absent	Epitrochleo-anconeus	Flexor carpi ulnaris (part)
Flexor carpi ulnaris	Flexor carpi ulnaris	Flexor carpi ulnaris	Flexor carpi ulnaris	Flexor carpi ulnaris
Flexor digitorum longus superficialis	Flexor digitorum longus superficialis	Flexor digitorum longus pars humeralis	Flexor digitorum longus (humeral head)	Palmaris longus
Flexor digitorum longus profundus	Flexor digitorum longus profundus	Flexor digitorum longus pars ulnaris	Flexor digitorum longus (ulnar head)	Flexor digitorum longus

TABLE 4.2. Homologies of the avian intrinsic manual musculature with crocodylians, lepidosaurs, and testudines.

Aves (Baumel et al., 1993)	**Crocodylia (Meers, 2003)**	**Lepidosauria (Russell & Bauer, 2008)**	**Testudines (Walker, 1973)**
Extensor longus digiti majorus pars proximalis	Extensor digitorum superficialis, digit II	Extensor digitorum brevis superficialis, digit II	Extensor digitorum brevis (part), digit II
Ulnimetacarpalis dorsalis	Extensor digitorum superficialis, digits III and/or IV	Extensor digitorum brevis superficialis, digits III and/or IV	Extensor digitorum brevis (part), digits III and/or IV
Extensor brevis alulae	Extensor digitorum profundus, digit I	Extensor digitorum brevis profundus, digit I	Extensor digitorum brevis (part), digit I
Extensor longus digiti majorus pars distalis	Extensor digitorum profundus, digit II	Extensor digitorum brevis profundus, digit II	Extensor digitorum brevis (part), digit II
Flexor alulae	Flexor digitorum brevis superificalis, digit I	Flexor digitorum brevis, digit I	Flexor brevis superficialis, digit I
Adductor alulae	Flexor digitorum brevis profundus, digit I	Lumbricals (part), digit I	Flexor brevis profundus, digit I
Abductor digiti majoris	Flexor digitorum brevis profundus, digit II	Lumbricals (part), digit II	Flexor brevis profundus, digit II
Flexor digiti minoris	Flexor digitorum brevis profundus, digit III	Lumbricals (part), digit III	Flexor brevis profundus, digit III
Abductor alulae	Abductor metacarpi I	Flexor digitorum brevis, digit I deep part	Abductor pollicis brevis
“Abductor digiti minimi” (only present in *Struthio*)	Abductor metacarpi V	Abductor digiti quinti	Abductor digiti minimi

FIGURE 4.1. Consensus phylogeny of all extant taxa used in this analysis, based on the recent phylogenies of Livezey and Zusi (2007), Jetz et al. (2012), Conrad (2008), and Sterli (2010).

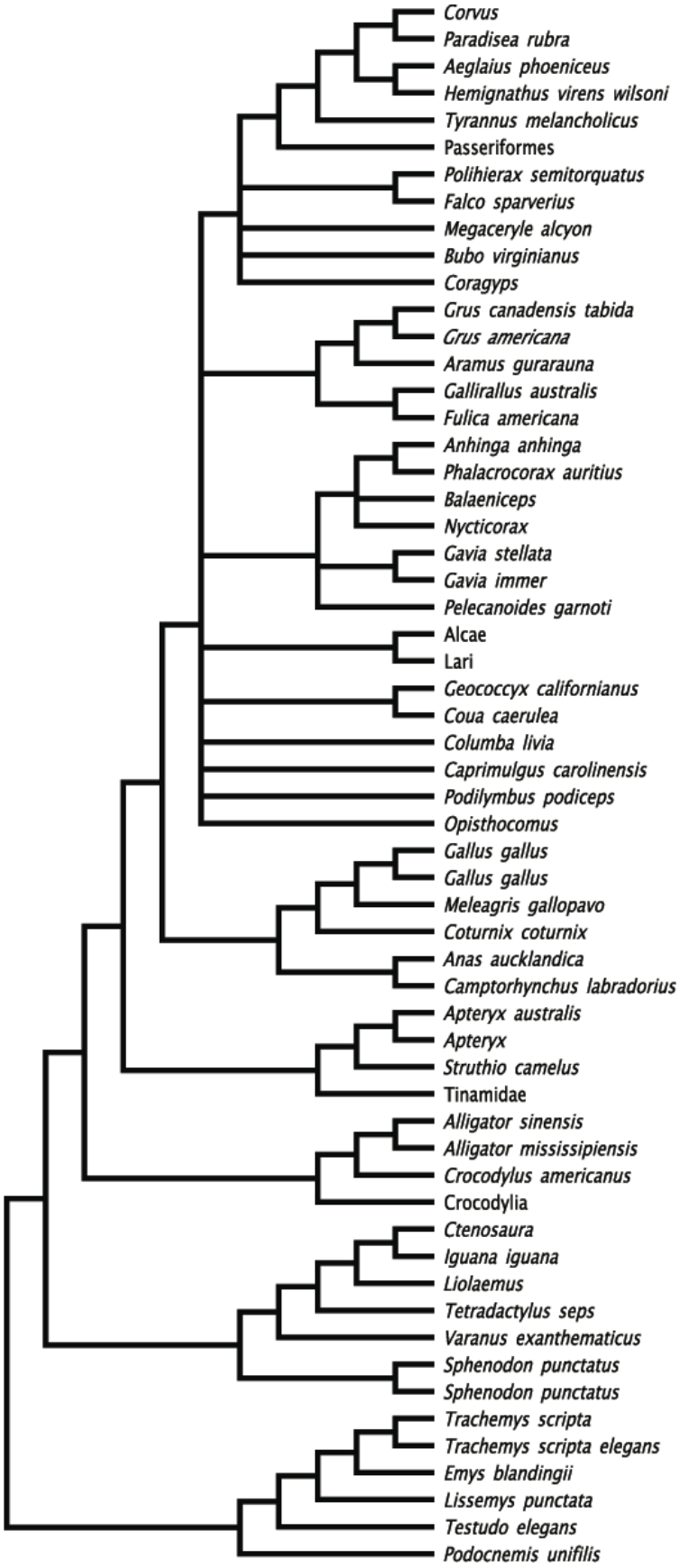
Corvus
Paradisea rubra
Aeglaius phoeniceus
Hemignathus virens wilsoni
Tyrannus melancholicus
Passeriformes
Polihierax semitorquatus
Falco sparverius
Megaceryle alcyon
Bubo virginianus
Coragyps
Grus canadensis tabida
Grus americana
Aramus gurarauna
Gallirallus australis
Fulica americana
Anhinga anhinga
Phalacrocorax auritius
Balaeniceps
Nycticorax
Gavia stellata
Gavia immer
Pelecanoides garnoti
Alcae
Lari
Geococcyx californianus
Coua caerulea
Columba livia
Caprimulgus carolinensis
Podilymbus podiceps
Opisthocomus
Gallus gallus
Gallus gallus
Meleagris gallopavo
Coturnix coturnix
Anas aucklandica
Camptorhynchus labradorius
Apteryx australis
Apteryx
Struthio camelus
Tinamidae
Alligator sinensis
Alligator mississipiensis
Crocodylus americanus
Crocodylia
Ctenosaura
Iguana iguana
Liolaemus
Tetradactylus seps
Varanus exanthematicus
Sphenodon punctatus
Sphenodon punctatus
Trachemys scripta
Trachemys scripta elegans
Emys blandingii
Lissemys punctata
Testudo elegans
Podocnemis unifilis

FIGURE 4.2. Myological reconstruction of the scapulocoracoid of *Tawa hallae* in lateral (**A**) and medial (**B**) views. Proposed muscle origins are indicated in red, proposed insertions are indicated in blue. **Abbreviations: BB**, Biceps brachii; **CB**, Coracobrachialis; **DC**, Deltoideus clavicularis; **DS**, Deltoideus scapularis; **LS**, Levator scapulae; **RH**, Rhomboideus; **SBC**, Subcoracoideus; **SBS**, Subscapularis; **SC**, Supracoracoideus; **SCA**, Supracoracoideus accessorius; **SHA**, Scapulohumeralis anterior; **SHP**, Scapulohumeralis posterior; **SP**, Serratus profundus; **SS**, Serratus superficialis; **TBS**, Triceps brachii scapularis; **TR**, Trapezius. Scale bar equals 5 cm.

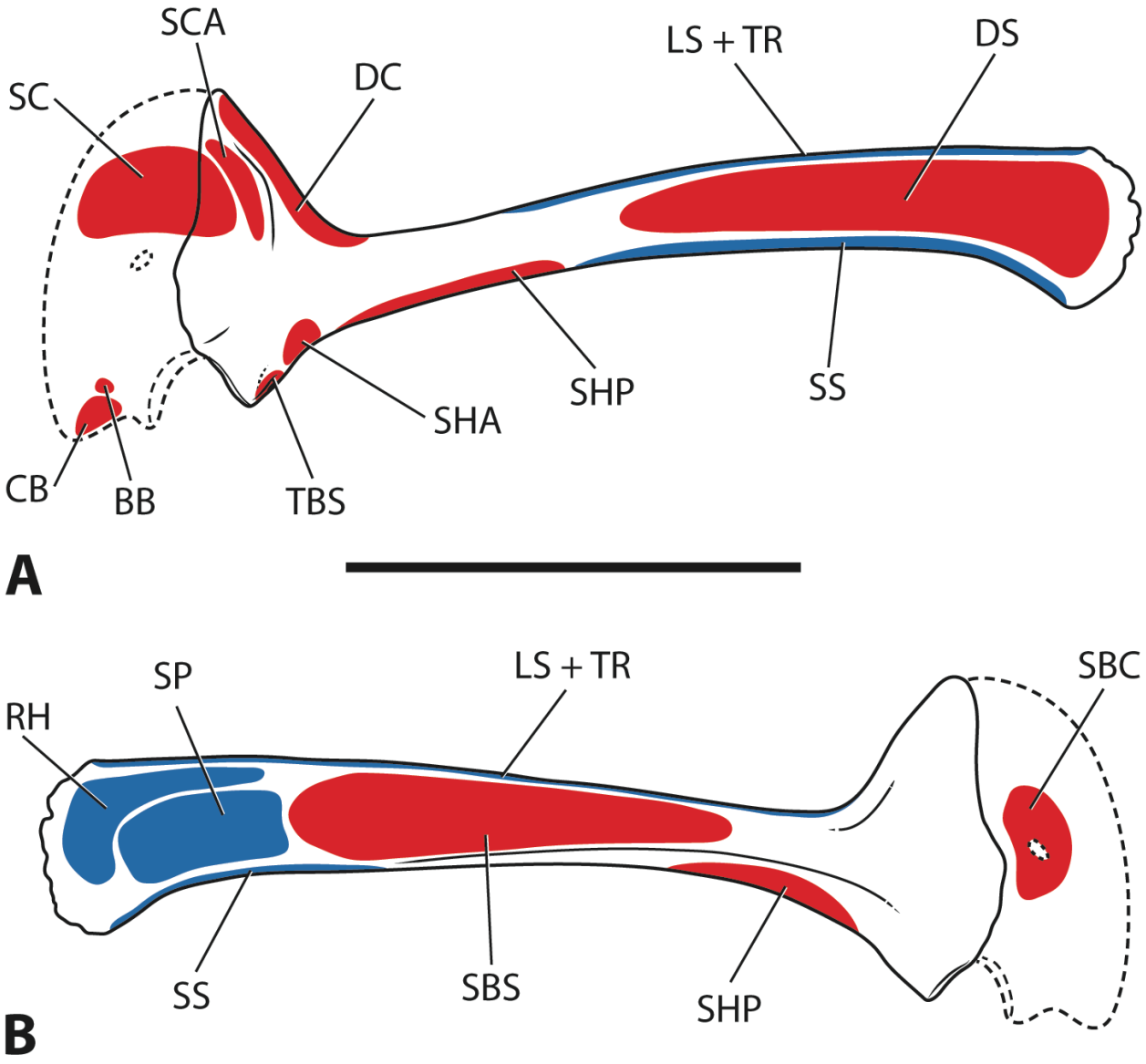
SCA
SC
DC
LS + TR
DS
SHP
SS
SHA
CB
BB
TBS
A
SP
RH
LS + TR
SBC
SS
SBS
SHP
B

FIGURE 4.3. Myological reconstruction of the humerus of *Tawa hallae* in lateral (**A**), posterior (**B**), anterior (**C**), and medial (**D**) views. Proposed muscle origins are indicated in red, proposed insertions are indicated in blue. **Abbreviations: AN**, Anconeus; **AR**, Abductor radialis; **BB**, Biceps brachii; **BR**, Brachialis; **CB**, Coracobrachialis; **DC**, Deltoideus clavicularis; **DS**, Deltoideus scapularis; **EA**, Epitrocheloanconeus; **ECR**, Extensor carpi radialis; **ECU**, Extensor carpi ulnaris; **EDL**, Extensor digitorum longus; **FCU**, Flexor carpi ulnaris; **FDLS**, Flexor digitorum longus superficialis; **HR**, Humeroradialis; **LD**, Latissimus dorsi; **P**, Pectoralis; **PA**, Pronator accessorius; **PT**, Pronator teres; **SBC**, Subcoracoideus; **SBS**, Subscapularis; **SC**, Supracoracoideus; **SCA**, Supracoracoideus accessorius; **SHA**, Scapulohumeralis anterior; **SHP**, Scapulohumeralis posterior; **SU**, Supinator; **TBL**, Triceps brachii longus; **TBM**, Triceps brachii medialis. Scale bar equals 5 cm.

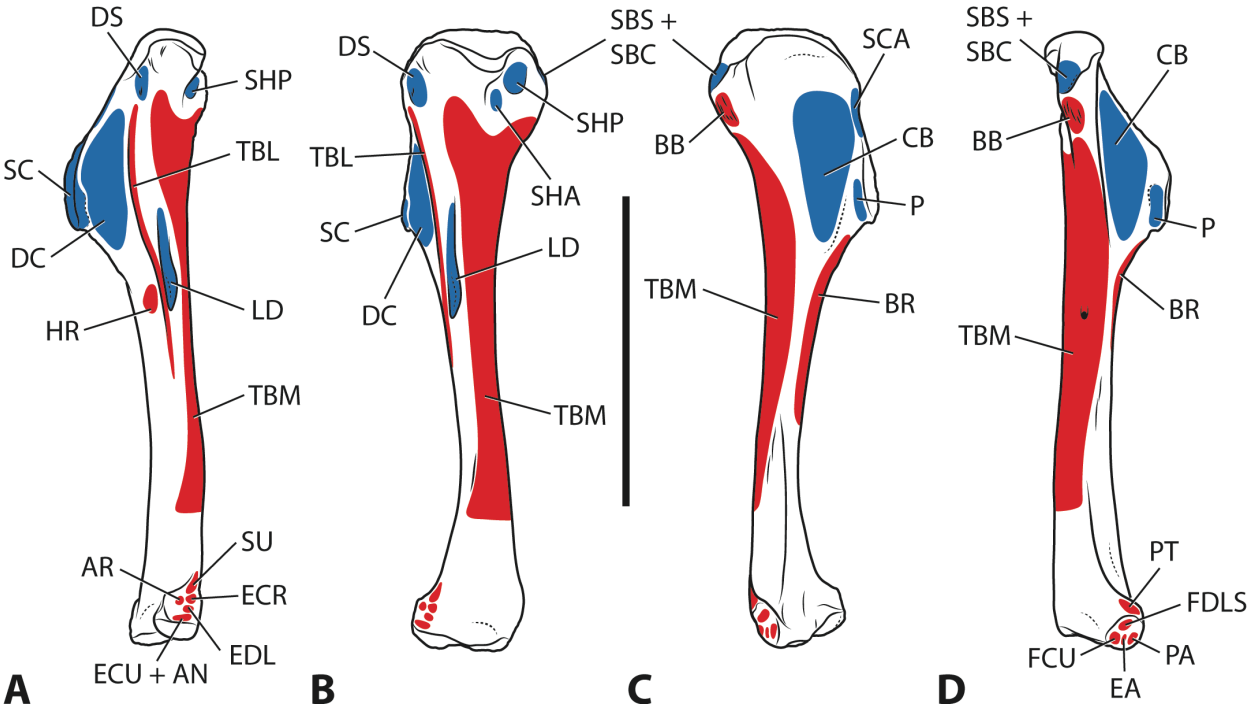
DS
SHP
TBL
SC
DC
LD
HR
TBM
SU
AR
ECR
EDL
ECU + AN
A
DS
SBS +
SBC
SHP
TBL
SHA
SC
LD
DC
TBM
B
SCA
BB
CB
P
TBM
BR
C
SBS +
SBC
CB
BB
P
BR
TBM
PT
FDLS
FCU
PA
EA
D

FIGURE 4.4. Myological reconstruction of the antebrachium of *Tawa hallae* in anterior (**A**), posterior (**B**), lateral (**C**), and medial (**D**) views. Proposed muscle origins are indicated in red, proposed insertions are indicated in blue. **Abbreviations: AN**, Anconeus; **APL**, Abuctor pollicis longus; **AR**, Abductor radialis; **BB**, Biceps brachii; **BR**, Brachialis; **EA**, Epitrocheloanconeus; **FDLP**, Flexor digitorum longus profundus; **HR**, Humeroradialis; **PA**, Pronator accessorius; **PQ**, Pronator quadratus; **PT**, Pronator teres; **R**, Radius; **SU**, Supinator; **TB**, Triceps brachii; **U**, Ulna. Scale bar equals 5 cm.

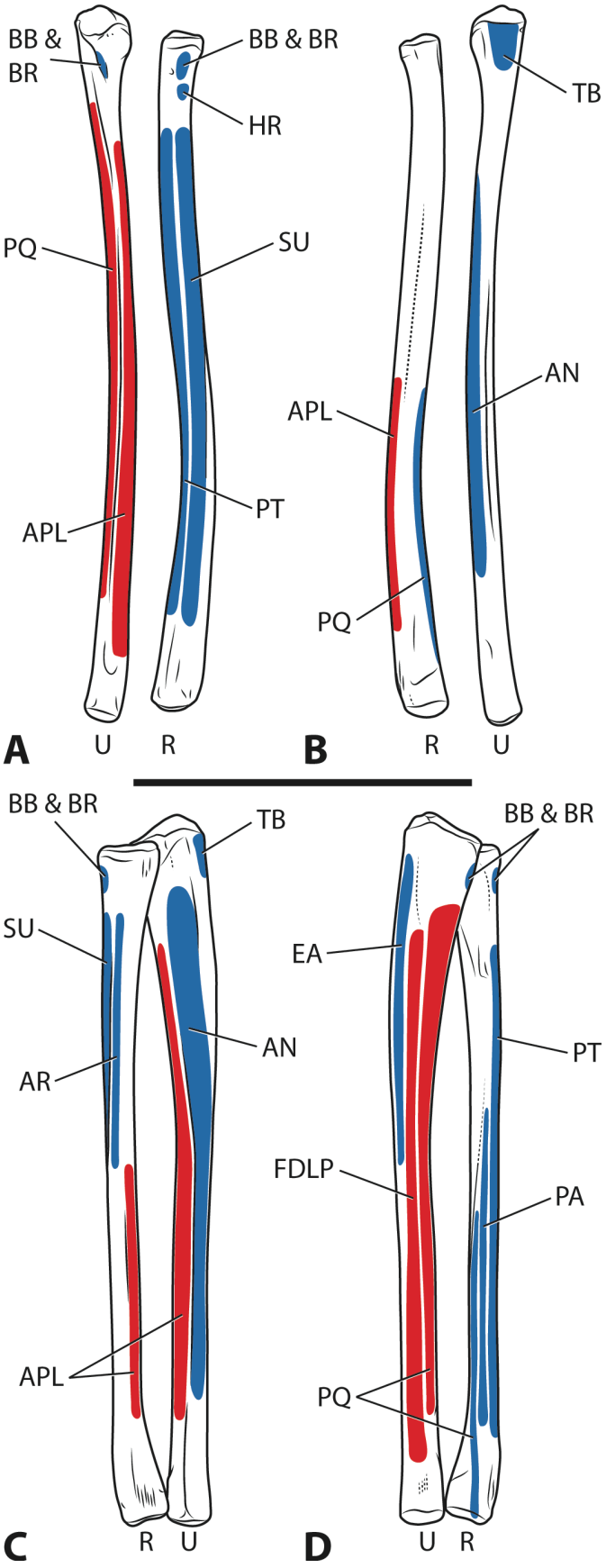
BB &
BR
BB & BR
HR
PQ
SU
APL
PT
A
U
R
TB
AN
APL
PQ
R
U
B
BB & BR
TB
SU
AN
AR
APL
C
R
U
BB & BR
EA
PT
FDLP
PA
PQ
D
U
R

FIGURE 4.5. Myological reconstruction of the carpus and manus of *Tawa hallae* in dorsal (**A**) and ventral (**B**) views. Proposed muscle origins are indicated in red, proposed insertions are indicated in blue. **Abbreviations: APB**, Abductor pollicis brevis; **APL**, Abductor pollicis longus; **ADM**, Abductor digiti minimi; **ECR**, Extensor carpi radialis; **ECU**, Extensor carpi ulnaris; **EDB**, Extensor digitorum brevis; **EDBP**, Extensor digitorum brevis profundus; **EDBS**, Extensor digitorum brevis superficialis; **EDL**, Extensor digitorum longus; **FCU**, Flexor carpi ulnaris; **FDBP**, Flexor digitorum brevis profundus; **FDBS**, Flexor digitorum brevis superficialis; **FDL**, Flexor digitorum longus; **I**, Digit I; **II**, Digit II; **III**, Digit III; **IV**, Digit IV; **PQ**, Pronator quadratus. Scale bar equals 5 cm.

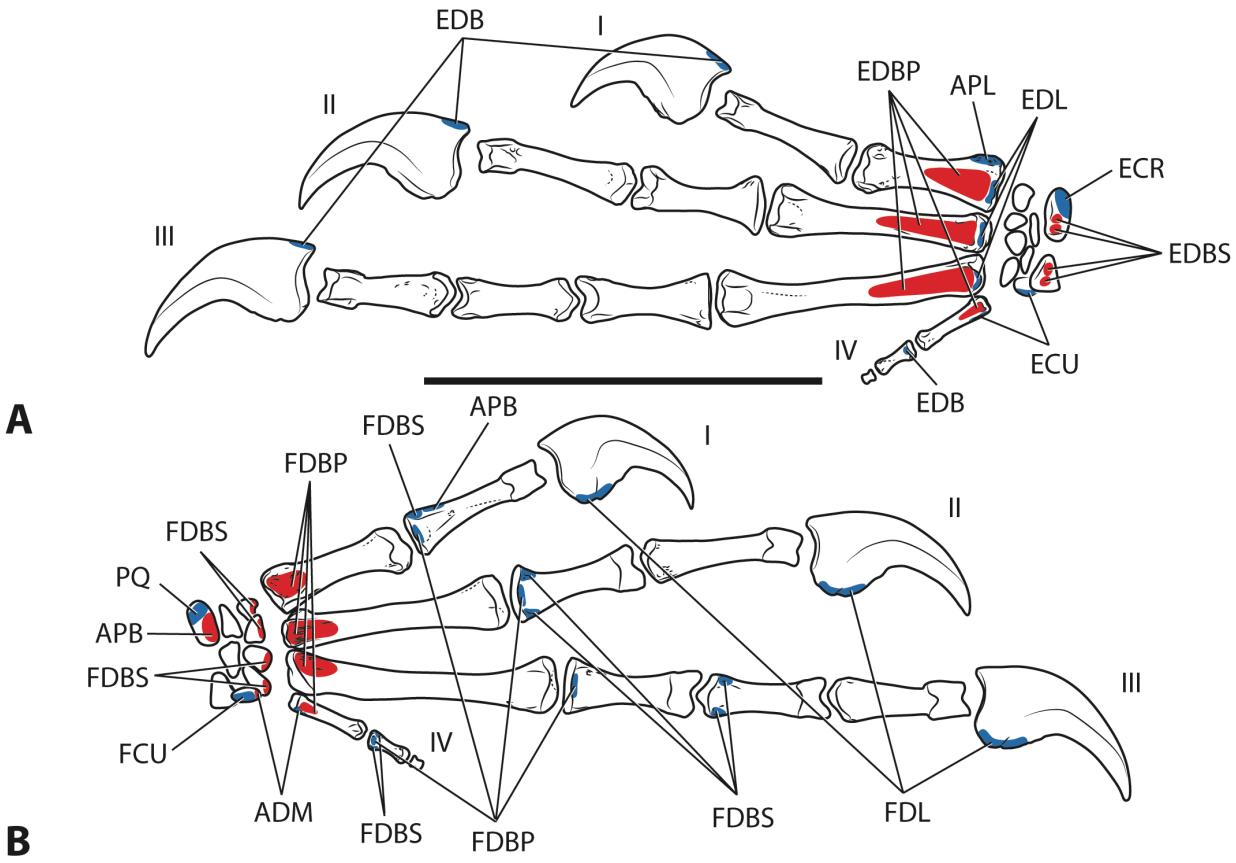
A
EDB
I
II
III
EDBP
APL
EDL
ECR
EDBS
ECU
IV
EDB
B
APB
FDBS
FDBP
I
II
III
FDBS
PQ
APB
FDBS
FCU
IV
ADM
FDBS
FDBP
FDBS
FDL

FIGURE 4.6. Comparison of published myological reconstructions of the shoulder in a generalized basal ornithiscian (**A**, adapted from Maidment & Barrett, 2011), the basal sauropodomorph *Saturnalia* (**B**, adapted from Langer et al., 2007), the basal theropod *Tawa* (**C**), and the dromaeosaurid *Saurornitholestes* (**D**, adapted from Jasinoski et al., 2006 and TMP 88.121.39). Muscles are labeled on *Tawa* and represented in the same color on other taxa. **Abbreviations: AE**, antebrachial extensors; **BB**, Biceps brachii; **CB**, Coracobrachialis; **DC**, Deltoideus clavicularis; **DS**, Deltoideus scapularis; **HR**, Humeroradialis; **LD**, Latissimus dorsi; **SC**, Supracoracoideus; **SHA**, Scapulohumeralis anterior; **SHP**, Scapulohumeralis posterior; **TBM**, Triceps brachii medialis; **TBS**, Triceps brachii caput scapulare. Scale bars each equal 5 cm.

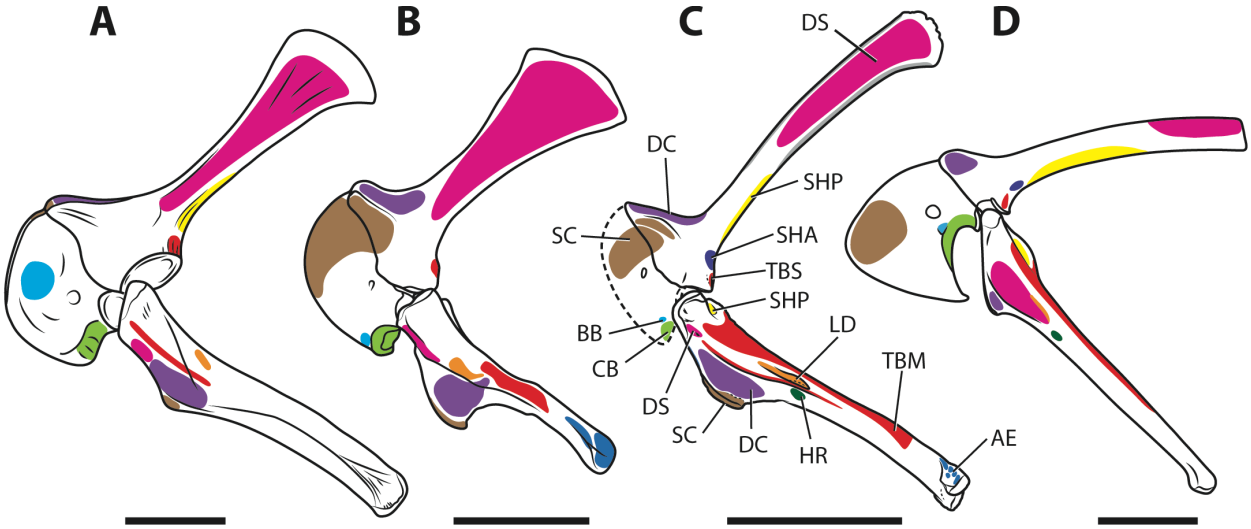
A
B
C
D
DS
DC
SHP
SC
SHA
TBS
SHP
BB
LD
CB
TBM
DS
SC
DC
HR
AE

APPENDIX

1. TABLES

TABLE 4.S1. List of extant taxa scored for analysis, with myological references.

Taxon	Reference
Emys blandingii	Haines 1939
Trachemys scripta elegans	Walker 1973
Trachemys scripta	Abdala et al. 2008
Podocnemis unifilis	Abdala et al. 2008
Lissemys punctata	Shah & Patel 1964
Testudo elegans	Shah & Patel 1964
Sphenodon punctatus	Haines 1939
Sphenodon punctatus	Miner 1925
Varanus exanthematicus	Haines 1939, 1950
Iguana iguana	Russell & Bauer 2008
Liolaemus sp.	Abdala & Moro 2006
Tetradactylus seps	Berger-Dell'mour 1983
Ctenosaura similis	Straus 1942
Alligator sinensis	Cong et al. 1998
Crocodylus americanus	Ribbing 1907
Alligator mississipiensis	Haines 1939
"Crocodylia"	Meers 2003
Struthio camelus	dissection
Apteryx sp.	Parker 1891
Apteryx australis	McGowan 1982
"Tinamidae"	Hudson et al. 1972
Camptorhynchus labradorius	Zusi & Bentz 1978
Anas aucklandica	Livezey 1990
Coturnix coturnix	Fitzgerald 1969
Meleagris gallopavo	Harvey et al. 1968
Gallus gallus	Sullivan 1962
Gallus gallus	Hudson & Lanzillotti 1964
Opisthocomus	Hudson & Lanzillotti 1964
Podilymbus podiceps	Sanders 1967
Caprimulgus carolinensis	OUVC 10642 (dissection)
Columba livia	George & Berger 1966
Geococcyx californianus	Berger 1954
Coua caerulea	Berger 1953
"Lari"	Hudson et al. 1969

Taxon	Reference
“Alcae”	Hudson et al. 1969
Pelecanoides garnoti	McKitrick 1991
Gavia immer	McKitrick 1991
Gavia stellata	McKitrick 1991
Nycticorax nycticorax	Vanden Berge 1970
Balaeniceps rex	Vanden Berge 1970
Phalacrocorax auritius	Owre 1967
Anhinga anhinga	Owre 1967
Fulica americana	Rosser 1980
Gallirallus australis	McGowan 1986
Grus americana	Fisher & Goodman 1955
Grus canadensis tabida	Berger 1956b
Aramus guarauna	Allen 1962
Coragyps atratus	Fisher 1946
Bubo virginianus	OUVC 10641 (dissection)
Megaceryle alcyon	OUVC 10643 (dissection)
Falco sparverius	Meyers 1992, 1996
Polihierax semitorquatus	Berger 1956a
“Passeriformes”	Swinebroad 1954
Tyrannus melancholicus	McKitrick 1985
Hemignathus virens wilsoni	Raikow 1977
Aeglaius phoeniceus	George & Berger 1966
Paradisea rubra	Berger 1956c
Corvus brachyrhynchos	Hudson & Lanzillotti 1955

TABLE 4.S2. Proportional likelihoods of each character state at the nodes Aves, Archosauria, and Archosauria + Lepidosauria based on maximum likelihood ancestral state reconstruction using the consensus phylogeny. Asterisk indicates state is significantly likely.

Char.	State	Proportional Likelihood at Aves	Proportional Likelihood at Archosauria	Proportional Likelihood at Archosauria + Lepidosauria
1	0	0.0125	0.9873*	0.9997*
	1	0.9875*	0.0127	0.0003
2	0	0.0567	0.9417*	0.9822*
	1	0.9433*	0.0583	0.0078
3	0	0.1787	0.5013	0.4659
	1	0.8213	0.4987	0.5341
4	0	0.9992*	0.9810*	0.4914
	1	0.0007	0.0190	0.5086
5	0	0.0104	0.9895*	0.9998*
	1	0.9896*	0.0105	0.0002
6	0	0.9987*	0.9986*	0.9976*
	1	0.0013	0.0014	0.0024
7.1	0	0.0108	0.9891*	0.9998*
	1	0.9892*	0.0109	0.0002
7.2	0	0.9117*	0.9812*	0.9891*
	1	0.0883	0.0188	0.0109
8.0	0	0.0166	0.9815*	0.9978*
	1	0.9831*	0.0180	0.0014
	2	0.0003	0.0006	0.0008
9.1	0	0.9999*	1.000*	1.000*
	1	0.0001	0.0000	0.0000
9.2	0	0.0022	0.0453	0.9152*

Char.	State	Proportional Likelihood at Aves	Proportional Likelihood at Archosauria	Proportional Likelihood at Archosauria + Lepidosauria
	1	0.9978*	0.9547*	0.0848
10	0	0.9997*	0.9834*	0.9994*
	1	0.0003	0.0163	0.0006
	2	0.0000	0.0003	0.0000
11	0	—	—	0.3141
	1	—	—	0.6869
12	0	—	—	0.0087
	1	—	—	0.9913*
13	0	0.9629*	—	0.9763*
	1	0.0371	—	0.0237
14.1	0	0.0130	—	0.4943
	1	0.9870*	—	0.5057
14.2	0	0.0007	—	0.0256
	1	0.9993*	—	0.9744*
14.3	0	0.6512	—	0.6693
	1	0.3488	—	0.3307
14.4	0	0.9451*	—	0.9938*
	1	0.0549	—	0.0062
15	0	1.000*	0.9995*	1.000*
	1	0.0000	0.0005	0.0000
16.1	0	0.0128	0.2632	0.5008
	1	0.9872*	0.7368	0.4992
16.2	0	0.0108	0.9891*	0.9998*
	1	0.9892*	0.0109	0.0002

Char.	State	Proportional Likelihood at Aves	Proportional Likelihood at Archosauria	Proportional Likelihood at Archosauria + Lepidosauria
16.3	0	0.0010	0.0426	0.9574*
	1	0.9990*	0.9574*	0.0426
16.4	0	0.0005	0.0223	0.9569*
	1	0.9995*	0.9777*	0.0431
16.5	0	0.0000	0.0000	0.0054
	1	1.000*	1.000*	0.9946*
16.6	0	0.0220	0.9770*	0.9990*
	1	0.9780*	0.0230	0.0010
17	0	0.9176*	0.9832*	0.9905*
	1	0.0824	0.0168	0.0095
18	0	0.0504	0.1291*	0.6705*
	1	0.8158*	0.8153*	0.2991*
	2	0.1338*	0.0556	0.0303
19	0	0.9999*	—	0.9999*
	1	0.0001	—	0.0001
20	0	0.9504*	—	0.1126
	1	0.0030	—	0.0096
	2	0.0466	—	0.8778*
21	0	0.1660	0.7560	0.8613
	1	0.8340	0.2440	0.1387
22.1	0	0.0676	0.9636*	0.9973*
	1	0.9324*	0.0364	0.0027
22.2	0	0.0272	0.2174	0.1733
	1	0.9728*	0.7826	0.8267

Char.	State	Proportional Likelihood at Aves	Proportional Likelihood at Archosauria	Proportional Likelihood at Archosauria + Lepidosauria
23	0	0.9026*	0.8633	0.9869*
	1	0.0974	0.1367	0.0131
23.1	0	0.4728	—	0.9406*
	1	0.5272	—	0.0594
24	0	0.8761*	—	0.6983
	1	0.1014	—	0.1808
	2	0.0224	—	0.1209
25	0	1.000*	1.000*	0.9999*
	1	0.0000	0.0000	0.0001
26.1	0	0.0220	0.9774*	0.9990*
	1	0.9780*	0.0226	0.0010
26.2	0	0.0459	0.8745	0.9138*
	1	0.9541*	0.1255	0.0862
27	0	1.000*	1.000*	1.000*
	1	0.0000	0.0000	0.0000
27.1	0	0.9999*	0.9999*	0.9999*
	1	0.0001	0.0001	0.0001
28.1	0	0.8854*	0.9790*	0.9901*
	1	0.1146	0.0210	0.0099
28.2	0	0.9944*	0.9983*	0.9978*
	1	0.0056	0.0017	0.0022
28.3	0	0.9869*	0.9960*	0.9956*
	1	0.0131	0.0040	0.0044
29.1	0	1.000*	1.000*	1.000*

Char.	State	Proportional Likelihood at Aves	Proportional Likelihood at Archosauria	Proportional Likelihood at Archosauria + Lepidosauria
	1	0.0000	0.0000	0.0000
29.2	0	1.000*	1.000*	0.9993*
	1	0.0000	0.0000	0.0007
29.3	0	1.000*	1.000*	0.9995*
	1	0.0000	0.0000	0.0005
29.4	0	0.9947*	0.9250*	0.9511*
	1	0.0053	0.0750	0.0489
30.1	0	0.8822*	0.9897*	0.9977*
	1	0.1178	0.0103	0.0023
30.2	0	1.000*	1.000*	1.000*
	1	0.0000	0.0000	0.0000
30.3	0	0.0431	0.9777*	0.9990*
	1	0.9569*	0.0223	0.0010
30.4	0	0.0010	0.0421	0.9574*
	1	0.9990*	0.9579*	0.0426
31.1	0	0.0016	0.0104	0.0970
	1	0.9984*	0.9896*	0.9030*
31.2	0	0.0083	0.0481	0.3002
	1	0.9917*	0.9519*	0.6998*
31.3	0	0.0041	0.0078	0.0226
	1	0.9959*	0.9922*	0.98774*
31.4	0	0.0071	0.0772	0.7856
	1	0.9929*	0.9228*	0.2144
32	0	0.0005	0.0170	0.0374

Char.	State	Proportional Likelihood at Aves	Proportional Likelihood at Archosauria	Proportional Likelihood at Archosauria + Lepidosauria
	1	0.0044	0.2592*	0.7755*
	2	0.0006	0.0252	0.0623
	3	0.0059	0.3493*	0.0624
	4	0.9887*	0.3491*	0.0624
33	0	—	—	0.0672
	1	—	—	0.1625
	2	—	—	0.3932
	3	—	—	0.3771
34	0	0.9886*	0.4950*	0.0493
	1	0.0052	0.2367*	0.8860*
	2	0.0005	0.0154	0.0388
	3	0.0056	0.2530*	0.0260
35	0	—	—	0.5926
	1	—	—	0.4074
36	0	0.9994*	0.9988*	0.9980*
	1	0.0006	0.0012	0.0020
37	0	0.5445*	0.4297*	0.5188*
	1	0.0388	0.0488	0.0660
	2	0.1535*	0.4197*	0.3545*
	3	0.2632*	0.1018*	0.0507
38	0	—	—	0.5586*
	1	—	—	0.0653
	2	—	—	0.2492*
	3	—	—	0.1270*

Char.	State	Proportional Likelihood at Aves	Proportional Likelihood at Archosauria	Proportional Likelihood at Archosauria + Lepidosauria
39	0	0.9993*	0.9984*	0.9770*
	1	0.0005	0.0008	0.0110
	2	0.0002	0.0008	0.0120
40	0	—	—	0.3148
	1	—	—	0.0968
	2	—	—	0.5885
41	0	0.0005	0.0206	0.9377*
	1	0.9995*	0.9789*	0.0614
	2	0.0003	0.0005	0.0009
42	0	0.0063	0.2128*	0.2123*
	1	0.9934*	0.7862*	0.7862*
	2	0.0002	0.0010	0.0020
43	0	—	—	0.8971*
	1	—	—	0.0976
	2	—	—	0.0054
44	0	—	—	0.9060*
	1	—	—	0.0940
45	0	—	—	0.4982
	1	—	—	0.1376
	2	—	—	0.3652
46	0	0.0181	0.9786*	0.9960*
	1	0.0003	0.0010	0.0020
	2	0.9815*	0.0204	0.0020
47	0	1.000*	1.000*	0.9988*

Char.	State	Proportional Likelihood at Aves	Proportional Likelihood at Archosauria	Proportional Likelihood at Archosauria + Lepidosauria
	1	0.0000	0.0000	0.0012
48	0	0.0128	0.1265	0.5401
	1	0.0459	0.1742	0.2158
	2	0.9323*	0.6993	0.2441
49	0	1.000*	1.000*	0.9986*
	1	0.0000	0.0000	0.0014
50	0	0.0054	0.1924	0.5664*
	1	0.0153	0.5817	0.4039*
	2	0.9793*	0.2259	0.0296
51	0	1.000*	1.000*	0.9987*
	1	0.0000	0.0000	0.0013
52	0	—	—	0.3268
	1	—	—	0.6732
53	0	—	—	0.9562*
	1	—	—	0.0438
54	0	—	—	0.8684
	1	—	—	0.1316
55	0	—	—	0.9562*
	1	—	—	0.0438
56	0	0.1284*	0.881*	0.9165*
	1	0.0091	0.0068	0.0075
	2	0.0594*	0.0274	0.0447
	3	0.8030*	0.0848	0.0313
57	0	0.0069	0.1628	0.1344

Char.	State	Proportional Likelihood at Aves	Proportional Likelihood at Archosauria	Proportional Likelihood at Archosauria + Lepidosauria
	1	0.9931*	0.8372	0.8658
58	0	—	0.9966*	0.9903*
	1	—	0.0016	0.0043
	2	—	0.0017	0.0054
59	0	—	0.8970*	0.2605
	1	—	0.1030	0.7395

2. CHARACTER LIST

1 Origin of Brachialis: from line along shaft of humerus (0), or from impression just proximal to distal humeral condyles on cranial/anterior surface of humerus (1)

2 Insertion of Brachialis: on proximal radius in common with Biceps brachii (0), or on impression just distal to ulnar cotyle on anterior surface of ulna (1)

3 Origin of Anconeus: on ectepicondyle of humerus, distal to origins of all other muscles (0), or in common with tendon of Extensor carpi ulnaris (1)

4 Insertion of Anconeus: fleshy on craniodorsal(aves)/craniolateral(croc) surface of ulna for greater than or equal to half its length (0), or less than half its length (1)

5 Origin of Supinator: on ectepicondyle of humerus, proximal to origins of all other muscles (0), or more distally on epicondyle, deep to origin of Extensor digitorum communis (1)

6 Insertion of Supinator: fleshy on cranial surface of radius for greater than or equal to half of its length (0), or proximally for less than half its length (1)

7 Origin of Extensor carpi radialis

7.1 Origin of Extensor carpi radalis: on ectepicondyle of humerus, between origin of supinator and extensor digitorum communis (0), or more proximally than origins of other muscles (1)

7.2 Secondary head that originates adjacent to the main head: absent (0), or present (1)

8 Insertion of Extensor carpi radialis: on the dorsal surface of proximal radiale (0), or on extensor process of carpometacarpus (base of metacarpal I) (1), or on distal radius (2)

9 Origin of Abductor pollicis longus

9.1 Head arising from cranial surface of shaft of ulna: present (0), or absent (1)

9.2 Head arising from caudal surface of shaft of radius: absent (0), or present (1)

10 Insertion of Abductor pollicis longus: on base of metacarpal I/extensor process of carpometacarpus (0), or on dorsal edge of proximal surface of radiale (1), or on second phalanx of first digit (2)

11 Origin of Abductor radialis: on ectepicondyle of humerus with primary head near origin of extensor carpi radialis longus and secondary head proximal to primary head and extensor carpi radialis longus (0), or lacking secondary head (1)

12 Insertion of the Abductor radialis: on proximal half of cranial surface of radius with a slip to dorsal surface of radiale (0), or lacking attachment to radiale (1)

13 Origin of Extensor carpi ulnaris: distally on ectepicondyle of humerus, near origin of Anconeus (0), or from L-shaped tendinous band with distal attachment on proximal end of craniodorsal surface of ulna (1)

14 Insertion of Extensor carpi ulnaris

14.1 Insertion on pisiform: present (0), or absent (1)

14.2 Insertion on ulnare: present (0), or absent (1)

14.3 Insertion on base of lateral-most metacarpal: present (0), or absent (1)

14.4 Insertion on base of metacarpal II: absent (0), or present (1)

15 Origin of Extensor digitorum longus: on ectepicondyle of humerus, between origins of extensor carpi radialis longus and extensor carpi ulnaris (0), or anterior to tendon of extensor carpi radialis longus (1)

16 Insertion of Extensor digitorum longus

16.1 Insertion on base of metacarpal I: present (0), or absent (1)

16.2 Insertion on base of metacarpal II: present (0), or absent (1)

16.3 Insertion on base of metacarpal III: present (0), or absent (1)

16.4 Insertion on base of metacarpal IV: present (0), or absent (1)

16.5 Insertion on base of metacarpal V: present (0), or absent (1)

16.6 Insertion on base of phalanx 1 of metacarpals I and II: absent (0), or present (1)

17 Origin of Pronator teres: on proximal portion of entepicondyle of humerus (0), or on area just proximal to entepicondyle of humerus, distal to ventral edge of origin of brachialis (1)

18 Insertion of Pronator teres: fleshy on cranioventral surface of distal radius for less than or equal to half its length (0), or for along radius for greater than half its length (1), or on proximal radius for less than or equal to half its length (2)

19 Origin of Pronator accessorius: only on entepicondyle of humerus distal to pronator teres, adjacent or deep to flexor digitorum superficialis and humerocarpal band (0), or also a fleshy head arising from humeroulnar pulley (1)

20 Insertion of Pronator accessorius: on ulnar/cranioventral surface of radius for most of its length (0), or proximally for less than half its length (1), or distally for less than half its length (2)

21 Origin of Prontor quadratus: fleshy from ventral surface of ulna for greater than or equal to half its length (0), or distally for less than half its length (1)

22 Insertion of Pronator quadratus

22.1 Insertion on ulnar surface of radius: present (0), or absent (1)

22.2 Insertion on craniodorsal corner of base of the carpals: absent (0), or present (1)

23 Epitrochleoanconeus: present (0), or absent (1)

23.1 Origin of Epitrochleoanconeus: or in close proximity to Flexor carpi ulnaris (0), or in common with Pronator accessorius from entepicondyle of humerus (1)

24 Insertion of Epitrochleoanconeus: fleshy on cranial surface of proximal 1/4 to 1/2 of ulna (0), or on distal 1/2 of ulna (1)

25 Origin of Flexor carpi ulnaris: on entepicondyle of humerus, posterodistal to origins of other muscles (0), or has secondary head (1)

26 Insertion of Flexor carpi ulnaris

26.1 Insertion on pisiform: present (0), or absent (1)

26.2 Insertion on ulnare: absent (0), or present (1)

27 Origin of Flexor digitorum longus superficialis: from single head on entepicondyle of humerus between origins of Flexor carpi ulnaris and Pronator teres (0), or origin is split into two heads (1)

27.1 Secondary attachment to proximal ulna: absent (0), or present (1)

28 Insertion of Flexor digitorum longus superficialis

28.1 Insertion together with tendons of Flexor digitorum longus profundus: present (0), or absent (1)

28.2 Insertion on second phalanx of digit II: absent (0), or present (1)

28.3 Insertion on first phalanx of digit II: absent (0), or present (1)

29 Origin of Flexor digitorum longus profundus

29.1 Origin on ulna: present (0), or absent (1)

29.2 Origin on radius: absent (0), or present (1)

29.3 Origin on humerus: absent (0), or present (1)

29.4 Origin on ulnare: absent (0), or present (1)

30 Insertion of Flexor digitorum longus profundus

30.1 Inserts on ventral surface of base of terminal phalanx of digit I: present (0), or absent (1)

30.2 Inserts on ventral surface of the base of terminal phalanx of digit II: present (0), or absent (1)

30.3 Inserts on ventral surface of the base of terminal phalanx of digit III: present (0), or absent (1)

30.4 Inserts on ventral surface of the base of terminal phalanges of digits IV-V: present (0), or absent (1)

31 Origin of Extensor digiti I brevis superficialis

31.1 Origin from dorsal surface of ulnare: present (0), or absent (1)

31.2 Origin from dorsal surface of intermedium: present (0), or absent (1)

31.3 Origin from dorsal surface of distal ulna: present (0), or absent (1)

31.4 Origin from dorsal surface of radiale: absent (0), or present (1)

32 Origin of Extensor digiti II brevis superficialis: from dorsal surface of distal ulna (0), intermedium (1), ulnare (2), or radiale (3), or distal radius (4)

33 Origin of Extensor digiti III brevis superficialis: from dorsal surface of distal ulna (0), intermedium (1), ulnare (2), or radiale (3)

34 Origin of Extensor digiti IV brevis superficialis: from dorsal surface of distal ulna (0), or only from ulnare (1), or also from intermedium (2), or also from radiale (3)

35 Origin of Extensor digiti V brevis superficialis: only from dorsal surface of ulnare (0), or also from distal ulna (1)

36 Origin of Extensor digiti I brevis profundus: from dorsal surface of base of metacarpal I (0), or from dorsal surface of base of metacarpals I and II (1)

37 Origin of Extensores digitorum II–IV breves profundi: from dorsal surface of their metacarpal (0), or also two adjacent metacarpals (1), or the also metacarpal medial to it (2), or from radiale (3)

38 Origin of Extensor digiti V brevis profundus: from dorsal aspect of metacarpal V (0), or metacarpals V and metacarpal IV (1), or from distal ulnare (2), or from distal ulna (3)

39 Insertion of Extensores digitorum breves superficiales et profundi: on dorsal surface of proximal end of each terminal phalanx (0), or only as far as penultimate phalanx (1), or only as far as first phalanx (2)

40 Insertion of Extensor digiti V brevis profundus: on terminal phalanx of digit V (0), on dorsal surface of first phalanx of digit V (1), or on dorsal surface of metacarpal V (2)

41 Origin of Flexores digitorum I–IV breves superficiales: from annular ligament over carpals (0), or from ventral surface of distal carpals and tendon of Flexor digitorum longus (1), or from distal radius (2)

42 Insertion of Flexor digiti I brevis superficialis: by means of bifurcated tendon on flexor processes on base of first phalanx (0), or on medial margin of base of first phalanx (1), or on terminal phalanx (2)

43 Insertion of Flexores digitorum II–IV breves superficiales: by means of bifurcated tendon on flexor processes on base of first phalanx (0), or tendons reunite to attach at base of second or third phalanx (1), or on terminal phalanx (2)

44 Origin of Flexor digiti V brevis superficialis: identical to those of digits I–IV (0), or from ventral surface of radiale (1)

45 Insertion of Flexor digiti V brevis superficialis: identical to those of digits I–IV (0), or by a single tendon on penultimate phalanx of digit V (1), or terminal phalanx of digit V (2)

46 Origin of Flexor digiti I brevis profundus: ventral surface of distal carpal row (0), or from both carpals and metacarpal I (1), or from metacarpal II (2)

47 Insertion of Flexor digiti I brevis profundus: on flexor process on ventral surface of first phalanx of digit I (0), or on either side of ventral surface on distal end of metacarpal I (1)

48 Origin of Flexor digiti II brevis profundus: ventral surface of distal carpal row (0), or from both carpals and metacarpal II (1), or from base of metacarpal II (2)

49 Insertion of Flexor digiti II brevis profundus: on flexor process on ventral surface of first phalanx of digit II (0), or on either side of ventral surface on distal end of metacarpal II (1)

50 Origin of Flexor digiti III brevis profundus: only ventral surface of distal carpal row (0), or from both carpals and metacarpal III (1), or only proximal half of metacarpal III (2)

51 Insertion of Flexor digiti III brevis profundus: on the flexor process on the ventral surface of first phalanx of digit III (0), or on either side of ventral surface on distal end of metacarpal III (1)

52 Origin of Flexor digiti IV brevis profundus: only ventral surface of distal carpal row (0), or also has attachments along proximal three-quarters of metacarpal IV (1)

53 Insertion of Flexor digiti IV brevis profundus: on flexor process on ventral surface of first phalanx of digit IV (0), or on either side of ventral surface on distal end of metacarpal IV (1)

54 Origin of Flexor digiti V brevis profundus: ventral surface of distal carpal row (0), or ventral surface of proximal end of metacarpal V (1)

55 Insertion of Flexor digiti V brevis profundus: on the flexor process on ventral surface of first phalanx of digit V (0), or on either side of ventral surface on distal end of metacarpal V (1)

56 Origin of Abductor pollicis brevis: from ventrolateral surface of radiale (0), or metacarpal I (1), or distal radius (2), or tendon of Extensor carpi radialis (3)

57 Insertion of Abductor pollicis brevis: on proximolateral surface of metacarpal I (0), or on lateral surface of first phalanx of digit I (1)

58 Origin of Abductor digiti minimi: only from distal surface of pisiform (0), or only from ulnar distal carpal (1), or also has ventral component that arises from annular ligament and Flexor carpi ulnaris (2)

59 Insertion of Abductor digiti minimi: on lateral surface of metacarpal V (0), or on ventrolateral surface of proximal first phalanx of digit V (1)

3. DATA MATRIX

```
Emys_blandingii     ?    ?    1    0    0    0    0    0
     0    0    0    0    0    0    0    0    0    1    0
     0    0    0    0    0    0

0    ?    ?    ?    ?    ?    ?    ?    ?    ?    ?    ?    ?
?    ?    ?    ?    ?    ?    ?    ?    ?    ?    ?    ?    ?
?    1    1    0    0    0    0    1    0    0    0    0
```

0

0 ? ? ? ? ? ? ? ? ? ? ? ? ?

? ? ? ? ? ? ?

Trachemys_scripta_elegans 0 1 1 0 0 0

0 0 0 0 0 0 0 1 0 0 0

1 0 0 0 0 0 0 0 0 0

0 ? ? 0 1 1 ? 0 1 0 0

1 1 0 0 0 0 0 0 0 ? 0

0 0 0 1 1 0 0 0 2 1 0

0 0 0 1 1 0 0 0 0 0 1

0 1 0 1 0 1 0 ? 0 1 1

1 1

Trachemys_scripta 0 0 1 0 0 0 0 0

2 0 0 0 1 1 ? ? ? ? ?

0 0 0 0 0 0 0 0 0 0 2

0 0 1 0 0 1 0 0 0 1 0

0 0 0 0 0 1 ? 0 0 0

0 ? ? ? ? ? ? ? ? 0 0

0 2 1 0 0 0 0 0 0 0 0

0 0 0 0 0 0 0 2 1 0 1

Podocnemis_unifilis 0 0 1 1 0 0 0 0

2 0 0 0 1 1 ? ? ? ? ?

0 0 0 0 0 0 0 0 0 0 2

0 0 1 0 0 1 0 0 0 1 0

0 0 0 0 0 1 ? 0 0 0

0 ? ? ? ? ? ? ? ? 0 0

0 2 1 0 0 0 0 0 0 0 0

0 0 0 0 0 0 0 2 1 0 1

Lissemys_punctata 0 1 0 ? 0 0 0 0

0 0 0 0 1 0 0 1 0 1 0

```
     0    1    0    0    0    0    0    0    0    0    2
     1    0    1    0    0    1    0    1    1    1    0
     0    0    0    0    1    0    0    0    0    0    0
     1    0    1    1    1    1    2    ?    ?    ?    ?
     1    2    0    0    0    0    2    0    0    0    0
     0    0    0    0    0    0    0    1    2    1
Testudo_elegans      0    0    0    0    0    0    0    0
     0    0    0    2    1    0    0    ?    ?    ?    ?
     0    0    0    0    0    0    0    0    0    0    2
     1    0    1    0    0    1    0    0    1    1    0
     0    0    0    0    1    0    0    0    0    0    0
     0    0    1    0    ?    ?    ?    ?    ?    ?    ?
     1    2    1    0    0    0    0    0    0    0    0
     0    0    0    0    0    0    ?    ?    ?    ?
Sphenodon_punctatus ?    ?    0    1    0    0    0    0
     0    0    0    0    0    1    0    0    1    0    0
     0    0    0    0    0    1

0    ?    ?    ?    ?    ?    ?    ?    ?    ?    ?    ?    ?
?    ?    ?    ?    ?    ?    ?    ?    ?    ?    ?    ?    ?
?    1    0    0    0    1    1    2    0    1    1    0
     0

0    ?    ?    ?    ?    ?    ?    ?    ?    ?    ?    ?    ?
?    ?    ?    ?    ?    ?    ?
Sphenodon_punctatus_2    0    0    1    1    0    0    0
     0    0    0    0    0    0    1    0    0    1    0
     0    0    0    0    0    0    1    0    0
     0    ?    ?    0    0    0    0    0    2    0    0
     0    1    0    0    0    0    0    0    0    0    0
     0    0    0    1    0    1    0    1    2    1    0
```

0 0 0 0 0 0 1 1 0 0 1
1 1 1 1 1 1 1 ? 1 0 0
0 1
Varanus_exanthematicus ? ? ? ? 0 0 0
0 0 0 0 0 0 1 0 0 0 0
0 0 1 0 0 0 1 0 0 1 0
2 0 0 1 0 0 0 0 0 1 1
0 0 0 0 0 0 0 1 0 0 0
0 0 1 1 0 2 2 1 1 0 2
2 0 0 0 ? 1 0 ? 0 0 0
0 0 0 0 0 0 0 0 1 0 1
Iguana_iguana 0 0 ? ? 0 0 ? ? ?
0 0 0 0 1 1 0 1 0 0 0
1 0 0 0 1 0 0 0 1 1 0
0 0 0 0 0 0 0 0 0 0 0
0 0 0 0 0 0 0 0 0 0 0
1 1 0 2 2 1 0 0 0 0 0
0 0 1 1 0 1 0 0 0 0 0
0 0 0 0 0 ? ? 2 1
Liolaemus ? ? ? ? 0 0 0 0 0 0
0 0 0 1 0 0 1 0 0 0 1
0 0 0 1 0 0 2 0 1 0 0
0 0 0 0 1 0 0 0 0 0 0
0 0 0 0 0 0 0 0 0 0 1
0 0 0 2 1 0 0 2 1 0 0
0 2 2 0 0 0 1 0 1 0 1
0 1 0 1 0 0 0 0
Tetradactylus_seps ? ? ? ? 0 0 0 0
0 0 0 0 1 1 0 0 1 0 0
0 1 0 0 0 1 0 0 0 0 2
0 0 1 0 0 2 0 0 0 0 0

0 0 0 0 0 0 1 0 0 0 0

0 1 1 0 2 2 1 0 0 2 1

0 0 0 1 1 0 1 0 0 0 0

0 0 0 0 0 0 1 1 0 1

Ctenosaura_similis ? ? ? ? ? ? ? ? ?

? ? ? ? ? ? ? ? ? ? ? ? ?

? ? ? ? 0 1 0 0 0 0 1 ?

0 0 1 0 0 0 0 0 0 0 0

0 0 1 0 0 0

0 ? ? ? ? ? ? ? ? ? ? ? ?

? ? ? ? ? ? ? ? ? ? ? ? ?

? ? ? ? ? ? ?

Alligator_sinensis 0 0 0 0 0 0 0 0

0 0 0 1 1 1 ? ? ? ? ?

0 1 0 1 1 1 1 0 1 ? ?

0 0 0 1 ? ? 0 0 0 1 1

0 0 0 0 0 0 0 0 0 0 0

1 1 1 1 ? ? ? ? ? 0 ?

0 ? 1 0 0 1

2 ? ? ? ? ? ? ? ? ? ?

0 ? ? ?

Crocodylus_americanus ? ? 0 0 0 0 0

0 0 0 1 1 1

1 ? ? ? ? ? 0 1 0 0 1

1 0 0 1 ? ? 0 0 0

1 ? ? 0 0 0 1 0 0 0 0

0 0 0 1 0 0 0 1 1 1 1

1 3 3 0 1 0 2 3 0 2 1

1 0 1 2 0 0 1 0 1 0 1

0 1 0 0 0 0 ?

```
Alligator_mississipiensis      ?    ?    0    0    0    0
     0    0    0    0    1    1    1
     1    ?    ?    ?    ?    ?    0    1    0    1    0
     1    0    ?    ?    ?    ?    ?    ?    ?

1    ?    ?    ?    ?    ?    ?    ?    ?    ?    ?    ?    ?
?    ?    ?    ?    ?    ?    1    1    1    1    3    3
     3    1    1    1    3    0

2    ?    ?    ?    ?    ?    ?    ?    ?    ?    ?    ?    ?
?    ?    ?    0    0    ?    ?
Crocodylia      0    0    0    0    0    0    0    0    0
     0    1    1    1    1    ?    ?    ?    ?    ?    1
     0    0    1    1    1    0    0    1    ?    ?    0
     0    0    1    ?    ?    0    0    0    1    0    0
     0    0    0    0    0    1    0    0    0    1    1
     1    1    1    3    3    3    1    0    2    2    0
     2    1    0    0    1    2    0    0    2    0    1
     0    1    0    1    0    0    0    0    0
Struthio_camelus     1    1    1    0    1    0    1    0
     1    1    1    0    ?    ?    0    1    1    0    0
     0    1    1    1    1    1    1    0    1    ?    ?
     1    0    1    1    ?    ?    0    1
     1    ?    ?    ?    ?    ?    0    0    0    0    0
     0    0    1    1    1    1    1    4    ?    0    ?
     0    0    ?    0    ?    ?    ?    ?    ?    ?    2
     0    2    0    2    0    ?    ?    ?    ?    2    1
     0    0
Apteryx    1    1    0    0    1    0    ?    ?    ?    0
     1    0    ?    ?    0    1    1    0
     0    ?    ?    ?    ?    ?    ?    ?    0
```

```
     1    ?    ?    ?    ?    ?    0    0    1    0
     1    ?    ?    ?    ?    ?    ?    0    1    0    0
     1    0    1

1    ?    ?    ?    ?    ?    ?    ?    ?    ?    ?    ?    ?
?    ?    ?    ?    ?    ?    ?    ?    ?    ?    ?    ?    ?
?    ?    ?    ?    ?    ?    ?
Apteryx_australis    1    0    0    0    1    0    1    0
     1    0    1

0    ?    ?    ?    ?    ?    ?    ?    ?    ?    ?    ?    ?
?    ?    0    1    ?    ?    1    1    0    0    0    1
     0    1    1    ?    ?    ?    ?    ?    0    0    0
     0    1    0    1    1    ?    ?    ?    ?    ?    ?

0    ?    ?    ?    ?    ?    ?    ?    ?    ?    ?    ?    ?
?    ?    ?    ?    ?    ?    ?    ?    ?    ?    ?    ?    ?
Tinamidae 1    1    1    0    1    0    1    0    1    0
     1    0    ?    ?    0    1    1    0    0    0    1
     1    1    1    1    1    0    1    0    0    1    1
     1    0    1    0    0    1    1    1    0    0    0
     0    0    0    0    0    0    0    1
     1    ?    ?    ?    ?    4    ?    0    ?    0
     0    ?    0    ?    1    1    ?    ?    ?    2    0
     2    0    2    0    ?    ?    ?    ?    3    1    ?    ?
Camptorhynchus_labradorius    1    1    1    0    1    0
     1    1    1    0    1    0    ?    ?    1    1    1
     1    1    0    1    1    1    1    1    1    1    2
     0    0    1    1    1    0    1    0    0    1    1
     1    0    1    1    1    0    0    0    0    1    0
     1    1    ?    ?    ?    ?    4    ?    0    ?
```

```
     0    ?    ?    1    ?    1    1    ?    ?    ?    2
     0    1    0    2    0    ?    ?    ?    ?    3
     1    ?    ?
Anas_aucklandica    1    1    1    0    1    0    1    1
     1    0    1    0    ?    ?    1    1    1    1    1
     0    1    1    1    1    1    1    1    2    0    0
     1    1    1    0    1    0    0    1    1    1    0
     1    1    1    0    0    0    0    1    0    1
     1    ?    ?    ?    ?    4    ?    0    ?
     0    ?    ?    1    ?    1    1    ?    ?    ?    2
     0    1    0    2    0    ?    ?    ?    ?    3
     1    ?    ?
Coturnix_coturnix   1    1    1    0    1    0    1    0
     1    0    1    0    ?    ?    0    1    1    0    0
     0    1    1    1    1    1    1    0    1    0    0
     1    1    1    0    1    0    0    1    1    1    1
     1    1    1    0    0    0    0    0    0    1
     1    ?    ?    ?    ?    4    ?    0    ?
     1    ?    ?    0    ?    ?    ?    ?    ?    ?    2
     0    2    0    2    0    ?    ?    ?    ?    1
     1    ?    ?
Meleagris_gallopavo 1    1    1    0    1    1    1    0
     1    0    1    0    ?    ?    0    1    1    1    1
     0    1    1    1    1    1    1    0    2    0    0
     1    1    1    0    1    0    0    1    1    1    0
     1    0    1    0    0    0    0    1    0    1
     1    ?    ?    ?    ?    4    ?    0    ?    0
     3    ?    1    ?    1    1    ?    ?    ?    2    0
     1    0    2    0    ?    ?    ?    ?    3    1    ?    ?
Gallus_gallus  1    1    0    0    1    0    1    0    1
     0    1    0    ?    ?    0    1    1    1    1    0
```

```
     1    1    1    1    1    1    0    1    0    0    0
     1    1    0    1    0    0    1    1    1    0    0
     0    0    0    0    0    0    1    0    1
     1    ?    ?    ?    ?    4    ?    0    ?    0
     0    ?    0    ?    1    1    ?    ?    ?    2    0
     2    0    2    0    ?    ?    ?    ?    3    1    ?    ?
Gallus_gallus_2      1    1    0    0    1    0    1    0
     1    0    1    0    ?    ?    0    1    1    1    1
     0    1    1    1    1    1    1    0    1    0    0
     0    1    1    0    1    0    0    1    1    1    0
     0    0    0    0    0    0    0    1    0    1
     1    ?    ?    ?    ?    4    ?    0    ?    0
     3    ?    0    ?    1    1    ?    ?    ?    2    0
     2    0    2    0    ?    ?    ?    ?    3    1    ?    ?
Opisthocomus    1    1    0    0    1    0    1    0    1
     0    1    0    ?    ?    0    1    1    1    1    0
     1    1    1    1    1    1    0    2    0    1    0
     1    1    0    1    ?    0    1    1    1    0    0
     0    0    0    0    0    0    0    0    1
     1    ?    ?    ?    ?    4    ?    0    ?    0
     3    ?    0    ?    1    1    ?    ?    ?    2    0
     2    0    2    0    ?    ?    ?    ?    3    1    ?    ?
Podilymbus_podiceps 1    1    1    0    1    1    1    1
     1    0    1    0    ?    ?    1    1    1    0    0
     0    1    1    1    1    1    1    0    2    0    0
     1    1    1    1    ?    ?    0    1    1    1    0
     0    0    0    0    0    0    0    1    0    1
     1    ?    ?    ?    ?    4    ?    0    ?
     0    ?    ?    0    ?    1    1    ?    ?    ?    2
     0    2    0    2    0    ?    ?    ?    ?    3
     1    ?    ?
```

Caprimulgus_carolinensis 1 1 1 0 1 0 1
1 1 0 1 0 ? ? 0 1 1 1
1 0 1 1 1 1 1 1 1 2 0
0 1 1 1 1 ? ? 0 1 1 1
0 1 0 0 0 0 0 0 1 0 1
1 ? ? ? ? 4 ? 0 ? 0
3 ? 0 ? 1 1 ? ? ? 2 0
2 0 2 0 ? ? ? ? 3 1 ? ?
Columba_livia 1 1 1 1 1 0 1 1 1
0 1 0 ? ? 1 1 1 1 1 0
1 1 1 1 1 1 1 1 0 0 1
1 1 1 ? ? 0 1 1 1 0 1
1 1 0 0 0 0 1 0 1
1 ? ? ? ? 4 ? 0 ? 0
3 ? 0 ? 1 1 ? ? ? 2 0
1 0 2 0 ? ? ? ? 3 1 ? ?
Geococcyx_californianus 1 1 0 0 1 0 1
0 1 0 1 0 ? ? 1 1 1 1
1 1 1 1 1 1 1 1 1 1 0
0 1 1 1 1 ? ? 0 1 1 1
0 1 0 1 0 0 0 0 1 0 1
1 1 1 1 1 4 ? 0 ?
0 ? ? 0 ? 1 1 ? ? ? 2
0 1 0 2 0 ? ? ? ? 3
1 ? ?
Coua_caerulea 1 1 0 0 1 0 1 1 1
0 1 0 ? ? 1 1 1 1 1 0
1 1 1 1 1 1 1 1 0 0 1
1 1 1 ? ? 0 1 1 1 0 1
0 1 0 0 0 0 1 0 1
1 ? ? ? ? 4 ? 0 ?

```
      0     ?     ?     0     ?     1     1     ?     ?     ?     2
      0     1     0     2     0     ?     ?     ?     ?     3
      1     ?     ?
Lari  1     1     1     0     1     0     1     0     1     0     1
      0     ?     ?     1     1     1     1     1     0     1     1
      1     1     1     1     1     2     0     0     0     1     1
      1     ?     ?     0     1     1     1     0     1     1     1
      0     0     0     0     1     0     1
      1     ?     ?     ?     ?     4     ?     0     ?     0
      0     ?     0     ?     1     1     ?     ?     ?     2     0
      2     0     2     0     ?     ?     ?     ?     3     1     ?     ?
Alcae       1     1     1     0     1     0     1     0     1     0
      1     0     ?     ?     1     1     1     1     1     0     1
      1     1     1     1     1     1     2     0     0     0     1
      1     1     ?     ?     0     1     1     1     0     1     1
      1     0     0     0     0     1     0     1
      1     ?     ?     ?     ?     4     ?     0     ?     0
      0     ?     0     ?     1     1     ?     ?     ?     2     0
      2     0     2     0     ?     ?     ?     ?     3     1     ?     ?
Pelecanoides_garnoti        1     1     ?     0     ?     ?     1
      1     1     0     1     0     ?     ?     0     1     1     1
      1     0     1     1     1     1     1     1     1     2     0
      0     1     1     1     1     ?     ?     0     1     1     1
      0     0     0     0     0     0     0     0     1     0     1
      1     ?     ?     ?     ?     4     ?     0     ?     0
      0     ?     1     ?     1     1     ?     ?     ?     2     0
      1     0     2     0     ?     ?     ?     ?     1     1     ?     ?
Gavia_immer       1     1     1     0     1     0     1     1     1
      0     1     0     ?     ?     0     1     1     1     1     0
      1     1     1     1     1     1     1     2     0     0     1
      1     1     1     ?     ?     0     1     1     1     0     0
```

0 0 0 0 0 0 1 0 1

1 ? ? ? ? 4 ? 0 ? 0

0 ? 1 ? 1 1 ? ? ? 2 0

1 0 2 0 ? ? ? ? 3 1 ? ?

Gavia_stellata 1 1 1 0 1 0 1 1 1

0 1 0 ? ? 0 1 1 1 1 0

1 1 1 1 1 1 1 2 0 0 1

1 1 1 ? ? 0 1 1 1 0 0

0 0 0 0 0 0 1 0 1

1 ? ? ? ? 4 ? 0 ? 0

0 ? 1 ? 1 1 ? ? ? 2 0

1 0 2 0 ? ? ? ? 1 1 ? ?

Nycticorax_nycticorax 1 1 1 0 1 1 1

1 1 0 1 0 ? ? 0 1 1 1

1 0 1 1 1 1 1 1 0 2 0

0 1 1 1 1 ? ? 0 1 1 1

0 0 0 0 0 0 0 0 1 0 1

1 ? ? ? ? 4 ? 0 ? 0

3 ? 0 ? 1 1 ? ? ? 2 0

1 0 2 0 ? ? ? ? 3 1 ? ?

Balaeniceps_rex 1 1 1 0 1 1 1 1

1 0 1 0 ? ? 0 1 1 1 1

0 1 1 1 1 1 1 0 2 0 0

1 1 1 1 ? ? 0 1 1 1 0

0 0 0 0 0 0 0 0 0 1

1 ? ? ? ? 4 ? 0 ? 0

3 ? 0 ? 1 1 ? ? ? 2 0

1 0 2 0 ? ? ? ? 3 1 ? ?

Phalacrocorax_auritius ? ? 1 0 1 1 1

0 1 0 1 0 ? ? 0 1 1 1

1 0 1 1 1 1 1 1 1 2 0

0 ? ? ? 1 ? ? 0 1 1 1

0 1 1 0 0 0 0 0 1 0 1

1 ? ? ? ? 4 ? 0 ? 1

0 ? 0 ? 1 1 ? ? ? 2 0

1 0 2 0 ? ? ? ? 3 1 ? ?

Anhinga_anhinga ? ? 1 0 1 1 1 0

1 0 1 0 ? ? 0 1 1 1 1

0 1 1 1 1 1 1 1 1 0

0 ? ? ? 1 ? ? 0 1 1 1

0 1 1 0 0 0 0 0 1 0 1

1 ? ? ? ? 4 ? 0 ? 1

0 ? 0 ? 1 1 ? ? ? 2 0

1 0 2 0 ? ? ? ? 3 1 ? ?

Fulica_americana 1 1 1 0 1 0 1 1

1 0 1 0 ? ? 1 1 1 1 1

0 1 1 1 1 1 1 0 1 0 0

1 1 1 1 ? ? 1 1 1 1 0

1 0 1 0 0 0 0 1 0 1

1 ? ? ? ? 4 ? 0 ?

1 ? ? 0 ? 1 1 ? ? ? 2

0 2 0 2 0 ? ? ? ? 1

1 ? ?

Gallirallus_australis 1 1 0 0 1 0 1

1 1 0 1 0 ? ? 0 1 1 1

1 0 1 1 1 1 1 1 0 1 0

0 1 1 1 1 ? ? 0 1 1 1

0 0 0 0 0 0 0 0 1 0 1

1 ? ? ? ? 4 ? 0 ?

1 ? ? 0 ? 2 1 ? ? ? 2

0 2 0 2 0 ? ? ? ? 1

1 ? ?

```
Grus_americana 1    1    0    0    1    0    1    1    1
     0    1    0    ?    ?    1    1    1    1    1    0
     1    1    1    1    1    1    0    2    0    0    0
     1    1    1    ?    ?    0    1    1    1    0    1
     1    0    0    0    0    0    1    0    1
     1    ?    ?    ?    ?    4    ?    0    ?
     1    ?    ?    0    ?    1    1    ?    ?    ?    2
     0    2    0    2    0    ?    ?    ?    ?    1
     1    ?    ?
Grus_canadensis_tabida   1    1    0    0    1    0    1
     1    1    0    1    0    ?    ?    0    1    1    1
     1    0    1    1    1    1    1    1    0    2    0
     0    0    1    1    1    ?    ?    0    1    1    1
     1    1    1    0    0    0    0    0    1    0    1
     1    ?    ?    ?    ?    4    ?    0    ?
     1    ?    ?    0    ?    1    1    ?    ?    ?    2
     0    2    0    2    0    ?    ?    ?    ?    1
     1    ?    ?
Aramus_guarauna     1    1    1    0    1    1    1    1
     1    0    1    0    ?    ?    0    1    1    1    1
     0    1    1    1    1    1    1    0    2    0    0
     1    1    1    1    ?    ?    0    1    1    1    0
     1    1    0    0    0    0    0    1    0    1
     1    ?    ?    ?    ?    4    ?    0    ?    1
     3    ?    0    ?    1    1    ?    ?    ?    2    0
     1    0    2    0    ?    ?    ?    ?    3    1    ?    ?
Coragyps  1    1    1    0    1    0    1    1    1    0
     1    0    ?    ?    0    1    1    1    1    0    1
     1    1    1    1    1    1    2    0    1    0    1
     1    1    ?    ?    0    1    1    1    0    1    1
     0    0    0    0    0    1    0    1
```

1 ? ? ? ? 4 ? 0 ? 0

3 ? 0 ? 1 1 ? ? ? 2 0

2 0 2 0 ? ? ? ? 3 1 ? ?

Bubo_virginianus 1 1 1 0 1 1 1 0

1 0 1 0 ? ? 0 1 1 1 1

0 1 1 1 1 1 1 0 2 0 1

0 1 1 1 ? ? 0 1 1 1 0

0 0 0 0 0 0 0 0 0 1

1 ? ? ? ? 4 ? 0 ? 0

3 ? 0 ? 1 1 ? ? ? 2 0

2 0 2 0 ? ? ? ? 1 1 ? ?

Megaceryle_alcyon 1 1 1 0 1 0 1 0

1 ? ? ? ? ? 0 1 1 1 1

0 1 1 1 1 1 1 0 2 0 1

0 1 1 1 ? ? 0 1 1 1 0

0 0 0 0 0 0 0 1 0 1

1 ? ? ? ? 4 ? 0 ?

0 ? ? 0 ? 1 1 ? ? ? 2

0 2 0 2 0 ? ? ? ? 3

1 ? ?

Falco_sparverius 1 1 0 0 1 1 1 1

1 0 1 0 ? ? 1 1 1 1 1

0 1 1 1 1 1 1 1 2 0 1

0 1 1 1 ? ? 0 1 1 1 0

1 0 1 0 0 0 0 1 0 1

1 ? ? ? ? 4 ? 0 ? 0

3 ? 0 ? 1 1 ? ? ? 2 0

1 0 2 0 ? ? ? ? 3 1 ? ?

Polihierax_semitorquatus 1 1 0 0 1 0 1

1 1 0 1 0 ? ? 1 1 1 1

1 0 1 1 1 1 1 1 1 1 0

0 1 1 1 1 ? ? 0 1 1 1

0 1 0 1 0 0 0 0 1 0 1

1 ? ? ? ? 4 ? 0 ?

0 ? ? 0 ? 1 1 ? ? ? 2

0 1 0 2 0 ? ? ? ? 3

1 ? ?

Passeriformes 1 1 0 0 1 0 1 1 1

0 0 0 ? ? 1 1 1 1 1 0

1 1 1 1 1 1 1 1 0 0 0

1 1 1 ? ? 0 1 1 1 0 1

0 1 0 0 0 0 1 0 1

1 ? ? ? ? 4 ?

0 ? ? ? ?

0 ? ? ? ? ? ? 2

0 ? ? ? ? ? ? ? ? 3

1 ? ?

Tyrannus_melancholicus 1 1 0 0 1 0 1

1 1 0 0 0 ? ? 1 1 1 0

0 0 1 1 1 1 1 1 1 1 0

0 0 1 1 1 ? ? 0 1 1 1

0 1 0 1 0 0 0 0 1 0 1

1 ? ? ? ? 4 ?

0 ? ? ? ?

0 ? ? ? ? ? ? 2 0 2 0

2 0 ? ? ? ? 3 1 ? ?

Hemignathus_virens_wilsoni 1 1 0 0 1 1

1 1 1 0 0 0 ? ? 1 1 1

0 0 0 1 1 1 1 1 1 1 1

1 0 1 1 1 1 ? ? 0 1 1

1 0 1 0 1 0 0 0 0 1 0

1 1 ? ? ? ? 4 ?

```
     0    ?    ?    ?    ?
     0    ?    ?    ?    ?    ?    ?    2    0    2    0
     2    0    ?    ?    ?    ?    3    1    ?    ?
Aeglaius_phoeniceus 1    1    0    0    1    1    1    0
     1    0    0    0    ?    ?    1    1    1    0    0
     0    1    1    1    1    1    1    1    1    1    0
     0    1    1    1    ?    ?    0    1    1    1    0
     1    0    1    0    0    0    0    1    0    1
     1    ?    ?    ?    ?
     4    ?    ?    ?    ?    ?    ?
     0    ?    ?    ?    ?    ?    ?    2    0    ?    ?
     2    0    ?    ?    ?    ?    3    1    ?    ?
Paradisea_rubra     1    1    0    0    1    0    1    0
     1    1    1    1    ?    ?    1    1    1    0    0
     0    1    1    1    1    1    1    1    1    0    0
     1    1    1    1    ?    ?    0    1    1    1    0
     1    0    1    0    0    0    0    1    0    1
     1    ?    ?    ?    ?    4    ?
     0    ?    ?    ?    ?
     0    ?    ?    ?    ?    ?    ?    2    0    1    0
     2    0    ?    ?    ?    ?    3    1    ?    ?
Corvus_brachyrhynchos    1    1    0    0    1    1    1
     1    1    0    0    0    ?    ?    1    1    1    0
     0    0    1    1    1    1    1    1    0    1    1
     0    0    1    1    1    ?    ?    0    1    1    1
     0    1    0    1    0    0    0    0    1    0    1
     1    ?    ?    ?    ?    4    ?
     0    ?    ?    ?    ?    0    ?    1
     1    ?    ?    ?    2    0    2    0    2
     0    ?    ?    ?    ?    3    1    ?    ?
```

4. SUPPLEMENTARY REFERENCES

Abdala V, Manzano AS, Herrel A. 2008. The distal forelimb musculature in aquatic and terrestrial turtles: phylogeny or environmental constraints? Journal of Anatomy 213:159–172.

Abdala V, Moro S. 2006. Comparative myology of the forelimb of *Liolaemus* sand lizards (Liolaemidae). Acta Zoologica 87:1–12.

Allen TT. 1962. Myology of the Limpkin [Doctoral]. Gainsville, FL: University of Florida. 339 p.

Berger AJ. 1953. On the locomotor anatomy of the Blue Coua, *Coua caerulea*. The Auk 70:49–93.

Berger AJ. 1954. The myology of the pectoral appendage of three genera of American cuckoos. Miscellaneous Publications Museum of Zoology, University of Michigan 85:1–35.

Berger AJ. 1956a. Appendicular myology of the Pygmy Falcon (*Polihierax semitorquatus*). American Midland Naturalist 55:326–333.

Berger AJ. 1956b. The appendicular myology of the Sandhill Crane, with comparative remarks on the Whooping Crane. The Wilson Bulletin 68:282–304.

Berger AJ. 1956c. On the anatomy of the Red Bird of Paradise, with comparative remarks on the Corvidae. The Auk 73:427–446.

Berger-Dell'mour. 1983. Der übergang von echse zu schleiche in der gattung *Tetradactylus* Merrem. Zoologische Jahrbücher Abteilung für Anatomie und Ontogenie der Tiere 110:1–152.

Cong L, Hou L, Wu X-C, Hou J. 1998. The Gross Anatomy of *Alligator sinensis* Fauvel. Beijing: Science Press. 388 p.

Fisher HI. 1946. Adaptation and comparative anatomy of the locomotor apparatus of New World vultures. American Midland Naturalist 35:545–727.

Fisher HI, Goodman DC. 1955. The myology of the Whooping Crane, *Grus americana*. Illinois Biological Monograph 24:1–127.

Fitzgerald TC. 1969. The Coturnix Quail: Anatomy and Histology. Des Moines, IA: The Iowa State University Press. 306 p.

George JC, Berger AJ. 1966. Avian Myology. New York, NY: Academic Press. 500 p.

Haines RW. 1939. A revision of the extensor muscles of the forearm in tetrapods. Journal of Anatomy 73:211–233.

Haines RW. 1950. The flexor muscles of the forearm and hand in lizards and mammals. Journal of Anatomy 84:13–29.

Harvey EB, Kaiser HE, Rosenberg LE. 1968. An Atlas of the Domestic Turkey (*Meleagris gallopavo*) Myology and Osteology. Washington, DC: U.S. Atomic Energy Commission, Division of Biology and Medicine. 247 p.

Hudson GE, Hoff KM, Vanden Berge JC, Trivette EC. 1969. A numerical study of the wing and leg muscles of Lari and Alcae. Ibis 111:459–524.

Hudson GE, Lanzillotti PJ. 1955. Gross anatomy of the wing muscles in the Family Corvidae. American Midland Naturalist 53:1–44.

Hudson GE, Lanzillotti PJ. 1964. Muscles of the pectoral limb in galliform birds. American Midland Naturalist 71:1–113.

Hudson GE, Schreiweis DO, Wang SYC, Lancaster DA. 1972. A numerical study of the wing and leg muscles of Tinamous (Tinamidae). Northwest Science 46:207–255.

Livezey BC. 1990. Evolutionary morphology of flightlessness in the Aukland Islands Teal. The Condor 92:693–673.

McGowan C. 1982. The wing musculature of the Brown kiwi *Apteryx australis mantelli* and its bearing on ratite affinities. Journal of Zoology 197:173–219.

McGowan C. 1986. The wing musculature of the Weka (*Gallirallus australis*), a flightless rail endemic to New Zealand. Journal of Zoology 210:305–346.

McKitrick MC. 1985. Myology of the pectoral appendage in kingbirds (*Tyrannus*) and their allies. The Condor 87:402–417.

McKitrick MC. 1991. Forelimb myology of loons (Gaviiformes),with comments on the relationship of loons and tubenoses (Procellariiformes). Zool J Linn Soc 102:115–152.

Meers MB. 2003. Crocodylian forelimb musculature and its relevance to Archosauria. The Anatomical Record Part A 274A:891–916.

Meyers RA. 1992. Morphology of the shoulder musculature of the American kestrel, *Falco sparverius* (Aves), with implications for gliding flight. Zoomorphology 112:91–103.

Meyers RA. 1996. Morphology of the antebrachial musculature of the American kestrel, *Falco sparverius*. Annals of Anatomy 178:49–60.

Miner RW. 1925. The pectoral limb of *Eryops* and other primitive tetrapods. Bulletin of the American Museum of Natural History 51:145–312.

Owre OT. 1967. Adaptations for locomotion and feeding in the Anhinga and the Double-Crested Cormorant. Ornithological Monographs 6:1–140.

Parker TJ. 1891. Observations on the anatomy and development of *Apteryx*. Philosophical Transactions of the Royal Society B 182:25–134.

Raikow RJ. 1977. Pectoral appendage myology of the Hawaiian honeycreepers (Drepanididae). The Auk 94:331–342.

Ribbing L. 1907. Die distale armmuskulatur der Amphibien, Reptilien und Säugetiere. Zoologische Jahrbücher 23:587–682.

Rosser BWC. 1980. The wing muscles of the American coot (*Fulica americana* Gmelin). Canadian Journal of Zoology 58:1758–1773.

Russell AP, Bauer AM. 2008. The appendicular locomotor apparatus of *Sphenodon* and normal-limbed squamates. In: Gans C, Gaunt AS, Adler K, editors. Biology of the Reptilia 24, Morphology 1. Ithaca, NY: Society for the Study of Amphibians and Reptiles. p 1–466.

Sanders SWH. 1967. The osteology and myology of the pectoral appendage of grebes [Doctoral], Ann Arbor, MI: University of Michigan. 562 p.

Shah RV, Patel VB. 1964. Myology of the chelonian pectoral appendage. Journal of Animal Morphology and Physiology 11:58–84.

Straus WL. 1942. The homologies of the forearm flexors: urodeles, lizards, mammals. American Journal of Anatomy 70:281–316.

Sullivan GE. 1962. Anatomy and embryology of the wing musculature of the domestic fowl (*Gallus*). Australian Journal of Zoology 10:458–518.

Swinebroad J. 1954. A comparative study of the wing myology of certain passerines. American Midland Naturalist 51:488–514.

Vanden Berge JC. 1970. A comparative study of the appendicular musculature of the Order Ciconiiformes. American Midland Naturalist 84:289–364.

Walker JWF. 1973. The locomotor apparatus of testudines. In: Gans C, Parsons TS, editors. Biology of the Reptilia 4. New York: Academic Press. p 1–100.

Zusi RL, Bentz GD. 1978. The appendicular myology of the Labrador Duck (*Camptorhynchus labradorius*). The Condor 80:407–418.

Chapter V: Myology of the forelimb of *Majungasaurus crenatissimus* (Theropoda, Abelisauridae) and the morphological consequences of extreme limb reduction

ABSTRACT

Forelimb reduction occurred independently in multiple lineages of theropod dinosaurs. Although tyrannosaurs are renowned for their tiny, two-fingered forelimbs, the degree of their reduction in length is surpassed by abelisaurids, which possess an unusual morphology distinct from that of other theropods. The forelimbs of abelisaurids are short but robust and exhibit numerous crests, tubercles, and scars that allow for inferences of muscle attachment sites. Phylogenetically-based reconstructions of the musculature were used in combination with close examination of the osteology in the Malagasy abelisaurid *Majungasaurus* to create detailed muscle maps of the forelimbs, and patterns of the muscular and bony morphology were compared with those of extant tetrapods with reduced or vestigial limbs. The lever arms of muscles crossing the glenohumeral joint are shortened relative to the basal condition, reducing the torque of these muscles but increasing the excursion of the humerus. Fusion of the antebrachial muscles into a set of flexors and extensors is common in other tetrapods and occurred to some extent in *Majungasaurus*. However, the presence of tubercles on the antebrachial and manual elements of abelisaurids indicates that many of the individual distal muscles acting on the wrist and digits were retained. *Majungasaurus* shows some signs of the advanced stages of forelimb reduction preceding limb loss, while also exhibiting features suggesting that the forelimb was not completely functionless. The conformation of abelisaurid forelimb musculature was unique among theropods and further emphasizes the unusual morphology of the forelimbs in this clade.

INTRODUCTION

Limb reduction can be found in nearly every known tetrapod clade and often occurs as a result of or alongside a shift in locomoto mode, such as forelimb reduction after the loss of flight in birds or reduction of all limbs upon elongation of the body and acquisition of concertina locomotion in lepidosaurs. Among extant taxa whose evolutionary lineages have undergone such reduction, oftentimes only a vestigial remnant of the girdle and limb remains, as is the case with the hind limbs of whales and basal snakes. However, within birds and lizards, there are several

extant species that exhibit intermediate stages of limb reduction between the full-sized limb and a completely vestigial one. Limb reduction in lepidosaurs has been the subject of numerous studies, most of which focus on its relationship to body elongation, variation in phalangeal formulas, and the developmental pathways driving reduction (e.g., Presch, 1975; Lande, 1978; Greer, 1987; Caputo et al., 1995; Greer et al., 1998; Shapiro, 2002; Brandley et al., 2008). Comparatively few studies have described or investigated the effects of reduction on the osteology of more proximal limb elements, the myology of the limb, or the functional role of the reduced limb (Fürbringer, 1870; Gans, 1975; Berger-Dell'mour, 1983; Gans and Fusari, 1994), although a recent analysis suggests that the so-called "intermediate" body form of reduced-limbed lizards has been selected for and undergone long periods of stability (Brandley et al., 2008). Variation in the osteology, myology, and pterylography (feather morphology) of neognathous birds has been extensively studied, revealing that, while many flightless neognaths show a very similar, albeit relatively smaller, morphology to their close volant relatives (Livezey, 1989, 1990, 2003), a few taxa show more substantial modification of the wing (Livezey, 1992a, 1992b, 2003). However, no forelimb of an extant neognath exhibit as much modification and reduction as those of ratites, for which there are remarkably few studies of wing morphology (McGowan, 1982; Maxwell and Larsson, 2007b), none of which analyzes changes in morphology across the entire clade. Thus, there is still little known about the effects of limb reduction on the myology of the forelimb and how these changes, in turn, affect the functional capabilities of the limb.

Nonavian theropod dinosaurs present another opportunity to investigate the morphology of highly reduced but potentially non-vestigial forelimbs. Reduction of the forelimb occurred in multiple independent theropod lineages, in some case resulting in a completely novel morphology within the clade. Nonavian theropods were obligate bipeds and primitively possessed long, well-developed forelimbs. The most famous example of reduced forelimbs in theropods is that of tyrannosaurids, and specifically *Tyrannosaurus rex*, which had an arm that was very small relative to its large body size and a manus reduced to two digits (e.g., Brochu, 2003). The mechanisms and evolutionary drivers of forelimb reduction in nonavian theropods is unknown, but in some clades it has been hypothesized to be a result of disuse and specialization

toward head-based predation (Lockley et al., 2009). The most unusual morphology and dramatic reduction in relative length, however, is found in the abelisaurids (Fig. 1), a clade of medium- to large-bodied Cretaceous theropod dinosaurs known almost exclusively from Gondwana. The detailed morphology of the forelimb is relatively well known for the most derived abelisaurids because it has been preserved in near or total articulation in three taxa: *Aucasaurus* (Coria et al., 2002), *Carnotaurus* (Bonaparte et al., 1990), and *Majungasaurus* (Burch and Carrano, 2012). In particular, the 2005–2010 field seasons of the Mahajanga Basin Project have yielded forelimb material from several individuals of the Late Cretaceous (Maastrichtian) Malagasy abelisaurid *Majungasaurus*, including one complete and mostly articulated specimen (Burch and Carrano, 2012). These specimens provide the opportunity to identify muscle scars, tubercles, and crests that are consistent not only between *Majungasaurus* and other abelisaurid taxa but also intraspecifically.

The extreme reduction of the distal elements of the abelisaurid forelimbs has led to the a priori assumption in some studies that the limbs lacked all function (e.g., Senter and Parrish, 2006). However, they possess several features that provide evidence against vestigialization of the limb. The bulbous, hemispherical humeral head and distal radius and ulna indicate that the shoulder and wrist had large ranges of motion; one extreme of this range of motion is even preserved in the articulated and extended wrist of *Aucasaurus* (Coria et al., 2002). Although the distal humeral condyles are flat, the highly concave proximal surfaces of the radius and ulna may indicate that the cartilage cap of this articular surface was also bulbous. The humerus and antebrachial elements are stout and feature several well-developed muscle scars. These features provide the opportunity for reconstruction of the musculature of this bizarre and reduced forelimb, which can then be compared to the musculature of the reduced forelimbs in extant taxa in order to assess how varying osteology affects forelimb myology. Additionally, muscle reconstructions provide functional clues by revealing the action of each muscle on the limb and allowing comparisons with more basal taxa to determine potential shifts in muscle function. The objective of this study is to provide an essential component to future testing of such hypotheses through reconstruction of the myology of the forelimb in *Majungasaurus*.

Institutional Abbreviations—BYU, Brigham Young University, Provo, UT, U.S.A.;

FMNH, The Field Museum, Chicago, Illinois, U.S.A.; **IVPP**, Institute of Palaeontology and Palaeoanthropology, Beijing, China; **MACN-CH**, Museo Argentino de Ciencias Naturales, Colección Chubut, Buenos Aires, Argentina; **MCF-PVPH**, Museo Municipal Carmen Fuñes, Paleontología de Vertebrados, Plaza Huincul, Argentina; **MNHN**, Muséum National d'Histoire Naturelle, Paris, France; **UA**, Université d'Antananarivo, Antananarivo, Madagascar, **UMNH**, Utah Museum of Natural History, Salt Lake City, UT, U.S.A.; **USNM**, National Museum of Natural History, Smithsonian Institution, Washington, DC, U.S.A.

MATERIALS AND METHODS

This reconstruction is based primarily on the osteology of a complete forelimb of *Majungasaurus crenatissimus* (FMNH PR2836), an isolated well-preserved ulna (UA 9860) and humerus (FMNH PR 2423), and several other previously described specimens (Burch and Carrano, 2012). These are supplemented by new specimens of the antebrachial elements collected in the 2010 Mahajanga Basin Project field season, including a mostly complete radius (MAD 10212) and ulna (MAD 10061) both from subadult individuals. Specimens of *Carnotaurus* (MACN-CH 894), *Aucasaurus* (MCF-PVPH-236), *Ceratosaurus* (UMNH VP 5278, USNM 4735, BYU VP 13024) and *Limusaurus* (IVPP V15924, V15923) were also examined to identify morphological features that provide additional information on osteological correlates of muscle attachment sites in ceratosaurs.

Identification of muscle attachment sites was based on the complete reconstruction of the forelimb musculature in the early theropod *Tawa hallae* (Chapter IV) and critical examination of scars, crests, and tubercles preserved on the *Majungasaurus* specimens. The methodological details of this initial reconstruction are detailed elsewhere (see Chapter IV), but are briefly summarized here. Data on the presence, morphology, and attachment sites of each muscle were collected from an Extant Phylogenetic Bracket (Witmer, 1995) of birds, crocodylians, lizards, and turtles. These data were coded as discrete characters and the ancestral states were reconstructed at each node along the backbone of a combined phylogeny of the extant taxa, allowing for designations of the muscles and their specific morphology as phylogenetically

unequivocal or equivocal. These were combined with functional inferences (Bryant and Russell, 1992) based on preserved muscle scars in the extinct taxa, the structure of the forelimb system, and comparisons with extant taxa featuring analogous morphology (e.g., chameleons) in order to reconstruct the most probable arrangement of the musculature in the basal taxon. For the present analysis, reports on the musculature in extant taxa with reduced forelimbs (Fürbringer, 1870; McGowan, 1982; Berger-Dell'mour, 1983; Livezey, 1992b; Maxwell and Larsson, 2007) were also employed to assess effects of reduction on the myology of the limb.

RESULTS

Scapulocoracoid

The scapulocoracoids of abelisaurids are characterized by large, elliptical coracoids and long, broad scapular blades with parallel edges. This provides large potential attachment areas for much of the pectoral musculature (Fig. 2). The insertion of Serratus superficialis is marked in *Majungasaurus* on the ventral edge of the medial aspect of the scapular blade by a shallow groove that extends distally from the approximate midpoint of the scapular blade (Fig. 2B). This groove is developed to various extents in other ceratosaurians; in *Aucasaurus* (MCF PVPH 236) it begins slightly more proximally on the blade whereas in *Carnotaurus* (MACN-CH 894) and *Ceratosaurus* (UMNH VP 5278, BYUVP 13024) it is more extensive, covering two-thirds of the scapular blade. The groove typically exhibits a well-defined dorsal edge proximally that becomes indistinct at the distal end of the scapular blade. The medial surface of the distal end of the scapular blade is marked by shallow grooves in a Y-shape that delineate the boundaries between the insertions of Serratus profundus, Rhomboideus, and the origin of Subscapularis (Fig. 2B).

Subscapularis originated broadly from the medial surface of the scapular blade, its dorsal and ventral edges bounded by the groove for Serratus superficialis ventrally and dorsally by a series of small grooves located at approximately the midpoint of the scapular blade, as in *Carnotaurus* (Fig. 2B). Because ceratosaurians do not possess a distinct medial mid-scapular ridge as seen in early theropods (Chapter IV) and their scapular blades do not narrow proximally before the acromial expansion, Subscapularis had a much more proximally extensive origin than

seen in other theropods. The small, dorsal grooves of *Majungasaurus* and *Carnotaurus* may indicate the ventral extent of the Trapezius and Levator scapulae musculature, which insert along the dorsal edge of the scapular blade (Fig. 2B) but, because they are only present for a short distance in the middle of the blade, this relationship is not clear. However, in *Ceratosaurus* (UMNH VP 5278), this insertion is distinctly marked by a long, narrow, depressed, and highly rugose groove extending along the entire dorsal surface of the scapular blade. As the scapula expands into the acromion this groove becomes less rugose and distinct, and likely represents the area of this scar devoted to the insertion of Trapezius.

The ventral surface of the scapula in *Majungasaurus* is marked by a distinct and slightly rugose lump near the glenoid that was previously identified as the scar for the insertion of Triceps brachii scapularis (Burch and Carrano, 2012). This lump is present as a distinct tubercle on the right scapula of *Carnotaurus* (MACN-CH 894), but it is elongated distally into a prominent fin on the left scapula of *Carnotaurus* as well as in *Aucasaurus* (MCF PVPH 236). A similar rugose lump is also found on the scapula of *Ceratosaurus*, but it is located further from the glenoid fossa. The fin-like morphology of this feature in some abelisaurids makes it an unlikely attachment for Triceps brachii scapularis, which has a limited tendinous insertion in archosaurs. It is much more probable that this lump and/or fin represents the area of origin of Scapulohumeralis posterior (Fig. 2). The lack of a mid-scapular medial ridge would have limited the medial extent of Scapulohumeralis posterior in ceratosaurians, causing the fin-like structure to develop to provide additional attachment area for this muscle. In addition, the lateral surface of the glenoid lip is rugose in *Ceratosaurus*, indicating an origin of Triceps brachii scapularis close to the edge of the glenoid. In *Majungasaurus* there is a small amount of rugosity between the lump and the edge of the glenoid lip, but in abelisaurids this origin is generally indistinct. The origin of Scapulohumeralis anterior is also difficult to place in ceratosaurians because the area dorsal and posterior to the glenoid fossa is smooth and lacks any kind of ridge demarcating the attachment of this muscle. Thus it is reconstructed here originating from a small area in this region (Fig. 2A), though its exact location is uncertain.

The broad, wide scapular blade of *Majungasaurus* also provides a large area of origin on its lateral surface for the Deltoideus scapularis (Fig. 2A). As with Subscapularis, the lack of

narrowing of the scapular blade allows for a much wider origin proximally and a more even distribution of muscle fibers over the length of the blade. The acromial expansion is the location of origin of Deltoideus clavicularis, and in *Majungasaurus* it is long and slopes gently, creating a broad, triangular surface posterodorsal to the subacromial depression (Fig. 2A). This area narrows to a point at the tip of the acromion, allowing some muscle fibers to originate slightly anterior to the glenoid fossa. The subacromial depression of *Majungasaurus* and *Carnotaurus* is divided into two portions by a low ridge. The smaller portion, restricted to the scapula, forms a long oval along its proximal edge and represents the site of origin for Supracoracoideus accessorius (Fig. 2A). The rest of the Supracoracoideus complex arose from the larger part of the depression, which is formed primarily by the coracoid but extends onto a small part of the proximal scapula just beyond the line of fusion between the two bones.

The biceps tubercle of *Majungasaurus* is low but distinct and clearly marks the point of origin for the coracoid head of Biceps brachii (Fig. 2A). It is located close to the coracoid lip of the glenoid fossa and helps to define the margin of the subglenoid fossa. The subglenoid ridge intersects with the margin of the coracoid a short distance from the point of inflection of the posteroventral process, creating a wide, subrectangular subglenoid fossa for the origin of Coracobrachialis (Fig. 2A). This fossa is set off from the lateral surface of the coracoid by the prominent subglenoid ridge and faces slightly posteroventrally. A low rugosity on the anterior edge of the coracoid in one specimen of *Majungasaurus* (FMNH PR 2836, left side) may represent an area of origin of Pectoralis (Fig. 2A); this broad muscle arose from presumably cartilaginous sternal elements but in some theropod taxa it may have also had an origin from the coracoid, as in *Struthio* (Jasinoski et al., 2006). A scar for Pectoralis may also be located on the right coracoid of *Aucasaurus* (MCF PVPH 236), which also has a low rugosity along the ventral portion of its margin. On the medial surface of the *Majungasaurus* coracoid there are no indications of the boundaries of the origin of Subcoracoideus, but in *Ceratosaurus* (UMNH VP 5278) there is a large, subcircular, lightly striated depression just anterior to the coracoid foramen that indicates that this muscle arose from this area of the expansive coracoid in ceratosaurians (Fig. 2B).

Humerus

Abelisaurids have stout, robust humeri that exhibit a low to moderate degree of scarring from the musculature. Nevertheless, there are several prominent features that are identifiable as muscle attachment sites. *Majungasaurus*, *Carnotaurus*, and *Aucasaurus* all possess well-developed internal tuberosities that project substantially beyond the medial border of the humeral head (Fig. 1). This is the insertion site for Subscapularis and Subcoracoideus, two of the main adductors of the forelimb (Fig. 3). Although these two muscles typically insert with a common tendon, separate insertions in abelisaurids may be indicated by a midline ridge present in some specimens (right humerus of FMNH PR 2836 of *Majungasaurus* and right humerus of MACN-CH 894 of *Carnotaurus*) that divides the proximal surface of the internal tuberosity into slightly anterior and posterior facing surfaces. In this case it would be expected that the anterior face would be occupied by the insertion of Subcoracoideus, being the more anteriorly located muscle, and the posterior face would be occupied by the insertion of Subscapularis.

Distal to the proximal surface of the internal tuberosity, a narrow, distinct oblong depression is present on the medial margin of its anterior surface in FMNH PR 2423, representing the site of origin of the humeral head of Biceps brachii (Fig. 3A, B); a small rugosity near this position is also present in the right humerus of *Aucasaurus*. The posterior surface of the internal tuberosity is marked in *Majungasaurus* (represented in both FMNH PR 2423 and the right humerus of FMNH PR 2836) by a small rugose area that corresponds to the insertion point of Scapulohumeralis posterior (Fig. 3C). As in other theropods, the insertion site of Scapulohumeralis anterior is not marked by a scar in *Majungasaurus* or in other abelisaurids. It is typically closely associated with the insertion of Scapulohumeralis posterior, so it is reconstructed here inserting in a small area just lateral to Scapulohumeralis posterior (Fig. 3C), similar to the condition reconstructed in early theropods (Chapter IV).

The humerus FMNH PR 2423 of *Majungasaurus* possesses a deep fossa on the anterior surface of the humeral shaft just distal to the humeral head, which represents the wide, fleshy insertion site of Coracobrachialis (Fig. 3A). The distal extent of this fossa is somewhat restricted, potentially limiting the distal range of this insertion to slightly less than half the length of the

deltopectoral crest. The area available for the insertion of Pectoralis on the medial surface of the deltopectoral crest is also limited given its low, broad morphology, so the insertion would have been restricted to a narrow area at the apex of the crest (Fig. 3A, B). However, at the tip of the deltopectoral crest its rugose edge is extremely wide and provides a large attachment site for the insertion of the Supracoracoideus complex of muscles. The greater tubercle is distally displaced, leaving a short stretch of the edge of the crest for the insertion of Supracoracoideus accessorius (Fig. 3A, D).

The posterior surface of the deltopectoral crest in abelisaurids exhibits numerous large, lumpy rugosities that do not obviously correspond to muscle attachment sites in this area in early theropods. Although their morphology is unusual, it is very similar across all abelisaurid taxa and smaller tubercles in an equivalent area also appear in the humerus of *Ceratosaurus* (UMNH VP 5278). In *Majungasaurus* there are two distinct tubercles preserved in multiple specimens: a proximal one close to the greater tubercle, and a distal tubercle separated from the edge of the deltopectoral crest by a flat, unmarked surface. Several large muscles of the shoulder insert in this area, and the proximity of the tubercles to both the greater tubercle and the deltopectoral crest suggests that they are related to the Deltoideus musculature. However, the posterior surface of the poorly-developed greater tubercle is covered by light rugosity in *Majungasaurus* and slightly larger rugosities in *Aucasaurus*, suggesting a limited insertion for Deltoideus scapularis in this area not associated with the tubercles (Fig. 3C, D). Deltoideus clavicularis typically has a wide insertion over the lateral surface of the deltopectoral crest, and in *Ceratosaurus* this area is heavily striated, extending up to the edge of the posterior tubercles, which form a ridge extending proximodistally. This ridge is aligned proximodistally with a smaller, more distally located ridge and together they may represent the triceps ridge, from which Triceps brachii lateralis originates. *Ceratosaurus* also lacks a distinct furrow for the insertion of Latissimus dorsi that is found in more basal taxa; instead, it is likely that the "tubercles" in *Ceratosaurus* are a product of a more proximally located insertion of Latissimus dorsi that is interacting with the triceps ridge in this taxon to create a highly rugose area. Although it is somewhat difficult to clearly assign the tubercles in *Aucasaurus* and *Carnotaurus* to this arrangement, the tubercles of *Majungasaurus* more closely align with the morphology of *Ceratosaurus*, and thus a similar

arrangement is tentatively reconstructed here (Fig. 3).

The origin of Triceps brachii medialis does not usually leave a scar on the bone surface, but it is large and fleshy, covering much of the posteromedial surface of the humerus. The humerus of *Majungasaurus* is smooth in this area and lacks any ridges or tuberosities that would potentially limit the area of origin, so it is here reconstructed with a similar morphology to the basal condition (Fig. 3). The origin of Brachialis is also difficult to position with accuracy because it too lacks any defining scars in early theropods, in which it arises linearly from the distal part of the deltopectoral crest and the anterolateral humeral shaft. The low apex of the deltopectoral crest wraps around the humeral shaft to a more anteriorly placed position in *Majungasaurus*, and so the origin is reconstructed in a position that is located closer to the midline of the anterior surface (Fig. 3A). The antebrachial muscles arising from the humeral ect- and entepicondyles would have likely done so in close association with one another, and there is little indication that their arrangement in *Majungasaurus* would have differed from that in a more basal taxon. However, the entepicondyle of both *Majungasaurus* and *Aucasaurus* projects far anteriorly, placing the origin of the muscles attaching to it more medially than in earlier theropods (Fig. 3A). It is difficult to locate a true ectepicondyle in *Majungasaurus*, although a slight depression on the posterolateral surface of the shaft just proximal to the articular surface may represent the area from which the ectepicondylar muscles originated (Fig. 3C, D). The relative posterior placement of the ectepicondyle and the proximal placement of the insertion of Supinator (see below) indicates that the origin of Supinator had migrated more proximally on the humeral shaft. In *Aucasaurus*, the radius possesses a proximal projection of this muscle attachment and concurrently exhibits a rugose ridge just proximal to the ectepicondyle, likely representing a proximally shifted origin for this muscle.

Antebrachium

The abelisaurid antebrachium has a highly unusual reduced morphology distinct from that of other theropods. Although the antebrachial elements are very short, they are also very robust with several large, rugose muscle scars. When articulated, the two bones lock tightly together and no long-axis rotation is possible for either element. Most of the supinators and pronators of

the forearm also have a role in flexion or extension and evidence from the scars in *Majungasaurus* indicates that they have shifted toward this function rather than disappearing. The exception to this is Pronator quadratus, which only has a function in pronation of the forearm and manus and thus would have been lost in abelisaurids. Additionally, the status of Pronator accessorius is unknown; there is a single, undifferentiated Pronator muscle in paleognaths (Beddard, 1898), and the fusion of two similarly acting muscles is also a common stage seen in limb reduction of lepidosaurs (Fürbringer, 1870). In the limited muscular space available in the abelisaurid forelimb, Pronator accessorius may have become lost or fused with Pronator teres. The insertion of Pronator teres on the radius of *Majungasaurus* is represented by a small triangular rugosity near the proximal end of the anterior surface that extends into a low ridge along the shaft of the bone (Fig. 4A, C). Just lateral to this is a very large triangular rugosity previously referred to as the lateral triangular rugosity and identified as the insertion of Supinator (Burch and Carrano, 2012). Inserting on the anterolateral surface of the radius in other theropods, Supinator is a major flexor of the forearm and this action seems to be retained in *Majungasaurus*. The rugosity runs the length of the radius and is widest proximally where the inclination and slight anterolateral projection of the radial articular surface gives it the most proximal insertion of the antebrachial muscles (Fig. 4).

Another previously named rugosity, the posterolateral triangular rugosity (Burch and Carrano, 2012), is smaller and located just above the distal articular surface at the posterolateral corner of the radius (Fig. 4B, D). This rugosity represents the combined insertion of Abductor radialis and/or Extensor carpi radialis (ECR). These two muscles are closely associated in tetrapods and may have become fused in the reduced forearm of *Majungasaurus*. In early theropods Abductor radialis inserts on the lateral surface of the radius and ECR inserts on the radiale. No ceratosaur is known to possess a radiale so the insertion of this muscle must have shifted or the muscle itself was lost in these taxa. In birds ECR inserts on the carpometacarpus in an area equivalent to the base of metacarpal I (George and Berger, 1966) and, although this may have served as an insertion point in ceratosaurs with more robust manual morphology, the first metacarpal of abelisaurids is small and already serves as the point of attachment for another muscle (see below). If this muscle has not been lost, the only other location for its insertion is on

the distal radius, as it is in some turtles (Abdala et al., 2008). The substantial rugosity on the distal radius does not obviously correspond to any other antebrachial muscle and may represent the fusion and common insertion of these two muscles in abelisaurids, where it would serve primarily as an extensor of the forearm.

On the anterior surface of the antebrachium, closely associated tubercles on the proximal edges of the radius and ulna correspond to the common insertion of Biceps brachii and Brachialis, as in early theropods (Fig. 4A). In *Majungasaurus* the ulnar tubercle (previously called the anterolateral ridge; Burch and Carrano, 2012) is slightly larger than the radial tubercle and this disparity is exaggerated in *Aucasaurus* and *Carnotaurus*, indicating that the ulnar attachment may be the primary insertion for this common tendon in abelisaurids. Anterior to the interosseus process of the ulna, Flexor digitorum longus profundus (FDLP) had a long, narrow origin extending along the shaft of the ulna distal to the tubercle for Biceps brachii (Fig. 4A, D). There is a distinct notch in the margin of the otherwise dramatically flaring distal articular surface, just anterior to the radial articular facet, to allow for passage of the tendon of this muscle into the manus. On the posterior surface of the antebrachium, a small Abductor pollicis longus muscle likely took origin from the facing surfaces of the radius and ulna, near the ridges for the interosseus membrane (Fig. 4A, D). Although the manus of *Majungasaurus* is very reduced, this muscle is often retained in extant taxa with reduced manus (McGowan, 1982; Berger-Dell'mour, 1983), so it is here reconstructed as present. The tendon of this muscle would have reached the manus via a shallow groove in the flaring distal margin of the radius, between the ulnar articular facet and the posterior projection of the radial distal articular surface.

A major muscle attaching to the posterior surface of the ulna but lacking a scar is Anconeus. The ulna of *Majungasaurus* has a wide, smooth posterior surface that provides a large potential area of insertion for this muscle (Fig. 4B), which has a large, fleshy insertion in early theropods. Inserting on the posterior surface of the ulna, Anconeus would have been one of the primary extensors of the forearm in abelisaurids. The other major antebrachial extensor was Triceps brachii, which inserted on the olecranon process of the ulna (Fig. 4B, C). The olecranon is extremely reduced in *Majungasaurus*, barely projecting beyond the level of the proximal articular surface, and lacks any striations on its posterior surface. Nevertheless the insertion of

Triceps brachii is extremely consistent among tetrapods and thus it would have inserted here in *Majungasaurus* as well. On the anterolateral surface of the ulna, a low ridge probably demarcates the posterior border of the insertion of Epitrochleoanconeus (Fig. 4C). This muscle's fleshy insertion was restricted to the anterior half of the ulna in early theropods, but some forelimb muscles have been shown to extend proportionately farther distally in a taxon with reduced limbs (Livezey, 1992b), so this muscle may have extended along the relatively short distance of the ulnar shaft in *Majungasaurus*.

The ceratosaurian wrist contained at most one ossified carpal; although no carpals are known from the articulated forelimbs of *Majungasaurus*, *Ceratosaurus* (Gilmore, 1920), or *Limusaurus* (Xu et al., 2009), a single rounded bony element that appears to be a carpal can be seen in the articulated arm of *Aucasaurus* (MCF-PVPH 236) and in the recently described *Eoabelisaurus* (Pol and Rauhut, 2012). A small round bone is also present on the distal ulna of *Carnotaurus* (MACN-CH 894) in nearly the same location as preserved in the *Aucasaurus* arm, but the manus of this taxon is jumbled as preserved so it is unknown whether this represents an homologous element. The transformation of the carpus into cartilage and retention of bony metacarpals has been described in extant lepidosaurs with reduced forelimbs (Fürbringer, 1870), although it is not as common in taxa that still possess a well-developed manus, as in *Ceratosaurus*. When their attachment sites become cartilaginous, muscles that previously attached to the carpals are either lost or their attachments shift to a nearby bone, as has been described for some lizards (Berger-Dell'mour, 1983). It is most common for distal attachments of muscles inserting on the carpals to shift to the proximal metacarpals (these attachments will be discussed below), but Flexor carpi ulnaris may have taken a more proximal insertion in *Majungasaurus* (Fig. 4A). Both adult *Majungasaurus* ulnae (FMNH PR 2836 and UA 9860) possess large round pits on the anterior expansion of the distal articular surface, and in the smaller ulna (MAD 10061) this is represented by a shallow divot in the same area. This pit appears to have been the site of a large tendinous attachment, but most of the muscles inserting on the ulna do so via long, fleshy attachments. Of the muscles attaching to the carpus in this region, only Flexor carpi ulnaris typically has a large enough tendon to make such a pit. This insertion of Flexor carpi ulnaris would have resulted in the loss of its action on the carpus and the

anterior projection of the distal ulna would have made this muscle a strong flexor of the antebrachium.

Manus

Majungasaurus retains four digits in its manus, each bearing one or two phalanges. The phalanx of digit IV is fused to the metacarpal in FMNH PR 2836, and it is unknown whether this is a typical morphology or if this phalanx was sometimes mobile. Both the left and right hands preservered in MCF-PVPH 236 of *Aucasaurus* also exhibit fusion within digit IV, so here it is assumed that the phalanx of digit IV was also non-mobile in *Majungasaurus*. The hands of early dinosaurs possessed several layers of short digital flexors and extensors for fine control of the fingers, but *Majungasaurus* certainly lacked a need for such fine control. The intrinsic manual muscles are the first to be lost and individual muscles with similar actions often fuse in lepidosaurs with reduced forelimbs (Fürbringer, 1870; Berger-Dell'mour, 1983). This, combined with the loss of the bony carpals in ceratosaurs, points to the loss of the superficial layers of each muscle group, which arise from the carpals. However, there are several features that suggest that the deep layers of the short digital muscles were present in the first three digits. On the ventral surface, metacarpals I–III each have a wide, projecting, proximal lip that likely served as the site of origin for Flexor digitorum brevis (FDB) of each digit (Fig. 5B). The slips for digits II and III would have divided to insert on the slightly striated projections at either corner of the proximal edge of the proximal (or only) phalanx. Although these projections are small, a split insertion is also supported by the proximal phalanges of *Aucasaurus*, which possess very large tubercles in these locations for the attachment of these tendons. Digit I has only one phalanx, and the ventral surface of phalanx I-1 has a major central ridge and proximal tubercle. The FDB slip to digit I typically does not divide and inserts only on the medial side of the phalanx, so it is reconstructed with this morphology here (Fig. 5B). The central tubercle of phalanx I-1 would have been the insertion point of the tendon of Flexor digitorum longus (FDL) to digit I (Fig. 5B). The FDL tendons to the other digits would have inserted on the proximal surfaces of the distal phalanges. It is uncertain whether digit III possessed one or two phalanges, so the FDL tendon is tentatively reconstructed as inserting on the fused potential second phalanx of this digit (Fig. 5B).

Dorsally, Extensores digitores breves (EDB) are the only muscles that insert on the distal phalanges and extend each digit, so they would have been present in all digits possessing mobile phalanges. These muscle slips originated from the wide, flat dorsal surfaces of metacarpals I–III and traveled a short distance to insert on the proximal edge of the distal phalanx of each digit (Fig. 5A). The tendons of Extensor digitorum longus (EDL) inserted on the base of each metacarpal, just proximal to the origin of EDB (Fig. 5A). Although an insertion by EDL on metacarpal IV is phylogenetically equivocal and not reconstructed in the early theropod *Tawa* (Burch, in prep), an attachment is reconstructed here based on the relative metacarpal sizes. In *Tawa*, metacarpal IV is very small relative to the other metacarpals but, in abelisaurids, metacarpal IV is as large or larger than the other metacarpals. Additionally, abelisaurids apparently exhibited an extreme range of manual extension (as preserved in *Aucasaurus*), which would be better served by having an extensor slip attaching to each digit.

The relatively large metacarpal IV would have also served as an attachment site for the insertion of Extensor carpi ulnaris (Fig. 5A). This muscle is reconstructed as inserting on both the pisiform and the lateral-most metacarpal in early theropods (Chapter IV), and solely on the lateral-most metacarpal once the pisiform is lost in more derived taxa (Chapters IV, VI). The proximal surface of metacarpal IV in *Majungasaurus* is highly angled such that the lateral side projects proximally, and this morphology is even more exaggerated in the manus of *Aucasaurus*. This projection corresponds well to the insertion of Extensor carpi ulnaris, where it would primarily provide extension and ulnar deviation of the wrist. On the opposite side of the manus, the tendon of Abductor pollicis longus would have inserted on the medial side of the first metacarpal (Fig. 5A). Although *Majungasaurus* lacks the prominent medial projection of the first metacarpal seen in early theropods, the proximal edge of the medial surface is characterized by a flat, slightly projecting surface for the insertion of this muscle. Two small manual muscles responsible for detailed movements of the digits, Abductor pollicis brevis and Abductor digiti minimi, were likely lost from the reduced abelisaurid manus. The digits of *Majungasaurus* probably did not have much autonomy, so it is unlikely that these muscles would have been maintained in the manus.

DISCUSSION

Comparative Myology

The scapulocoracoid morphology of *Majungasaurus* suggests few major shifts in the musculature of the shoulder girdle from the basal condition (Fig. 6). The most prominent of these are the changes caused by the parallel scapular margins in abelisaurids, which most greatly affect the origins of Deltoideus scapularis and Subscapularis. The relative narrowing of the distal scapular blade (i.e., loss of the distal flare) and the relative widening of the proximal scapular blade results in a shift in the distribution of the muscle fibers such that a much larger proportion of the muscle is located proximally. The origin of Scapulohumeralis posterior was also shifted proximally in abelisaurids, although *Ceratosaurus* (UMNH VP 5278) maintained a more plesiomorphic origin further from the edge of the glenoid. These muscles are the primary retractors of the humerus and, by shifting their origins proximally, the length of their moment arms, and thus the torque they would be able to generate, was reduced. This is somewhat counteracted in both Deltoideus scapularis and Scapulohumeralis posterior by the slight distal displacement of their insertion sites on the humeral shaft, which served to lengthen their lever arms. The insertion for Deltoideus scapularis in abelisaurids also is very poorly developed relative to that in more basal taxa including *Ceratosaurus*, which possesses a robust, rugose greater tubercle.

The insertion site for Subscapularis is very well developed in abelisaurids, although the orientation of the internal tuberosity is such that its projection creates a line of action that is more advantageous for medial rotation than humeral retraction. The projecting internal tuberosity may also be driven by the insertion of Subcoracoideus, which has a large potential area of origin on the medial surface of the coracoid, providing a substantial capacity for humeral adduction. The shift of more of the muscle fibers of Subscapularis proximally also improved this muscle's role as an adductor of the humerus, though it would have still remained a secondary action. Abelisaurids maintain the wide triangular area of origin for Deltoideus clavicularis as seen in *Ceratosaurus* as well as in earlier theropods (e.g., *Dilophosaurus*, UCMP 37302), but the reduction of the deltopectoral crest greatly limited the potential area of insertion as well as nearly

eliminated any protractional capabilities of this muscle.

The role of the humeral protractor in abelisaurids is filled by the Supracoracoideus complex of muscles, whose large potential area of origin from the subacromial depression and lateral surface of the coracoid indicates substantial development of this muscle group in ceratosaurs. Because the projection of the deltopectoral crest is extremely low in abelisaurids, this muscle group would have inserted nearly flush with the humeral shaft and thus had a shorter moment arm for protraction. Its moment arm for abduction was also reduced due to the medial deviation of the deltopectoral crest onto the anterior shaft of the humerus. Protraction of the humerus was also assisted by Coracobrachialis. Abelisaurids retained a relatively large area of origin for this muscle as well as a subglenoid fossa that faces primarily posteroventrally, which resulted in a more direct line of action for this muscle. Although the insertion is somewhat restricted in *Majungasaurus*, the humeri of *Aucasaurus* possess large, low rugose areas distal and medial to the anterior fossa that may indicate a larger area of insertion in this taxon.

The Pectoralis muscle of *Majungasaurus* may have had a broad origin that included the anterior edge of the scapular blade, but the reduced deltopectoral crest again pulled the point of insertion close to the humeral shaft and shortened the moment arm for this muscle. Similarly, the insertion of Latissimus dorsi moved proximally relative to its position in early theropods, thus shortening the lever arm of this muscle for retraction of the humerus, but this arrangement was also present in *Ceratosaurus* (UMNH VP 5278) and *Limusaurus* (IVPP V15924). Triceps brachii retained all three of its heads in abelisaurids, although the scapular head seems to have had a smaller, less well-developed, and less rugose origin than in other large theropods, including *Ceratosaurus*. There is no indication of reduction in either of the other two heads, and scarring around the origin of the lateral head seems to indicate that this part was well developed. However, the olecranon processes on the ulnae of *Majungasaurus* and *Aucasaurus* are very reduced and hardly project beyond the proximal articular surface. This is not the case in *Carnotaurus*, which possesses an extremely well-developed olecranon process bearing slight striations on its posterior surface.

The lack of any rotation of the antebrachial elements relative to each other would have resulted in the loss or modification of all the antebrachial muscles with roles in pronation or

supination. In *Majungasaurus* and *Aucasaurus* the entepicondyle projects anteriorly, reorienting the lines of action of these muscles to flexion. The ectepicondyle is less well developed in both taxa, although in *Aucasaurus* it is not quite as reduced as in *Majungasaurus*, and it is oriented more posteriorly, enhancing the extensor action of most of the muscles originating from this epicondyle. The exception to this is Supinator, a flexor, whose origin had to move proximally in order to maintain this role. In *Carnotaurus* both epicondyles are large and retain their medial and lateral orientations, similar to the arrangement in *Ceratosaurus* and other early theropods.

The insertions of the antebrachial muscles of abelisaurids were highly modified and difficult to compare to the basal condition. Furthermore, little is known about the antebrachium of abelisauroids or about any transitional stages in the evolution of this bizarre morphology within the clade. Even the basal abelisaurid *Eoabelisaurus* possesses a radius and ulna that are morphologically more similar to those of early theropods than to those of more derived abelisaurids (Pol and Rauhut, 2012). Although slightly more elongate than those of *Majungasaurus* and *Carnotaurus*, the antebrachial elements of *Aucasaurus* bear the same general morphology and arrangement of scars and tubercles, though with a few notable differences. The radius of *Aucasaurus* lacks a distinct posterolateral triangular rugosity for the insertion of Abductor radialis and Extensor carpi radialis and, although the fleshy insertion of Abductor radialis may not have left a scar on the posterior surface of the radius, the tendinous insertion of ECR likely would have. It is possible that in *Aucasaurus* the insertion of ECR was located on the medial surface of metacarpal I; this insertion corresponds with the area of insertion in birds (George and Berger, 1966), and it is also the likely area of insertion in *Ceratosaurus* and other ceratosaurs that had well-developed hands but lacked an ossified carpus. In this case, the muscle would have retained its ability to extend and possibly abduct the wrist.

Another distinct scar in *Aucasaurus* is a large rugosity located distally on the medial surface of the ulna. This rugosity does not obviously correspond to any muscle, but it may represent a distal insertion of Epitrochleoanconeus in this taxon. Flexor carpi ulnaris may have had a different insertion point in *Aucasaurus* and *Carnotaurus*, both of which lack the anterior pit on the distal articular surface present in *Majungasaurus*. This is possibly related to the round bone found at nearly the exact same location at the anteromedial corner of the distal articular

surface of the ulna in the right arm of *Aucasaurus* and the left arm of *Carnotaurus*. Located in the vicinity of the insertion of Flexor carpi ulnaris (FCU), this bone may either represent a carpal or potentially a sesamoid found in the tendon of FCU, assisting it to wrap around the projecting distal articular surface of the ulna. In either case, it is hypothesized here that FCU inserted on this bone, which was then connected distally to the lateral side of metacarpal IV via a ligament or the continuation of the FCU tendon. The insertion of Extensor carpi ulnaris (ECU) also had an attachment to the pisiform in early theropods, but it also attached to the lateral-most metacarpal, which typically possesses a lateral fin that relates to this insertion (Chapter IV). This morphology is present in the metacarpal IV of *Ceratosaurus* (USNM 4735), but this metacarpal does not display increased development of this fin due to the loss of the pisiform. Both the left and right metacarpal IVs preserved in the holotype of *Aucasaurus*, however, bear extremely well-developed lateral processes that also project proximally and, although the metacarpal IV of *Majungasaurus* is relatively reduced, it still has a distinct proximal inclination laterally.

The intrinsic manual musculature was likely reduced to a single layer in all ceratosaurs given the lack of more than one ossified carpal. However, in lepidosaurs, Flexores digitorum breves superficiales originate from an annular ligament, so it is possible that this layer was retained at least in ceratosaurs with well-developed manus and possessed a similar non-bony origin. The manus of *Aucasaurus* possesses a digit I that is more reduced than that of *Majungasaurus*, consisting of a pyramidal metacarpal lacking a phalanx or even a distal articular surface for a phalanx. In this case, the short flexors would have been reduced to only the second and third digits. However, unlike that of *Majungasaurus*, the hands of *Carnotaurus* and *Aucasaurus* both seem to have possessed unguals. In *Aucasaurus*, the distal phalanx of digit II possesses a distal articular surface and a pit for a collateral ligament on its medial condyle, and the manual elements known from *Carnotaurus* seem to include unguals, although further preparation of the specimen is necessary to confirm this. An ungual present on digit II in these taxa would serve as the insertion point for the tendons of Flexor digitorum longus and Extensor digitorum brevis for this digit, as in earlier theropods. *Aucasaurus* and *Ceratosaurus* both possess very large tubercles on the proximal ventral surfaces of phalanges II-1 and III-1; in both taxa these tubercles are greatly enlarged relative to the overall length of the phalanx, and indicate

enlarged flexor musculature despite the small size of the phalanges.

Consequences of Extreme Forelimb Reduction in Abelisaurids

As is typical in tetrapod limb reduction (Fürbringer, 1870; Lande, 1978), forelimb reduction in abelisaurids is greatest in the distal elements. Abelisaurids take this to the extreme; although their antebrachial and manual elements are among the shortest relative to body size in Theropoda, their scapulocoracoids do not exhibit reduction in comparison to basal ceratosaurs (Chapter VII). The retention of large scapulocoraoids in nonavian theropod taxa with reduced limbs may be due to a close developmental association between the scapular blade and the axial skeleton (Kuijper et al., 2005; Valasek et al., 2011), but some of the muscles attaching to the scapulocoracoid possibly had important roles in other activities. Those muscles attaching to the neck (e.g., Levator scapulae) could have played a part in feeding, as may be the case in extant crocodylians (Meers, 2003), and those muscles attaching to the ribs (e.g., Serratus muscles) could have had a role in respiration, as they appear to have in extant birds and crocodylians (Codd et al., 2005; Munns et al., 2012). Although several studies have investigated the functional morphology of respiration and craniocervical muscle dynamics in nonavian dinosaurs (e.g., O'Connor and Claessens, 2005; Snively and Russell, 2007b; Tsuihiji, 2010; Tickle et al., 2012), these studies have focused on the axial musculature and the role of the muscles attaching to the pectoral girdle has not been explored. Furthermore, these muscles predominantly attach to the perimeter of the scapulocoracoid, so their potential areas of origin would be increased through lengthening of the scapular blade, but not by widening it, as is demonstrated in the scapula of *Majungasaurus*. Muscles attaching to the flat surfaces, such as Deltoideus scapularis and Subscapularis, maintain relatively wide, fleshy sites of origin. At the same time, movement of the origins of these muscles toward the glenoid fossa, as well as reduction of the deltopectoral crest in the humerus, result in an overall shortening in moment arms of most of the muscles crossing the glenohumeral joint. A shorter moment arm reduces the torque a muscle can produce for a given action but creates a large angular displacement for the distal end of the bone. That the shoulder of *Majungasaurus* was well-suited for a wide range of motion is also supported by the presence of a bulbous, hemispherical humeral head, which would have allowed the humerus to

move in nearly any direction.

The morphology of the antebrachial elements of *Majungasaurus* is distinct from that of any extant tetrapod, including those with reduced limbs. Besides their unusual shape, the presence of substantial muscle scars on their surfaces indicates the retention of a well-developed musculature and a lack of vestigialization of the distal elements. The radius and ulna of the vestigial forelimbs of the kiwi and emu have been described as simple (McGowan, 1982) and "essentially featureless" (Maxwell and Larsson, 2007b:428) but, in ostriches, which make use of their forelimbs for display and other purposes (Davies, 2002), the radius and ulna retain scars and distinct intermuscular lines (pers. obs.). These differences in osteology are reflected in the development of the musculature: the antebrachial musculature of the former two species, particularly that of the emu, is highly reduced and many muscles have been lost altogether (McGowan, 1979; Maxwell and Larsson, 2007b), whereas the ostrich retains a nearly full complement of antebrachial muscles (Burch, in prep.). In lepidosaurs with forelimbs that show extreme reduction to a single digit, the distal muscles have undergone a reduction and fusion similar to that seen in the emu, and the osteology is similarly indistinct (Berger-Dell'mour, 1983). Although distinct muscle scars present on the antebrachium in *Majungasaurus* provide evidence against extensive fusion of these muscles, the actions of the individual antebrachial muscles have all converged on either flexion or extension, limiting the potential movements of the elbow.

The highly reduced manus of *Majungasaurus* is unusual in that it retains the plesiomorphic ceratosaurian state of four digits. The first stages of limb reduction in tetrapods are typically a reduction in the number of phalanges and loss of pre- and post-axial digits. In lepidosaurs, digit reduction and loss typically follows the sequence of I > V > II > (III, IV), with digits III and IV being retained in taxa that also possess a manus (Fig. 7A), whereas in theropod dinosaurs and birds, this sequence is V > IV > III > I > II (Fig. 7B; Shapiro et al., 2007). Although these two sequences differ in order, they both share the retention of one or two larger central digits subsequent to complete loss of the pre- and postaxial digits. This type of forelimb reduction is found in other theropods, such as tyrannosaurs (Fig. 7C), but it is notably not present among ceratosaurs. Basal ceratosaurs and abelisauroids do show a substantial reduction in the medial and lateral digits relative to digits II and III (Gilmore, 1920; Xu et al., 2009; Pol and Rauhut,

2012) but, unlike the typical progression, these digits are not lost in derived abelisaurids and the metacarpals become nearly subequal in length (Burch and Carrano, 2012). Uniform reduction of the manus, in which the metacarpals are subequal and one or two short phalanges are present on each digit, is not as common and is found in large graviportal animals including tortoises, sauropods, and elephants (Fig. 7D, E; Shapiro et al., 2007). As it is virtually impossible for the abelisaurid forelimb to have been used in such a manner, the reasons for its convergence on this type of reduction are unclear. The retention of the medial and lateral metacarpals may be a result of their roles as attachment sites for Abductor pollicis longus and Extensor carpi ulnaris, respectively, and the evidently large range of motion possible in the wrist of abelisaurids. The bulbous distal articular surfaces of the radius and ulna would have allowed not only substantial flexion and extension (the latter being preserved in the right forelimb of *Aucasaurus*), but also potentially a relatively wide range of abduction and adduction of the wrist.

With the loss of mobile phalanges in digit IV (and digit I in *Aucasaurus*), the small intrinsic muscles of the hand also disappeared in these digits. The extremely small size of the remaining phalanges would have hardly extended beyond the palm of the hand, yet the large ventral tubercles on the phalanges of *Aucasaurus* provide evidence that the short flexors of digits II and III were retained. As in the antebrachium, the condition of the manual muscles in extant flightless birds seems to reflect the utilization of the wing. Although the nonfunctional wings of kiwis and emus actually possess more phalanges in the major digit than is seen in other birds, they have lost all intrinsic manual muscles (McGowan, 1982; Maxwell and Larsson, 2007a), whereas the ostrich retains all muscles present in volant birds and even exhibits primitive muscles not found in other avian taxa (Burch, in prep.). The flightless Galápagos Cormorant, which displays the greatest degree of wing reduction among extant neognaths, also retains a complete manual musculature and possesses an additional intrinsic muscle to the alula absent from other birds; although they do not engage in wing-propelled diving, Galápagos Cormorants likely do make use of their wings and particularly the feathers attaching to the alula during dives for hydrodynamic stabilization (Livezey, 1992b). The retention of the intrinsic manual musculature in the central digits in the hand of abelisaurids suggests that these digits possess some function, even at their extremely reduced size.

Among extant flightless birds, one of the most common functions of non-vestigial wings is that of display, and even at their small size the forelimbs of abelisaurids may have been used for similar species-recognition or mating displays. Another possibility is that of stimulation of the partner during mating. The hind limb booid snakes possesses only the femur and a claw-like 'spur,' and these limbs are actively used during copulation to provide stimulation of the female. During the spurring behavior in pythons, the pelvic spurs move in a wide arc to accomplish a stroke, and also are used to slightly lift the scales of the female (Gillingham and Chambers, 1982). In some cases, the spurs appear to be used to move the female slightly for positioning of the cloaca (Murphy et al., 1978). Spurs are also used in combat interactions determining male dominance in boids, and in this role they can tear up scales and gouge the skin (Carpenter et al., 1978; Barker et al., 1979). The osteology and myology of abelisaurids like *Majungasaurus* indicate that the forelimb was able to be moved in a wide range of motion, which is congruent with the action of completing a stimulating stroke. Additionally, the presence of substantial tubercles for the digital flexors may indicate that the manus played some role in scale lifting or raking the skin. The relatively well-developed shoulder adductor musculature of abelisaurids supports a potential role in clamping or positioning the female between the two forelimbs. The spurs of boid snakes are sexually dimorphic, particularly among mature individuals (Stickel and Stickel, 1946). As future fossil discoveries are made, identification of sexual dimorphism in the forelimbs of abelisaurid theropods would lend further support to this functional hypothesis.

CONCLUSIONS

The reduction of the forelimb in *Majungasaurus* and other derived abelisaurids has resulted in a muscular morphology that exhibits some of the hallmarks of forelimb reduction and loss in extant tetrapods. The low deltopectoral crest provides smaller attachment areas for several brachial muscles, and unossified carpals and a highly reduced manus likely limited the intrinsic manual musculature to a single layer. At the same time, sizable muscle scars on the radius and ulna indicate that a well-developed antebrachial musculature was present in these taxa, and tubercles on the phalanges suggest that digital flexion was a possible action for at least some

digits of the manus. Abelisaurids also exhibit a shoulder myology that is specialized for pulling the forelimb through a large excursion instead of muscles capable of powerful actions. Taken together, the osteology and reconstructed musculature suggest that the forelimbs of abelisaurids were not truly vestigial (lacking any function). Possible functions for this limb include intraspecific display or parter stimulation or clasping during mating.

The unusual morphology of the abelisaurid forelimb makes straightforward functional hypotheses difficult because of the lack of an extant analogue, but the reconstruction presented here provides the first step in future analyses of the functional capabilities of such a limb. Future studies that involve modeling the muscle lines of action and moment arms in three-dimensions (e.g., Hutchinson et al., 2005a) will allow for more detailed insights on the action of each muscle and how they worked together. Unfortunately, the forelimb is unknown for more basal abelisauroid and abelisaurid taxa that may have possessed transitional antebrachial morphologies; future discoveries may shed light on some of the unusual muscle scars that lack obvious correlates in early theropods and how the musculature has evolved stepwise within the clade. The effects of limb reduction and the changing osteology on the myology of the limb is not well understood, but the musculature of *Majungasaurus* provides an example of the results of extreme reduction and will be an important comparative model for future analyses of the musculature of reduced limbs in other extant and extinct species.

ACKNOWLEDGEMENTS

I thank D. Krause, A. Turner, B. Demes, and S. Gatesy for their help and support in the development of this study and comments on early drafts of the manuscript. M. Carrano (USNM), R. Coria (MCF), F. Novas (MACN), A. Kramerz (MACN), R. Sheetz (BYU), R. Irmis (UMNH), M. Getty (UMNH), C. Levitt (UMNH), and Xu X. (IVPP) generously provided access to specimens in their care. I also acknowledge the members of the 2005, 2007, and 2010 Mahajanga Basin Project field expeditions for the collection of these specimens, and A. Rasoamiaramanana of the Université d'Antananarivo, B. Andriamihaja and his staff of the Madagascar Institute pour la Conservation des Ecosystèmes Tropicaux, and the villagers of Berivotra for logistical support

in the field. I thank J. Groenke, V. Heisey, and the volunteers of the Science Museum of Minnesota for their skilled preparation of these materials and A. Pritchard, J. Sertich, and W. Simpson for curation. I thank J. McCartney for support and feedback during this project, and for comments on early drafts of this manuscript. Funding for the Mahajanga Basin Project has been provided by the National Science Foundation (DEB- 9224396, EAR-9418816, EAR-9706302, EAR-0106477, EAR- 0446488, EAR-1123642), the Dinosaur Society (1995), and the National Geographic Society (1999, 2001, 2004, 2009). Support for this project was provided by a National Science Foundation Graduate Research Fellowship and a National Science Foundation Doctoral Dissertation Improvement Grant (DEB 111036).

LITERATURE CITED

Abdala, V., A. S. Manzano, and A. Herrel. 2008. The distal forelimb musculature in aquatic and terrestrial turtles: phylogeny or environmental constraints? Journal of Anatomy 213:159–172.

Barker, D. G., J. B. Murphy, and K. W. Smith. 1979. Social behavior in a captive group of Indian pythons, *Python molurus* (Serpentes, Boidae) with formation of a linear social hierarchy. Copeia 1979:466–471.

Beddard, F. E. 1898. The Structure and Classification of Birds. Longmans, Green, and Co., London.

Berger-Dell'mour. 1983. Der übergang von echse zu schleiche in der gattung *Tetradactylus* Merrem. Zoologische Jahrbücher. Abteilung für Anatomie und Ontogenie der Tiere 110:1–152.

Bonaparte, J. F., F. E. Novas, and R. A. Coria. 1990. *Carnotaurus sastrei* Bonaparte, the horned, lightly built carnosaur from the Middle Cretaceous of Patagonia. Natural History Museum of Los Angeles County Contributions in Science 416:1–41.

Brandley, M. C., J. P. Huelsenbeck, and J. J. Wiens. 2008. Rates and patterns in the evolution of snake-like body form in squamate reptiles: Evidence for repeated re-evolution of lost digits and long-term persistence of intermediate bodyforms. Evolution 62:2042–2064.

Brochu, C. A. 2003. Osteology of *Tyrannosaurus rex*: Insights from a nearly complete skeleton and high-resolution computed tomographic analysis of the skull. Journal of Vertebrate Paleontology 22:1–138.

Bryant, H. N., and A. P. Russell. 1992. The role of phylogenetic analysis in the inference of unpreserved attributes of extinct taxa. Philosophical Transactions: Biological Sciences 337:405–418.

Burch, S. H., and M. T. Carrano. 2012. An articulated pectoral girdle and forelimb of the abelisaurid theropod *Majungasaurus crenatissimus* from the Late Cretaceous of Madagascar. Journal of Vertebrate Paleontology 32:1–16.

Caldwell, M. W. 2003. "Without a leg to stand on": on the evolution and development of axial elongation and limblessness in tetrapods. Canadian Journal of Earth Science 40:573–588.

Caputo, V., B. Lanza, and R. Palmieri. 1995. Body elongation and limb reduction in the genus *Chalcides* Laurenti 1768 (Squamata Scincidae): a comparative study. Tropical Zoology 8:95–152.

Carpenter, C. C., J. B. Murphy, and L. A. Mitchell. 1978. Combat bouts with spur use in the Madagascan boa (*Sanzinia madagascariensis*). Herpetologica 34:207–212.

Codd, J. R., D. F. Boggs, S. F. Perry, and D. R. Carrier. 2005. Activity of three muscles associated with the uncinate processes of the giant Canada Goose *Branta canadensis maximus*. Journal of Experimental Biology 208:849–857.

Coria, R. A., L. M. Chiappe, and L. Dingus. 2002. A new close relative of *Carnotaurus sastrei* Bonaparte 1985 (Theropoda: Abelisauridae) from the Late Cretaceous of Patagonia. Journal of Vertebrate Paleontology 22:460–465.

Davies, S. J. J. F. 2002. Ratites and Tinamous, Bird Families of the World, Volume 9. Oxford University Press, Oxford, UK, 310 pp.

Fürbringer, M. 1870. Die Knochen und Muskeln der Extremitäten bei den Schlangenähnlichen Sauriern. Vergleichend-anatomische Abhandlung. W. Engelmann, Leipzig, 135 pp.

Gans, C. 1975. Tetrapod limblessness: evolution and functional corollaries. American Zoologist 15:455–467.

Gans, C., and M. Fusari. 1994. Locomotor analysis of surface propulsion by three species of reduced-limbed fossorial lizards (*Lerista*: Scincidae) from Western Australia. Journal of Morphology 222:309–326.

George, J. C., and A. J. Berger. 1966. Avian Myology. Academic Press, New York, 500 pp.

Gillingham, J. C., and J. A. Chambers. 1982. Courtship and pelvic spur use in the Burmese python, *Python molurus bivittatus*. Copeia 1982:193–196.

Gilmore, C. W. 1920. Osteology of the carnivorous Dinosauria in the United States National Museum, with special reference to the genera *Antrodemus* (*Allosaurus*) and *Ceratosaurus*. Bulletin of the United States National Museum 110:1–159.

Greer, A. E. 1987. Limb reduction in the lizard genus *Lerista*. 1. Variation in the number of phalanges and presacral vertebrae. Journal of Herpetology 21:267–276.

Greer, A. E., V. Caputo, B. Lanza, and R. Palmieri. 1998. Observations on limb reduction in the scincid lizard genus *Chalcides*. Journal of Herpetology 32:244–252.

Hutchinson, J. R., F. C. Anderson, S. S. Blemker, and S. L. Delp. 2005. Analysis of hindlimb muscle moment arms in *Tyrannosaurus rex* using a three-dimensional musculoskeletal computer model: implications for stance, gait and speed. Paleobiology 31:676–701.

Jasinoski, S. C., A. P. Russell, and P. J. Currie. 2006. An integrative phylogenetic and extrapolatory approach to the reconstruction of dromaeosaur (Theropoda: Eumaniraptora) shoulder musculature. Zoological Journal of the Linnean Society 146:301–344.

Kuijper, S., A. Beverdam, C. Kroon, A. Brouwer, S. Candille, G. Barsh, and F. Meijlink. 2005. Genetics of shoulder girdle formation: roles of Tbx15 and aristaless-like genes. Development 132:1601–1610.

Lande, R. 1978. Evolutionary mechanisms of limb loss in tetrapods. Evolution 32:73–92.

Livezey, B. C. 2003. Evolution of flightlessness in rails (Gruiformes: Rallidae): phylogenetic, ecomorphological, and ontogenetic perspectives. Ornithological Monographs 53:1–654.

Livezey, B. C. 1989. Flightlessness in Grebes (Aves, Podicipedidae): its independent evolution in three genera. Evolution 43:29–54.

Livezey, B. C. 1992a. Morphological corollaries and ecological implications of flightlessness in the Kakapo (Psittaciformes: *Strigops habroptilus*). Journal of Morphology 213:105–145.

Livezey, B. C. 1992b. Flightlessness in the Galápagos cormorant (*Compsohalieus* [*Nannopterum*] *harrisi*): heterochrony, giantism and specialization. Zoological Journal of the Linnean Society 105:155–224.

Livezey, B. C. 1990. Evolutionary morphology of flightlessness in the Aukland Islands Teal. The Condor 92:693–673.

Lockley, M., R. Kukihara, and L. Mitchell. 2009. Why *Tyrannosaurus rex* had puny arms: an integral morphodynamic solution to a simple puzzle in theropod paleobiology; pp. 131–164 in P. Larson and K. Carpenter (eds.), *Tyrannosaurus rex*: the Tyrant King. Indiana University Press.

Maxwell, E. E., and H. C. E. Larsson. 2007a. Osteology and myology of the wing of the Emu (*Dromaius novaehollandiae*), and its bearing onf the evolution of vestigial structures. Journal of Morphology 268:423–441.

Maxwell, E. E., and H. C. E. Larsson. 2007b. Osteology and myology of the wing of the Emu (*Dromaius novaehollandiae*), and its bearing on the evolution of vestigial structures. Journal of Morphology 268:423–441.

McGowan, C. 1979. The hind limb musculature of the Brown Kiwi, *Apteryx australis mantelli*. Journal of Morphology 160:33-74.

McGowan, C. 1982. The wing musculature of the Brown kiwi *Apteryx australis mantelli* and its bearing on ratite affinities. Journal of Zoology 197:173–219.

Meers, M. B. 2003. Crocodylian forelimb musculature and its relevance to Archosauria. The Anatomical Record Part A 274A:891–916.

Munns, S. L., T. Owerkowicz, S. J. Andrewartha, and P. B. Frappell. 2012. The accessory role of the diaphragmaticus muscle in lung ventilation in the estuarine crocodile *Crocodylus porosus*. Journal of Experimental Biology 15:845–852.

Murphy, J. B., D. G. Barker, and B. W. Tryon. 1978. Miscellaneous notes on the reproductive biology of reptiles. II. Eleven species of the family Boidae, genera *Candoia*, *Corallus*, *Epicrates* and *Python*. Journal of Herpetology 12:385–390.

O'Connor, P. M., and L. P. A. M. Claessens. 2005. Basic avian pulmonary design and flow-through ventilation in non-avian theropod dinosaurs. Nature 436:253–256.

Pol, D., and O. W. M. Rauhut. 2012. A Middle Jurassic abelisaurid from Patagonia and the early diversification of theropod dinosaurs. Proceedings of the Royal Society B 279:3170–3175.

Presch, W. 1975. The evolution of limb reduction in the teiid lizard genus *Bachia*. Bulletin of the Southern California Academy of Sciences 74:113–121.

Senter, P., and J. M. Parrish. 2006. Forelimb function in the theropod dinosaur *Carnotaurus sastrei*, and its behavioral implications. PaleoBios 26:7–17.

Shapiro, M. D. 2002. Developmental morphology of limb reduction in *Hemiergis* (Squamata: Scincidae): chondrogenesis, osteogenesis, and heterochrony. Journal of Morphology 254:211–231.

Shapiro, M. D., N. H. Shubin, and J. P. Downs. 2007. Limb diversity and digit reduction in reptilian evolution; pp. 225–244 in B. K. Hall (ed.), Fins into Limbs. University of Chicago Press, Chicago.

Snively, E., and A. P. Russell. 2007. Functional morphology of neck musculature in the Tyrannosauridae (Dinosauria, Theropoda) as determined via a hierarchical inferential approach. Zoological Journal of the Linnean Society 151:759–808.

Stickel, W. H., and L. F. Stickel. 1946. Sexual dimorphism in the pelvic spurs of *Enygrus*. Copeia 1946:10–12.

Tickle, P. G., M. A. Norell, and J. R. Codd. 2012. Ventilatory mechanics from maniraptoran theropods to extant birds. Journal of Evolutionary Biology 25:740–747.

Tsuihiji, T. 2010. Reconstructions of the axial muscle insertions in the occipital region of dinosaurs: evaluation of past hypotheses on Marginocephalia and Tyrannosauridae using the Extant Phylogenetic Bracket approach. The Anatomical Record 293:1360–1386.

Valasek, P., S. Theis, A. DeLaurier, Y. Hinits, G. N. Luke, A. M. Otto, J. Minchin, L. He, B. Christ, G. Brooks, H. Sang, D. J. Evans, M. Logan, R. Huang, and K. Patel. 2011. Cellular and molecular investigations into the development of the pectoral girdle. Developmental Biology 357:108–116.

Witmer, L. M. 1995. The extant phylogenetic bracket and the importance of reconstructing soft tissues in fossils; pp. 9-33 in J. J. Thomason (ed.), Functional Morphology in Vertebrate Paleontology. Cambridge University Press, Cambridge, UK.

Xu, X., J. M. Clark, J. Mo, J. Choiniere, C. A. Forster, G. M. Erickson, D. W. E. Hone, C. Sullivan, D. A. Eberth, S. J. Nesbitt, Q. Zhao, R. Hernandez, C. Jia, F.-l. Han, and Y. Guo. 2009. A Jurassic ceratosaur from China helps clarify avian digital homologies. Nature 459:940–944.

FIGURE 5.1. Reconstruction of articulated right scapulocoracoid and forelimb of *Majungasaurus crenatissimus* in lateral view. Model is composed of CT scans of FMNH PR 2836, right scapulocoracoid and humerus; UA 9860, left ulna (reversed); and FMNH PR 2836, left radius, metacarpals, and phalanges (reversed). **Abbreviations: H**, humerus; **MC I**, metacarpal I; **MC IV**, metacarpal IV; **P**, phalanges; **R**, radius; **SC**, scapulocoracoid; **U**, ulna. Scale bar equals 5 cm.

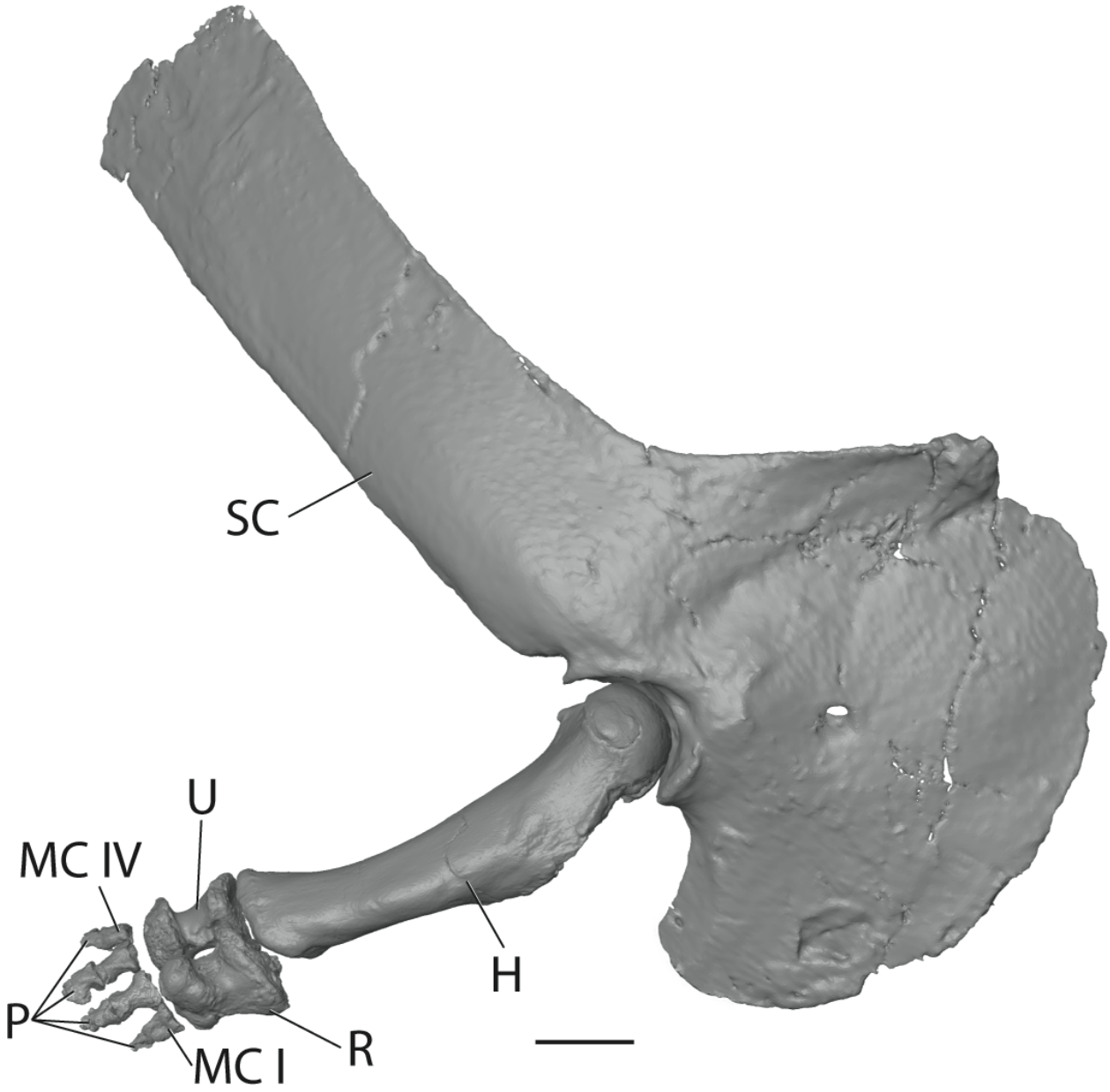
SC
U
MC IV
H
P
R
MC I

FIGURE 5.2. Myological reconstruction of the right scapulocoracoid (FMNH PR 2836) of *Majungasaurus crenatissimus* in lateral (**A**) and medial (**B**) views. Proposed muscle origins are indicated in red, proposed insertions are indicated in blue. **Abbreviations: BB**, Biceps brachii; **CB**, Coracobrachialis; **DC**, Deltoideus clavicularis; **DS**, Deltoideus scapularis; **LS**, Levator scapulae; **P**, Pectoralis; **RH**, Rhomboideus; **SBC**, Subcoracoideus; **SBS**, Subscapularis; **SC**, Supracoracoideus; **SCA**, Supracoracoideus accessorius; **SHA**, Scapulohumeralis anterior; **SHP**, Scapulohumeralis posterior; **SP**, Serratus profundus; **SS**, Serratus superficialis; **TBS**, Triceps brachii scapularis; **TR**, Trapezius. Scale bar equals 5cm.

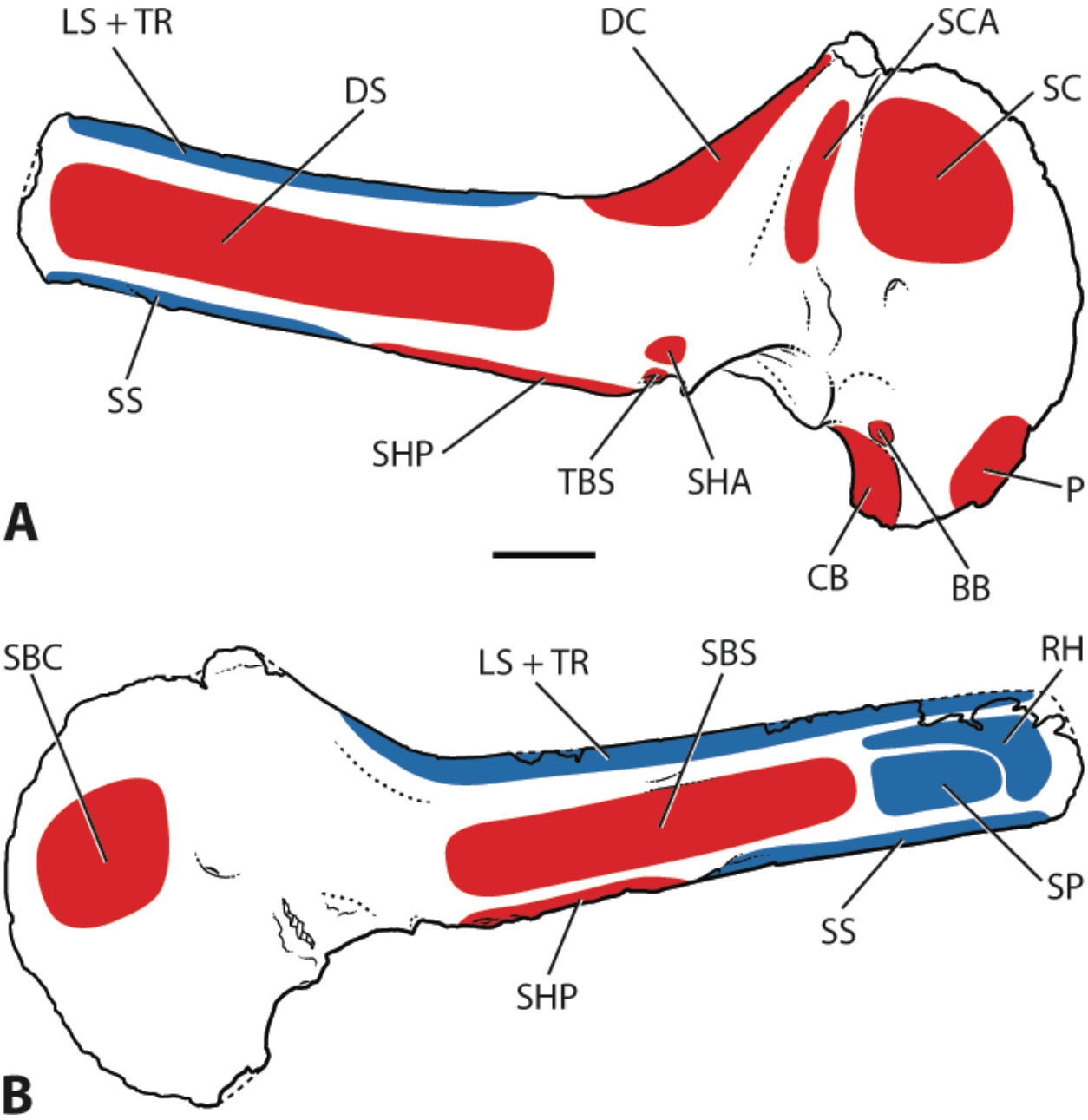
LS + TR
DS
DC
SCA
SC
SS
SHP
TBS
SHA
P
A
CB
BB
SBC
LS + TR
SBS
RH
SP
SS
SHP
B

FIGURE 5.3. Myological reconstruction of the humerus of *Majungasaurus crenatissimus* in anterior (**A**), medial (**B**), posterior (**C**), and lateral (**D**) views. Proposed muscle origins are indicated in red, proposed insertions are indicated in blue. The humerus is a composite reconstruction based on the right humerus of FMNH PR 2836 and the isolated humerus FMNH PR 2423. **Abbreviations: AN**, Anconeus; **AR**, Abductor radialis; **BB**, Biceps brachii; **BR**, Brachialis; **CB**, Coracobrachialis; **DC**, Deltoideus clavicularis; **DS**, Deltoideus scapularis; **EA**, Epitrocheloanconeus; **ECR**, Extensor carpi radialis; **ECU**, Extensor carpi ulnaris; **EDL**, Extensor digitorum longus; **FCU**, Flexor carpi ulnaris; **FDLS**, Flexor digitorum longus superficialis; **LD**, Latissimus dorsi; **P**, Pectoralis; **PT**, Pronator teres; **SBC**, Subcoracoideus; **SBS**, Subscapularis; **SC**, Supracoracoideus; **SCA**, Supracoracoideus accessorius; **SHA**, Scapulohumeralis anterior; **SHP**, Scapulohumeralis posterior; **SU**, Supinator; **TBL**, Triceps brachii longus; **TBM**, Triceps brachii medialis. Scale bar equals 5cm.

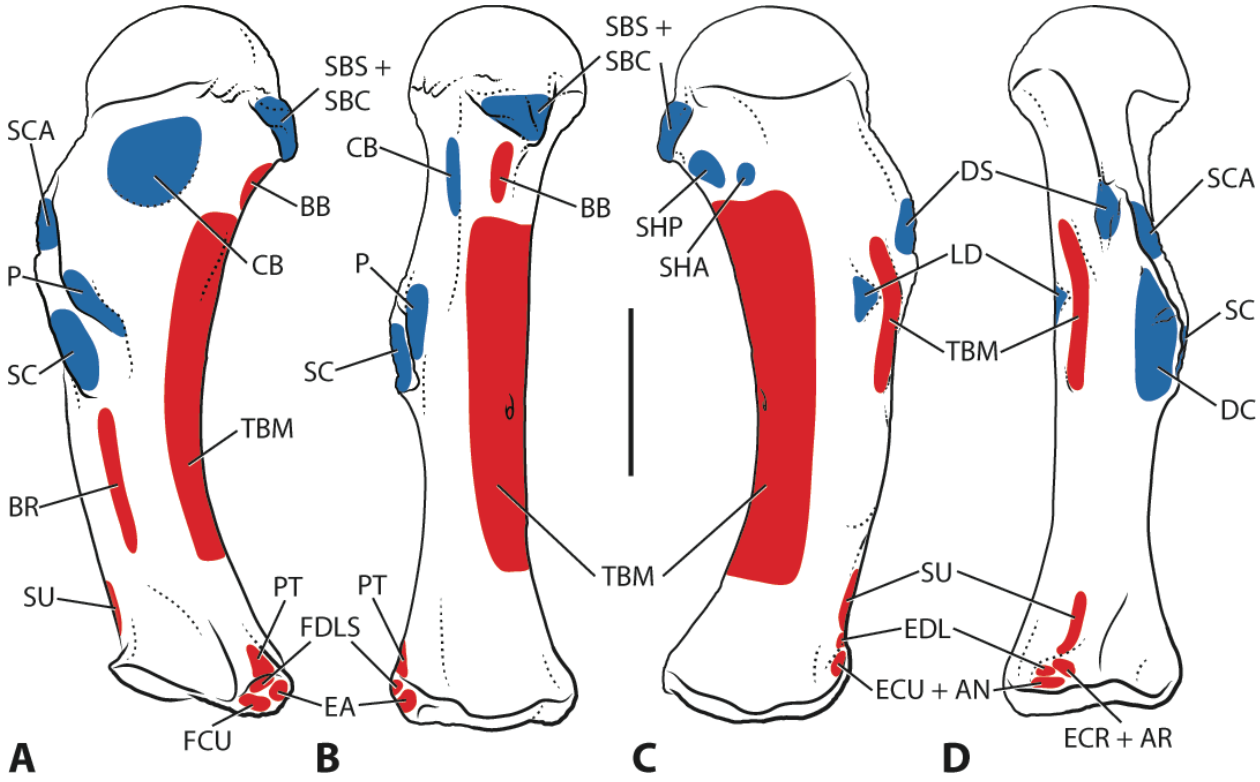
SCA
SBS +
SBC
BB
CB
P
SC
TBM
BR
SU
PT
FDLS
EA
FCU
A
SBS +
SBC
CB
BB
P
SC
PT
TBM
B
SBS +
SBC
SHP
SHA
TBM
C
DS
SCA
LD
SC
TBM
DC
SU
EDL
ECU + AN
ECR + AR
D

FIGURE 5.4. Myological reconstruction of the antebrachium of *Majungasaurus crenatissimus* in anterior (**A**), posterior (**B**), medial (**C**), and lateral (**D**) views. Proposed muscle origins are indicated in red, proposed insertions are indicated in blue. Radius is FMNH PR 2836, ulna is UA 9860 (reversed). Cross-hatching indicates broken bone surface, shaded areas indicate matrix. **Abbreviations: AN**, Anconeus; **APL**, Abuctor pollicis longus; **AR**, Abductor radialis; **BB**, Biceps brachii; **BR**, Brachialis; **EA**, Epitrocheloanconeus; **ECR**, Extensor carpi radialis; **FCU**, Flexor carpi ulnaris; **FDLP**, Flexor digitorum longus profundus; **PT**, Pronator teres; **R**, Radius; **SU**, Supinator; **TB**, Triceps brachii; **U**, Ulna. Scale bar equals 5cm.

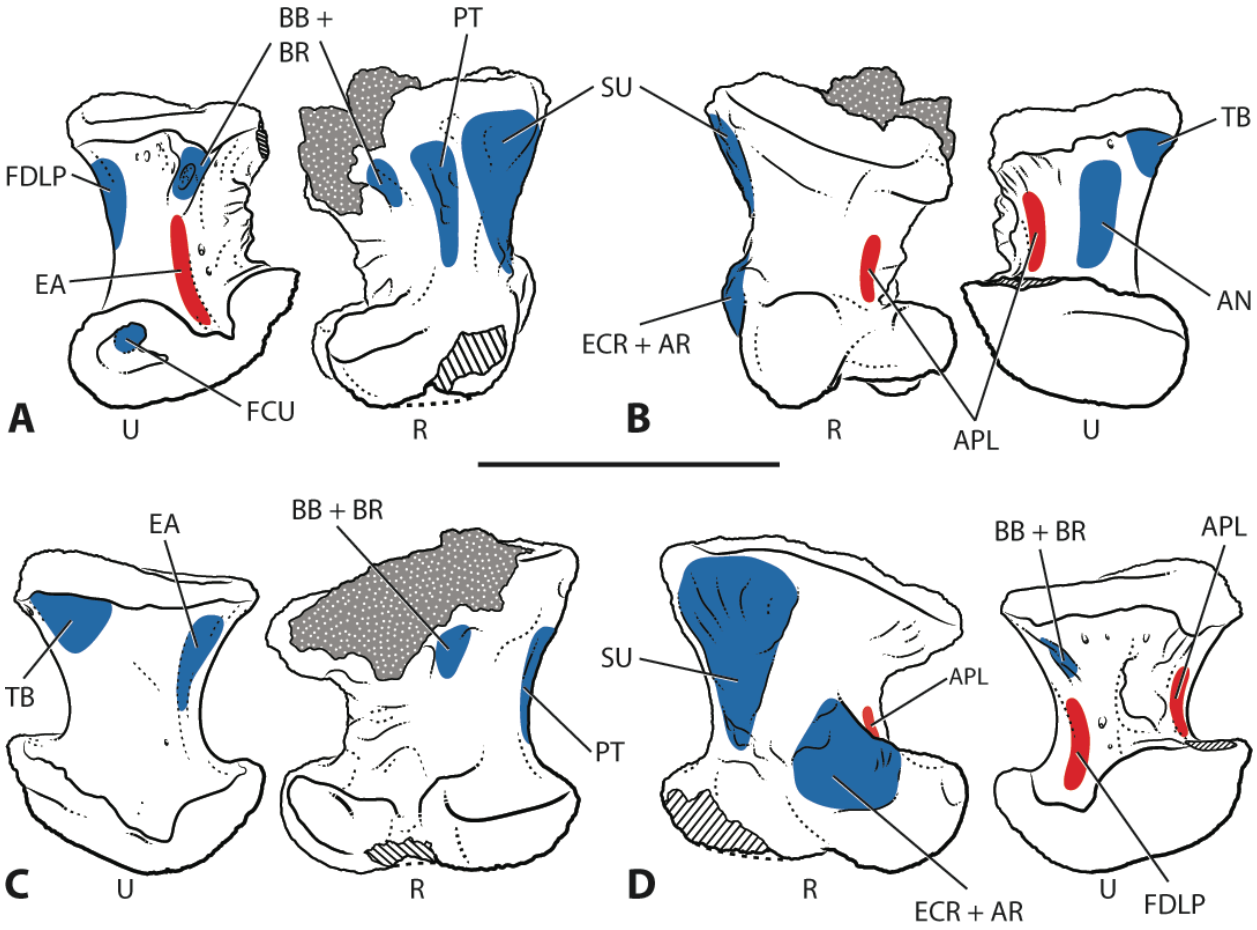
BB +
BR
PT
FDLP
EA
FCU
A
U
R
SU
TB
ECR + AR
AN
B
R
APL
U
EA
BB + BR
TB
PT
C
U
R
SU
APL
BB + BR
APL
D
R
ECR + AR
U
FDLP

FIGURE 5.5. Myological reconstruction of the manus (FMNH PR 2836) of *Majungasaurus crenatissimus* in dorsal (**A**) and ventral (**B**) views. Proposed muscle origins are indicated in red, proposed insertions are indicated in blue. Cross-hatching indicates broken bone surface, shaded areas indicate matrix. **Abbreviations: APL**, Abductor pollicis longus; **ECU**, Extensor carpi ulnaris; **EDB**, Extensor digitorum brevis; **EDB**, Extensor digitorum brevis; **EDL**, Extensor digitorum longus; **FDB**, Flexor digitorum brevis; **FDL**, Flexor digitorum longus; **I**, Digit I; **II**, Digit II; **III**, Digit III; **IV**, Digit IV. Scale bar equals 5cm.

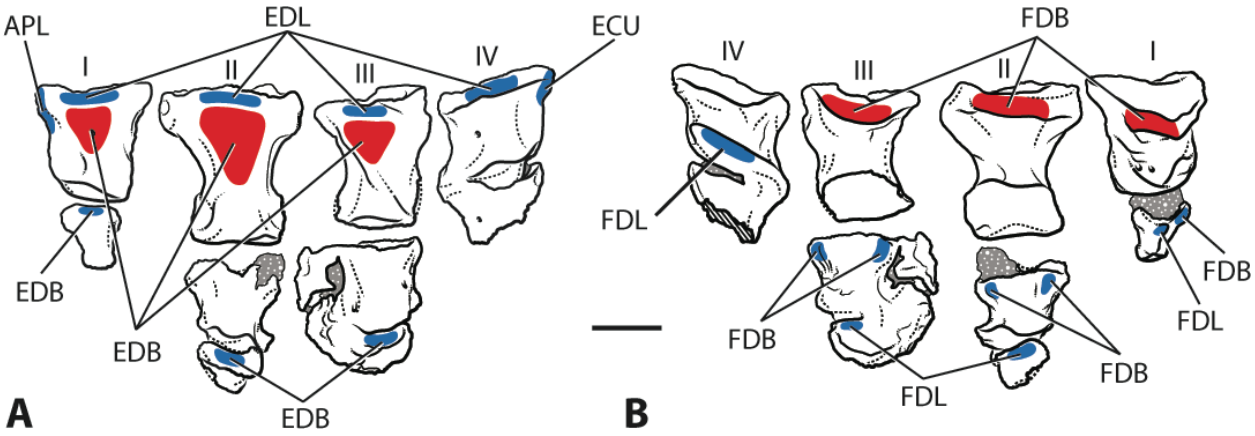
APL
EDL
ECU
I
II
III
IV
EDB
EDB
EDB
A
FDB
IV
III
II
I
FDL
FDB
FDB
FDL
FDB
FDL
B

FIGURE 5.6. Comparison of myological reconstructions of the shoulder in the early theropod *Tawa hallae* (**A**) and *Majungasaurus crenatissimus* (**B**). Muscles are labeled on *Tawa* and represented in the same color on *Majungasaurus*. **Abbreviations: AE**, antebrachial extensors; **BB**, Biceps brachii; **CB**, Coracobrachialis; **DC**, Deltoideus clavicularis; **DS**, Deltoideus scapularis; **HR**, Humeroradialis; **LD**, Latissimus dorsi; **LS**, Levator scapulae; **SC**, Supracoracoideus; **SHA**, Scapulohumeralis anterior; **SHP**, Scapulohumeralis posterior; **SS**, Serratus superficialis; **TBL**, Triceps brachii lateralis; **TBM**, Triceps brachii medialis; **TBS**, Triceps brachii scapularis; **TR**, Trapezius. Scale bars equal 5cm for each taxon.

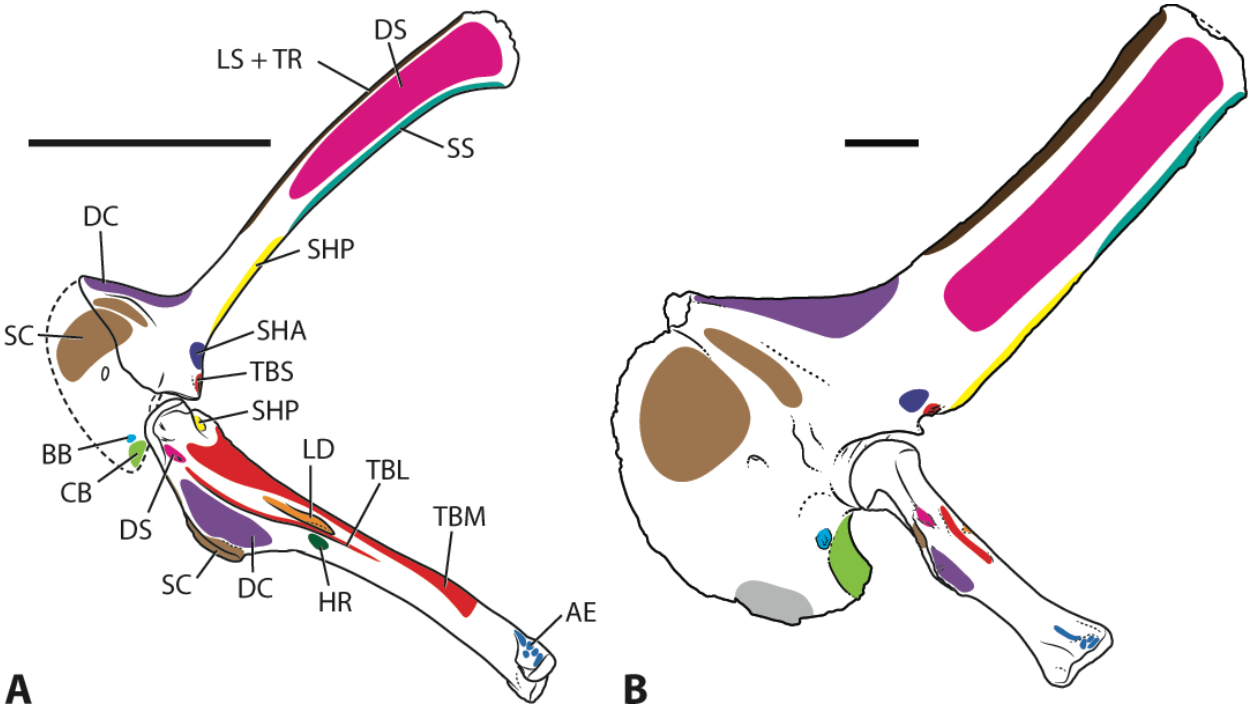
DS
LS + TR
SS
DC
SHP
SC
SHA
TBS
SHP
BB
CB
LD
TBL
TBM
DS
SC
DC
HR
AE
A
B

FIGURE 5.7. Patterns of manual reduction among tetrapods showing typical reduction of external digits (**A–C**), and the less common uniform digital reduction (**D–F**). All diagrams show a dorsal view of the right manus, and phalangeal formulae are given below each manus. Examples shown are the lepidosaur *Hemiergis quadrilineata* (**A**), the paleognathous bird *Struthio camelus* (**B**), the nonavian theropod *Tyrannosaurus rex* (**C**), the tortoise *Testudo* (**D**), the sauropod *Diplodocus* (**E**), and *Majungasaurus crenatissimus* (**F**). All diagrams except B and E after Shapiro et al. (2007).

A X-0-3-4-0

B 2-3-1-X-X

C 2-3-0-X-X

D 2-2-2-2-2

E 2-1-1-1-1

F 1-2-2?-1-X

Chapter VI: Myological trends of forelimb reduction in Tyrannosauroidea (Dinosauria: Theropoda)

ABSTRACT

The highly reduced forelimbs of tyrannosaurid theropods have sparked many hypotheses about their function or potential lack thereof. Although a few studies have attempted to address this question through basic biomechanical analyses of an exemplar taxon (*Tyrannosaurus rex*), the evolutionary pattern of acquisition of key myological characters over the tyrannosauroid lineage and the interactions of the musculature as a whole have never been investigated. In this study, osteological correlates of muscle attachment were identified in the forelimbs of tyrannosauroid, tetanuran, and basal theropod taxa and coded with discrete character states. Optimization of the character changes over the lineage leading to tyrannosaurids revealed that most of the major myological features of the forelimb in the most derived tyrannosaurids were acquired rapidly at or just before the node Tyrannosauridae, concurrent with the substantial overall reduction of the forelimb relative to body size. Many of these characters correspond to relative increases in muscle size and mechanical advantage in tyrannosaurids and are not consistent with the hypothesis of a functionless limb. Overall reduction in the adductors of the shoulder do not support a role for the forelimb in rising from the ground, but evidence for development of the shoulder extensors and elbow flexors are consistent with the functional demands of close-quarters grappling with struggling prey or a potential mate. The myology and osteology of the shoulder joint also support a new hypothesis of forelimb use in intraspecific displays such as those used in mating, territorial dominance, or species recognition.

INTRODUCTION

Reconstructing the behavior of extinct organisms has long been a major area of interest in the field of paleontology and the subject of many functional analyses. These studies can be generally divided into those primarily relating to either feeding (e.g., Barrett and Rayfield, 2006; Snively and Russell, 2007a; Zanno and Makovicky, 2011) or locomotion (e.g., Gatesy, 1990; Hutchinson, 2006; Maidment and Barrett, 2012). The forelimbs of nonavian theropod dinosaurs do not quite exclusively fit into either category, but are instead related to both; the elongate,

raptorial forelimbs of most theropods presumably served some role in prey acquisition and, in more derived theropods, the forelimbs once again regained a locomotory role in the evolution of flight. This second role has received the most attention, with recent studies focusing on the evolution of feathers and wing shape (X. Wang et al., 2011), the creation of aerodynamic models (Koehl et al., 2011), and changes in forelimb proportions relating to flight (Dececchi and Larsson, 2009). Nevertheless, the role that the forelimbs played in interspecific predator-prey interactions and intraspecific interactions in more basal taxa has the potential to reveal much about the biology and behavior of these animals.

Among nonavian theropods, the forelimbs that have been the source of perhaps the most attention and speculation are those of *Tyrannosaurus rex*. Due to their extremely reduced size relative to the overall massive size of the animal, it has generally been assumed that the forelimbs were vestigial, having lost all function as a result of a more cranially-based mode of predation (Horner and Lessem, 1993; Giffin, 1995; Lockley et al., 2009). Nevertheless, the morphology of the *Tyrannosaurus* forelimb is relatively robust (Brochu, 2003), eliciting other hypotheses as to its function, including assisting the animal from rising from the ground (Newman, 1970), partner clasping during mating (Osborn, 1906), or holding onto struggling prey once it has been brought close to the chest (Brown, 1915). Although these hypotheses are not mutually exclusive, they have never been considered together in a functional analysis of the forelimb.

One of the first steps in any functional analysis in an extinct taxon is the reconstruction of the relevant soft tissues. Although osteological convergence can be indicative of functional convergence, the same function can be achieved by a range of morphologies (Lauder, 1995) and convergent skeletal morphology may falsely indicate functional similarity when soft tissues are not accounted for (Maidment and Barrett, 2012). In the case of the forelimbs of tyrannosaurids, it is nearly impossible to assess function using a wholly analogous approach because no appropriate modern analogs exist. The integrative phylogenetic and extrapolatory analysis (Bryant and Russell, 1992) and Extant Phylogenetic Bracket (EPB; Witmer, 1995) methods can be used to create a well-constrained muscular reconstruction through identification of homologous osteological correlates and analysis of soft tissue data of the most closely related

extant taxa in an explicit phylogenetic context. Although the forelimb musculature of *Tyrannosaurus rex* has been reconstructed twice, both reconstructions rely on very limited extant samples and were performed with no regard to either the phylogenetic bracket (Carpenter and Smith, 2001) or to the homology of bone surfaces and osteological correlates (Lipkin and Carpenter, 2009). Additionally, the subsequent biomechanical analyses only investigated the action of a single muscle (Biceps brachii) on the antebrachium (Carpenter and Smith, 2001; Lipkin and Carpenter, 2009). Despite the interest in tyrannosaurid forelimb function, the relative contributions of all the pectoral and forelimb muscles and their ability to resist biologically relevant forces has never been considered.

Attempting to quantify absolute muscle size from the size of rugosities or other osteological correlates requires many assumptions that are not tenable, such as those about the relationship between muscle size and factors such as tendon size (Bryant and Seymour, 1990). However, comparing the musculature of a derived taxon to that of a more basal taxon and tracing the changes over the evolutionary lineage has been shown to be a useful method for investigating limb function in extinct taxa and the sequence of character acquisition leading to the evolution of novel morphologies (Hutchinson, 2001a, 2001b; Maidment and Barrett, 2012). By using these methods to assess the morphological shifts of the pectoral and forelimb musculature along the lineage of Tyrannosauroidea, I demonstrate the patterns of myological evolution and use the relative development of osteological correlates to test established hypotheses of forelimb function in *Tyrannosaurus rex* and other tyrannosaurid theropods.

Institutional Abbreviations—BYU, Brigham Young University, Provo, UT; **FMNH**, Field Museum, Chicago, IL; **IVPP**, Institute of Palaeontology and Palaeoanthropology, Beijing, China; **MOR**, Museum of the Rockies, Bozeman, MT; **MPC**, Paleontological Center of the Mongolian Academy of Sciences, Ulaanbaatar, Mongolia; **MUCPv**, Museo de Geología y Paleontología, Universidad Nacional del Comahue, Neuquén, Argentina; **ZCDM**, Zhucheng Dinosaur Museum, Shandong, China.

MATERIALS AND METHODS

The complete reconstruction of the forelimb musculature of the basal theropod *Tawa hallae* (see Chapter IV) was used as the basis for inferring the musculature in other theropods and served as the exemplar of the basal condition of the muscles. The methodological details of this initial reconstruction are detailed elsewhere (see Chapter IV). Through identification of the basic arrangement of the muscles and the osteological correlates of muscle attachment in a basal taxon, this reconstruction may be applied to other theropod taxa in combination with critical examination of scars, crests, and tubercles preserved on specimens of the species of interest and those of closely related taxa. As discussed by Hutchinson (2001a, 2001b), interpretation of osteological correlates of soft tissue attachment is complex and requires caution. Although muscles with tendinous attachments often leave scars on the bone surface, those with fleshy attachments usually do not, and defining their borders depends on the presence of intermuscular lines and the presence of other muscle scars (Bryant and Russell, 1992). In the theropod pectoral girdle and forelimb, many fleshy muscle attachments are not clearly demarcated by bony landmarks, and so the area of attachment on these surfaces must be interpreted only as a *potential* area of attachment. However, the development of these muscles may be assessed in a qualitative comparative context, even though quantifications of muscle size are problematic (Hutchinson, 2001a).

Using the myology of the pectoral girdle and forelimb of *Tawa* as a template, a full reconstruction of the forelimb musculature was completed for *Tyrannosaurus rex* as the exemplar for the derived condition. Although the complete musculature was not reconstructed for every tyrannosauroid taxon with preserved forelimb material, the osteology of each taxon was considered when assessing the muscle attachment sites in *Tyrannosaurus*. This is particularly important for muscle scars that are novel among tyrannosaurids; by identifying the early appearance of these scars on the tyrannosauroid lineage, it is possible to assign them to a particular muscle attachment with more confidence. To assess the osteological variation along the tyrannosauroid lineage and among more basal theropods, I examined a total of 100 specimens belonging to 35 genera of nonavian theropod dinosaurs. In cases where the original material could not be examined, taxa were coded from published photographs, illustrations, and descriptions (for a complete list of taxa and sources, see Supplemental Table 1). Among

tyrannosauroids, only one taxon (*Dryptosaurus aquilungius*) was not coded from personal observation of the specimen. Basal tetanuran and ceratosaurian taxa were included in order to more comprehensively trace the evolution of the osteological features over the taxa basal to Tyrannosauroidea and to identify potential myological convergence due to factors such as large body size. Abelisaurid taxa such as *Majungasaurus crenatissimus* were also considered so that characters relating to forelimb reduction in both clades could be identified.

The osteological features of the forelimb and pectoral girdle relating directly to the development and morphology of muscle attachment sites were formulated into characters with discrete states and scored for all taxa to create a data matrix (for a complete list of characters and codings, see Table S1). These characters were optimized onto a phylogenetic tree of the study taxa. Due to the lack of a recent large-scale phylogenetic analysis incorporating the study taxa, the current tree was concatenated from recent narrower phylogenetic analyses of Tyrannosauroidea (Xu et al., 2012), Tetanurae (Carrano et al., 2012), Ceratosauria (Carrano and Sampson, 2008; Xu et al., 2009), and basal Theropoda (Nesbitt et al., 2009a; Martinez et al., 2011). The placement of most of the study taxa is relatively uncontroversial; given the reduced number of taxa in the tree, even the relationships of fragmentary 'wild card' taxa such as *Poekilopleuron* are often resolved among their closest relatives. The exception to this is the relationships of the most basal taxa (i.e., *Herrerasaurus* and *Eoraptor*) and the monophyly (or lack thereof) of Coelophysoidea. To account for this, the node at the base of the tree and that of Coelophysoidea were collapsed into hard polytomies. Each character was traced over the tree and the character state transformations were optimized employing maximum likelihood using Mesquite 2.75 (Maddison and Maddison, 2010).

RESULTS

A full reconstruction of the musculature of *Tyrannosaurus rex* is provided in the supplementary information (Section 2, Figures S1–S4), along with justifications for novel muscle attachment sites; justification for muscle homologies and the basal pattern can be found in Chapter IV of this dissertation. A simplified lateral view of the musculature of *Tyrannosaurus*

in comparison with that of *Tawa* is shown in Figure 1. Node-by-node character optimizations are given in Table 1 and mapped onto the tree in Figure 2. The greatest number of state changes (six) occurs at the Tyrannosauridae node and the node before Tyrannosauridae (Tyrannosauridae + *Raptorex*), although all of the changes at the latter node are equivocal below this node due to their unknown status in *Dryptosaurus*. Six changes are also optimized at the Abelisauroidea node, and five changes are present at Tetanurae; all other nodes exhibit three or fewer changes.

The most derived tyrannosaurids (node 67) are characterized by a large rugosity on the greater tubercle of the humerus and substantial reduction in the height of the flexor tubercle of the ungual of digit I. An extremely prominent rugosity on the lateral surface of the deltopectoral crest is found among these large-bodied taxa (node 65), although this rugosity first appears among stem tyrannosauroids (node 55). Tyrannosaurids as a whole (node 59) are characterized by a prominent tubercle for Scapulohumeralis posterior on the scapula, a strongly flaring distal scapula, a sharp angle of expansion of the acromion, proximal excursion of the ectepicondylar muscle origins, anterior excursion of the insertion of supinator, and reduction of the manus to two functional digits. *Raptorex* shares with tyrannosaurids a narrow proximal scapula, low and anteriorly placed biceps tubercle, laterally directed subglenoid fossa of the scapula, reduced internal tuberosity of the humerus, and reduced medial projection of metacarpal I; these character states are unambiguously present at node 57, but are all ambiguous at node 55 and in some cases node 53 due to the fragmentary preservation of *Dryptosaurus* and *Eotyrannus*. The humerus of *Dryptosaurus* does indicate the acquisition of a relatively proximal shift of the tip of the deltopectoral crest and light rugosity on its lateral surface at this node (55). The unequivocal presence of light rugosity on the posterior surface of the greater tubercle of the humerus and a reduction in the size of the humeral entepicondyle are optimized to have appeared first in *Eotyrannus*, at node 53. *Yutyrannus* exhibits a ventrally positioned medial scapular ridge and a twisting insertion of supinator, indicating the unambiguous acquisition of these characters at node 51. At the base of Tyrannosauroidea (node 48), the slight distal displacement of the greater tubercle and the loss of the lateral triceps ridge are unequivocally optimized, as well as a reversal to the absence of a prominent tubercle for Scapulohumeralis posterior, a character that is reacquired higher in the tree.

The suite of characters acquired at Tetanurae (node 30) includes a prominent Scapulohumeralis posterior tubercle on the scapula, substantially projecting internal tuberosities and entepicondyles of the humerus, the loss of a tubercle on the edge of the proximal ulna, and the presence of a lateral process on the lateral-most metacarpal. Among the nine characters that distinguish Abelisauroidea (node 25) and Abelisauridae (node 27), only a low biceps tubercle, a laterally directed subglenoid fossa of the coracoid, lightly rugose posterior surface of the greater tubercle, and anterior orientation of the insertion of supinator are features that are shared with tyrannosauroids and tyrannosaurids. Other characters optimized at these nodes are related to the unique muscular morphology and forelimb reduction seen among abelisaurids (see Chapter V).

DISCUSSION

Pectoral and Humeral Evolution

The majority of changes in the forelimb myology of tyrannosauroid theropods are concentrated in those muscles that cross the glenohumeral joint. Although the scapulocoracoids and humeri of theropods along the line to tyrannosaurs appear grossly similar, inspection of their detailed morphology reveals shifts that have major consequence for the forelimb musculature. In particular, tyrannosaurids show substantial modifications of the Deltoideus complex of muscles that are distinct from taxa with robust forelimbs as well as from the reduced forelimbs of abelisaurids. Deltoideus clavicularis (DC) originates from the entire edge of the acromial expansion and inserts on the lateral surface of the deltopectoral crest (Chapter IV). In most other theropods the acromial expansion is subtriangular, placing the anteriormost fibers of DC considerably anterior to the glenoid fossa. However, in tyrannosaurids the acromial expansion is subrectangular and flares away from the scapular blade at nearly a 90° angle, limiting the anterior excursion of the origin of DC. This alters the relationship of the line of action of this muscle to the glenohumeral joint, shifting its action from primarily abduction to primarily extension. Unlike the reduced area of insertion seen in abelisaurids (Chapter V), the insertion of DC in tyrannosaurids and some tyrannosauroids is marked by a novel rugosity on the lateral surface of the plesiomorphically unreduced deltopectoral crest (for discussion of the identity of

this rugosity, see supplemental information). This rugosity becomes extremely robust and extensive in derived tyrannosaurids (node 65, Figs. 1, 3). Although the overall size of a rugosity does not give an indication of the size of the attached muscle, the degree of scarring and rugosity may indicate the relative development of a muscle (Bryant and Seymour, 1990; Jasinoski et al., 2006); thus, it is likely that the DC was relatively larger in derived tyrannosaurids than in more basal tyrannosaurids with only light scarring and other theropods that lack any scarring at all in this area.

The broad, flat scapular blade of theropods provides a large potential area of origin on its lateral surface for Deltoideus scapularis (DS; Chapter IV). The distal expansion of the scapula of early theropods is greatly enhanced in Tyrannosauridae, and this is coupled with a relative narrowing of the proximal portion of the blade, optimized to have been acquired slightly earlier along the lineage (node 57, Tyrannosauridae + *Raptorex*). The combination of these two characters limits the proximal excursion of DS and, at the same time, creates a larger potential area of origin distally. Shifting the majority of the fibers of this muscle posteriorly would slightly lengthen its moment arm and improve its action as an extensor of the humerus. Similar to that of DC, the insertion of DS is marked by a large rugose tubercle on the greater tubercle of the humerus, suggesting that both Deltoideus muscles were substantially developed in tyrannosaurids. Extension of the humerus would also be enacted by the Scapulohumeralis posterior (SHP), the origin of which exhibits relative enlargement at the node Tyrannosauridae. In this case, a distinct fin or tubercle extending along the posteroventral edge of the scapular blade a short distance from the glenoid is present in tyrannosaurids as well as allosauroids, but is not found in tyrannosauroids (Fig. 1). This fin may indicate an enlargement of SHP in these taxa, further adding to the ability to extend the humerus. The emphasis of these muscles on extension is followed quickly by the loss of the elongate furrow marking the insertion of the Latissimus dorsi (LD) on the humerus (at node 63). Although loss of an osteological correlate does not necessarily indicate loss of its associated muscle, it may correspond to a reduction of that muscle (Hutchinson, 2001a). However, a depression at the distal end of the DC rugosity in at least some specimens of *Tyrannosaurus* (MOR 980, right humerus) may represent a distal shift in the insertion of LD. This would lengthen the lever arm of this muscle, increasing its mechanical

advantage even if its overall size may have been reduced. These muscles all show modifications that improve their actions as extensors, suggesting that extension of the humerus was an important part of the function of the forelimb in derived tyrannosaurids.

The shape of the acromial expansion also affects the origin of the Supracoracoideus musculature, which originates from the subacromial depression of the scapula and adjacent surface of the coracoid (Fig. 1). The subrectangular acromial expansion of tyrannosaurids results in a larger scapular portion of the subacromial depression. Combined with the broad coracoid of tyrannosauroids, this may indicate that one or both parts of the Supracoracoideus complex are relatively large in these taxa. However, when two muscles have a fleshy attachment in one depression, it is difficult to discern the exact boundaries of their attachments (Bryant and Seymour, 1990), so in this case the two muscles of the Supracoracoideus complex are considered together. As with DC, the broad acromial expansion of tyrannosaurids results in a posterior shift of the dorsal-most muscle fibers, in turn shifting the line of action of this muscle posteriorly. For the Supracoracoideus complex, this results in a change in the primary action of the muscle from flexion and abduction of the humerus in the basal taxon (Chapter IV) to almost exclusively abduction. Additionally, the proximal shift of the tip of the deltopectoral crest acquired along the tyrannosauroid lineage (node 55) would have shifted the attachment site of the Supracoracoideus complex proximally and shortened its lever arm, resulting in reduced torque for the muscle but a wider humeral excursion provided by the muscle.

Another major change that occurs just before the tyrannosaurid node is a reduction of the adductor musculature of the humerus. The narrowing of the proximal scapular blade not only affects DS on its lateral surface, but also the Subscapularis (SBS) on its medial surface (Fig. S1). However, unlike DS, the distal expansion of SBS is limited by the Rhomboideus and Serratus profundus muscles inserting on the medial surface of the distal scapula. This distal limit is indicated in tyrannosaurids by two angled grooves in this area (*Tyrannosaurus*, FMNH PR 2081), resulting in a very limited potential area of origin for SBS relative to more basal taxa with broader proximal scapulae. This is accompanied at the same node by a reduction in the internal tuberosity of the humerus, which is the attachment point for SBS as well as Subcoracoideus (SBC). Reduction in the size of this tuberosity, which is very large in more basal tyrannosauroids

(e.g., *Yutyrannus*, ZCDM 5001), reduces the length of the moment arms for both muscles and this, combined with the reduction in potential area of origin of SBS, strongly suggests that the capabilities for adduction of the humerus was reduced in tyrannosaurids. Although there is no evidence for a reduction in the origin area of SBC, shortening of the moment arm of this muscle would have limited its abilities for strong adduction.

Shifts in the morphology of the coracoid occurring in the lineage just before Tyrannosauridae (node 59) indicate that changes in several muscles relating to flexion of the humerus occurred simultaneously. The projection of the biceps tubercle away from the surface of the coracoid is greatly reduced, and its location relative to the glenoid fossa is shifted anterodorsally. The reduction of the tubercle may indicate a reduction in overall size of the Biceps brachii (BB), but at the same time the anterior excursion lengthens its moment arm, making it a stronger flexor of the glenohumeral joint. Nearly simultaneously, the orientation and development of the subglenoid fossa shifts from deep and posteroventrally directed in tetanurans and basal theropods to flat and laterally directed in tyrannosaurids. This may indicate a relative reduction in the overall size of the Coracobrachialis (CB), which originates from this fossa and serves as the primary flexor of the glenohumeral joint (Chapter IV).

Antebrachial and Manual Evolution

Among tetrapods, limb reduction typically occurs in a distal-to-proximal pattern, with the distal elements exhibiting a greater degree of reduction than the proximal elements (Fürbringer, 1870; Lande, 1978). This is also true in tyrannosaurids yet, despite their reduced state, the forelimb and manus exhibit relatively few changes in their musculature in comparison with the pectoral girdle and humerus. As with the proximal elements, these changes mostly take place at the node Tyrannosauridae or slightly before. The humeral entepicondyle and ectepicondyle both display shifts in their morphology that affect the antebrachial muscles originating from them. The ectepicondyle of tyrannosaurids possesses a raised, rugose area that is slightly displaced proximally and separated from the edge of the humeral distal articular surface. This rugosity is not found in other theropods and likely indicates a proximal displacement of the origin of the extensor compartment of muscles, lengthening their moment arm for action on the elbow. This

would have particularly affected the most proximally located of these muscles, Supinator (SU), which also exhibits a modification in its insertion occurring at the Tyrannosauridae node (Figs. 1, 3). Longitudinal ridges on the radii in these taxa indicate that SU likely possessed an entirely anterior insertion on the radius, in contrast to the entirely or partially lateral insertion seen in more basal taxa. This shift would greatly reduce the ability of this muscle to supinate the antebrachium, instead redirecting its action to flexion of the elbow. Expansion of its fibers proximally on the humerus would further improve the leverage of this muscle for flexion.

The entepicondyle exhibits a reversal to the lower, more moderately developed morphology seen in basal theropods, in contrast to the extremely enlarged entepicondyle of tetanurans. This reversal occurs near the base of Tyrannosauroidea (node 53), though the most basal tyrannosauroids still possess a relatively enlarged entepicondyle. In this case, the limitations on the muscles originating from this epicondyle may have been relatively minimal because this morphology is similar to that of the most basal theropod taxa, which possess relatively long forelimbs. One character that shows no clear pattern of evolution is the development of the olecranon process of the ulna. It is unclear whether the presence of a well-developed olecranon process is ontogenetic or not (Raath, 1990), but even small specimens of tyrannosaurids (*Albertosaurus*, TMP 86.64.01) possess relatively large olecranon processes on the same scale as those of tetanurans. This likely indicates that, despite the reduction of the forelimb in tyrannosaurids, the Triceps brachii musculature remained unreduced.

Tyrannosaurids possess functionally two-digit hands, although it is uncertain how far this character extends down the tree due to a lack of completely preserved manus in most tyrannosauroids. Despite this, there is little evidence in the manus that the musculature attaching in this area was greatly modified, with most of the osteological correlates of these muscles (e.g., depressions on the dorsal and ventral proximal surfaces of the metacarpals for the short flexors of the digits) still present and well developed in the most derived tyrannosaurids. One correlate that shows a distinct shift in morphology is the medial projection at the proximal end of metacarpal I (Fig. 1). This process is the insertion site for Abductor pollicis longus (APL) and is typically well developed among most theropods, with some tetanurans exhibiting very pronounced projections (e.g., *Megaraptor*, MUCPv 341). It is effectively lost at the node before

Tyrannosauridae (node 57), which greatly shortens the moment arm of the action of this muscle on the wrist. However, it is somewhat sporadically reduced among the other study taxa and may be primarily related to the modifications of the tetanuran and especially the coelurosaurian wrist limiting radial deviation (Sullivan et al., 2010). The most derived tyrannosaurids (node 67) also exhibit a distinct reduction in the height of the flexor tubercle of the ungual of digit I, which is plesiomorphically large even in basal tyrannosaurids. The reduction of this tubercle creates relatively short moment arms for the Flexor digitorum longus at the distal phalangeal joint, resulting in a reduced moment in digital flexion.

Tyrannosaurid Forelimb Function

When considering the sum of the changes that have occurred in the musculature of the tyrannosaurid pectoral girdle and forelimb, several patterns begin to emerge relating to the function of the limb. At the shoulder, alterations in the origins and insertions of the Deltoideus musculature and Scapulohumeralis posterior all emphasize extension of the humerus. Although anterior excursion of the biceps tubercle of the coracoid suggests some importance of flexion of the humerus, other modifications of the Supracoracoideus complex and Coracobrachialis indicate a general reduction in this action among tyrannosaurids. A trade off between antagonistic actions also seems to occur between adduction and abduction of the humerus, with evidence of emphasis on abduction (Supracoracoideus) and a concomitant reduction of adduction (Subscapularis). At the elbow, the retention of a well developed Triceps brachii and modifications of Supinator suggest that flexion and extension likely retained importance, and were potentially even emphasized, in tyrannosaurids. Although the movements of the wrist would have been restricted relative to those of basal theropods based on the osteology of the carpus, there is little evidence that the musculature acting on the wrist would have been reduced. Finally, the morphology of the unguals indicate that digital flexion would only have been limited in the most derived tyrannosaurids.

Of the hypotheses concerning the forelimb function of tyrannosaurids, the most prevalent is that they were vestigial, i.e., they lacked all function (e.g., Horner and Lessem, 1993; Giffin, 1995; Lockley et al., 2009). This hypothesis is based in the idea that such small arms could not

be useful to an animal that large and, in some cases, that the forelimbs became reduced as a consequence of cranial enlargement (Lockley et al., 2009). The osteological signals of complete vestigiality have not yet been studied, but evidence from the wings of flightless birds suggests that complete loss of function is accompanied by extensive reduction in the osteological correlates of muscles, even among large-bodied birds (McGowan, 1982; Maxwell and Larsson, 2007b; pers. obs.). In tyrannosaurids, the presence of muscle scars exhibiting greater robustness than those of taxa with relatively longer forelimbs, as well as a general lack of reduction of the size of many osteological correlates, suggests that the forelimbs of these taxa were not completely useless. In fact, no nonavian theropod is known to possess forelimbs exhibiting a morphology consistent with complete vestigiality; all have relatively more robust osteological correlates of muscle attachment than even flightless birds (e.g., ostriches, flightless cormorants) that still utilize their wings for other functions (Livezey, 1992b; pers. obs.).

In considering the potential functional role of assisting the animal in rising from the ground, the forelimb has been hypothesized to have served as only a "kick-stand," providing a prop for the body as it rose (Stevens et al., 2009), as well as straightening the forelimb as in a 'push-up' to propel the anterior portion of the body upward (Newman, 1970). Placing the forelimb in this position causes the ground reaction forces to exert an abductor moment on the shoulder, and a well developed adductor musculature would be necessary in order for the forelimbs to provide enough force to push the considerable mass of the anterior body upward (Fig. 3). Tyrannosaurids exhibit the exact opposite trend, reducing the size and mechanical advantage of the adductor musculature. The relatively weakened adductor musculature of tyrannosaurids would not have been capable of performing a 'push-up,' and would likely have lacked the force to hold the animal's chest off the ground in a static support pose. The large deltoideus muscles may have assisted by providing lateral rotation of the humerus, causing movement of the elbow medially and reduction of the abductor moment at the shoulder (Maidment and Barrett, 2012), but this movement would have been limited due to the shortness of the forelimbs relative to the broad chest in tyrannosaurids. The specific modifications of the musculature in tyrannosaurids indicate that it is unlikely that the forelimbs of tyrannosaurids had much of a role in body support while rising from the ground.

The acts of holding onto struggling prey (Brown, 1915; Carpenter and Smith, 2001; Carpenter, 2002; Lipkin and Carpenter, 2009) or clasping a partner during mating (Osborn, 1906) can be considered to have similar requirements on the forelimb. In each case, the primary resulting force vector would have likely been forward, away from the body of the animal (Fig. 3). This vector would exert a flexor moment on the shoulder, an extensor moment on the elbow, and an extensor moment at the digits. To counteract these moments, the forelimb would need to possess a large extensor muscle mass at the shoulder, and substantial flexion at the elbow and digits. The musculature of the tyrannosaurid forelimb conforms to this with the exception of the development of the digital flexors in the most derived taxa. The reduced flexor tubercles of the unguals (e.g., *Tarbosaurus bataar*, MPC 107/2) would have provided a lower mechanical advantage for the Flexor digitorum longus relative to the morphology of more basal theropods. However, flexor tubercles with relatively reduced heights are also found in the extremely hypertrophied unguals of tetanurans (e.g., *Megaraptor namunhuaiquii*, MUCPv 341), suggesting that the moment arm provided by a tall flexor tubercle may not have been necessary among some of these large-bodied taxa. The Biceps brachii does not exhibit any evidence of a trend toward hypertrophy in tyrannosaurids (contra Carpenter and Smith, 2001; Lipkin and Carpenter, 2009), but the anterior orientation of the insertion of Supinator and the proximal excursion of its origin does suggest that flexion of the antebrachium was important. The extensor musculature of the shoulder of tyrannosaurids appears to have been particularly enlarged relative to the other muscle groups crossing the glenohumeral joint. Furthermore, the short humerus of tyrannosaurids would actually improve the mechanical advantage of many shoulder muscles by reducing the length of the load arm. This, combined with the robust morphology of the limb, would likely make the forelimbs of tyrannosaurs well equpped to resist the forces of large, struggling prey.

An additional possible function for the reduced forelimbs of tyrannosaurids is that of display. Display is the primary function of the reduced wings of ostriches and rheas (Davies, 2002), and provides enough functional constraint to retain well-developed forelimb musculature in these taxa (Burch, in prep.). Recent discoveries have shown that a filamentous feather structures were present in the large-bodied basal tyrannosauroid *Yutyrannus huali* (see Xu et al., 2012), and evidence for elongate, quill-like structures have been found in the antebrachium of

the allosauroid *Concavenator corcovatus* (see Ortega et al., 2010). Regardless of whether or not large tyrannosaurids had a feathery covering over large portions of their body, it is possible that the forelimbs bore feather structures large enough to be useful for intraspecific displays related to species recognition or mating. The nearly hemispherical humeral head of tyrannosaurids is uncommon among theropods (but is present in Abelisauridae; see Chapter V) and allows for a wide range of motion at the shoulder (Carpenter, 2002), which would have been advantageous for creating conspicuous displays with a small forelimb.

CONCLUSIONS

The morphology of the forelimb in basal tyrannosauroids indicates that the musculature of these taxa was generally similar to that of more basal theropods, with no distinct forelimb morphology characterizing the entire clade. Instead, the majority of character changes appear to have been rapidly acquired at the node Tyrannosauridae and just before it. The acquisition of these muscular traits appears to be correlated with the dramatic reduction of the forelimb relative to body size, although the incomplete forelimb preservation in several stem tyrannosauroid taxa occupying the 'middle' of the lineage hinder the exact placement of the reduction as well as the unambiguous optimization of many of the myological characters. Additionally, the presence of many derived tyrannosaurid muscular characters in the small-bodied *Raptorex kreigsteini* (LH PV18) indicates that their development was not tied to body size, reinforcing the idea that the tyrannosaurid body plan was present at small body sizes (Sereno et al., 2009). Instead, the development of these characters is likely related to functional shifts in the forelimb concurrent with reduction in overall proportions of the limb.

Utilization of phylogenetically rigorous soft tissue reconstruction permits the identification and assessment of functionally significant osteological characters, and consideration of the changes across the entire musculature enables the first tests of several established hypotheses of forelimb function in tyrannosaurids. The retention and development of robust osteological correlates of muscle attachment in the forelimbs of even the most derived tyrannosaurids suggests strongly that the forelimbs of these animals were not completely useless. Although the

muscle groups required for supporting the body when rising from the ground show evidence of reduction, the development of other groups is consistent with the functional demands of close-quarters grappling with struggling prey and potential mates. Additionally, the forelimb musculature and arthrology also supports the potential use of the forelimbs in intraspecific display, a common use of reduced forelimbs in modern birds.

LITERATURE CITED

Barrett, P. M., and E. J. Rayfield. 2006. Ecological and evolutionary implications of dinosaur feeding behaviour. Trends in Ecology and Evolution 21:217–224.

Brochu, C. A. 2003. Osteology of *Tyrannosaurus rex*: insights from a nearly complete skeleton and high-resolution computed tomographic analysis of the skull. Journal of Vertebrate Paleontology 22:1–138.

Brown, B. 1915. *Tyrannosaurus*, the largest flesh-eating animal that ever lived. The American Museum Journal 15:271–274.

Bryant, H. N., and K. L. Seymour. 1990. Observations and comments on the reliability of muscle reconstruction in fossil vertebrates. Journal of Morphology 206:109–117.

Bryant, H. N., and A. P. Russell. 1992. The role of phylogenetic analysis in the inference of unpreserved attributes of extinct taxa. Philosophical Transactions: Biological Sciences 337:405–418.

Carpenter, K. 2002. Forelimb biomechanics of nonavian theropod dinosaurs in predation. Senckenbergiana Lethaea 82:59–76.

Carpenter, K., and M. Smith. 2001. Forelimb osteology and biomechanics of *Tyrannosaurus rex*; pp. 90–116 in D. Tanke and K. Carpenter (eds.), Mesozoic Vertebrate Life. Indiana University Press, Bloomington, IN.

Carrano, M. T., and S. D. Sampson. 2008. The phylogeny of Ceratosauria (Dinosauria: Theropoda). Journal of Systematic Palaeontology 6:183–236.

Carrano, M. T., R. B. J. Benson, and S. D. Sampson. 2012. The phylogeny of Tetanurae (Dinosauria: Theropoda). Journal of Systematic Palaeontology 10:211–300.

Davies, S. J. J. F. 2002. Ratites and Tinamous, Bird Families of the World, Volume 9. Oxford University Press, Oxford, UK, 310 pp.

Dececchi, T. A., and H. C. E. Larsson. 2009. Patristic evolutionary rates suggest a punctuated pattern in forelimb evolution before and after the origin of birds. Paleobiology 35:1–12.

Fürbringer, M. 1870. Die Knochen und Muskeln der Extremitäten bei den Schlangenähnlichen Sauriern. Vergleichend-anatomische Abhandlung. W. Engelmann, Leipzig, 135 pp.

Gatesy, S. M. 1990. Caudofemoral musculature and the evolution of theropod locomotion. Paleobiology 16:170–186.

Giffin, E. B. 1995. Postcranial paleoneurology of the Diapsida. Journal of Zoology 235:389–410.

Gilmore, C. W. 1920. Osteology of the carnivorous Dinosauria in the United States National Museum, with special reference to the genera *Antrodemus* (*Allosaurus*) and *Ceratosaurus*. Bulletin of the United States National Museum 110:1–159.

Horner, J. R., and D. Lessem. 1993. The Complete *T. rex*. Simon & Schuster, New York, 239 pp.

Hutchinson, J. R. 2001a. The evolution of femoral osteology and soft tissues on the line to extant birds (Neornithes). Zoological Journal of the Linnean Society 131:169–197.

Hutchinson, J. R. 2001b. The evolution of pelvic osteology and soft tissues on the line to extant birds (Neornithes). Zoological Journal of the Linnean Society 131:123–168.

Hutchinson, J. R. 2006. The evolution of locomotion in archosaurs. Comptes Rendus Palevol 5:519–530.

Jasinoski, S. C., A. P. Russell, and P. J. Currie. 2006. An integrative phylogenetic and extrapolatory approach to the reconstruction of dromaeosaur (Theropoda: Eumaniraptora) shoulder musculature. Zoological Journal of the Linnean Society 146:301–344.

Koehl, M. A. R., D. Evangelista, and K. Yang. 2011. Using physical models to study the gliding performance of extinct animals. Integrative and Comparative Biology 51:1002–1018.

Lande, R. 1978. Evolutionary mechanisms of limb loss in tetrapods. Evolution 32:73–92.

Lauder, G. V. 1995. On the inference of function from structure; pp. 1–9 in J. J. Thomason (ed.), Functional Morphology in Vertebrate Paleontology. Cambridge University Press, Cambridge, UK.

Lipkin, C., and K. Carpenter. 2009. Looking again at the forelimb of *Tyrannosaurus rex*; pp. 167–190 in P. Larson and K. Carpenter (eds.), *Tyrannosaurus rex*: the Tyrant King. Indiana University Press, Bloomington, IN.

Livezey, B. C. 1992. Flightlessness in the Galápagos cormorant (*Compsohalieus* [*Nannopterum*] *harrisi*): heterochrony, giantism and specialization. Zoological Journal of the Linnean Society 105:155–224.

Lockley, M., R. Kukihara, and L. Mitchell. 2009. Why *Tyrannosaurus rex* had puny arms: an integral morphodynamic solution to a simple puzzle in theropod paleobiology; pp. 131–164 in P. Larson and K. Carpenter (eds.), *Tyrannosaurus rex*: the Tyrant King. Indiana University Press, Bloomington, IN.

Maddison, W. P., and D. R. Maddison. 2010. Mesquite: a modular system for evolutionary analysis. 2.73. http://mesquiteproject.org.

Maidment, S. C. R., and P. M. Barrett. 2012. Does morphological convergence imply functional similarity? A test using the evolution of quadrupedalism in ornithischian dinosaurs. Proceedings of the Royal Society B 279:3765–3771.

Martinez, R. N., P. C. Sereno, O. A. Alcober, C. E. Colombi, P. R. Renne, I. P. Montañez, and B. S. Currie. 2011. A basal dinosaur from the dawn of the dinosaur era in southwestern Pangaea. Science 331:206–210.

Maxwell, E. E., and H. C. E. Larsson. 2007. Osteology and myology of the wing of the Emu (*Dromaius novaehollandiae*), and its bearing on the evolution of vestigial structures. Journal of Morphology 268:423–441.

McGowan, C. 1982. The wing musculature of the Brown kiwi *Apteryx australis mantelli* and its bearing on ratite affinities. Journal of Zoology 197:173–219.

Nesbitt, S. J., N. D. Smith, R. B. Irmis, A. H. Turner, A. Downs, and M. A. Norell. 2009. A complete skeleton of a Late Triassic saurischian and the early evolution of dinosaurs. Science 326:1530–1533.

Newman, B. H. 1970. Stance and gait in the flesh-eating dinosaur *Tyrannosaurus*. Biological Journal of the Linnean Society 2:119–123.

Ortega, F., F. Escaso, and J. L. Sanz. 2010. A bizarre, humped Carcharodontosauria (Theropoda) from the Lower Cretaceous of Spain. Nature 467:203–206.

Osborn, H. F. 1906. *Tyrannosaurus*, Upper Cretaceous carnivorous dinosaur (second communication). Bulletin of the American Museum of Natural History 22:281–296.

Raath, M. A. 1990. Morphological variation in small theropods and its meaning in systematics: evidence from *Syntarsus rhodesiensis*; pp. 91–105 in K. Carpenter and P. J. Currie (eds.), Dinosaur Systematics. Cambridge University Press, Cambridge, UK.

Sereno, P. C., L. Tan, S. L. Brusatte, H. J. Kriegstein, X. Zhao, and K. Cloward. 2009. Tyrannosaurid skeletal design first evolved at small body size. Science 326:418–422.

Snively, E., and A. P. Russell. 2007. Craniocervical feeding dynamics of *Tyrannosaurus rex*. Paleobiology 33:610–638.

Stevens, K. A., P. Larson, E. D. Wills, and A. Anderson. 2009. Rex, sit: digital modeling of *Tyrannosaurus rex* at rest; pp. 192–203 in P. Larson and K. Carpenter (eds.), *Tyrannosaurus rex*: the Tyrant King. Indiana University Press, Bloomington, IN.

Sullivan, C., D. W. E. Hone, X. Xu, and F. Zhang. 2010. The asymmetry of the carpal joint and the evolution of wing folding in maniraptoran theropod dinosaurs. Proceedings of the Royal Society B doi:10.1098.

Wang, X., R. L. Nudds, and G. J. Dyke. 2011. The primary feather lengths of early birds with respect to avian wing shape evolution. Journal of Evolutionary Biology 24:1226–1231.

Witmer, L. M. 1995. The extant phylogenetic bracket and the importance of reconstructing soft tissues in fossils; pp. 9-33 in J. J. Thomason (ed.), Functional Morphology in Vertebrate Paleontology. Cambridge University Press, Cambridge, UK.

Xu, X., K. Wang, K. Zhang, Q. Ma, L. Xing, C. Sullivan, D. Hu, S. Cheng, and S. Wang. 2012. A gigantic feathered dinosaur from the Lower Cretaceous of China. Nature 484:92–95.

Xu, X., J. M. Clark, J. Mo, J. Choiniere, C. A. Forster, G. M. Erickson, D. W. E. Hone, C. Sullivan, D. A. Eberth, S. J. Nesbitt, Q. Zhao, R. Hernandez, C. Jia, F.-l. Han, and Y. Guo. 2009. A Jurassic ceratosaur from China helps clarify avian digital homologies. Nature 459:940–944.

Zanno, L. E., and P. J. Makovicky. 2011. Herbivorous ecomorphology and specialization patterns in theropod dinosaur evolution. Proceedings of the National Academy of Sciences 108:232–237.

TABLE 6.1. Character state optimizations for nodes along the evolutionary lineage of Tyrannosauroidea. A full list of characters and states is given in the supplementary information. Format is character number (state number). Asterisks indicate the character state optimization is equivocal at the nodes immediately preceding that one, and thus the change may have occured earlier in the lineage. Node names are given when available, otherwise the numbers correspond to those in Figure 2.

Node	Character Optimizations
Node 2, Theropoda	2(1)*, 4(1), 14(1)*
Node 7	14(0)
Node 11, Neotheropoda	12(0)*, 21(1)
Node 19, Ceratosauria	4(0), 5(1), 18(1)
Node 25, Abelisauroidea	7(1)*, 9(1), 11(3), 12(1), 15(1), 17(1)
Node 27, Abelisauridae	1(2), 14(2), 21(2)
Node 30, Tetanurae	1(1), 10(1)*, 19(1), 22(1)*, 26(1)*
Node 36, Avetheropoda	14(1)
Node 48, Tyrannosauroidea	1(0), 11(1)*, 17(1)*
Node 51	2(2)*, 21(0)
Node 53	12(1)*, 19(0)
Node 55	13(1), 16(1)
Node 57	5(2)*, 7(1)*, 8(1)*, 9(1)*, 10(2)*, 25(1)*
Node 59, Tyrannosauridae	1(1), 4(2), 6(1), 20(1), 21(2), 24(1)*
Node 63	18(2)*
Node 65	16(2)
Node 67	12(2), 27(2)*

FIGURE 6.1. Comparison of myological reconstructions of the shoulder and forelimb in *Tawa hallae* (**A**), *Allosaurus fragilis* (**B**), *Guanlong wucaii* (**C**), and *Tyrannosaurus rex* (**D**). Muscles are labeled on *Tawa* and represented in the same color in the other taxa. **Abbreviations: APB**, abductor pollicis brevis; **BB**, Biceps brachii; **CB**, Coracobrachialis; **DC**, Deltoideus clavicularis; **DS**, Deltoideus scapularis; **ECU**, Extensor carpi ulnaris; **HR**, Humeroradialis; **LD**, Latissimus dorsi; **SC**, Supracoracoideus; **SHP**, Scapulohumeralis posterior; **SU**, Supinator; **TB**, Triceps brachii. Line drawings based on the following specimens: *Tawa hallae*, GR 242; *Allosaurus fragilis*, BYU 671/8901, and after Gilmore, 1920; *Guanlong wucaii*, IVPP V14531, V14532; *Tyrannosaurus rex*, FMNH PR 2081, MOR 555. Not to scale.

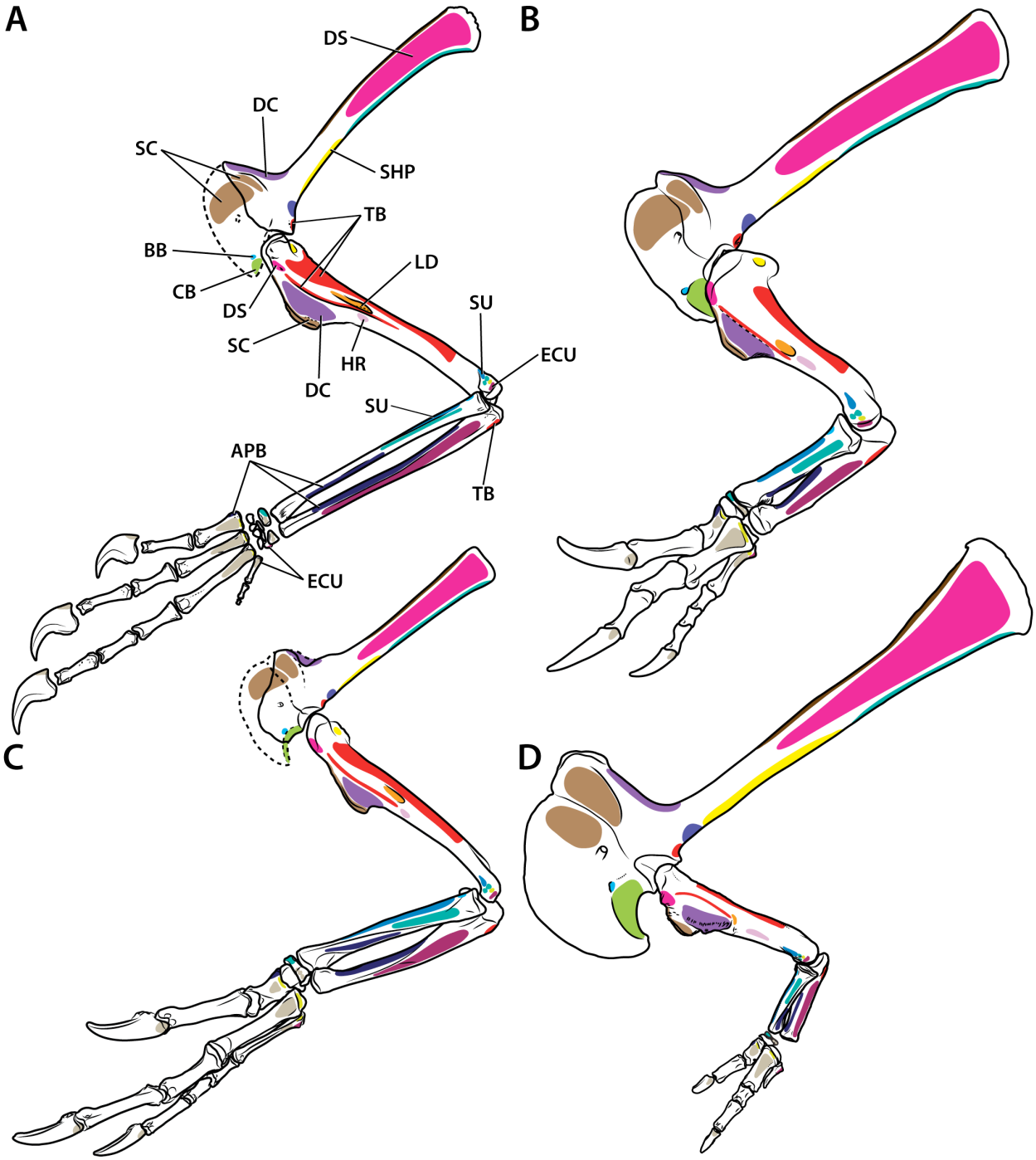
A
DS
DC
SC
SHP
TB
BB
LD
CB
DS
SU
SC
HR
ECU
DC
SU
APB
TB
ECU
B
C
D

FIGURE 6.2. Phylogeny of theropod dinosaurs coded in this analysis with character optimizations plotted at each node. Node numbers correspond to those given in Table 1, and character numbers and states correspond to those give in Supplementary Information section 4. Characters are color coded based on the element to which they pertain. Species collapsed into higher-level OTUs for Herrerasauridae, Coelophysidae, Abelisauridae, Megalosauroidea, and Allosauroidea.

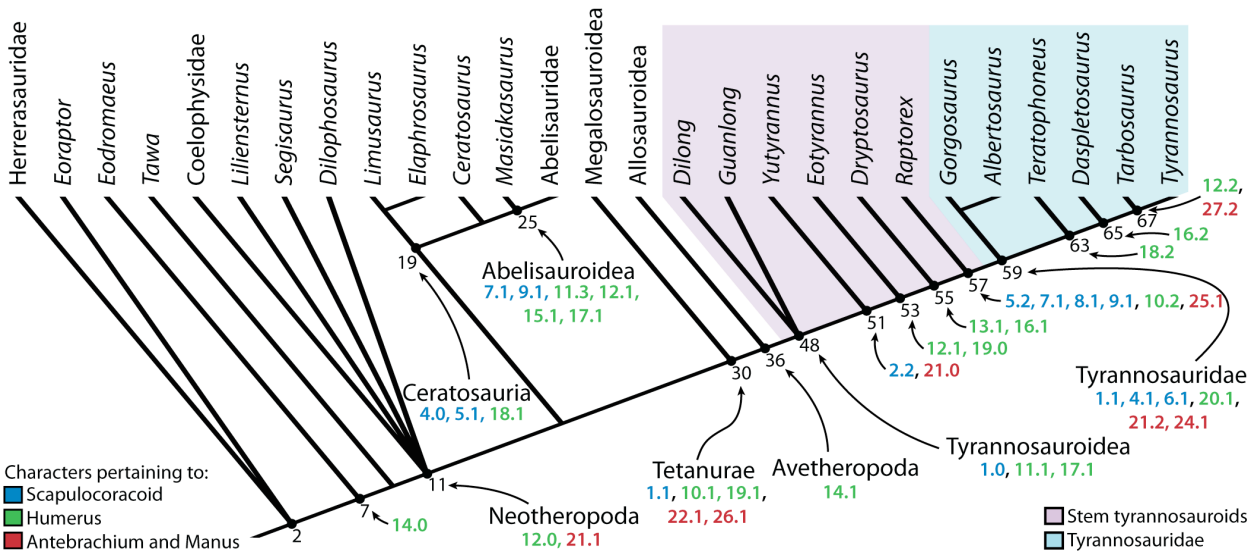
Herrerasauridae
Eoraptor
Eodromaeus
Tawa
Coelophysidae
Liliensternus
Segisaurus
Dilophosaurus
Limusaurus
Elaphrosaurus
Ceratosaurus
Masiakasaurus
Abelisauridae
Megalosauroidea
Allosauroidea
Dilong
Guanlong
Yutyrannus
Eotyrannus
Dryptosaurus
Raptorex
Gorgosaurus
Albertosaurus
Teratophoneus
Daspletosaurus
Tarbosaurus
Tyrannosaurus
25
19
Abelisauroidea
7.1, 9.1, 11.3, 12.1, 15.1, 17.1
Ceratosauria
4.0, 5.1, 18.1
11
Neotheropoda
12.0, 21.1
7
14.0
2
30
Tetanurae
1.1, 10.1, 19.1, 22.1, 26.1
36
Avetheropoda
14.1
48
Tyrannosauroidea
1.0, 11.1, 17.1
51
2.2, 21.0
53
12.1, 19.0
55
13.1, 16.1
57
5.2, 7.1, 8.1, 9.1, 10.2, 25.1
59
Tyrannosauridae
1.1, 4.1, 6.1, 20.1, 21.2, 24.1
63
18.2
65
16.2
67
12.2, 27.2
Characters pertaining to:
Scapulocoracoid
Humerus
Antebrachium and Manus
Stem tyrannosauroids
Tyrannosauridae

FIGURE 6.3. Biomechanical reconstruction of hypothetical forces exerted on the forelimb of *Tyrannosaurus rex* with relevant muscles as discussed in text. **A**, depicts the forces encountered from struggling prey or a mate; **B**, depicts the forces encountered during pushing up from the ground. Large red arrows indicate the direction of the external force; dashed black arrows indicate the moments inflicted on the joint as a result of the external force; solid black arrows indicate the muscle actions required to resist these moments. Approximate muscle fiber directions are indicated by color-coded lines between origin and insertion. Pastel colors indicate the attachment site is located on the non-visible surfaces of the bone. **Abbreviations**: **DC**, Deltoideus clavicularis; **DS**, Deltoideus scapularis; **GRF**, ground reaction force; **HR**, Humeroradialis; **LD**, Latissimus dorsi; **RF**, resistive force; **SBC**, Subcoracoideus; **SBS**, Subscapularis; **SHP**, Scapulohumeralis posterior; **SU**, Supinator.

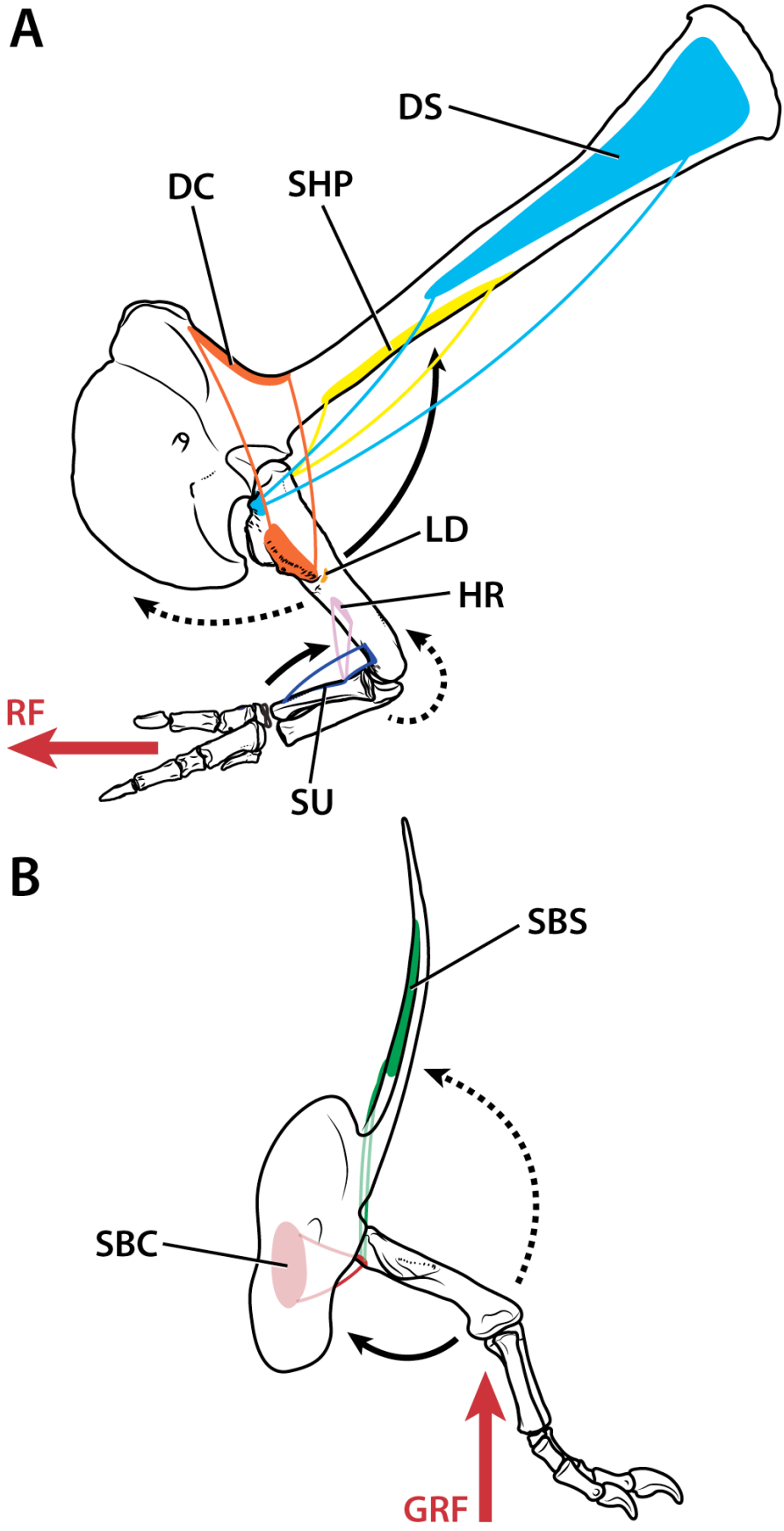
A
DS
DC
SHP
LD
HR
RF
SU
B
SBS
SBC
GRF

APPENDIX

1. INSTITUTIONAL ABBREVIATIONS

AMNH, American Museum of Natural History, New York, NY, U.S.A.; **ANSP**, Academy of Natural Sciences, Philadelphia, PA, U.S.A.; **AODF**, Australian Age of Dinosaurs Fossil, Winton, Australia; **BMNH**, Natural History Museum, London, UK; **BYU**, Brigham Young University, Provo, UT, U.S.A.; **CMN**, Canadian Museum of Nature, Ottawa, ON, Canada; **FMNH**, Field Museum, Chicago, IL, U.S.A.; **GR**, Ghost Ranch Ruth Hall Museum of Paleontology, Abiquiu, NM, U.S.A.; **HMN**, Humboldt Museum für Naturkunde, Berlin, Germany; **IVPP**, Institute of Palaeontology and Palaeoanthropology, Beijing, China; **LH**, Long Hao Institute of Geology and Paleontology, Hohhot, China; **MCF**, Museo Municipal 'Carmen Fuñes', Plaza Huincul, Argentina; **MIWG**, Museum of Isle of Wight Geology, Sandown, UK; **MNA**, Museum of Northern Arizona, Flagstaff, AZ, U.S.A.; **MNHN**, Musée National d'Histoire Naturelle, Paris, France; **MOR**, Museum of the Rockies, Bozeman, MT, U.S.A.; **MPC**, Paleontological Center of the Mongolian Academy of Sciences, Ulaanbaatar, Mongolia; **MUCPv**, Museo de Geología y Paleontología, Universidad Nacional del Comahue, Neuquén, Argentina; **NCSM**, North Carolina Museum of Natural Sciences, Raleigh, NC, U.S.A.; **PVSJ**, Museo de Ciencias Naturales, San Juan, Argentina; **QG**, National Museum of Natural History, Bulawayo, South Africa; TMP, Royal Tyrrell Museum of Paleontology, Drumheller, Alberta, Canada; **UCMP**, University of California Museum of Paleontology, Berkeley, CA, U.S.A.; **UMNH**, Utah Museum of Natural History, Salt Lake City, UT, U.S.A.; **USNM**, National Museum of Natural History, Smithsonian Institution, Washington, DC, U.S.A.; **ZCDM**, Zhucheng Dinosaur Museum, Shandong, China; **ZPAL**, Institute of Palaeobiology of the Polish Academy of Sciences, Warsaw, Poland.

2. FORELIMB MYOLOGY OF *TYRANNOSAURUS REX*

The musculature of the pectoral girdle and forelimb of *Tyrannosaurus rex* (Figs. S1, S2, S3, and S4) was reconstructed by identifying homologous osteological correlates, including bone

surfaces (Hutchinson, 2001a, 2001b), in this taxon and *Tawa hallae*, a basal theropod for which the full musculature was reconstructed using Integrative Phylogenetic/Extant Phylogenetic Bracket methods (Bryant and Russell, 1992; Witmer, 1995). Justification for the reconstruction of most of the muscle attachments are given in Chapter IV; below, I provide justification for muscle attachments in *Tyrannosaurus rex* that depart from those seen in *Tawa hallae*.

Rhomboideus (RH) and Serratus profundus (SP)—In *Tawa* these muscles were reconstructed as inserting adjacent to each other on the distal portion of the medial aspect of the scapular blade, with the Rhomboideus extending further distally based on the likely orientation of the scapular blade and its morphology of the extant phylogenetic bracket, but it lacked other osteological correlates (Chapter IV). However, some specimens of *Tyrannosaurus* exhibit two subtriangular fossae on the medial surface of the distal scapular blade (FMNH PR 2081, MOR 980), which likely indicate the areas of insertion of these two muscles, separated by the origin of Subscapularis (SBS; Fig. S1B). Grooves on the medial surface of the scapular blade separate similar fossae in *Majungasaurus crenatissimus* (FMNH PR 2836, Chapter IV), but are not present in other basal theropods. Thus, the phylogenetic bracket is still ambiguous for these muscles at the base of the tree.

Supracoracoideus (SC) and Supracoracoideus accessorius (SCA)—The tyrannosaurid scapulocoracoid is unique in possessing a ridge along the scapulocoracoid suture that separates the subacromial depression, which typically extends from the scapula to the coracoid, into two distinct fossae, each isolated to one element (*Daspletosaurus*, CMN 8506; *Tarbosaurus*, MPC 107/2; *Tyrannosaurus* MOR 555). This ridge likely divided the Supracoracoideus complex of muscles (Fig. S1A), but whether it represents an enlarged origin of SCA or the separation of the Supracoracoideus into additional heads as in crocodylians (Meers, 2003) is uncertain. The Supracoracoideus has been treated as possessing a continuous area of origin with the exception of SCA based on the phylogenetic bracket (Chapter IV), and so it is reconstructed in this way in *Tyrannosaurus* as well, giving the SCA a wide area of origin. These muscles have close areas of insertion on the deltopectoral crest, so they are considered together as part of one complex in the primary text given the uncertainty of the distribution of fibers at their origin.

Scapulohumeralis posterior (SHP)—Tyrannosaurids, allosauroids and some ceratosaurs possess distinct fin-like tubercles on the posteroventral edge of the scapular blade. The development of these tubercles varies from low, elongate tubercles (*Tyrannosaurus*, MOR 555; *Teratophoneus*, BYU 8120/9396; *Ceratosaurus*, UMNH VP 5278) to prominent, distinct fins (*Giganotosaurus* MUCPv Ch1; *Allosaurus*, BYU 725/17124). These rugosities appear to be distinct from those sometimes present for Serratus superficialis more distally (*Tyrannosaurus*, MOR 555). They are often rugose or striated on their medial surface, continuous with the area ventral to the medial scapular ridge (*Teratophoneus*, BYU 8120/9396), and so seem to represent a portion of a larger muscle attachment instead of a single tendinous attachment point. Thus, these tubercles are reconstructed here as representing the proximal edge of the origin of SHP (Fig. S1A), which attached along this edge, extending slightly onto each side of the scapular blade (Chapter IV).

Deltoideus clavicularis (DC), Latissimus dorsi (LD), and Humeroradialis (HR)—One of the most unique things about the forelimb in derived tyrannosaurids is the presence of an enormous rugosity extending along the lateral surface of the deltopectoral crest for approximately the distal half of the crest and often extending further distally onto the humeral shaft (*Tyrannosaurus*, FMNH PR 2081; Fig. S2B). The identity of the muscle attaching to this scar has been proposed to be part of Pectoralis (Carpenter and Smith, 2001), a combination of part of Supracoracoideus and Humeroradialis (Lipkin and Carpenter, 2009), or part of Teres major and/or Latissimus dorsi (Brochu, 2003). However, in the current muscular reconstruction (Chapter IV), this scar seems to most closely relate to the insertion of Deltoideus clavicularis. The possibility of an anterior migration of LD is difficult to rule out when considering only the morphology of the most derived tyrannosaurids because the furrow for LD is absent in these taxa but, when more basal tyrannosaurids are considered, the distinction becomes clearer. The humeri of *Gorgosaurus* (TMP 86.144.01) and *Albertosaurus* (TMP 2002.46.43) possess both furrows for LD and low rugosities matching the morphology of the larger rugosity in derived tyrannosaurids, indicating that the latter rugosity is associated with a muscle independent from LD. Additionally, at least one specimen of *Tyrannosaurus rex* (MOR 980, right humerus) possesses a depression

posterior to the distal end of this rugosity that may represent the retained furrow of LD in this specimen.

The association of this scar with Humeroradialis is difficult to completely rule out due to the position of the substantial origin of this muscle from this region in crocodylians (Meers, 2003). However, some tyrannosaurid humeri have low tubercles present distal to this scar on the lateral humeral shaft (*Daspletosaurus*, TMP 2001.36.01), and one humerus exhibits an extremely large tubercle in this region, possibly a result of a pathology (*Tyrannosaurus*, TMP 81.6.1). Similar tubercles are also found variably in other large theropod taxa (*Aucasaurus*, MCF PVPH 236; *Poekilopleuron*, MNHN 1897-2), and these distal scars may represent the distal migration of the origin of Humeroradialis in these taxa (Fig. S2B).

Flexor carpi ulnaris (FCU)—The insertion of FCU is plesiomorphically on the pisiform or ulnare in theropods (Chapter IV). Tyrannosauroids minimally possessed four carpal elements, including a radiale and several distal carpals (Lambe, 1917; Brochu, 2003), but the identity of the other carpals is difficult due to the lack of completely preserved carpus in many taxa. It seems likely that an ulnare was also present (Lambe, 1917), but it may have become relatively reduced (*Yutyrannus,* ZCDM 5001) and therefore a relatively poor area for muscle insertion. Distinct lateral and ventral projections on the proximal end of metacarpal III in tyrannosaurids (*Daspletosaurus*, TMP 2001.36.01; *Tyrannosaurus*, MOR 980) may indicate that this reduced metacarpal served as a site of muscle insertion for the FCU as well as for the Extensor carpi ulnaris (Fig. S4), which plesiomorphically inserted on the pisiform as well as the proximal end of the lateral-most metacarpal.

3. TABLES

TABLE 6.S1. List of taxa and specimen numbers scored for analysis. References are provided for taxa in which published photographs, illustrations, or descriptions were used.

Taxon	Specimens and/or Reference
Herrerasaurus ischigualastensis	PVSJ 373, 53, 407
Eoraptor lunensis	PVSJ 512
Sanjuansaurus	PVSJ 605
Eodromaeus murphi	PVSJ 562
Tawa hallae	GR 242, 241
Coelophysis bauri	AMNH 7227, 7228, 7230, 7231, 7238
Coelophysis bauri	TMP 84.63.29, 84.63.30, 84.63.32, 84.63.33, 84.63.40, 84.63.50, 84.63.52
"Syntarsus" rhodesiensis	QG 1, 514, 545, 568 573; Raath, 1969, 1990
"Syntarsus" kayentakatae	MNA V2623; Rowe, 1989
Segisaurus halli	UCMP 32101
Dilophosaurus wetherelli	UCMP 37302, 37303, 77270
Liliensternus liliensteri	HMN MB.R. 2175
Elaphrosaurus bambergi	HMN MB.R. (unnumbered)
Limusaurus inextricabilis	IVPP V15923, V15924
Ceratosaurus nasicornis	USNM 4735
Ceratosaurus dentisulcatus	UMNH VP 5278
Masiakasaurus knopfleri	FMNH PR 2621, 2676, 2481
Aucasaurus garridoi	MCF PVPH 236
Majungasaurus crenatissimus	FMNH PR 2836
Baryonyx walkeri	BMNH 9951
Poekilopleuron bucklandii	MNHN 1897-2 (Plastotype)
Torvosaurus tanneri	BYU 725/2002, 725/2011, 725/2012, 725/2018, 725/2021, 725/5013, 725/5019, 725/17697
Xuanhanosaurus quilixiaensis	IVPP V6729
Allosaurus fragilis	BYU 671/8901, 725/8895, 725/10600, 725/17124, 725/4897, 725/17488, 725/13260, 725/5097, 725/11567
Allosaurus fragilis	UMNH VP 6396, 9654, 9822, 13814, 10131, 7794, 7795, 8161, 8150, 8151, 8157, 8143, 8144, 8146, 8147
Megaraptor namunhuaiguii	MUCPv 341
Australovenator wintonensis	AODF 604; White et al., 2012
Giganotosaurus carolinii	MUCPv Ch1
Acrocanthosaurus atokensis	NCSM 14345; Currie & Carpenter, 2000
Dilong paradoxus	IVPP V14243

Taxon	Specimens and/or Reference
Guanlong wucaii	IVPP V14531, V14532
Yutyrannus huali	ZCDM 5000, 5001
Eotyrannus lengi	MIWG 1997.550
Dryptosaurus aquilunguis	ANSP 9995; Brusatte et al., 2011
Raptorex kriegsteini	LH PV18
Albertosaurus sarcophagus	TMP 86.64.01, 2002.46.43, 2004.56.27, 79.01.02, 81.19.94
Gorgosaurus libratus	TMP 91.36.500, 99.33.01, 99.55.340, 86.144.01
Gorgosaurus libratus	CMN 2120; Lambe, 1917
Teratophoneus curriei	BYU 8120/9396, 8120/9397
Daspletosaurus torosus	TMP 96.12.143, 2001.36.1
Daspletosaurus torosus	CMN 8506
Tarbosaurus bataar	ZPAL MgD-I/3, MgD-I/177
Tarbosaurus bataar	MPC 107/2
Tyrannosaurus rex	MOR 555, 980, 002, 1125
Tyrannosaurus rex	TMP 81.6.1
Tyrannosaurus rex	FMNH PR 2081

4. CHARACTER LIST

1) Placement of tubercle marking origin of Scapulohumeralis posterior: no tubercle (0), separated from scapular glenoid lip by gap (1), or near scapular glenoid lip (2)

2) Location of medial longitudinal ridge of scapula: at 1/2 the blade width (0), at 1/3 blade width from ventral edge (1), or very near ventral edge or no ridge (2)

3) Development of scar for Triceps brachii scapularis: surface rugosity (0), distinct tubercle (1), or no marking (2)

4) Expansion of distal scapula, relative to minimum width: less than or equal to 150% (0), between 150% and 300% (1), or greater than 300% (2).

5) Proximal constriction of scapular blade: moderately broad with flat lateral surface (0), extremely broad (1) or narrow with rounded lateral surface (2)

6) Angle of acromial expansion, relative to scapular blade: greater than 90° (0), or approximately 90° (1).

7) Biceps tubercle: prominent tubercle (0), or low and rounded (1)

8) Placement of biceps tubercle: posterior to anteriormost projection of glenoid (0), or anterior to that point (1)

9) Subglenoid fossa: facing primarily posteroventrally (0), or facing primarily laterally (1)

10) Internal tuberosity: moderately developed (0), substantial projection (1), or reduced (2)

11) Greater tubercle: level with humeral head (0), distal to top of humeral head, level with internal tuberosity (1), projecting proximal to humeral head (2), or distal to internal tuberosity (3)

12) Posterior surface of greater tubercle: smooth (0), moderately rugose (1), or highly rugose (2)

13) Tip of deltopectoral crest: 1/3 from proximal end of humerus (0), or 1/4 from proximal end of humerus (1)

14) Direction of projection of deltopectoral crest: lateral of directly anterior (0), directly anterior (1), or medial of directly anterior (2)

15) Development of deltopectoral crest: projects from humeral shaft for a distance at least as long as the anteroposterior midshaft diameter (0), or does not (1).

16) Rugosity on anterior edge of lateral surface of deltopectoral crest: absent (0), light rugosity (1), or extremely large rugosity (2)

17) Lateral triceps ridge: present (0), or absent (1)

18) Furrow for insertion of Latissimus dorsi: located distal to end of deltopectoral crest (0), level with end of deltopectoral crest (1), or absent (2)

19) Entepicondyle: moderately developed (0), or expanded (1)

20) Main insertion area for ectepicondyle: near articular surface edge (0), or rugose lump located more proximally (1)

21) Supinator insertion surface: twisting around radius, lateral to anterior (0), entirely lateral (1), or entirely anterior (2)

22) Tubercle on proximal anterior ulna: present (0), or absent (1)

23) Olecranon process: low and rounded (0), or well developed (1)

24) Functional digits: three (0), or two (1)

25) Medial proximal projection on metacarpal I: present (0), or reduced (1)

26) Lateral process on proximal end of lateralmost metacarpal: absent (0), or present (1)

27) Projection of flexor tubercle of ungual of digit I: 30% or more of articular height (0), 20–30% of articular height (1), or 0–20% of articular height (2)

5. DATA MATRIX

Herrerasaurus	001001??0000010000000010000
Sanjuansaurus	00100100???????????????1????
Eoraptor	0?2100000000?0100??00?000?00
Eodromaeus	0101000000010000001?0?01000?
Tawa	010100???011000000000000000
Coelophysis	0?2100000001?00000?0?1010000
Syntarsus	0?2100000000?0100??00???0100
Dilophosaurus	0101000000000000000101010102
Segisaurus	0?2100000??00100111101?????2
Liliensternus	012000000000000010001100???
Elaphrosaurus	??0?1?10101102100?00???????
Ceratosaurus	120010000102010001001010?1?
Limusaurus	0?201?100210020001000101l0?
Masiakasaurus	120010101231011012000??????
Aucasaurus	2200??101131021011002101l1?
Majungasaurus	220010101131021011002001l1?
Allosaurus	110100000101010100100110001
Baryonyx	110?00101110000010101l1???1
Poekilopleuron	???????????????0100121010l?0??
Australovenator	?????????120010010101100l?1
Giganotosaurus	1?0?00111???????????????????
Acrocanthosaurus	1??100000120010?0010111011?
Megaraptor	112?01000???????????1010002
Xuanhanosaurus	110???000110?????101111110
Torvosaurus	?????????100020000100l1?111
Dilong	0?210?????00?1?00200???????
Guanlong	0??10????1100100101111000l0
Yutyrannus	0201000101l?0100??100110010
Eotyrannus	0??000000?110100?000???????

```
Dryptosaurus      ???????????11?110????????0
Raptorex          02212011121111?11200011?1?2
Gorgosaurus       1??2211112111101100121111110
Albertosaurus     ???2211112111101100121111?0
Teratophoneus     120?2?11101111?11201?11????
Daspletosaurus    12022111121111021201211111l
Tarbosaurus       02012111121211021201211111l2
Tyrannosaurus     12022111121211021201211111l2
```

6. SUPPLEMENTARY REFERENCES

Brochu, C. A. 2003. Osteology of *Tyrannosaurus rex*: insights from a nearly complete skeleton and high-resolution computed tomographic analysis of the skull. Journal of Vertebrate Paleontology 22:1–138.

Brusatte, S. L., R. B. J. Benson, and M. A. Norell. 2011. The anatomy of *Dryptosaurus aquilunguis* (Dinosauria: Theropoda) and a review of its tyrannosauroid affinities. American Museum Novitates 3717:1–53.

Bryant, H. N., and A. P. Russell. 1992. The role of phylogenetic analysis in the inference of unpreserved attributes of extinct taxa. Philosophical Transactions: Biological Sciences 337:405–418.

Carpenter, K., and M. Smith. 2001. Forelimb osteology and biomechanics of *Tyrannosaurus rex*; pp. 90–116 in D. Tanke and K. Carpenter (eds.), Mesozoic Vertebrate Life. Indiana University Press, Bloomington, IN.

Currie, P. J., and K. Carpenter. 2000. A new specimen of *Acrocanthosaurus atokensis* (Theropoda, Dinosauria) from the Lower Cretaceous Antlers Formation (Lower Cretaceous, Aptian) of Oklahoma, USA. Geodiversitas 22:207–246.

Hutchinson, J. R. 2001a. The evolution of pelvic osteology and soft tissues on the line to extant birds (Neornithes). Zoological Journal of the Linnean Society 131:123–168.

Hutchinson, J. R. 2001b. The evolution of femoral osteology and soft tissues on the line to extant birds (Neornithes). Zoological Journal of the Linnean Society 131:169–197.

Lambe, L. M. 1917. The Cretaceous theropodous dinosaur *Gorgosaurus*. Memoirs of the Geological Survey of Canada 100:1–84.

Lipkin, C., and K. Carpenter. 2009. Looking again at the forelimb of *Tyrannosaurus rex*; pp. 167–190 in P. Larson and K. Carpenter (eds.), *Tyrannosaurus rex*: the Tyrant King. Indiana University Press, Bloomington, IN.

Meers, M. B. 2003. Crocodylian forelimb musculature and its relevance to Archosauria. The Anatomical Record Part A 274A:891–916.

Raath, M. A. 1969. A new coelurosaurian dinosaur from the Forest Sandstone of Rhodesia. Arnoldia Series of Miscellaneous Publicatons 4:1–25.

Raath, M. A. 1990. Morphological variation in small theropods and its meaning in systematics: evidence from *Syntarsus rhodesiensis*; pp. 91–105 in K. Carpenter and P. J. Currie (eds.), Dinosaur Systematics. Cambridge University Press, Cambridge, UK.

Rowe, T. A. 1989. A new species of the theropod dinosaur *Syntarsus* from the Early Jurassic Kayenta Formation of Arizona. Journal of Vertebrate Paleontology 9:125–136.

White, M. A., A. G. Cook, S. A. Hocknull, T. Sloan, G. H. K. Sinapius, and D. A. Elliot. 2012. New forearm elements discovered of holotype specimen *Australovenator wintonensis* from Winton, Queensland, Australia. PLoS ONE 7:e39364.

Witmer, L. M. 1995. The extant phylogenetic bracket and the importance of reconstructing soft tissues in fossils; pp. 9–33 in J. J. Thomason (ed.), Functional Morphology in Vertebrate Paleontology. Cambridge University Press, Cambridge, UK.

FIGURE 6.S1. Myological reconstruction of the scapulocoracoid of *Tyrannosaurus rex* (FMNH PR 2081) in lateral (**A**) and medial (**B**) views. Proposed muscle origins are indicated in red, proposed insertions are indicated in blue. **Abbreviations: BB**, Biceps brachii; **CB**, Coracobrachialis; **DC**, Deltoideus clavicularis; **DS**, Deltoideus scapularis; **LS**, Levator scapulae; **RH**, Rhomboideus; **SBC**, Subcoracoideus; **SBS**, Subscapularis; **SC**, Supracoracoideus; **SCA**, Supracoracoideus accessorius; **SHA**, Scapulohumeralis anterior; **SHP**, Scapulohumeralis posterior; **SP**, Serratus profundus; **SS**, Serratus superficialis; **TBS**, Triceps brachii scapularis; **TR**, Trapezius.

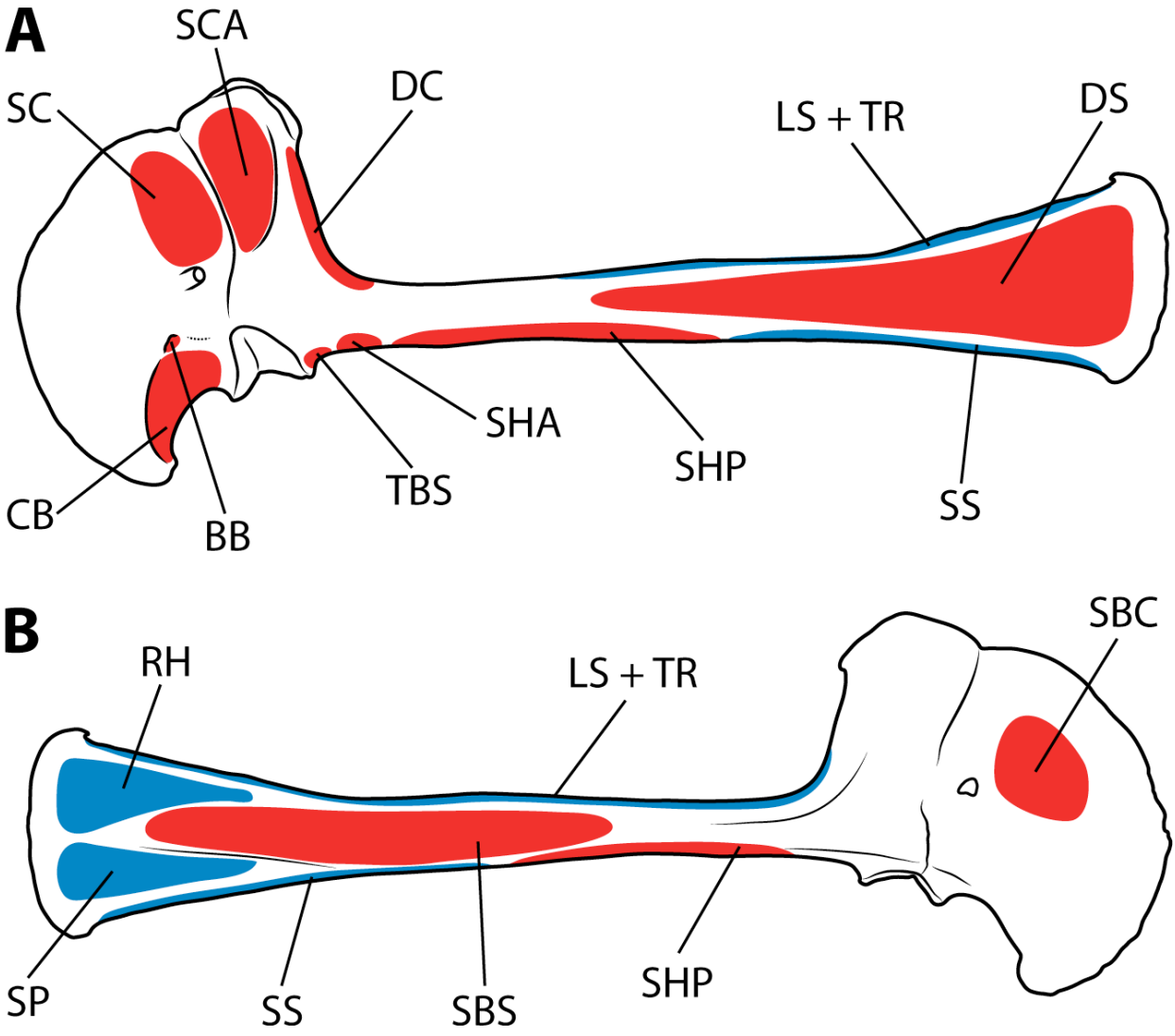
A
SCA
SC
DC
LS + TR
DS
SHA
SHP
TBS
CB
BB
SS
B
RH
LS + TR
SBC
SP
SS
SBS
SHP

FIGURE 6.S2. Myological reconstruction of the humerus of *Tyrannosaurus rex* (FMNH PR 2081) in anterior (**A**), lateral (**B**), and posterior (**C**) views. Proposed muscle origins are indicated in red, proposed insertions are indicated in blue. **Abbreviations: AN**, Anconeus; **AR**, Abductor radialis; **BB**, Biceps brachii; **BR**, Brachialis; **CB**, Coracobrachialis; **DC**, Deltoideus clavicularis; **DS**, Deltoideus scapularis; **EA**, Epitrocheloanconeus; **ECR**, Extensor carpi radialis; **ECU**, Extensor carpi ulnaris; **EDL**, Extensor digitorum longus; **FCU**, Flexor carpi ulnaris; **FDLS**, Flexor digitorum longus superficialis; **HR**, Humeroradialis; **LD**, Latissimus dorsi; **P**, Pectoralis; **PA**, Pronator accessorius; **PT**, Pronator teres; **SBC**, Subcoracoideus; **SBS**, Subscapularis; **SC**, Supracoracoideus; **SCA**, Supracoracoideus accessorius; **SHA**, Scapulohumeralis anterior; **SHP**, Scapulohumeralis posterior; **SU**, Supinator; **TBL**, Triceps brachii longus; **TBM**, Triceps brachii medialis.

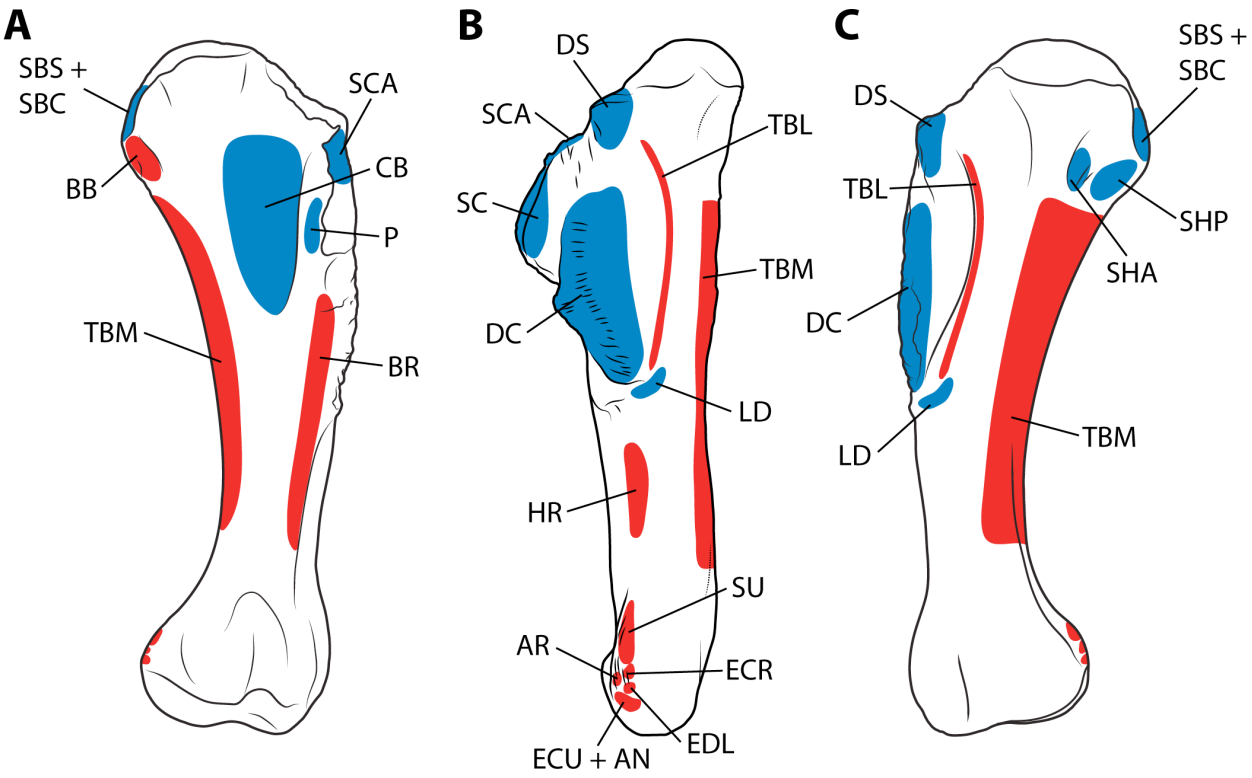
A
SBS +
SBC
SCA
BB
CB
P
TBM
BR
B
DS
SCA
TBL
SC
TBM
DC
LD
HR
SU
AR
ECR
ECU + AN
EDL
C
SBS +
SBC
DS
TBL
SHP
SHA
DC
LD
TBM

FIGURE 6.S3. Myological reconstruction of the antebrachium of *Tyrannosaurus rex* (FMNH PR 2081) in lateral (**A**), anterior (**B**), and medial (**C**) views. Proposed muscle origins are indicated in red, proposed insertions are indicated in blue. **Abbreviations: AN**, Anconeus; **APL**, Abuctor pollicis longus; **AR**, Abductor radialis; **BB**, Biceps brachii; **BR**, Brachialis; **EA**, Epitrocheloanconeus; **FDLP**, Flexor digitorum longus profundus; **HR**, Humeroradialis; **PA**, Pronator accessorius; **PQ**, Pronator quadratus; **PT**, Pronator teres; **R**, Radius; **SU**, Supinator; **TB**, Triceps brachii; **U**, Ulna.

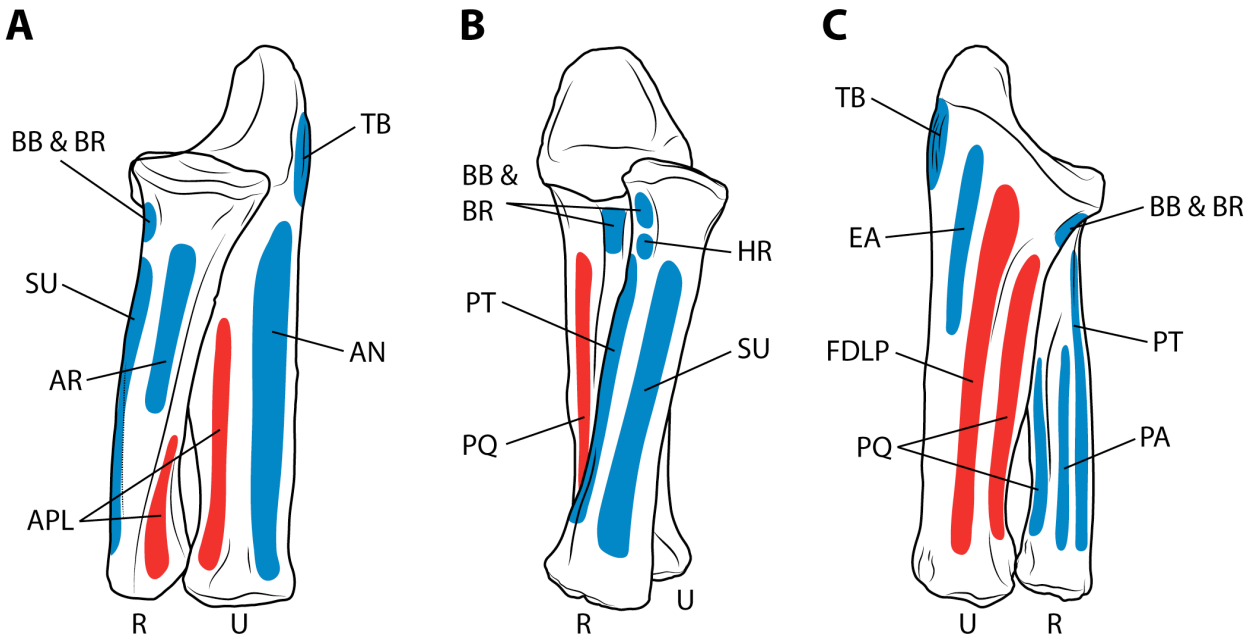
A
BB & BR
TB
SU
AN
AR
APL
R
U
B
BB &
BR
HR
PT
SU
PQ
R
U
C
TB
BB & BR
EA
FDLP
PT
PQ
PA
U
R

FIGURE 6.S4. Myological reconstruction of the carpus and manus of *Tyrannosaurus rex* (based on FMNH PR 2081 and MOR 555) in dorsal (**A**) and ventral (**B**) views. Proposed muscle origins are indicated in red, proposed insertions are indicated in blue. **Abbreviations: APB**, Abductor pollicis brevis; **APL**, Abductor pollicis longus; **ECR**, Extensor carpi radialis; **ECU**, Extensor carpi ulnaris; **EDB**, Extensor digitorum brevis; **EDBP**, Extensor digitorum brevis profundus; **EDBS**, Extensor digitorum brevis superficialis; **EDL**, Extensor digitorum longus; **FCU**, Flexor carpi ulnaris; **FDBP**, Flexor digitorum brevis profundus; **FDBS**, Flexor digitorum brevis superficialis; **FDL**, Flexor digitorum longus; **I**, Digit I; **II**, Digit II; **III**, Digit III.

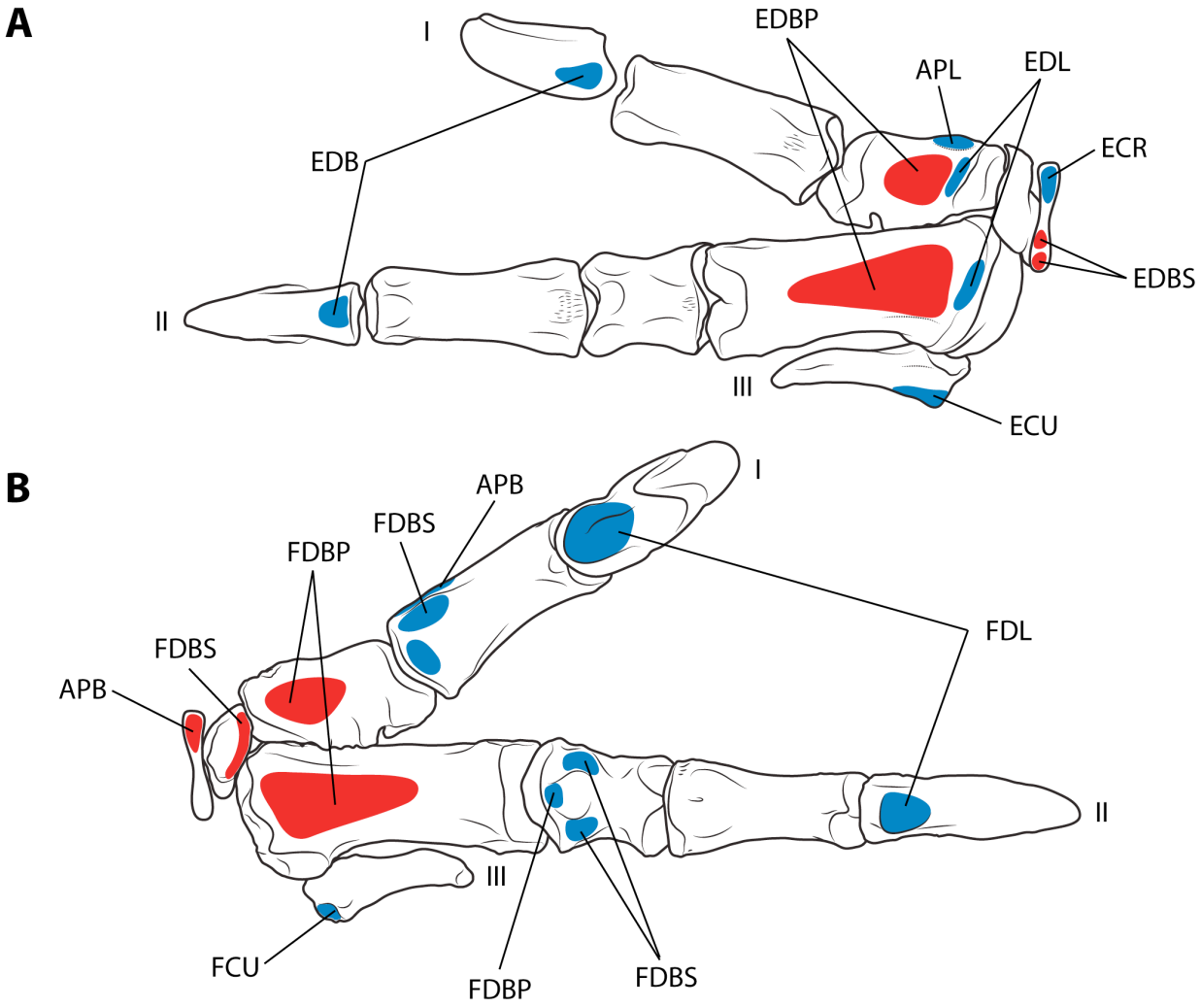
A
I
EDBP
APL
EDL
EDB
ECR
EDBS
II
III
ECU
B
APB
I
FDBS
FDBP
FDL
FDBS
APB
II
III
FCU
FDBP
FDBS

Chapter VII: Allometric and evolutionary trends of the pectoral girdle and forelimb of nonavian theropod dinosaurs

ABSTRACT

Nonavian theropod dinosaurs represent a taxonomically large and ecologically and morphologically diverse clade of bipedal tetrapods in which the forelimb did not have a primary locomotory role. This apparent lack of constraint has resulted in negative allometric scaling of the forelimb being invoked as the primary driving force behind the variation of forelimb size within the clade, particularly when considering forelimb reduction of tyrannosaurs and elongation of the forelimb along the avian lineage. This study assesses the allometric relationships of the forelimb and pectoral girdle within specialized theropod lineages and across the clade as a whole using phylogenetic comparative methods. Varying scenarios of forelimb evolution are modeled as Ornstein-Uhlenbeck processes to test for specific adaptive regimes within clades undergoing forelimb reduction and elongation, and the patterns of forelimb evolution over time are investigated using Bayesian ancestral state reconstruction (ASR) methods. Results of standard regressions recover a negative allometric pattern of forelimb length across the clade as reported in other studies, but the phylogenetically informed regressions reveal an overall pattern of isometry of the forelimb and positive allometry of the scapula. The best-fitting evolutionary model and the results of the ASR both show at least three distinct optima of relative forelimb length and demonstrate that the forelimbs of tyrannosaurs, ceratosaurs, and paravians were undergoing active selection for their distinctive proportions. The results also indicate that the relative forelimb length of most theropods and the scapular length across the entire clade exhibit a high degree of conservatism due to strong stabilizing selection, suggesting that biomechanical, developmental, or functional constraints were important in influencing forelimb proportions in most members of this clade.

INTRODUCTION

Over their ~165 million year evolutionary history, nonavian theropod dinosaurs occupied a wide variety of trophic categories, from hypercarnivory to herbivory (Zanno and Makovicky, 2011), and exhibited an enormous range of body sizes, from crow-sized dromaeosaurids (Xu et

al., 2000; Turner et al., 2007) to gigantic tyrannosaurids (Holtz, 2004). Unlike ornithischians and sauropodomorphs, theropods never re-evolved quadrupedality, retaining the bipedal posture of the most basal dinosauromorph taxa (Gatesy and Middleton, 1997a; Farlow et al., 2000). This 'fixed' bipedalism removed the biomechanical constraints of locomotion on the forelimb within the clade, permitting its diversification into a wide range of morphologies. However, despite substantial differences among theropods in the morphology of the individual elements of the forelimb, the intramembral proportions of the limb segments (that is, their proportions relative to each other) are conserved in most theropod taxa. This suggests that the proportions of the forelimb may have undergone selection due to factors such as spatial access, limb folding, or developmental pathways even if the forelimb was not experiencing constraint through ground reaction forces (Middleton and Gatesy, 2000). As Middleton and Gatesy (2000) pointed out, it is perhaps the relationship of forelimb length to hind limb length or overall body size that provides a stronger signal of function and ecology among nonavian theropods.

The importance of the scaling of limbs relative to body size has received much attention across Tetrapoda, in particular how large animals "solve" the problems of the differential scaling of body mass and cross-sectional parameters of muscle, tendon, and bone (McMahon, 1975; Alexander, 1981; Schmidt-Nielsen, 1984). In these cases, limb proportions, geometry, and posture are limited by the biomechanical requirements of body support and locomotion, which can cause departure from geometric similarity (isometry) in some scaling relationships. Similarly, the allometric scaling of bird wing length exhibits departure from geometric similarity due to the biomechanical demands of wing-based body support during flight (Prange et al., 1979; Olmos et al., 1996; Nudds, 2007). However, what constraints, if any, exist on the forelimb length of flightless bipedal animals are unclear. It is considered advantageous for a bipedal cursor to have relatively small forelimbs because they are non-propulsive "dead weight" and may create problems with balance (Coombs, 1978), although the specific allometric relationships of the forelimbs in flightless extant bipedal animals are unknown.

Nonavian theropods seem to exhibit a huge range of forelimb proportions relative to their body sizes, from extremely long to extremely short forelimbs. Forelimb reduction has evolved independently in multiple lineages, spawning various questions as to why and how this

morphology evolved. In one of these clades, the tyrannosaurids, reduction of forelimb length is accompanied by a substantial increase in body size in the derived taxa, which has led to speculation that forelimb reduction is merely a consequence of large size in nonavian theropods and that the forelimbs in these taxa were completely vestigial and possibly evolving toward complete loss (Horner and Lessem, 1993; Lockley et al., 2009). This idea has been supported by the finding of a negative allometric relationship between humeral length and body size in a sample of large nonavian theropods (Bybee et al., 2006), but evidence of reduced forelimbs at small body size among these lineages calls this trend into question (Sereno et al., 2009). At the other end of the spectrum, the forelimb of maniraptoran theropods is thought to exhibit relative elongation due to functional demands imposed by the evolution of flight (Padian and Chiappe, 1998a; Novas et al., 2009), but recent identification of a trend in body size reduction among this clade (Turner et al., 2007) has led to the idea that forelimb elongation in this clade is a passive allometric effect of small body size, just as forelimb reduction is a passive allometric effect of large body size (Bybee et al., 2006; Dececchi and Larsson, 2013).

This study provides a broad-scale analysis of the allometric scaling and evolutionary trends of nonavian theropod forelimbs, and is the first to look in detail at the relationship of forelimb length to large body size. Standard allometric and phylogenetically informed regressions are used to test for the presence of a trend of negative allometry of the forelimb with increasing body size across Theropoda as a whole, and whether these trends are reflected in the elements of the pectoral girdle. Analyses of different functional or phylogenetic groups are undertaken to identify potentially unique allometric patterns that do not affect the entire clade. The presence of directional evolutionary trends within specific clades, notably a trend of reduction within tyrannosauroids and one of elongation within maniraptorans, are tested through the use of phylogenetic model fitting that allow for the identification of potential selection toward independent optimal values for each clade. Finally, the ancestral pectoral and forelimb proportions are reconstructed in order to investigate the evolution of forelimb proportions through time and the role of basic functional constraints of the forelimb in the early evolution of these clades.

MATERIALS AND METHODS

Sample

Pectoral girdle and forelimb size was quantified by collecting measurements of the lengths of the scapular blade, humerus, radius, ulna, and metacarpal II for 111 specimens representing 82 taxa, taken either directly from specimens using calipers or a tape measure or from the literature. Due to the potential for interactions from ontogenetic allometric limb scaling (Kilbourne and Makovicky, 2010), specimens were limited to adult or near-adult individuals. A complete list of specimens, taxa, and measurements is given in Table S1, along with their sources. Measurements of circumference and diameter of the limb elements and various other metrics of scapulocoracoid size were also collected, but the limited sample size and non-normal distribution of these data rendered them unsuitable for statistical analysis. Femoral length was also collected to serve as a proxy for body size. This metric has been shown to have a strong relationship to overall body size in theropod dinosaurs (Christiansen and Fariña, 2004) and has been used commonly in studies of archosaurian body size evolution (Turner et al., 2007; Dececchi et al., 2012; Sookias et al., 2012; Turner and Nesbitt, 2013). Furthermore, femoral length was recently shown to scale isometrically with Snout-Vent Length in a large sample of theropods (Dececchi and Larsson, 2013). Using the length itself as a proxy instead of generating mass estimates is preferred to limit confounding errors introduced by the mass regression equations.

Standard Regressions

Data were log-transformed to meet parametric statistical assumptions. Bivariate regressions were performed in two major groups: 1) scapular length on femoral length (S/F), humeral length on femoral length (H/F), antebrachial length on femoral length (A/F), and metacarpal II length on femoral length (M/F) to explore element scaling in relation to body size; and 2) humeral length on scapular length (H/S), antebrachial length on humeral length (A/H), metacarpal II length on humeral length (M/H), and metacarpal II length on antebrachial length (M/A) to explore intralimb proportions and scaling. Antebrachial length was defined as radial

length, with ulnar length used in cases where the radius was not available. Regressions were run under a Reduced Major Axis (RMA) model using the lmodel2 package (Legendre, 2013) in the R statistical framework (R Development Core Team, 2013). This regression model was preferred over least squares methods because it assumes that both X and Y variables contain error, as is the case when both variables contain osteometric data (Rayner, 1985). Allometry is considered to be statistically significant when a value lies outside of the 95% confidence intervals for the isometric exponent of 1.0 (slope of the regression [Jungers et al., 1998]). These regressions were performed across all theropod taxa as well as for subsets of taxa representing functional or phylogenetic groups of interest, including the set of all taxa not typically classified as exhibiting forelimb reduction (NR), the set of taxa typically classified exhibiting forelimb reduction (RE), Tyrannosauroidea (TY), and Maniraptoriformes (MA, sensu Turner et al., 2012). Although Ceratosauria and its subclade Abelisauroidea are of considerable interest, the small number of taxa with preserved forelimb material was not sufficient for robust statistical analysis of this clade on its own.

Phylogenetic Regressions

Phylogenetic comparative methods take into account the non-independence of interspecific data due to shared evolutionary history of the taxa in the analysis (Felsenstein, 1985; Harvey and Pagel, 1991). Although differences in phylogenetic hypotheses (topology of the tree, branch lengths) can yield different patterns in the results, analyses incorporating a phylogenetic hypothesis have been shown to be more accurate than those assuming no phylogenetic signal, even when there are errors in the phylogeny (Nunn, 2011). Among other methods, the Phylogenetic Generalized Least Squares (PGLS, Martins and Hansen, 1997) approach was used in this study because of its ability to estimate a value for Pagel's lambda (λ), a measure of phylogenetic signal in the data (Pagel, 1999). After estimating this parameter using maximum likelihood, PGLS incorporates this value into the regression model. In cases where $\lambda=1.0$, this method is equivalent to Felsenstein's (1985) Phylogenetic Independent Contrast (PIC) method, which assumes evolution of the trait under Brownian Motion (random walk); when $\lambda=0.0$, there is no phylogenetic signal in the data. However, the model may also take

intermediate values of λ, indicating phylogenetic signal in the data under selection other than pure Brownian Motion (Pagel, 1999), and allowing for more accurate estimation of allometric trends. PGLS regressions were performed for each bivariate regression pair given above in all theropod taxa as well as the Tyrannosauroidea and Maniraptoriformes subsets using the caper package (Orme et al., 2012) implemented in the R statistical framework (R Development Core Team, 2013).

The phylogenetic tree for this method was constructed using an informal supertree method (Butler and Goswami, 2008; Brusatte et al., 2011; Sookias et al., 2012) by combining several recent, comprehensive theropod phylogenies for basal theropods (Nesbitt et al., 2009a; Martinez et al., 2011), ceratosaurs (Carrano and Sampson, 2008), tetanurans (Carrano et al., 2012), tyrannosaurs (Xu et al., 2012), and maniraptoriforms (Turner et al., 2012), grafting in several otherwise unsampled taxa (Choiniere et al., 2010; Choiniere et al., 2012; Pol and Rauhut, 2012). Given the taxon sampling dictated by preserved forelimb material, relatively few polytomies were present in the pruned tree (Fig. 1). The inclusion of only theropod taxa in the dataset renders the debate about whether *Herrerasaurus* and/or *Eoraptor* were non-theropod basal saurischians (Martinez et al., 2011) as a single, trifurcating polytomy at the base of the tree. Of potentially larger significance is the monophyly (or lack thereof) of Coelophysoidea (Nesbitt et al., 2009a; Martinez et al., 2011). The results presented here follow a paraphyletic Coelophysoidea as recovered by Nesbitt et al. (2009), but a reduced 'consensus' phylogeny of a polytomy at this node was also tested and found to give negligibly different values (<0.001 absolute difference). Branch lengths were applied via two methods: all branches set to equal length (unity), and branch lengths calibrated chronostratigraphically using geological ages of specimens and incorporating a 1-Myr adjustment for sister taxa with equivalent ages (Laurin, 2004; Kilbourne and Makovicky, 2010). Testing trees using species averages versus those retaining each individual specimen as a tip with hard polytomies at their 'base' yielded negligible differences and so individual specimens were retained in the dataset so as not to unnecessarily reduce sample size.

Evolutionary Trend Analysis and Ancestral State Reconstruction

The presence of directional trends in the evolution of the pectoral girdle and forelimb size in Theropoda can be explicitly tested by modeling various hypotheses of trait evolution within the clade. A common way to test for directional trends within a clade is to fit a model of Brownian motion with a directional trend, that is, a stochastic random walk model in one direction, typically increasing size or decreasing size (e.g., Sookias et al., 2012; Zanno and Makovicky, 2012). However, if one expects trends in different directions among subclades, each subclade must be tested individually, which becomes problematic in smaller clades with low sample size. Furthermore, the stochastic trend model assumes that the trait will continue to evolve in the given direction indefinitely, and that no stabilizing selection would occur to bound the trait to an optimum value (Hansen, 1997; Butler and King, 2004). Although this may be possible for some traits, it is not a biologically realistic assumption when modeling the elongation or reduction of a limb, which will possess developmental and anatomical constraints. Modeling the evolution of a trait as an Ornstein-Uhlenbeck (OU) process allows for the incorporation of the parameters of selection, drift, and one or more optima within a clade, and permits multiple trends to be mapped onto a single clade (Hansen, 1997; Butler and King, 2004). This method is also able to test the hypothesis that multiple, independent clades are evolving toward the same optimum value, such as whether ceratosaurs and tyrannosauroids share a single optimum ratio for forelimb reduction.

Nine models were tested in this analysis, and graphical representations are given in Figure 2. The null model was represented by pure Brownian motion (BM), implying that forelimb evolution proceeded in a stochastic, random walk fashion. The second model was that of Brownian motion plus a directional trend (BM+T), representing a directional random walk in one direction, with no optimum value. The third model (OU.1) was an OU model with one optimum for the entire clade of Theropoda. The models OU.3a, OU.3b, and OU.3c all contained three optima, each testing a different permutation of selection for forelimb reduction and elongation. The OU.3a model tests the hypothesis that tyrannosauroids and ceratosaurs independently evolved toward the same optimum and that maniraptoriforms as a whole exhibited selection toward a single optimum. The OU.3b model retains the same parameters for

tyrannosaurs and ceratosaurs, but tests the hypothesis that only Paraves underwent selection toward an optimum. The OU.3c model tests the hypothesis that large-bodied tetanuran theropods also evolved toward the same reduced-length optimum as ceratosaurs and tyrannosauroids by breaking the tree in to a basal optimum, a "middle" optimum (encompassing Ceratosauria, Tyrannosauroidea, and all taxa between them), and a maniraptoriform optimum. Models testing four optima on the theropod tree include OU.4a and OU.4b, which are identical to OU.3a and OU.3b except that in the four-optima models tyrannosauroids and ceratosaurs are modeled as having experienced selection for different optima. The final model is OU.7, which tests the hypothesis that each major clade (in this case, basal taxa, Ceratosauria, Megalosauroidea, Allosauroidea, Tyrannosauroidea, non-paravian Maniraptoriforms, and Paraves) evolved toward its own unique optimum.

The alvarezsauroids are a group of small-bodied maniraptorans that also exhibit extreme forelimb reduction, and it would be desirable to test for evolutionary trends within this clade as well. Unfortunately, the fragmentary nature of the forelimbs of most alvarezsauroid taxa have limited the sample in this clade to only two taxa: the most basal taxon, *Haplocheirus sollers*, and one of the most derived members, *Mononykus olecranus* (Fig. 1). Although this clade in general shows strong signs of a trend toward forelimb reduction (e.g., Chiappe, 2002), any signal obtained from isolating the clade in this dataset from the rest of Maniraptora would be an artifact of the poor sample. Future discoveries of more complete forelimbs of both derived and stem taxa of this clade will allow for tests of the presence of trends toward reduction and whether Alvarezsauroidea is converging on the same optimum as other clades of nonavian theropods with reduced limbs.

To test these models for theropod forelimb evolution, ratios of scapular length, humeral length, and forelimb length to femoral length (SF, HF, and FLF, respectively) were employed to provide a "size free" way of analyzing the evolution of limb proportions in the clade. Forelimb length was computed as the humeral length plus antebrachial length; although the length of metacarpal II is also often incorporated into the calculation of forelimb length, it was omitted in this analysis in order to maximize the number of taxa that could be included. Although forelimb length and humeral length ratios are expected to exhibit similar trends based on the inclusion of

humeral length in both values, testing forelimb length ratio has the potential to capture differential trends due to the relative scaling of the distal forelimb elements (Middleton and Gatesy, 2000). Species means for each ratio and the supertree incorporating geologically scaled branch lengths were used as the input data for this analysis. Tests of these models for the SF, HF, and FLF ratios were performed using the ouch (King and Butler, 2012) package as implemented in the R statistical framework (R Development Core Team, 2013); tests of the BM+T model were run in the geiger package (Harmon et al., 2013). Both the corrected Akaike Information Criterion (AICc) and the more conservative Schwartz Information Criterion (SIC) values were used to assess model fit, as the SIC is less likely to overestimate the goodness of fit of models with a large number of variables, such as the OU.7 model. ΔAICc scores were calculated for each model based on the AICc score for the best fitting model and were judged on the following recommended scale: if $\Delta AICc < 2$, there is strong evidence for the model; if $3 < \Delta AICc < 7$, there is slight evidence for the model; and if $\Delta AICc > 10$, there is no evidence for the model (Burnham and Anderson, 2004). Maximum likelihood estimates of the values of the optima for each model (θ) were also collected from the model testing results.

Results from the model testing (see below) indicated that the assumption of Brownian motion required for most ancestral state reconstruction methods was not met by the data, given the geologically scaled branch lengths. In order to account for this, branch-scaling parameters were estimated and incorporated into Bayesian ancestral state reconstructions following the methods of Boyer et al. (2013). Parameters were estimated using BayesTraits V 2.0 (Beta) (Pagel and Meade, 2013) by running two independent Markov chain Monte Carlo (MCMC) chains for each of the following combinations: 1) non-directional model (model "A") with no scaling parameters; 2) non-directional model with parameter δ; 3) non-directional model with parameter κ; 4) non-directional model with parameter λ; 5) directional model (model "B") with no scaling parameters; 6) directional model with parameter δ; 7) directional model with parameter κ; and 8) directional model with parameter λ. Each chain was run for 10,050,000 iterations with a burn-in of 50,000 iterations, and RateDev set to AutoTune to achieve acceptances between 20–40%. Tracer 1.5 (Rambaut and Drummond, 2009) was used to ensure convergence in each pair of chains and to calculate log Bayes Factor values to assess model fit; if the log Bayes Factor is > 5,

the model was considered to have strong support (Pagel and Meade, 2013). The directional versus non-directional models for each parameter were first compared against each other, and if no support for a directional model was found, the non-directional model for each parameter was compared against the null non-directional model with no parameters. Parameters identified as significant were then incorporated into the Ancestral State Reconstructions using BayesTraits, based on two independent MCMC runs of 10,050,000 iterations. Mean values and posterior densities for ancestral SF, HF and FLF ratios were reconstructed for nodes of interest using the combined results of the two MCMC runs.

RESULTS

Standard Regressions

Scaling relationships for scapular length versus femoral length were positively allometric in Theropoda as a whole, with all subsets (Table 1) exhibiting significant, strong correlation (R^2 = 0.935–0.962, $p < 0.001$). Lack of spread in the data resulted in closely positioned regression lines for all subsets (Fig. 3A), without major differences in slope or intercept. The scaling relationship of humeral length versus femoral length exhibited more variation, being negatively allometric for all taxa and in Tyrannosauroidea, but isometric in all other subsets (Table 1). The regressions for all taxa and Tyrannosauroidea show slightly lower, but still significant, correlations (R^2 = 0.826 and 0.782, $p < 0.001$) than those of the other subsets. Comparison of the allometric coefficients for the non-reduced and the reduced subsets shows nearly identical slopes (0.924 and 0.937, respectively), with the primary difference being the value of the intercepts, giving them a distinct separation when plotted (Fig. 3B). The antebrachium and metacarpal II show weaker correlations with femoral length for the complete dataset (R^2 = 0.532 and 0.516, $p < 0.001$); overall, the antebrachium scales with negative allometry and metacarpal II exhibits isometry. These correlations improve for some subsets (non-reduced taxa, reduced, and maniraptoriforms) but are very weak in Tyrannosauroidea, with metacarpal II length to femoral length showing no significant correlation (R^2 = 0.0153, p = 0.6602). The odd result of positive allometry in metacarpal II among reduced-forelimb taxa is probably related to this poor

relationship in tyrannosauroids, as well as the extreme reduction of the manus in abelisauroids (Fig. 3D, see discussion below).

The scaling relationship of humeral length versus scapular length is negatively allometric for all taxa and all subsets except for maniraptoriforms, in which it is isometric (Table 1). Tyrannosauroidea exhibits the strongest negative allometry, with an allometric coefficient of 0.552 (95% CI: 0.426, 0.698). The antebrachium scales isometrically with the humerus in all groups except in the non-reduced subset, where it exhibits negative allometry (Table 1). Metacarpal II also exhibits isometry in relation to humeral length in all groups, with the exception of the reduced subset; as in metacarpal II length versus femoral length above, this is likely due in part to the extreme reduction of the manus in abelisaurids and the position of *Carnotaurus*, *Majungasaurus*, and *Aucasaurus* well below the remainder of the taxa (Fig. 4C). The regression of metacarpal II on antebrachial length exhibits a relatively strong correlation in all groups (R^2 = 0.893–0.964, $p < 0.001$; Fig. 4D), and exhibits positive allometry in both the entire dataset as well as the reduced subset, although in this case it is not caused by abelisaurids falling outside the range of other theropod taxa.

Phylogenetic Regressions

The PGLS analysis found high values of lambda (equal to 1.0 or nearly so) for almost all of the bivariate regressions and, as such, yielded different allometric patterns in these cases (Table 2). The exception is the scaling relationship of scapular length on femoral length, for which every subset-branch length combination had a lambda of 0.0 (no phylogenetic signal) except for the unity model of Tyrannosauroidea ($\lambda = 0.653$). Even with the added scaling parameter, this model still showed strong positive allometry. The allometric exponent (slope) of this and each other model do not differ greatly from the values obtained from the standard RMA regressions. The humerus and antebrachium both have the same pattern of scaling against the femur in this analysis, with all groups exhibiting isometry under both branch length models except for Tyrannosauroidea under the geologically calibrated model, which is strongly negatively isometric (Table 2). This correlation is weak but still significant for the antebrachium (R^2 = 0.290, p = 0.0035). In both of these cases, lambda indicates a lack of phylogenetic signal

within the clade under the geologically calibrated branch lengths ($\lambda = 0.0$), but pure Brownian Motion under the unity model ($\lambda = 1.0$). This discrepancy is likely due to the large temporal gap between basal tyrannosauroids and derived tyrannosaurids (Fig. S1), which is incorporated into the scaled branch lengths.

The regressions for metacarpal II length on femoral length were unable to be calculated for the set of all taxa and Tyrannosauroidea for the geologically calibrated branch length model, and the unity model for Tyrannosauroidea yielded a low but significant correlation ($R^2 = 0.347$, $p = 0.0045$) exhibiting negative allometry; all other subsets exhibited isometry. As in the standard regressions, the humerus scales with negative allometry in relation to the scapular length in all cases except for maniraptoriforms, where it exhibited isometry (Table 2). For this relationship, high values of lambda ($\lambda = 0.956–1.0$), and thus the significant influence of phylogeny, did not greatly affect the allometric exponents. The pattern of antebrachial length in relationship to humeral length does not differ from isometry in any case (Table 2). Metacarpal II exhibits quite a different pattern from that of the standard regression in relation to both the humerus and the antebrachium, with all cases following isometry except maniraptoriforms, which scale with significant negative allometry under both branch length models (Table 2).

Trend Analysis and Ancestral State Reconstruction

For the ratio of scapular length to femoral length (SF ratio), all OU models performed considerably better than BM or BM+T (Table 3), with the BM+T performing the worst. The OU.1 model (single optimum) performed better than the other models by >4 ΔAICc (the minimum difference), but no other OU possessed a ΔAICc value of >10 (no support). Furthermore, the values for the maximum likelihood estimates of the selective optima in each model (θ_x) do not greatly differ from the optimum estimated by the OU.1 model ($\theta = 0.6608$). The BM model performed worst by a large difference for both the ratios of humeral to femoral length and forelimb to femoral length, with the BM+T model exhibiting a similarly poor fit. Among OU models, OU.3b (three optima, with dual origin of reduced forelimb size and the third optimum encompassing only Paraves) performed better by a ΔAICc of >4 than all models except for OU.4b (four optima, with ceratosaurs and tyrannosauroids having separate optima and the third

optimum encompassing only Paraves), which also exhibited strong support (ΔAICc ≤ 2). The OU.3a model (three optima, with dual origin of reduced forelimb size and the third optimum encompassing all Maniraptoriforms) exhibited weak support (ΔAICc < 4) for the HF ratio but not for the FLF ratio. All OU models with multiple optima performed better (ΔAICc < 10) than the single optimum OU model in both datasets.

For each ratio, kappa and lambda scaling parameters were found to be significant (log Bayes Factors >10) and were estimated during the ancestral state reconstruction (ASR) analysis. As expected from previous model testing (above), the directional model of trait evolution never provided a better fit than pure Brownian motion and thus was not used in ASRs. The reconstructed values of the ratios for each node of interest are given in Table 4 along with the 95% HPD intervals for each value. In general, the 95% HPD intervals are extremely wide and extensively overlap; these intervals are generally "over-conservative" (Losos, 1999; Martins, 1999; Boyer et al., 2013), as is clear from the values presented here, for which some ratios of have a lower bound of zero. Plotting the reconstructed values for each node against time yields patterns that are similar to those found in the model-fitting analysis (Fig. 5). The scapula to femur ratio exhibits a large expansion in the range of values toward the middle of the theropod lineage, with no clade-specific trends evident. Convergence on a single optimum value of relative scapular length can be observed as multiple lineages approach a midline ratio that is similar to those exhibited by more basal taxa (Fig. 5A). Relative forelimb length experiences a slight decrease during the early evolution of Theropoda, but shows a continued increase after the ceratosaurian lineage branches off. Tyrannosauroidea exhibits forelimb proportions similar to basal Maniraptoriformes at its base, but quickly converges on the trajectory of Abelisauridae. By the end of the Mesozoic there is a large gap between the lineages exhibiting forelimb reduction and those maintaining longer forelimb lengths or exhibiting a trend of elongation (Fig. 5B).

DISCUSSION

Patterns of Forelimb Allometry in Theropods

Similar to other studies that have found negative allometric relationships between forelimb elements and body size (Vargas, 1999; Bybee et al., 2006; Dececchi and Larsson, 2013), the standard RMA regressions found negative allometric relationships for humeral length versus femoral length and antebrachial length versus femoral length in the theropod clade as a whole (Table 1, Fig. 2). However, when phylogeny is taken into account, both relationships are isometric (Table 2). The strong phylogenetic signal in the data indicates that the reduced forelimbs of large theropods are a result of shared phylogenetic history and not representative of the clade as a whole. This is further illustrated by the fact that the slope of the PGLS regression of humeral length versus femoral length for all taxa (b = 0.948–0.953 [note that the range of values indicates differences based on branch lengths used, not confidence intervals]) is similar to the slope of the RMA regression when all taxa that are typically identified as possessing reduced forelimbs are removed (b = 0.924). Notably, the PGLS regression of the forelimb elements on femoral length for only the clade Tyrannosauroidea are negatively allometric when the geologically-calibrated branch lengths are used but isometric with the unity branch lengths; as the results of the model testing indicate, it is unlikely that forelimb evolution of this clade is undergoing pure Brownian motion, an assumption of the unity model. Thus it appears that the tyrannosauroid clade does exhibit a negatively allometric relationship of forelimb length to body size, although this is a clade-specific trend.

At the other end of the scale, even when phylogenetically uncorrected, maniraptoriforms do not exhibit negative allometry of the forelimb elements relative to femoral length, which would be expected if forelimb elongation was merely a result of small body size. In fact, the standard RMA regression has a slightly positively allometric slope (b = 1.102), although it is not significantly different from isometry and a negative allometric trend is certainly not supported by the PGLS regressions. Although the results of this analysis differ from a similar study of forelimb allometry in a more coelurosaurian-focused dataset, which found negative allometry of the forelimb across Theropoda (Dececchi and Larsson, 2013), the overall conclusions do not. Dececchi and Larsson (2013) reported no support for an evolutionary trend of increasing forelimb length throughout Coelurosauria to Aves, and this trend is also not supported by the

findings of this study of forelimb isometry among Maniraptoriformes (but see below on the trend modeling results for Paraves). The allometric slopes of Dececchi and Larsson (2013) for the individual forelimb elements on snout-vent length are consistently lower than those reported here, but they fall within the 95% confidence intervals for the RMA slopes of this study. Furthermore, their results are all based on phylogenetically uninformed statistics, and thus are likely exhibiting the confounding trends of the Tyrannosauroidea.

In general, the relationships of antebrachial and metacarpal lengths to femoral lengths are not strong, although the PGLS regressions of antebrachial length are better correlated than the uncorrected RMA regressions (R^2 of 0.727–0.731 vs. 0.516, respectively). This relationship is particularly poor in tyrannosauroids, indicating that the scaling of the manus likely exhibits no clear trend relative to body size. The metacarpus and antebrachium are, however, highly correlated with each other and the humerus and exhibit isometric trends across all taxa. This generally agrees with the high level of conservatism found in the intramembral proportions of nonavian theropods by Middleton and Gatesy (2000), but the trends do not clearly match the expected proportional reduction of distal elements relative to proximal elements that have been described for limb reduction (Fürbringer, 1870; Lande, 1978). For a given humeral length, tyrannosaurids possess slightly shorter antebrachii and metacarpals than do most other theropod taxa, but they are within the range of all nonavian theropods (Fig. 4B, C). Abelisauroids, however, clearly exhibit this pattern of forelimb reduction, with antebrachial and metacarpal lengths much shorter than would be expected based on humeral length (Fig. 4B, C), reflecting the same morphological isolation for the entire clade as found by Middleton and Gatesy (2000) for *Carnotaurus*.

The strong positive allometry of the scapula relative to femoral length, lacking any phylogenetic signal ($\lambda = 0.0$ for most regressions), is a unique result of this study in comparison to the only other studies that analyze this relationship (Dececchi et al., 2012; Dececchi and Larsson, 2013). Dececchi and Larsson (2013) recover scapular length as isometric to snout-vent length in their complete dataset that includes basal avian taxa, but the confidence intervals for the reported slope nearly exclude isometry when only nonavian theropod taxa are included (b = 1.0668 [CI 0.999995, 1.133605], Table S2C, D; Dececchi and Larsson, 2013). It is possible that

scapular length scales slightly differently with snout-vent length than it does with femoral length, and this is supported by the results of Dececchi et al. (2012; Fig. 3), although in that study scapular length exhibited a stronger positive allometry with snout-vent length than with femoral length. Furthermore, there are only 28 taxa in common between the two studies for this regression, with their sample focusing more on coelurosaurs as opposed to more basal taxa. The strong correlation between scapular length and body size may be due to a close developmental association between the scapular blade and the axial skeleton (Kuijper et al., 2005; Valasek et al., 2011; Dececchi and Larsson, 2013), but this does not explain the significant positive allometry exhibited by the scapular blade.

One possibility is that hypaxial muscles such as Trapezius and Levator scapulae that attach to the scapula played an important role in craniocervical support or feeding in large theropods; for instance, the Levator scapulae is an effective abductor of the neck in crocodylians, and may be used in feeding strikes (Meers, 2003). However, these muscles do not leave clear osteological correlates of their proximal attachments on the vertebral column (see Chapter IV), and their role in craniocervical muscle dynamics has not been explored (Snively and Russell, 2007c, 2007b; Tsuihiji, 2010). The size of the scapulocoracoid as a whole may also be related to its connection to the sternum and gastral basket. Although the sternum is not preserved and is presumed to be cartilaginous in most non-maniraptoran theropods (Padian, 2004), it would have linked the coracoids to the anterior edge of the gastral basket, which is thought to be a major driver of lung ventilation in nonavian theropods (Claessens, 2004). The relationship of the scapulocoracoid to this system could constrain its overall size. Furthermore, the Serratus musculature, which attaches to the scapula and the ribs, appears to have a role in ventilation in both extant birds and crocodylians (Codd et al., 2005; Munns et al., 2012), although its importance in the breathing of these taxa is not well understood. Nevertheless, it is possible that these muscles had a substantial role in respiration in nonavian theropod dinosaurs and may have helped to constrain the scaling of the scapula.

Evolutionary Trends of Forelimb Size

Results of the evolutionary model fitting analysis reinforce the idea that theropod clades with reduced forelimbs underwent unique evolutionary trajectories. A key hypothesis of tetrapod limb reduction is that unused limbs become reduced due to evolutionary drift and that reduced morphologies become fixed in part because they are developmentally less costly (Fong et al., 1995). In that case, Brownian motion would be expected to be the major driver behind theropod limb proportions because they lack the functional constraints of body support and locomotion. However, analyzing the limb proportions of nonavian theropods reveals that the best model is one of selection toward an optimum value in specific clades. Using the ratio data for this analysis allows for the testing of size-independent evolutionary trends; in this way, more basal, small-bodied taxa with reduced limbs such as *Raptorex* and *Masiakasaurus* reinforce a trend of forelimb reduction that is not an effect of allometric scaling but active selection for a reduced limb, regardless of body size (e.g., Sereno et al., 2009). It is possible that tyrannosauroids and ceratosaurs share a single optimum value for the proportions of reduced forelimbs, but an alternate model where they each have unique optima is also well supported (Table 3). This uncertainty is likely due to the relatively small number of ceratosaur taxa with preserved forelimbs that could be analyzed for this study, the lack of many taxa exhibiting an intermediate forelimb morphology between the basal and derived taxa, and the lack of inclusion of the manus in this analysis. The highly unusual forelimb morphology of derived abelisaurids (e.g., Burch and Carrano, 2012) suggests that they possessed a distinct trajectory from that of tyrannosauroids. However, the reconstructed ancestral states for the forelimb to femur ratio at nodes along the phylogenetic "backbones" of these clades clearly show convergence in their values and a similar evolutionary trajectory (Fig. 5B).

The estimated optima for Ceratosauria and Tyrannosauroidea from the OU.4b model are larger proportions than those observed in the derived taxa, which is possibly due to the large temporal distances between basal and derived members of each clade. In comparison to the reconstructed values for ancestral nodes within the tree, the optima for forelimb to femur ratio for Ceratosauria and Tyrannosauroidea are similar to the value reconstructed for the node just outside the most derived family (Abelisauridae and Tyrannosauridae, respectively). Optima

estimates may also be affected by the relatively small sample size of taxa exhibiting the most derived morphologies in each clade, leading to an estimated value that is more affected by basal taxa. Filling in these gaps with future fossil discoveries will likely improve the estimations of these optima.

The results of this analysis also indicate that tyrannosauroids and ceratosaurs are unique among theropod clades in experiencing selection for a reduced forelimb morphology; the model that incorporated separate optima for each major theropod clade performed comparatively poorly, indicating that the forelimbs of most other theropods are all undergoing the same selective regime for a "medium" length forelimb. Despite the large degree of variation in the overall forelimb morphology within many of these clades, the relative size of the forelimbs and their individual elements are conserved, as is the case for the intramembral proportions of the forelimb (Middleton and Gatesy, 2000). The model-fitting also confirms that no overarching trend exists for forelimb elongation within all of Maniraptoriformes (Dececchi and Larsson, 2013). However, the best fitting models do find a distinct trend for forelimb elongation within the sister taxa to birds, Paraves. Although not discussed, some evidence of this trend also appears in the results of Dececchi and Larsson (2013); specifically, the nodal reconstruction for the relative forelimb length of paravians falls above the expected value based on linear regressions (Dececchi and Larsson, 2013; Fig. 4A), indicating that paravians exhibit longer forelimbs than expected based on body size alone. Similar to the other clades, the optima estimated for paravian forelimb proportions in this study consistently underestimate the observed proportions in the most derived taxa. In this case, the omission of basal avian taxa from the dataset may be the source of this underestimation. Nevertheless, these models indicate that elongation of the forelimb was undergoing selection in the taxa most closely related to birds, even though no trend of elongation was acting on the clade of Maniraptoriformes as a whole.

The hypothesis that a 'decoupling' of the forelimb module from body size was necessary for the evolution of flight (e.g., Dececchi and Larsson, 2013) is not supported by these results, which indicate that no overarching scaling trend of forelimb length encompassed all nonavian theropods. Instead, the pattern of evolution in the forelimb shows evidence of selection toward different optima, including selection toward forelimb elongation along the lineage to birds. The

evolution of bipedalism in archosaurs involved the localization of the locomotory module to the hind limb and tail (Gatesy and Dial, 1996), and thus the loss of locomotion-based constraint on the forelimb until the forelimb itself became a locomotory module at the evolution of flight. Although other constraints may have existed on forelimb proportions of most nonavian theropods (e.g., Middleton and Gatesy, 2000), these may be due to similar functional demands of food acquisition (see below) and do not necessarily suggest that forelimb morphology was dependent on body size.

Given the results of significant positive allometry within the scapula of nonavian theropods, it is somewhat unexpected to find strong evidence for a single selected-for optimal ratio of scapular length to femoral length. Similar to the tight correlation of these two values discussed above, this selection may be due to the constraint imposed on scapular size by its connection to the trunk through the hypaxial musculature. The reconstructed ancestral states for the scapula to femur ratio reinforce the lack of clade specificity in scapular evolution, showing a relative random scattering of values over time (Fig. 5A). Visualizing the trends of the ancestral states at each node through time also clearly shows a trend in most clades toward a single optimum, as found in the model testing. Although there is only weak support for the other models of scapular evolution, the estimated optimal ratios for Tyrannosauroidea in the models of OU.4a, OU.4b, and OU.7 are slightly higher than those reconstructed for other clades, which may indicate that tyrannosauroids experience selection for slightly longer scapulae than do other theropods.

Functional Implications

The strong correlations of forelimb elements with femur length and significant evidence for selection of an optimal relative forelimb length for most theropod taxa support the hypothesis that there are constraints on the forelimb proportions of nonavian theropods, perhaps due to similar forelimb function for many members of the clade. One factor that may influence limb proportions and effect conservatism within the clade is spatial access (Middleton and Gatesy, 2000). The ability for the manus to access the area near the shoulder and, to a larger extent, the space immediately in front of the animal, may be a driving factor behind the overall isometry of

the forelimb within Theropoda. Although joint morphology is thought to limit the forward reach and spatial access of theropod forelimbs (Carpenter, 2002), these ranges of motions are likely conservative, as cartilage caps have been found to extend the range of motion in extant archosaurs (Hutson and Hutson, 2012). The reduced forelimb morphology of tyrannosaurids appears to limit their spatial range, but this may be partially compensated for by their joint morphology, which permits a relatively wide range of motion (Carpenter, 2002; Chapter IV).

The question remains: why is there selection for forelimb reduction? And why only in some clades of large theropods? Although it has been suggested that forelimb reduction was a compensatory measure in order to maintain balance in taxa with very large crania (Fastovsky and Weishampel, 2005), it is unlikely that the relatively small forelimbs of bipedal predatory dinosaurs had much effect on their center of mass. A recent study estimated the total mass of the forelimb to make up only 0.15% the total mass of *Tyrannosaurus rex* (Bates et al., 2009)*;* even quadrupling the size of the forelimbs would likely have had an exceedingly small effect on the center of mass and balance of the animal. Furthermore, examples that contradict this hypothesis can be found in spinosaurids such as *Suchomimus*, in which large body size and large heads are accompanied by relatively long forelimbs as well (Sereno et al., 1998), as well as in abelisaurids such as *Carnotaurus*, which possess relatively small crania as well as extremely reduced forelimbs (Bonaparte et al., 1990). Paradoxically, the shortening of the forelimb elements in tyrannosaurids increases the effective mechanical advantage of certain muscles within the limb by reducing the length of the load arm, which may be necessary when grappling with large prey (Chapter VI). Further investigations into the functional morphology of the forelimbs in clades exhibiting forelimb reduction will likely help to elucidate the factors contributing to the selection for this unusual morphology.

CONCLUSIONS

It is a long-standing hypothesis that variations in forelimb length of nonavian theropods, whether reduction in Tyrannosauridae or elongation in Paraves, are directly dependent on overall body size and that this relationship is due to passive evolutionary effects (Vargas, 1999; Xu et al.,

2004; Bybee et al., 2006; Dececchi and Larsson, 2013). However, the results of this study show that there is no evidence of negative allometric scaling of the forelimb elements across the entire clade when phylogeny is taken into account. Furthermore, although a negative allometric trend may be present within Tyrannosauroidea, models of forelimb size evolution show that it was not a passive process, but instead the forelimbs underwent active selection possibly due to shifts in the center of mass in derived tyrannosaurids. Additionally, although this study confirms previous results that there is no trend of forelimb elongation across the entire clade of Maniraptoriformes, forelimb elongation within Paraves is not a result of negative allometry and also underwent active selection toward forelimb proportions that characterize basal avians. The absence of an overarching ancestral scaling relationship of forelimb length that encompassed all nonavian theropods suggests that no 'decoupling' of the theropod forelimb was necessary for the evolution of flight (e.g., Dececchi and Larsson, 2013), as the forelimb maintained its own module separate from that of the hind limbs after the evolution of bipedalism in archosaurs (Gatesy and Dial, 1996; Gatesy and Middleton, 1997a).

These results also reinforce previous findings of a high degree of conservatism in forelimb proportions in most members of Theropoda (Middleton and Gatesy, 2000), suggesting that the forelimb of bipedal nonavian dinosaurs did not necessarily experience fewer biomechanical, functional, or developmental constraints than the forelimbs of quadrupedal dinosaurs. There have been a wide range of forelimb functions proposed for nonavian theropods, including prey apprehension mechanisms of grasping, raking, and clasping (Sereno, 1993; Carpenter, 2002), as well as clamping or hooking of foliage among herbivorous clades (Nicholls and Russell, 1985; Russell and Russell, 1993). Despite the differences in these actions, they may share common biomechanical requirements; unfortunately, few if any studies have created full biomechanical models of these activities to assess the functional demands on the forelimb and how they vary. Furthermore, the allometric relationships of extant flightless bipedal animals remain essentially unknown, so it is unclear whether the forelimb conservatism shown by nonavian theropods is typical of flightless bipeds or a unique characteristic of the clade. Future work in these areas will greatly enhance our understanding of the factors affecting forelimb size and shape of bipedal animals.

ACKNOWLEDGMENTS

I thank D. Krause, A. Turner, B. Demes, and S. Gatesy for their help and support in the development of this study and for comments on early drafts of the manuscript. R. Allain (MNHN), J. Calvo (MUCPv), J. Canale (MEB), M. Carrano (USNM), S. Chapman (BMNH), Chinzorig T. (MPC), R. Coria (MCF), M. Getty (UMNH), M. Goodwin (UCMP), A. Halamski (ZPAL), D. Henderson (TMP), S. Hutt (MIWG), R. Irmis (UMNH), T. Keillor (University of Chicago), A. Kramarz (MACN), C. Levitt (UMNH), R. Martinez (PVSJ), C. Mehling (AMNH), M. Norell (AMNH), F. Novas (MACN), K. Padian (UCMP), D. Pol (MPEF), J. Porfiri (MUCPv), E. Ruigómez (MPEF), D. Schwartz-Wings (HMN), P. Sereno (University of Chicago), R. Sheetz (BYU), B. Strilisky (TMP), H. Woodward (MOR), Xu X. (IVPP), and Zheng F. (IVPP) generously provided access to specimens in their care. Thanks to P. O'Connor, R. Felice, and E. Gorscak for statistical and methodological discussions, and to A. Pritchard for assistance with data collection. I thank J. McCartney for support and feedback during this project. Funding for this project was provided by a National Science Foundation Graduate Research Fellowship, a National Science Foundation Doctoral Dissertation Improvement Grant (DEB 111036), and the Doris O. and Samuel P. Welles Research Fund of the UCMP.

LITERATURE CITED

Alexander, R. M. 1981. Allometry of the leg muscles of mammals. Journal of Zoology 194:539–552.

Bates, K. T., P. L. Manning, D. Hodgetts, and W. I. Sellers. 2009. Estimating mass properties of dinosaurs using laser imaging and 3D computer modeling. PLoS ONE 4:e4532.

Bonaparte, J. F., F. E. Novas, and R. A. Coria. 1990. *Carnotaurus sastrei* Bonaparte, the horned, lightly built carnosaur from the Middle Cretaceous of Patagonia. Natural History Museum of Los Angeles County Contributions in Science 416:1–41.

Boyer, D. M., E. R. Seiffert, J. T. Gladman, and J. I. Bloch. 2013. Evolution and allometry of calcaneal elongation in living and extinct primates. PLoS ONE 8:e67792.

Brusatte, S. L., M. J. Benton, D. G. Lloyd, M. Ruta, and S. C. Wang. 2011. Macroevolutionary patterns in the evolutionary radiation of archosaurs (Tetrapoda: Diapsida). Earth and Environmental Science Transactions of the Royal Society of Edinburgh 101:367–382.

Burch, S. H., and M. T. Carrano. 2012. An articulated pectoral girdle and forelimb of the abelisaurid theropod *Majungasaurus crenatissimus* from the Late Cretaceous of Madagascar. Journal of Vertebrate Paleontology 32:1–16.

Burnham, K. P., and D. R. Anderson. 2004. Multimodal inference: understanding AIC and BIC in model selection. Sociological Methods Research 33:261–304.

Butler, M. A., and A. S. King. 2004. Phylogenetic comparative analysis: a modeling approach for adaptive evolution. The American Naturalist 164:683–695.

Butler, R. J., and A. Goswami. 2008. Body size evolution in Mesozoic birds: little evidence for Cope's rule. Journal of Evolutionary Biology 21:1673–1682.

Bybee, P. J., A. H. Lee, and E.-T. Lamm. 2006. Sizing the Jurassic theropod dinosaur *Allosaurus:* assessing growth strategy and evolution of ontogenetic scaling of limbs. Journal of Morphology 267:347–359.

Carpenter, K. 2002. Forelimb biomechanics of nonavian theropod dinosaurs in predation. Senckenbergiana Lethaea 82:59–76.

Carrano, M. T., R. B. J. Benson, and S. D. Sampson. 2012. The phylogeny of Tetanurae (Dinosauria: Theropoda). Journal of Systematic Palaeontology 10:211–300.

Carrano, M. T., and S. D. Sampson. 2008. The phylogeny of Ceratosauria (Dinosauria: Theropoda). Journal of Systematic Palaeontology 6:183–236.

Chiappe, L. M. 2002. The Cretaceous, short-armed Alvarezsauridae, *Mononykus* and its kin; pp. 87–120 in L. M. Chiappe and L. M. Witmer (eds.), Mesozoic Birds: Above the Heads of Dinosaurs. University of California Press.

Choiniere, J. N., J. M. Clark, C. A. Forster, and X. Xu. 2010. A basal coelurosaur (Dinosauria: Theropoda) from the Late Jurassic (Oxfordian) of the Shishugou Formation in Wucaiwan, People's Republic of China. Journal of Vertebrate Paleontology 30:1773–1796.

Choiniere, J. N., C. A. Forster, and W. J. de Klerk. 2012. New information of *Nqwebasaurus thwazi*, a coelurosaurian theropod from the Early Cretaceous Kirkwood Formation in South Africa. Journal of African Earth Sciences 71–72:1–17.

Christiansen, P., and R. A. Fariña. 2004. Mass prediction in theropod dinosaurs. Historical Biology 16:85–92.

Claessens, L. P. A. M. 2004. Dinosaur gastralia: origin, morphology, and function. Journal of Vertebrate Paleontology 24:89–106.

Codd, J. R., D. F. Boggs, S. F. Perry, and D. R. Carrier. 2005. Activity of three muscles associated with the uncinate processes of the giant Canada Goose *Branta canadensis maximus*. Journal of Experimental Biology 208:849–857.

Coombs, W. P. 1978. Theoretical aspects of cursorial adaptations in dinosaurs. The Quarterly Review of Biology 53:393–418.

Dececchi, T. A., and H. C. E. Larsson. 2013. Body and limb size dissociation at the origin of birds: uncoupling allometric constraints across a macroevolutionary transition. Evolution doi:10.1111/evo.12150.

Dececchi, T. A., H. C. E. Larsson, and D. W. E. Hone. 2012. *Yixianosaurus longimanus* (Theropoda: Dinosauria) and its bearing on the evolution of Maniraptora and ecology of the Jehol fauna. Vertebrata PalAsiatica 50:111–139.

Farlow, J. O., S. M. Gatesy, T. R. Holtz, J. R. Hutchinson, and J. M. Robinson. 2000. Theropod locomotion. American Zoologist 40:640–663.

Fastovsky, D. E., and D. B. Weishampel. 2005. The Evolution and Extinction of the Dinosaurs. Cambridge University Press, Cambridge, UK, 485 pp.

Felsenstein, J. 1985. Phylogenies and the comparative method. The American Naturalist 125:1–15.

Fong, D. W., T. C. Kane, and D. C. Culver. 1995. Vestigialization and loss of nonfunctional characters. Annual Review of Ecology and Systematics 26:249–268.

Fürbringer, M. 1870. Die Knochen und Muskeln der Extremitäten bei den Schlangenähnlichen Sauriern. Vergleichend-anatomische Abhandlung. W. Engelmann, Leipzig, 135 pp.

Gatesy, S. M., and K. P. Dial. 1996. Locomotor modules and the evolution of avian flight. Evolution 50:331–340.

Gatesy, S. M., and K. M. Middleton. 1997. Bipedalism, flight and the evolution of theropod locomotor diversity. Journal of Vertebrate Paleontology 17:308–329.

Hansen, T. F. 1997. Stabilizing selection and the comparative analysis of adaptation. Evolution 51:1341–1351.

Harmon, L., J. Weir, C. Brock, R. Glor, W. Challenger, G. Hunt, R. FitzJohn, M. Pennell, G. Slater, J. Brown, J. Uyed, and J. Eastman. 2013. geiger: Analysis of evolutionary diversification. 1.99-3.

Harvey, P. H., and M. D. Pagel. 1991. The Comparative Method in Evolutionary Biology. Oxford University Press, Oxford, UK, 239 pp.

Holtz, T. R. 2004. Tyrannosauroidea; pp. 111–136 in D. B. Weishampel, P. Dodson, and H. Osmolska (eds.), The Dinosauria (Second Edition). University of California Press, Berkeley, CA.

Horner, J. R., and D. Lessem. 1993. The Complete *T. rex*. Simon & Schuster, New York, 239 pp.

Hutson, J. D., and K. N. Hutson. 2012. A test of the validity of range of motion studies in fossil archosaur elbow mobility using repeated-measures analysis and the extant phylogenetic bracket. Journal of Experimental Biology 215:2030–2038.

Jungers, W. L., D. B. Burr, and M. S. Cole. 1998. Body size and scaling of long bone geometry, bone strength, and positional behavior in cercopithecoid primates; pp. 309–335 in E. Strasser, J. Fleagle, A. L. Rosenberger, and H. McHenry (eds.), Primate Locomotion: Recent Advances. Plenum Press, New York, USA.

Kilbourne, B. M., and P. J. Makovicky. 2010. Limb bone allometry during postnatal ontogeny in non-avian dinosaurs. Journal of Anatomy 217:135–152.

King, A. S., and M. A. Butler. 2012. ouch: Ornstein-Uhlenbeck models for phylogenetic comparative hypotheses. 2.8-2.

Kuijper, S., A. Beverdam, C. Kroon, A. Brouwer, S. Candille, G. Barsh, and F. Meijlink. 2005. Genetics of shoulder girdle formation: roles of Tbx15 and aristaless-like genes. Development 132:1601–1610.

Lande, R. 1978. Evolutionary mechanisms of limb loss in tetrapods. Evolution 32:73–92.

Laurin, M. 2004. The evolution of body size, Cope's Rule and the origin of amniotes. Systematic Biology 53:594–622.

Legendre, P. 2013. lmodel2: Model II Regression. R package version 1.7-1.

Lockley, M., R. Kukihara, and L. Mitchell. 2009. Why *Tyrannosaurus rex* had puny arms: an integral morphodynamic solution to a simple puzzle in theropod paleobiology; pp. 131–164 in P. Larson and K. Carpenter (eds.), *Tyrannosaurus rex*: the Tyrant King. Indiana University Press, Bloomington, IN.

Losos, J. B. 1999. Commentaries — Uncertainty in the reconstruction of ancestral character states and limitations on the use of phylogenetic comparative methods. Animal Behavior 58:1319–1324.

Martinez, R. N., P. C. Sereno, O. A. Alcober, C. E. Colombi, P. R. Renne, I. P. Montañez, and B. S. Currie. 2011. A basal dinosaur from the dawn of the dinosaur era in southwestern Pangaea. Science 331:206–210.

Martins, E. P. 1999. Estimation of ancestral states of continuous characters: a computer simulation study. Systematic Biology 48:642–650.

Martins, E. P., and T. F. Hansen. 1997. Phylogenies and the comparative method: a general approach to incorporating phylogenetic information into the analysis of interspecific data. The American Naturalist 149:646–667.

McMahon, T. A. 1975. Using body size to understand the structural design of animals: quadrupedal locomotion. Journal of Applied Physiology 39:619–627.

Meers, M. B. 2003. Crocodylian forelimb musculature and its relevance to Archosauria. The Anatomical Record Part A 274A:891–916.

Middleton, K. M., and S. M. Gatesy. 2000. Theropod forelimb design and evolution. Zoological Journal of the Linnean Society 128:149–187.

Munns, S. L., T. Owerkowicz, S. J. Andrewartha, and P. B. Frappell. 2012. The accessory role of the diaphragmaticus muscle in lung ventilation in the estuarine crocodile *Crocodylus porosus*. Journal of Experimental Biology 15:845–852.

Nesbitt, S. J., N. D. Smith, R. B. Irmis, A. H. Turner, A. Downs, and M. A. Norell. 2009. A complete skeleton of a Late Triassic saurischian and the early evolution of dinosaurs. Science 326:1530–1533.

Nicholls, E. L., and A. P. Russell. 1985. Structure and function of the pectoral girdle and forelimb of *Struthiomimus altus* (Theropoda: Ornithomimidae). Palaeontology 28:643–677.

Novas, F. E., D. Pol, J. I. Canale, J. D. Porfiri, and J. O. Calvo. 2009. A bizarre Cretaceous theropod dinosaur from Patagonia and the evolution of Gondwanan dromaeosaurids. Proceedings of the Royal Society of London Series B 276:1101–1107.

Nudds, R. L. 2007. Wing-bone length allometry in birds. Journal of Avian Biology 38:515–519.

Nunn, C. L. 2011. The Comparative Approach in Evolutionary Anthropology and Biology. University of Chicago Press, Chicago, 392 pp.

Olmos, M., A. Casinos, and J. Cubo. 1996. Limb allometry in birds. Annales Des Sciences Naturelles, Zoologie 17:39–49.

Orme, D., R. Freckleton, G. H. Thomas, T. Petzoldt, S. Fritz, N. Isaac, and W. Pearse. 2012. caper: Comparative Analyses of Phylogenetics and Evolution in R. 0.5.

Padian, K. 2004. Basal Avialae; pp. 210–231 in D. B. Weishampel, P. Dodson, and H. Osmolska (eds.), The Dinosauria, Second Edition. University of California Press, Berkeley, CA.

Padian, K., and L. M. Chiappe. 1998. The origin and early evolution of birds. Biological Review 73:1-42.

Pagel, M. 1999. Inferring the historical patterns of biological evolution. Nature 401:877–884.

Pagel, M., and A. Meade. 2013. BayesTraits. V 2.0 (Beta).

Pol, D., and O. W. M. Rauhut. 2012. A Middle Jurassic abelisaurid from Patagonia and the early diversification of theropod dinosaurs. Proceedings of the Royal Society B 279:3170–3175.

Prange, H. D., J. F. Anderson, and H. Rahn. 1979. Scaling of skeletal mass to body mass in birds and mammals. The American Naturalist 113:103–122.

R Development Core Team. 2013. R: A language and environment for statistical computing. 3.0.1. R Foundation for Statistical Computing, Vienna, Austria.

Rambaut, A., and A. Drummond. 2009. Tracer. V 1.5.

Rayner, J. M. V. 1985. Linear relationships in biomechanics: the statistics of scaling functions. Journal of Zoology 206:415–439.

Russell, D. A., and D. E. Russell. 1993. Mammal-dinosaur convergence. National Geographic Research & Exploration 9:70–79.

Schmidt-Nielsen, K. 1984. Scaling: Why is Animal Size so Important? Cambridge University Press, Cambridge, UK, 256 pp.

Sereno, P. C. 1993. The pectoral girdle and forelimb of the basal theropod *Herrerasaurus ischigualastensis*. Journal of Vertebrate Paleontology 13:425–450.

Sereno, P. C., A. L. Beck, D. B. Dutheil, B. Gado, H. C. E. Larsson, G. H. Lyon, J. D. Marcot, O. W. M. Rauhut, R. W. Sadlier, C. A. Sidor, D. J. Varricchio, G. P. Wilson, and J. A. Wilson. 1998. A long-snouted predatory dinosaur from Africa and the evolution of spinosaurids. Science 282:1298–1302.

Sereno, P. C., L. Tan, S. L. Brusatte, H. J. Kriegstein, X. Zhao, and K. Cloward. 2009. Tyrannosaurid skeletal design first evolved at small body size. Science 326:418–422.

Snively, E., and A. P. Russell. 2007a. Functional morphology of neck musculature in the Tyrannosauridae (Dinosauria, Theropoda) as determined via a hierarchical inferential approach. Zoological Journal of the Linnean Society 151:759–808.

Snively, E., and A. P. Russell. 2007b. Functional variation of neck muscles and their relation to feeding style in Tyrannosauridae and other large theropod dinosaurs. The Anatomical Record 290:934–957.

Sookias, R. B., R. J. Butler, and R. B. J. Benson. 2012. Rise of dinosaurs reveals major body-size transitions are driven by passive processes of trait evolution. Proceedings of the Royal Society B doi:10.1098/rspb.2011.2441.

Tsuihiji, T. 2010. Reconstructions of the axial muscle insertions in the occipital region of dinosaurs: evaluation of past hypotheses on Marginocephalia and Tyrannosauridae using the Extant Phylogenetic Bracket approach. The Anatomical Record 293:1360–1386.

Turner, A. H., P. J. Makovicky, and M. A. Norell. 2012. A review of dromaeosaurid systematics and paravian phylogeny. Bulletin of the American Museum of Natural History 371:1–206.

Turner, A. H., and S. J. Nesbitt. 2013. Body size evolution during the Triassic archosauriform radiation. Geological Society, London, Special Publications 379:doi 10.1144/SP379.15.

Turner, A. H., D. Pol, J. A. Clarke, G. M. Erickson, and M. A. Norell. 2007. A basal dromaeosaurid and size evolution preceding avian flight. Science 317:1378–1380.

Valasek, P., S. Theis, A. DeLaurier, Y. Hinits, G. N. Luke, A. M. Otto, J. Minchin, L. He, B. Christ, G. Brooks, H. Sang, D. J. Evans, M. Logan, R. Huang, and K. Patel. 2011. Cellular and molecular investigations into the development of the pectoral girdle. Developmental Biology 357:108–116.

Vargas, A. O. 1999. Evolution of arm size in theropod dinosaurs: a developmental hypothesis. Noticiario Mensual 338:16–19.

Xu, X., M. A. Norell, X. Kuang, X.-L. Wang, Q. Zhao, and C. Jia. 2004. Basal tyrannosauroids from China and evidence for protofeathers in tyrannosauroids. Nature 431:680–684.

Xu, X., K. Wang, K. Zhang, Q. Ma, L. Xing, C. Sullivan, D. Hu, S. Cheng, and S. Wang. 2012. A gigantic feathered dinosaur from the Lower Cretaceous of China. Nature 484:92–95.

Xu, X., Z. Zhou, and X.-L. Wang. 2000. The smallest known non-avian theropod dinosaur. Nature 408:705–708.

Zanno, L. E., and P. J. Makovicky. 2011. Herbivorous ecomorphology and specialization patterns in theropod dinosaur evolution. Proceedings of the National Academy of Sciences 108:232–237.

Zanno, L. E., and P. J. Makovicky. 2012. No evidence for directional evolution of body mass in herbivorous theropod dinosaurs. Proceedings of the Royal Society B 280:20122526.

TABLE 7.1. Results of Reduced Major Axis regressions for each subset of theropod taxa, with scaling pattern indicated as positive allometry (P), negative allometry (N), or isometry (I).

		N	Intercept	Slope	95% CI, Lower	95% CI, Upper	R^2	*p*	Pattern
S/F									
	All	69	-1.34	1.15	1.09	1.22	0.945	<0.001	P
	NR	50	-1.39	1.17	1.08	1.26	0.935	<0.001	P
	TY	16	-2.27	1.28	1.11	1.49	0.940	<0.001	P
	RE	19	-1.75	1.20	1.09	1.33	0.962	<0.001	P
	MA	21	-1.46	1.19	1.08	1.31	0.961	<0.001	P
H/F									
	All	87	0.269	0.829	0.751	0.916	0.826	<0.001	N
	NR	63	-0.148	0.924	0.850	1.00	0.905	<0.001	I
	TY	22	0.825	0.712	0.552	0.909	0.782	<0.001	N
	RE	24	-0.770	0.937	0.839	1.05	0.940	<0.001	I
	MA	26	-1.00	1.10	0.933	1.31	0.862	<0.001	I
A/F									
	All	76	0.117	0.774	0.662	0.908	0.532	<0.001	N
	NR	56	0.0796	0.820	0.714	0.943	0.795	<0.001	N
	TY	19	0.873	0.614	0.234	1.34	0.315	0.0125	I
	RE	20	-2.27	1.04	0.835	1.33	0.824	<0.001	I
	MA	24	-1.20	1.10	0.874	1.37	0.797	<0.001	I
M/F									
	All	61	-1.74	0.971	0.760	1.27	0.516	<0.001	I
	NR	43	-1.44	0.971	0.826	1.15	0.787	<0.001	I
	TY	15	-3.35	1.16	NA	NA	0.0153	0.6602	—
	RE	18	-4.89	1.34	1.05	1.79	0.800	<0.001	P
	MA	21	-1.87	1.09	0.844	1.43	0.772	<0.001	I
H/S									
	All	68	1.37	0.693	0.625	0.766	0.853	<0.001	N
	NR	48	1.20	0.746	0.679	0.819	0.911	<0.001	N

		N	Intercept	Slope	95% CI, Lower	95% CI, Upper	R^2	*p*	Pattern
	TY	18	2.09	0.552	0.426	0.698	0.826	<0.001	N
	RE	20	0.654	0.767	0.685	0.859	0.951	<0.001	N
	MA	21	0.218	0.960	0.789	1.17	0.858	<0.001	I
A/H									
	All	78	-0.221	0.949	0.861	1.05	0.845	<0.001	I
	NR	56	0.0280	0.924	0.865	0.988	0.944	<0.001	N
	TY	21	-0.268	0.935	0.695	1.26	0.730	<0.001	I
	RE	22	-0.962	1.03	0.867	1.23	0.879	<0.001	I
	MA	24	-0.272	0.997	0.925	1.08	0.972	<0.001	I
M/H									
	All	61	-1.72	1.11	0.964	1.28	0.774	<0.001	I
	NR	41	-1.18	1.03	0.926	1.15	0.900	<0.001	I
	TY	17	-2.79	1.29	0.839	2.16	0.600	<0.001	I
	RE	20	-3.50	1.38	1.06	1.88	0.753	<0.001	P
	MA	21	-0.579	0.927	0.826	1.04	0.945	<0.001	I
M/A									
	All	63	-1.41	1.16	1.07	1.26	0.906	<0.001	P
	NR	43	-1.11	1.09	0.996	1.20	0.924	<0.001	I
	TY	16	-0.201	0.943	0.820	1.09	0.944	<0.001	I
	RE	20	-2.17	1.34	1.13	1.60	0.893	<0.001	P
	MA	21	-0.289	0.922	0.840	1.01	0.964	<0.001	I

Model abbreviations: A/F, antebrachium length on femur length; A/H, antebrachium length on humerus length; H/F, humerus length on femur length; H/S, humerus length on scapula length; M/A, manus length on antebrachium length; M/F, manus length on femur length; M/H, manus length on humerus length; S/F, scapula length on femur length. Subset abbreviations: MA, maniraptoriforms; NR, nonavian theropods with non-reduced forelimbs; RE, nonavian theropods with reduced forelimbs; TY, tyrannosauroids.

TABLE 7.2. Results of PGLS regressions for each subset of theropod taxa, with scaling pattern indicated as positive allometry (P), negative allometry (N), or isometry (I).

	N	BL	λ	Int	Slope	95% CI, Lower	95% CI, Upper	R^2	*p*	Pattern
S/F										
All	68	U	0.00	-1.18	1.12	1.06	1.19	0.945	<0.001	P
All	68	S	0.00	-1.15	1.12	1.05	1.19	0.943	<0.001	P
TY	15	U	0.653	-2.66	1.36	1.13	1.58	0.917	<0.001	P
TY	15	S	0.00	-1.93	1.23	1.06	1.40	0.939	<0.001	P
MA	20	U	0.00	-1.34	1.17	1.06	1.28	0.959	<0.001	P
MA	20	S	0.00	-1.34	1.17	1.06	1.28	0.961	<0.001	P
H/F										
All	86	U	0.953	-0.381	0.960	0.875	1.05	0.854	<0.001	I
All	86	S	0.948	-0.264	0.940	0.854	1.03	0.847	<0.001	I
TY	21	U	1.00	-0.289	0.936	0.733	1.14	0.814	<0.001	I
TY	21	S	0.00	1.34	0.636	0.480	0.791	0.773	<0.001	N
MA	25	U	0.959	-0.526	0.990	0.825	1.16	0.858	<0.001	I
MA	25	S	0.985	0.172	0.855	0.698	1.01	0.834	<0.001	I
A/F										
All	75	U	1.00	-0.507	0.935	0.805	1.06	0.731	<0.001	I
All	75	S	0.979	-0.409	0.922	0.792	1.05	0.727	<0.001	I
TY	18	U	1.00	-0.164	0.864	0.546	1.18	0.642	<0.001	I
TY	18	S	0.00	2.39	0.383	0.098	0.669	0.290	0.0035	N
MA	23	U	1.00	-1.08	1.03	0.831	1.23	0.832	<0.001	I
MA	23	S	0.986	-0.599	0.944	0.771	1.12	0.847	<0.001	I
M/F										
All	60	U	1.00	-1.87	0.985	0.815	1.16	0.690	<0.001	I
All	60	S	—	—	—	—	—	—	—	—
TY	14	U	1.00	1.54	0.502	0.125	0.878	0.347	0.0045	N
TY	14	S	—	—	—	—	—	—	—	—
MA	20	U	0.939	-1.40	0.985	0.742	1.23	0.781	<0.001	I

	N	BL	λ	Int	Slope	95% CI, Lower	95% CI, Upper	R^2	*p*	Pattern
MA	20	S	0.967	-1.01	0.925	0.690	1.16	0.770	<0.001	I
H/S										
All	47	U	0.986	0.968	0.785	0.710	0.860	0.867	<0.001	N
All	47	S	0.956	1.02	0.774	0.705	0.843	0.881	<0.001	N
TY	17	U	1.00	1.73	0.655	0.490	0.819	0.806	<0.001	N
TY	17	S	0.00	2.28	0.523	0.398	0.649	0.819	<0.001	N
MA	20	U	1.00	0.107	0.958	0.809	1.11	0.906	<0.001	I
MA	20	S	0.965	0.422	0.894	0.743	1.04	0.884	<0.001	I
A/H										
All	77	U	1.00	-0.173	0.977	0.907	1.05	0.910	<0.001	I
All	77	S	0.977	-0.213	0.986	0.915	1.06	0.908	<0.001	I
TY	20	U	1.00	-0.204	0.985	0.829	1.14	0.897	<0.001	I
TY	20	S	0.985	-0.958	1.12	0.972	1.27	0.926	<0.001	I
MA	23	U	1.00	-0.239	0.985	0.907	1.06	0.967	<0.001	I
MA	23	S	0.968	-0.206	0.978	0.901	1.05	0.968	<0.001	I
M/H										
All	60	U	1.00	-1.37	0.994	0.895	1.09	0.869	<0.001	I
All	60	S	0.981	-1.37	1.01	0.906	1.11	0.869	<0.001	I
TY	16	U	1.00	0.065	0.825	0.529	1.12	0.685	<0.001	I
TY	16	S	0.984	-0.050	0.846	0.553	1.14	0.698	<0.001	I
MA	20	U	0.00	-0.401	0.890	0.788	0.992	0.943	<0.001	N
MA	20	S	0.00	-0.422	0.895	0.791	1.000	0.941	<0.001	N
M/A										
All	62	U	1.00	-1.13	1.01	0.927	1.09	0.905	<0.001	I
All	62	S	0.938	-1.18	1.04	0.951	1.12	0.903	<0.001	I
TY	15	U	0.00	-0.033	0.908	0.795	1.02	0.952	<0.001	I
TY	15	S	0.00	-0.051	0.913	0.787	1.04	0.941	<0.001	I
MA	20	U	0.00	-0.188	0.899	0.817	0.981	0.963	<0.001	N
MA	20	S	0.00	-0.209	0.905	0.818	0.992	0.960	<0.001	N

Model abbreviations: A/F, antebrachium length on femur length; A/H, antebrachium length on humerus length; H/F, humerus length on femur length; H/S, humerus length on scapula length; M/A, manus length on antebrachium length; M/F, manus length on femur length; M/H, manus length on humerus length; S/F, scapula length on femur length. Subset abbreviations: MA, maniraptoriforms; TY, tyrannosauroids. Other abbreviations: BL, branch length model; CI, confidence interval; Int, intercept of regression equation; S, geologically scaled branch lengths; U, branch lengths set to unity (1.0).

TABLE 3. Results of phylogenetic model fitting for the evolution of the scapular-femoral ratio (SF Ratio), humeral-femoral ratio (HF Ratio), and forelimb-femoral ratio (FLF Ratio). **Bold** indicates the AICc and SIC (Schwartz Information Criterion) values for the best performing model; *italics* indicates the values of the worst performing model.

	AICc	Δ_{AICc}	SIC	α	σ^2	θ_{other}	θ_R	θ_T	θ_C	θ_M	θ_P
SF Ratio											
BM	3.895	37.17	7.719	—	0.6481	—	—	—	—	—	—
BM+T	*5.349*	*38.62*	—	—	0.5467	—	—	—	—	—	—
OU.1	**-33.28**	**0**	**-27.66**	16.73	1.147	0.661	—	—	—	—	—
OU.3a	-28.71	4.569	-19.78	17.57	1.189	0.679	0.663	—	—	0.646	—
OU.3b	-29.03	4.244	-20.1	17.86	1.198	0.679	0.664	—	—	—	0.619
OU.3c	-28.81	4.464	-19.89	18.09	1.215	0.629	0.678	—	—	0.647	—
OU.4a	-26.43	6.844	-15.99	18.35	1.226	0.682	—	0.693	0.638	0.646	—
OU.4b	-26.76	6.511	-16.33	18.63	1.234	0.681	—	0.694	0.639	—	0.618
OU.7	-24.92	8.353	-10.61	296.7	15.05	0.555	—	0.718	0.657	—	0.611
HF Ratio											
BM	*-64.99*	*29.06*	*-60.77*	—	0.2410	—	—	—	—	—	—
BM+T	-66.88	27.17	—	—	0.5670	—	—	—	—	—	—
OU.1	-76.37	17.68	-70.14	5.913	0.3506	0.499	—	—	—	—	—
OU.3a	-90.51	3.536	-80.47	28.39	0.7993	0.471	0.389	—	—	0.645	—
OU.3b	**-94.05**	**0**	**-84.01**	33.08	0.8671	0.501	0.389	—	—	—	0.710
OU.3c	-88.59	5.463	-78.55	20.99	0.6380	0.503	0.422	—	—	0.644	—
OU.4a	-88.47	5.575	-76.65	30.74	0.8519	0.472	—	0.370	0.408	0.646	—
OU.4b	-92.11	1.942	-80.28	34.79	0.9003	0.501	—	0.369	0.409	—	0.711
OU.7	-89.56	4.487	-72.88	37.75	0.8965	0.488	—	0.369	0.399	—	0.718
FLF Ratio											
BM	*13.14*	*19.67*	*16.92*	—	0.7684	—	—	—	—	—	—
BM+T	12.95	19.49	—	—	1.016	—	—	—	—	—	—
OU.1	10.16	16.70	15.72	4.103	1.059	0.835	—	—	—	—	—
OU.3a	-0.503	6.032	8.309	18.10	2.006	0.772	0.568	—	—	1.13	—
OU.3b	**-6.535**	**0**	**2.277**	28.19	2.604	0.846	0.569	—	—	—	1.30

	AICc	Δ_{AICc}	SIC	α	σ^2	θ_{other}	θ_R	θ_T	θ_C	θ_M	θ_P
OU.3c	1.768	8.303	10.58	12.21	1.552	0.822	0.644	—	—	1.12	—
OU.4a	1.620	8.155	11.91	17.02	1.896	0.771	—	0.604	0.505	1.13	—
OU.4b	-4.333	2.202	5.961	27.33	2.520	0.846	—	0.597	0.524	—	1.30
OU.7	-0.104	6.431	13.96	33.27	2.785	0.815	—	0.597	0.528	—	1.31

Subscripts for θ parameters indicate different selective optima: C, ceratosaurs; M, maniraptoriforms; other, all tip species (OU.1) or tip species unassigned to other optima (other models); P, paravians; T, tyrannosauroids. Model abbreviations given in text.

TABLE 7.4. Ancestral state reconstruction of the ratios for scapula length to femur length (SF Ratio), humerus to femur length (HF Ratio), and forelimb (humerus + antebrachium) to femur length (FLF Ratio). Node names as given in Figure 1.

Clade	SF Ratio			HF Ratio			AF Ratio		
	M	L95%	U95%	M	L95%	U95%	M	L95%	U95%
Theropoda Root	0.565	0.297	0.846	0.559	0.346	0.766	0.953	0.577	1.36
Neotheropoda	0.608	0.327	0.873	0.554	0.336	0.785	0.899	0.491	1.32
Node 01	0.625	0.332	0.895	0.499	0.251	0.728	0.831	0.396	1.25
Averostra	0.643	0.399	0.889	0.484	0.227	0.729	0.780	0.340	1.23
Ceratosauria	0.633	0.352	0.946	0.468	0.263	0.664	0.688	0.245	1.13
Node 02	0.779	0.492	1.07	0.458	0.200	0.720	—	—	—
Abelisauroidea	0.876	0.579	1.16	0.448	0.184	0.711	0.738	0.500	0.964
Node 03	0.760	0.467	1.07	0.405	0.138	0.681	0.533	0.008	0.996
Noasauridae	0.633	0.338	0.919	0.388	0.198	0.587	—	—	—
Abelisauridae	0.763	0.480	1.08	0.372	0.007	0.640	0.485	0.001	0.935
Tetanurae	0.671	0.368	0.964	0.484	0.222	0.741	0.797	0.342	1.23
Megalosauroidea	0.707	0.413	0.991	0.490	0.232	0.755	0.809	0.377	1.26
Avetheropoda	0.649	0.364	0.957	0.474	0.270	0.679	0.830	0.385	1.28
Allosauroidea	0.735	0.434	1.03	0.485	0.224	0.754	0.837	0.385	1.28
Coelurosauria	—	—	—	0.482	0.208	0.740	0.849	0.389	1.30
Node 04	0.560	0.251	0.863	0.492	0.224	0.780	0.867	0.417	1.36
Tyrannosauroidea	0.523	0.218	0.819	0.505	0.295	0.739	0.903	0.428	1.37
Node 05	0.683	0.371	0.987	0.452	0.152	0.732	0.766	0.299	1.27
Node 06	0.628	0.330	0.942	0.378	0.009	0.687	0.602	0.137	1.12
Tyrannosauridae	0.652	0.358	0.974	0.348	0.003	0.627	0.535	0.003	1.04
Albertosaurinae	0.708	0.402	1.02	0.330	0.002	0.643	0.484	0.0	0.991
Node 07	0.630	0.316	0.930	0.331	0.002	0.636	0.512	0.001	1.03
Tyrannosaurinae	0.702	0.377	0.999	0.324	0.0	0.615	0.489	0.0	0.984
Node 08	0.710	0.414	0.710	0.297	0.0	0.628	0.442	0.0	0.939
Node 09	0.493	0.197	0.802	0.484	0.215	0.760	0.817	0.340	1.28
Maniraptoriformes	0.576	0.278	0.889	0.537	0.256	0.824	0.921	0.435	1.41

Clade	SF Ratio			HF Ratio			AF Ratio		
	M	L95%	U95%	M	L95%	U95%	M	L95%	U95%
Ornithomimosauria	0.633	0.331	0.931	0.568	0.288	0.868	0.965	0.469	1.45
Maniraptora	—	—	—	0.566	0.280	0.858	0.960	0.479	1.47
Node 10	0.663	0.358	0.982	0.553	0.268	0.861	0.968	0.449	1.46
Therizinosauria	0.781	0.492	1.01	0.590	0.284	0.875	1.01	0.504	1.48
Node 11	0.613	0.314	0.923	0.550	0.261	0.830	0.916	0.407	1.42
Alverzsauroidea	0.612	0.308	0.926	0.488	0.182	0.784	0.797	0.303	1.32
Node 12	0.626	0.321	0.964	0.560	0.263	0.878	1.01	0.496	1.50
Oviraptorosauria	0.627	0.306	0.928	0.570	0.259	0.872	1.04	0.512	1.53
Paraves	0.605	0.275	0.915	0.608	0.376	0.862	1.07	0.560	1.56
Troodontidae	0.569	0.265	0.885	0.595	0.287	0.920	1.06	0.538	1.57
Dromaeosauridae	0.628	0.307	0.936	0.584	0.346	0.832	1.15	0.647	1.68

Column heading abbreviations: L95%, lower 95% HPD value; M, mean; U95%, upper 95% HPD value.

FIGURE 7.1. Chronostratigraphically calibrated phylogeny of theropod taxa used in the present analyses, with branch lengths calculated as discussed in the text. Clades of interest used in Ancestral State Reconstructions are labeled and given numbers in the absence of standardized node names. Numbers in parentheses following selected taxa indicate the number of specimens included in the analysis; lack of a following number indicates taxon is represented by a single specimen.

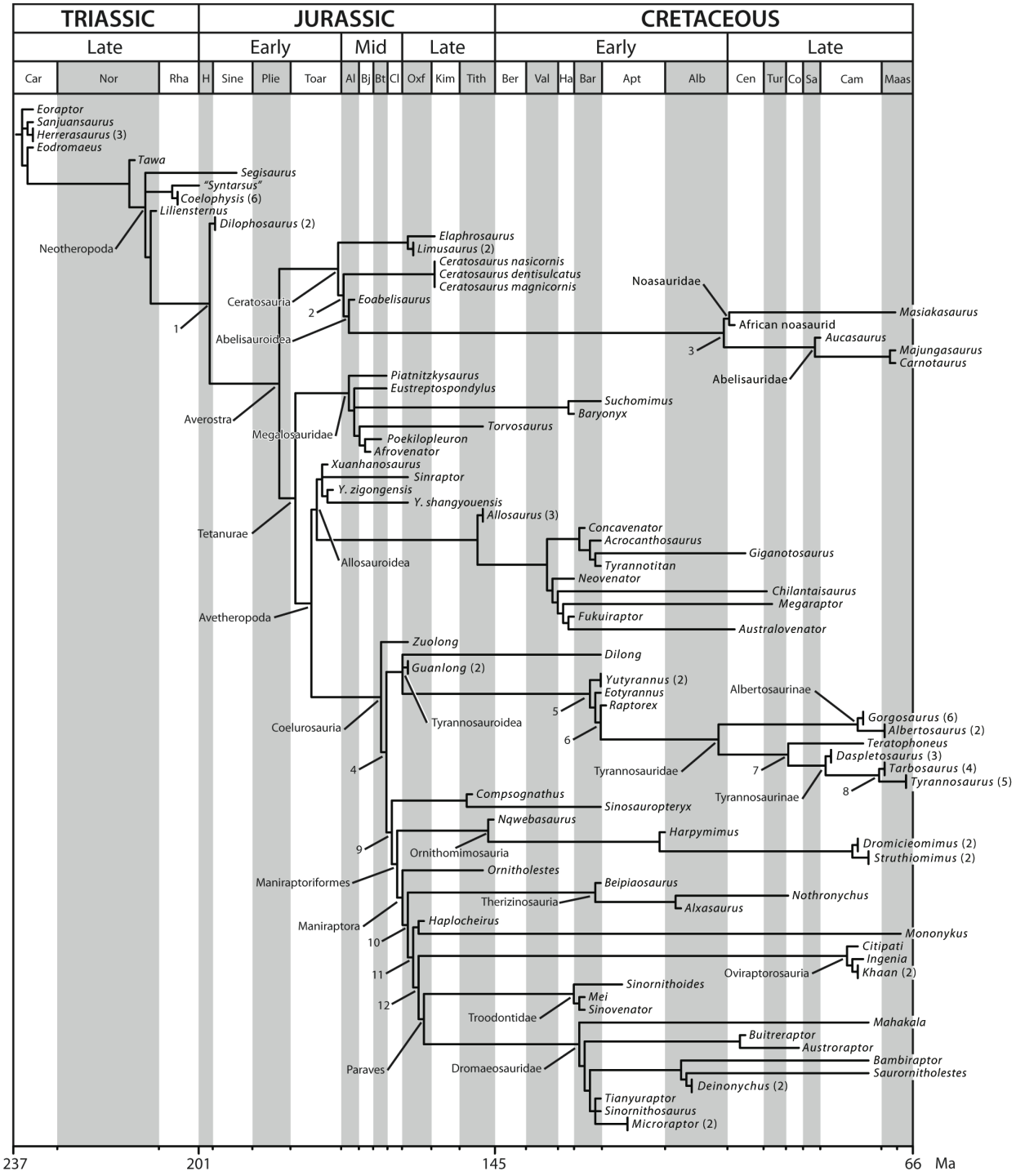
TRIASSIC
JURASSIC
CRETACEOUS
Late
Early
Mid
Late
Early
Late
Car
Nor
Rha
H
Sine
Plie
Toar
Al
Bj
Bt
Cl
Oxf
Kim
Tith
Ber
Val
Ha
Bar
Apt
Alb
Cen
Tur
Co
Sa
Cam
Maas
Eoraptor
Sanjuansaurus
Herrerasaurus (3)
Eodromaeus
Tawa
Segisaurus
"Syntarsus"
Coelophysis (6)
Liliensternus
Dilophosaurus (2)
Neotheropoda
Elaphrosaurus
Limusaurus (2)
Ceratosaurus nasicornis
Ceratosaurus dentisulcatus
Ceratosaurus magnicornis
Ceratosauria
Eoabelisaurus
Noasauridae
Masiakasaurus
African noasaurid
Aucasaurus
Majungasaurus
Carnotaurus
Abelisauridae
Abelisauroidea
Piatnitzkysaurus
Eustreptospondylus
Suchomimus
Baryonyx
Averostra
Megalosauridae
Torvosaurus
Poekilopleuron
Afrovenator
Xuanhanosaurus
Sinraptor
Y. zigongensis
Y. shangyouensis
Allosaurus (3)
Tetanurae
Concavenator
Acrocanthosaurus
Giganotosaurus
Tyrannotitan
Allosauroidea
Neovenator
Chilantaisaurus
Megaraptor
Fukuiraptor
Australovenator
Avetheropoda
Zuolong
Dilong
Guanlong (2)
Yutyrannus (2)
Eotyrannus
Raptorex
Albertosaurinae
Gorgosaurus (6)
Albertosaurus (2)
Teratophoneus
Daspletosaurus (3)
Tarbosaurus (4)
Tyrannosaurus (5)
Tyrannosauridae
Tyrannosaurinae
Coelurosauria
Tyrannosauroidea
Compsognathus
Sinosauropteryx
Nqwebasaurus
Harpymimus
Dromicieomimus (2)
Struthiomimus (2)
Ornithomimosauria
Ornitholestes
Maniraptoriformes
Beipiaosaurus
Therizinosauria
Nothronychus
Alxasaurus
Maniraptora
Haplocheirus
Mononykus
Citipati
Ingenia
Khaan (2)
Oviraptorosauria
Sinornithoides
Mei
Sinovenator
Troodontidae
Mahakala
Buitreraptor
Austroraptor
Bambiraptor
Saurornitholestes
Deinonychus (2)
Paraves
Dromaeosauridae
Tianyuraptor
Sinornithosaurus
Microraptor (2)
1
2
3
4
5
6
7
8
9
10
11
12
237
201
145
66
Ma

FIGURE 7.2. Alternative adaptive regime models pectoral girdle and forelimb proportion evolution in nonavian theropods. Diagrammed are models OU.3a (**A**), OU.3b (**B**), OU.3c (**C**), OU.4a (**D**), OU.4b (**E**), and OU.7 (**F**). Color codes indicate varying hypotheses of optima for different clades (see text): blue, reduction of the forelimb in various clades toward one optimum (A–C) or reduction of the forelimb in Ceratosauria toward a unique optimum (D–F); red, elongation of the forelimb in Maniraptoriformes (A, C, D) or elongation only within Paraves (B, E, F); orange, reduction of the forelimb in Tyrannosauroidea toward a unique optimum; pink, reduction of the forelimb in Megalosauroidea toward a unique optimum; purple; reduction of the forelimb in Allosauroidea toward a unique optimum; yellow, elongation of the forelimb in Maniraptoriformes other than Paraves; green, fixation of forelimb proportions at a "medium" length in all other taxa.

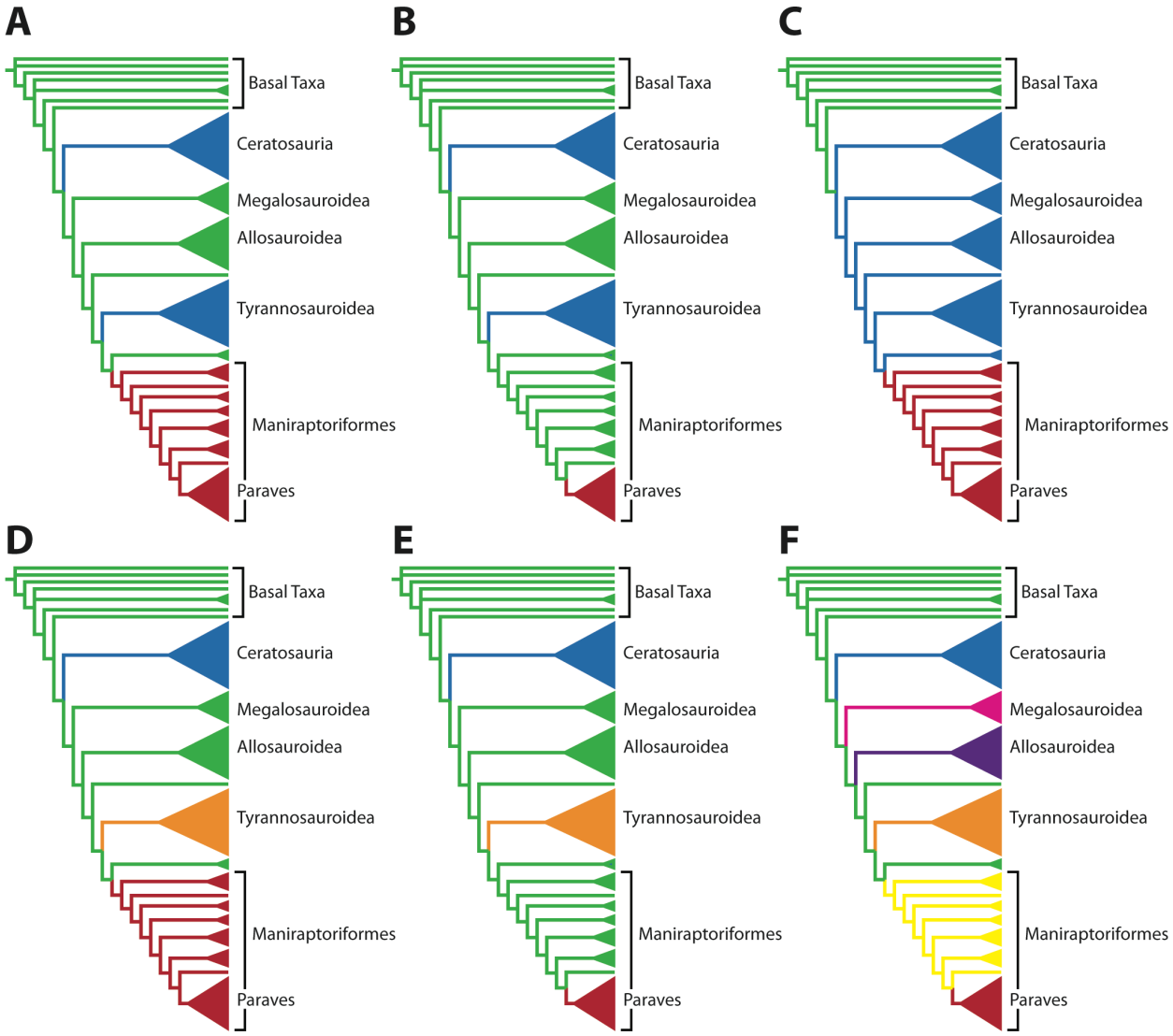
A
Basal Taxa
Ceratosauria
Megalosauroidea
Allosauroidea
Tyrannosauroidea
Maniraptoriformes
Paraves
B
Basal Taxa
Ceratosauria
Megalosauroidea
Allosauroidea
Tyrannosauroidea
Maniraptoriformes
Paraves
C
Basal Taxa
Ceratosauria
Megalosauroidea
Allosauroidea
Tyrannosauroidea
Maniraptoriformes
Paraves
D
Basal Taxa
Ceratosauria
Megalosauroidea
Allosauroidea
Tyrannosauroidea
Maniraptoriformes
Paraves
E
Basal Taxa
Ceratosauria
Megalosauroidea
Allosauroidea
Tyrannosauroidea
Maniraptoriformes
Paraves
F
Basal Taxa
Ceratosauria
Megalosauroidea
Allosauroidea
Tyrannosauroidea
Maniraptoriformes
Paraves

FIGURE 7.3. Standard Reduced-Major Axis linear regressions of log-transformed pectoral girdle and forelimb elements against femoral length: scapular length versus femoral length (**A**), humeral length versus femoral length (**B**), antebrachial length versus femoral length (**C**), and metacarpal II length versus femoral length (**D**). Taxa are color- and symbol-coded by clade, and regression lines for each subset are plotted. Graph A shows the strong relationship of scapula length to femur length regardless of partitioning of the data. The regression lines of graphs B and C show that the negative allometric relationship of humeral and antebrachial lengths found in the regression of the entire sample is driven mostly by the stronger negative allometry within the clade of Tyrannosauroidea; when these taxa are removed from the dataset, the regression line is not different from isometry. Furthermore, when only taxa with reduced limbs are considered, the allometric slope is also not different from isometry. Graph D shows the generally poor relationship of metcarpal length to femur length.

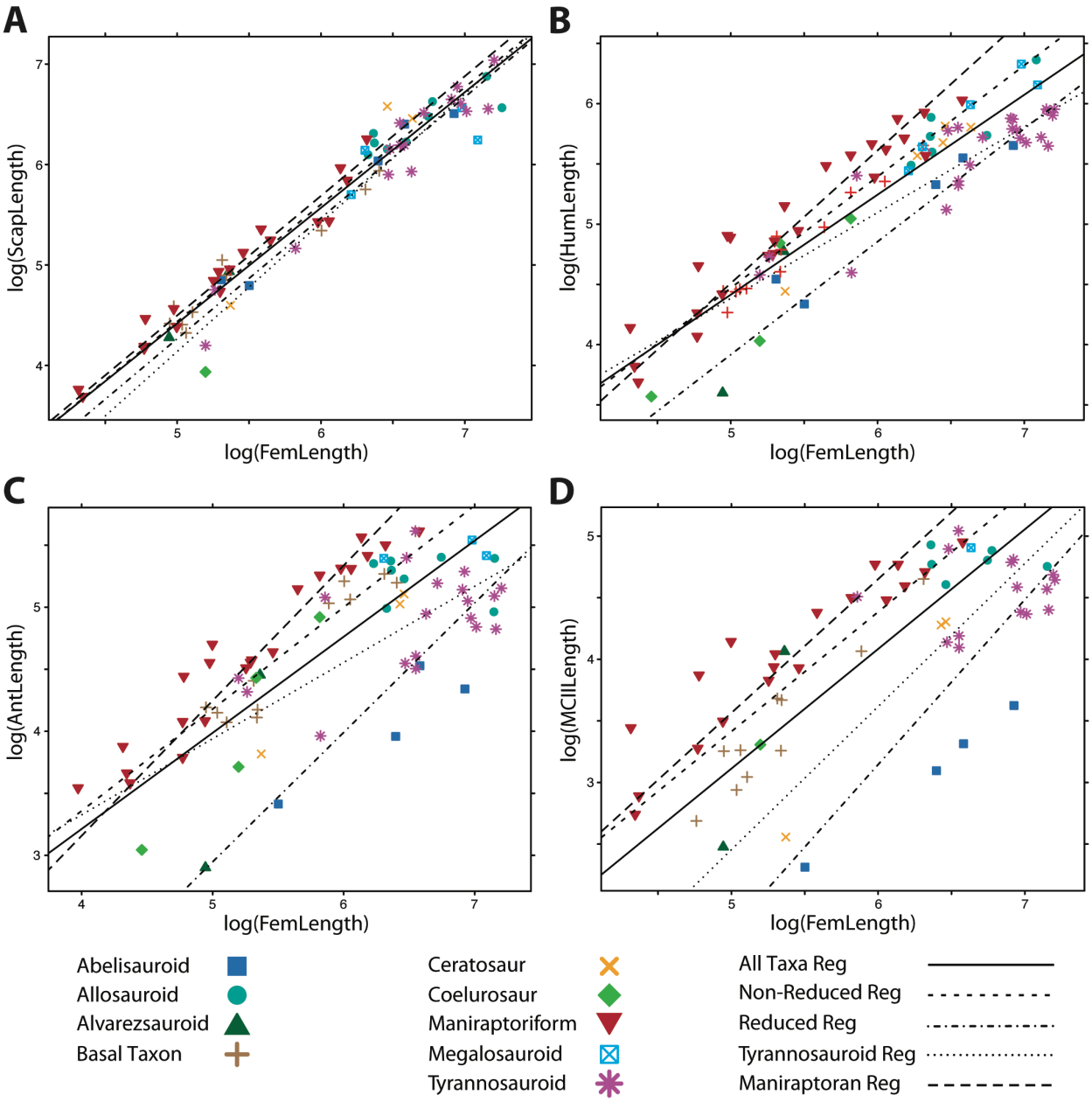
A
log(ScapLength)
log(FemLength)
B
log(HumLength)
log(FemLength)
C
log(AntLength)
log(FemLength)
D
log(MCIILength)
log(FemLength)
Abelisauroid
Allosauroid
Alvarezsauroid
Basal Taxon
Ceratosaur
Coelurosaur
Maniraptoriform
Megalosauroid
Tyrannosauroid
All Taxa Reg
Non-Reduced Reg
Reduced Reg
Tyrannosauroid Reg
Maniraptoran Reg

FIGURE 7.4. Standard Reduced-Major Axis linear regressions of log-transformed intramembral relationships: humeral length versus scapular length (**A**), antebrachial length versus humeral length (**B**), metacarpal II length versus humeral length (**C**), and metacarpal II length versus antebrachial length (**D**). Taxa are color- and symbol-coded by clade, and regression lines for each subset are plotted. The regression lines of graph A show the negative allometric relationship of humeral length to scapular length in all data subsets except Maniraptoriformes, which exhibit isometry. Graphs B and C show the isometric relationships of antebrachial and metacarpal length to humeral length most subsets, with the abelisaurid taxa (solid blue boxes) falling well below the rest of the sample. Graph D shows the generally strong relationship of metcarpal length to antebrachial length, with subsets exhibiting either isometry (non-reduced, tyrannosauroid, manirpatoriform) or positive allometry (all taxa, reduced).

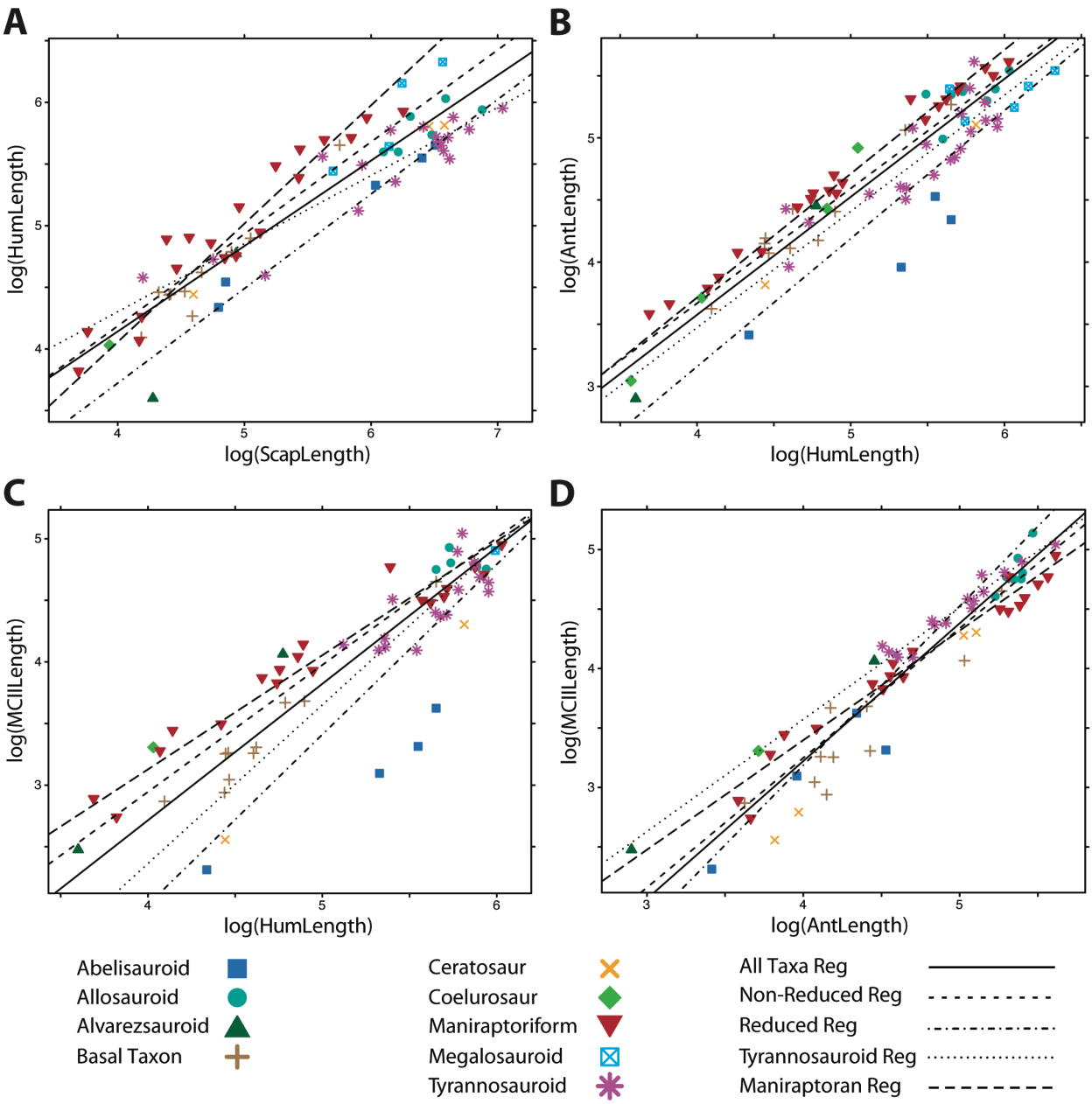
A
log(HumLength)
log(ScapLength)
B
log(AntLength)
log(HumLength)
C
log(MCIILength)
log(HumLength)
D
log(MCIILength)
log(AntLength)
Abelisauroid
Allosauroid
Alvarezsauroid
Basal Taxon
Ceratosaur
Coelurosaur
Maniraptoriform
Megalosauroid
Tyrannosauroid
All Taxa Reg
Non-Reduced Reg
Reduced Reg
Tyrannosauroid Reg
Maniraptoran Reg

FIGURE 7.5. Plots of ancestral state reconstructions for nodes of interest in theropod forelimb evolution for the scapula to femur ratio (**A**) and forelimb to femur ratio (**B**), plotted over the history of the clade. Clades are color coded as in Figure 1F (OU.7) to represent unique evolutionary trajectories. Estimated optima from the model-fitting analyses are indicated with an arrow: θ_S, optimum for scapular ratio based on OU.1; θ_R, optimum for reduced forelimb ratio based on OU.3b; θ_P, optimum for elongate forelimb ratio of Paraves based on OU.3b.

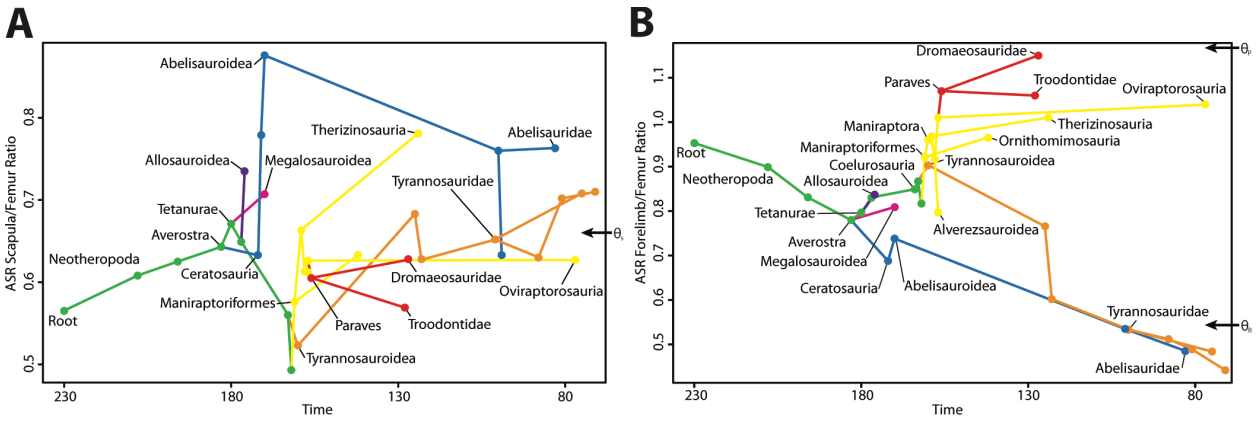
A
ASR Scapula/Femur Ratio
0.5
0.6
0.7
0.8
230
180
130
80
Time
Abelisauroidea
Therizinosauria
Abelisauridae
Allosauroidea
Megalosauroidea
Tyrannosauridae
Tetanurae
Averostra
Neotheropoda
Ceratosauria
Dromaeosauridae
Oviraptorosauria
Maniraptoriformes
Root
Paraves
Troodontidae
Tyrannosauroidea
θx
B
ASR Forelimb/Femur Ratio
0.5
0.6
0.7
0.8
0.9
1.0
1.1
230
180
130
80
Time
Dromaeosauridae
θp
Paraves
Troodontidae
Oviraptorosauria
Maniraptora
Therizinosauria
Maniraptoriformes
Ornithomimosauria
Coelurosauria
Tyrannosauroidea
Root
Neotheropoda
Allosauroidea
Tetanurae
Alverezsauroidea
Averostra
Megalosauroidea
Ceratosauria
Abelisauroidea
Tyrannosauridae
θx
Abelisauridae

APPENDIX

1. INSTITUTIONAL ABBREVIATIONS

AM, Albany Museum, Grahamstown, South Africa; **AMNH**, American Museum of Natural History, New York, NY, U.S.A.; **AODF**, Australian Age of Dinosaurs Fossil, Winton, Australia; **BMNH**, Natural History Museum, London, UK; **BYU**, Brigham Young University, Provo, UT, U.S.A.; **CAGS**, Chinese Academy of Geological Sciences, Beijing, China; **CMN**, Canadian Museum of Nature, Ottawa, ON, Canada; **CV**, Municipal Museum of Chongqing, Chongqing, China; **FMNH**, Field Museum, Chicago, IL, U.S.A.; **FPDM**, Fukui Prefectural Dinosaur Museum, Katsuyama, Japan; **GR**, Ghost Ranch Ruth Hall Museum of Paleontology, Abiquiu, NM, U.S.A.; **HMN**, Humboldt Museum für Naturkunde, Berlin, Germany; **IVPP**, Institute of Palaeontology and Palaeoanthropology, Beijing, China; **LH**, Long Hao Institute of Geology and Paleontology, Hohhot, China; **MACN**, Museo Argentino de Ciencias Naturales, Colección Chubut, Buenos Aires, Argentina; **MCCM**, Museo de las Ciencias de Castilla-La Mancha, Cuenca, Spain; **MCF**, Museo Municipal 'Carmen Fuñes', Plaza Huincul, Argentina; **MCZ**, Museum of Comparative Zoology, Cambridge, MA, U.S.A.; **MIWG**, Museum of Isle of Wight Geology, Sandown, UK; **MLP**, Museo La Plata, La Plata, Argentina; **MML**, Museo Municipal de Lamarque, Río Negro, Argentina; **MNHN**, Musée National d'Histoire Naturelle, Paris, France; **MNN**, Musée National du Niger, Niamy, Niger; **MOR**, Museum of the Rockies, Bozeman, MT, U.S.A.; **MPC**, Paleontological Center of the Mongolian Academy of Sciences, Ulaanbaatar, Mongolia; **MPCA**, Museo Carlos Ameghino, Cipolletti, Río Negro Province, Argentina; **MPEF**, Museo Paleontológico Egidio Feruglio, Trélew, Argentina **MUCPv**, Museo de Geología y Paleontología, Universidad Nacional del Comahue, Neuquén, Argentina; **MWC**, Museum of Western Colorodo, Fruita, CO, U.S.A.; **NCSM**, North Carolina Museum of Natural Sciences, Raleigh, NC, U.S.A.; **NGIP**, Nanjing Institute of Geology and Palaeontology, Nanjing, China; **OUM**, Oxford University Museum, Oxford, UK; **PIN**, Paleontological Institute, Russian Academy of Sciences, Moscow, Russia; **PVL**, Fundación Miguel Lillo, Universidad Nacional de Tucumán, San Miguel de Tucumán, Argentina; **PVSJ**, Museo de Ciencias Naturales, San Juan, Argentina; **QG**, National Museum of Natural History, Bulawayo, South Africa; **TMP**, Royal

Tyrrell Museum of Paleontology, Drumheller, AB, Canada; **ROM**, Royal Ontario Museum, Toronto, ON, Canada; **STM**, Shandong Tianyu Museum of Nature, Shandong, China; **UC**, University of Chicago, Chicago, IL, U.S.A.; **UCMP**, University of California Museum of Paleontology, Berkeley, CA, U.S.A.; **UMNH**, Utah Museum of Natural History, Salt Lake City, UT, U.S.A.; **USNM**, National Museum of Natural History, Smithsonian Institution, Washington, DC, U.S.A.; **ZCDM**, Zhucheng Dinosaur Museum, Shandong, China; **ZDM**, Zigong Dinosaur Museum, Zigong, China; **ZPAL**, Institute of Palaeobiology of the Polish Academy of Sciences, Warsaw, Poland.

2. TABLES

TABLE 7.S1. Raw data used in the analyses with specimen number and source of measurements given. Asterisks indicate estimated values based on other specimens of the same taxon. Dagger indicates ulnar length was used. Abbreviations: AL, antebrachial length; FL, femoral length; HL, humeral length; ML, metacarpal II length, PM, personal measurement; SL, scapular length.

Taxon	Specimen	Source	FL	SL	HL	AL	ML
Acrocanthosaurus atokensis	NCSM 14345	Currie & Carpenter, 2000	1277	970	380	220	116
African noasaurid	UC uncat.	PM	245	121	76.5	30.4	10.1
Afrovenator abakensis	UC OBA 1	Sereno et al., 1994	760	?	400	?	135
Albertosaurus sarcophagus	ROM 807	Parks, 1928	1066	740	303	136	80
Albertosaurus sarcophagus	TMP 86.64.01	PM; Carrano, 1998	?	?	213	99.1	61.6
Allosaurus fragilis	USNM 4734	Gilmore, 1920	850	652	310	222	122
Allosaurus sp.	BYU 671/8901	PM	?	727	416	256	?
Allosaurus sp.	DINO 11541	PM	640	470	?	186.4	100
Alxasaurus elesitaensis	IVPP V88402	Dececchi & Larsson, 2013	555	520	375	245	111
Aucasaurus garridoi	MCF-PVPH-236	PM	722	603	257	92.6	27.5
Australovenator wintonensis	AODF 604	White et al., 2012	578	?	307.4	215.4	138
Austroraptor cabazai	MML 195	Novas et al., 2009	560	?	262	?	?
Bambiraptor feinbergorum	AMNH 30556	Burnham et al., 2000	119	87	105	85	48
Baryonyx walkeri	BMNH 9951	PM	1200	515	471	225	?
Beipiaosaurus inexpectus	IVPP V11559	PM	266	212.1	?	?	79.8
Buitreraptor gonzalezorum	MPCA 245	Makovicky et al., 2005	145	96	135	95	?
Carnotaurus sastrei	MACN-CH 894	PM	1018	670	285	76.8	37.5
Ceratosaurus dentisulcatus	UMNH VP 5278	PM	762	638	332	?	?
Ceratosaurus magnicornis	MWC 1	Madsen & Welles, 2000	630	?	292	?	?
Ceratosaurus nasicornis	USNM 4735	PM	620	?	?	152.3	72.1
Chilantaisaurus tashuikouensis	IVPP V2884	Hu, 1964	1190	?	580	?	?
Citipati osmolksae	MPC 100/1004	PM	395	228	219	203.0	118.0
Coelophysis bauri	AMNH 7224	Colbert, 1989	203	156	134	82	39.7
Coelophysis bauri	AMNH 7223	Colbert, 1989	209	134	120	65	39.2
Coelophysis bauri	AMNH 7227	PM	165.1	92.8	87	58.7	21
Coelophysis bauri	TMP 84.63.32	PM	?	65.8	60.0	37.5	17.6
Coelophysis bauri	TMP 84.63.33	PM	157.9	75.5	86.5	?	26.1
Coelophysis bauri	TMP 84.63.50	PM	116.9	?	?	?	14.7
Compsognathus longipes	MNHN CNJ 79	Peyer, 2006	180.8	51.2	56.3	41.0	27.3
Concavenator corcovatus	MCCM-LH 6666	Ortega et al., 2010	560	445	270	147	?
Daspletosaurus torosus	CMN 8506	Russell, 1970	1000	772	357	171	120
Daspletosaurus torosus	TMP 2001.36.1	PM	1015	?	355	197.8	123
Daspletosaurus torosus	FMNH PR 5336	Carrano, 1998	1010	?	327	?	?
Deinonychus antirrhopus	AMNH 3015	Ostrom, 1969	284	190	241	172	?
Deinonychus antirrhopus	MCZ 4371	Ostrom, 1976	336	?	263	192	90
Dilong paradoxus	IVPP V14243	PM	180.8	66.6	97.3	83.8	?
Dilophosaurus wetherilli	UCMP 37302	PM	550	315	285	194.1	105
Dilophosaurus wetherilli	UCMP 77270	PM	605	379	?	180.8	?
Dromiceiomimus brevitertius	AMNH 5201	PM	388	?	289	?	?

Taxon	Specimen	Source	FL	SL	HL	AL	ML
Dromiceiomimus samueli	TMP 95.110.1	PM	427	230	276	202.6	88.3
Elaphrosaurus bambergi	HMN dd	Janensch, 1925; PM	529	?	262	?	?
Eoabelisaurus mefi	MPEF PV 3990	Pol & Rauhut, 2012	640	720	335	165	74
Eodromaeus murphi	PVSJ 562	PM	141	82.9	85.2	66.2	25.9
Eoraptor lunensis	PVSJ 512	PM	153.7	82	84.7	63.4	18.9
Eotyrannus lengi	MIWG 1997.550	PM	?	275	260	?	?
Eustreptospondylus oxoniensis	OUM J13558	Sadlier et al., 2008	498	299	231	?	?
Fukuiraptor kitadaniensis	FPDM 97122	Azuma & Currie, 2000	507	?	242	211†	?
Giganotosaurus carolinii	MUCPv-Ch1	PM	1420	710	?	?	?
Gorgosaurus libratus	TMP 91.163.1	PM; Carrano, 1998	720	490	?	?	?
Gorgosaurus libratus	TMP 91.36.500	PM; Carrano, 1998	645	365	167.4	94.4	62.7
Gorgosaurus libratus	CMN 2120	Lambe, 1917	1040	876	324	156	98
Gorgosaurus libratus	TCM 2001.89.1	Larson, 2008	825	675	305	180†	?
Gorgosaurus libratus	AMNH 5664	Matthew & Brown, 1923	700	?	205	100	60
Guanlong wucaii	IVPP V14531	PM	350	?	222	160.5	?
Guanlong wucaii	IVPP V14532	PM	193	116	113	75†	?
Haplocheirus sollers	IVPP V15988	PM	213	139.1	118.4	86.0	58.2
Harpymimus okladnikovi	MPC 100/29	PM	?	279	298	218	92.8
Herrerasaurus ischigualastensis	PVSJ 373	PM	360	?	?	153.1	58.3
Herrerasaurus ischigualastensis	MACN 18.060	Reig, 1963	280.6	?	144.7	?	?
Herrerasaurus ischigualastensis	MLP 61-VIII-2-3	Reig, 1963	336.0	?	192.9	?	?
Ingenia yanshini	MPC 100/30	PM	235	168.1	140.6	103.5	50.9
Khaan mckennai	MPC 100/1002	PM	198.1	139	116.2	95.2	51.3
Khaan mckennai	MPC 100/1127	PM	191.3	127.1	114.4	91	46.0
Liliensternus liliensterni	HMN MB.R. 2175	PM	424	?	211.5	158.0	?
Limusaurus inextricabilis	IVPP V15923	PM	215	99.3	85.0	45.5	12.9
Limusaurus inextricabilis	IVPP V15924	PM	?	?	?	53.0	16.3
Mahakala omnogovae	MPC 100/1033	Turner et al., 2007	79	?	40	36	18
Majungasaurus crenatissimus	FMNH PR 2836	PM	600*	418	206	52.4	22.1
Masiakasaurus knopfleri	FMNH PR 2621, 2676, 2481	PM	202	128	94	?	?
Megaraptor namunhuaiguii	MUCPv 341	PM	?	395	?	237	171
Mei long	IVPP V12733	PM	77.0	40.1	45.6	39	15.5
Microraptor zhaoianus	CAGS 20-8-001	Hwang et al., 2002	74.77	43.01	62.88	48.3	31.3
Microraptor zhaoianus	IVPP V12330	PM	53.1	?	?	34.6	?
Mononykus olecranus	MPC 107/6	PM	140.4	72.1	36.6	18.2	11.9
Neovenator salerii	MIWG 6348	Brusatte et al., 2008	730	505	?	?	?
Nothronychus graffami	UMNH VP 16420	PM	718	?	415	274	141
Nqwebasaurus thwazi	AM 6040	Choiniere et al., 2012	118	64.7	58.5	44.2	26.5
Ornitholestes hermanni	AMNH 619	Osborn, 1903, Carpenter, et al. 2005	207	?	127	84	?
Piatnitzkysaurus floresi	PVL 4073	Bonaparte, 1986	548.0	465	282	220†	?
Poekilopleuron bucklandii	MNHN 1897-2	PM	?	?	312	170	?
Raptorex kriegsteini	LH PV18	PM	338	175	99.2	52.6	?
Sanjuansaurus gordilloi	PVSJ 605	PM	405	209	?	183†	?
Saurornitholestes langstoni	TMP 88.121.39	PM	214	142.5	172.8	?	?
Segisaurus halli	UCMP 32101	PM	145	98.4	71.3	?	?
Sinornithoides youngi	IVPP V9612	PM	140	?	83.1	59.4	33

Taxon	Specimen	Source	FL	SL	HL	AL	ML
Sinornithosaurus millenii	IVPP V12811	PM	148	80.3	133	110†	63
Sinosauropteryx prima	NGIP 127587	Chen et al., 1998	86.4	?	35.5	21	?
Sinovenator changii	IVPP V12615	Makovicky et al., 2005	118	66	71	59†	?
Sinraptor dongi	IVPP 10600	Currie & Zhao, 1993	876	755	?	?	132
Struthiomimus altus	TMP 85.08.03	PM	484	345	303	225	99
Struthiomimus sp.	TMP 90.26.1	PM	462	390	356	261	117.9
Suchomimus tenerensis	MNN GDF500	Sereno et al., 1998	1075	710	560	255	?
Syntarsus rhodesiensis	QG 1	Raath, 1969	208	?	100	61	26
Tarbosaurus bataar	MPC 107/2	PM	1290	702	284	124.4	81.5
Tarbosaurus bataar	PIN 552-1	Maleev, 1974	?	750	255	110	60
Tarbosaurus bataar	ZPAL MgD-I/3	PM	700	489	212	90.5	66
Tawa hallae	GR 242	PM	?	106	101.6	83.7	27.3
Teratophoneus curriei	BYU 8120/13719	PM	757	376	242.5	140.7†	?
Tianyuraptor ostromi	STM1-3	Zheng et al., 2010	200	114	129	97	57
Torvosaurus tanneri	BYU 725/2002	PM	?	?	430	189.4	?
Tyrannosaurus rex	MOR 555	PM	1275	?	385	162.4	96.5
Tyrannosaurus rex	MOR 980	PM	1330	?	366	?	109
Tyrannosaurus rex	MOR 002	PM	?	715	272	?	?
Tyrannosaurus rex	FMNH PR 2081	PM; Brochu, 2003	1345	1140	385	173	104
Tyrannosaurus rex	TMP 81.6.1	PM	1230	?	305	?	?
Tyrannotitan chubutensis	MPEF-PV 1156	PM	1270	?	?	143†	?
Xuanhanosaurus quilixiaensis	IVPP V6729	PM	?	?	285	210	115.6
Yangchuanosaurus shangyouensis	CV 00214	Dong et al., 1984	585	500	270	?	?
Yangchuanosaurus zigongensis	ZDM 9011	Gao, 1993	396	550	360	200	118
Yutyrannus huali	ZCDM 5001	PM	652	471	322	221	134
Yutyrannus huali	ZCDM 5000	PM	698	610	331	274	155
Zuolong salleei	IVPP V15912	Choiniere et al., 2010	336	?	155.4	137.0	?

3. SUPPLEMENTARY REFERENCES

Azuma, Y., and P. J. Currie. 2000. A new carnosaur (Dinosauria: Theropoda) from the Lower Cretaceous of Japan. Canadian Journal of Earth Sciences 37:1735–1753.

Bonaparte, J. F. 1986. Les dinosaures (Carnosaures, Allosauridés, Sauropodes, Cétosauridés) du Jurassique Moyen de Cerro Cóndor (Chubut, Argentina). Annales de Paléontologie (Vert.-Invert.) 72:247–289.

Brochu, C. A. 2003. Osteology of *Tyrannosaurus rex*: insights from a nearly complete skeleton and high-resolution computed tomographic analysis of the skull. Journal of Vertebrate Paleontology 22:1–138.

Brusatte, S. L., R. B. J. Benson, and S. Hutt. 2008. The osteology of *Neovenator salerii* (Dinosauria: Theropoda) from the Wealden Group (Barremian) of the Isle of Wight. Palaeontographical Society Monographs 162:1–75.

Burnham, D. A., K. L. Derstler, P. J. Currie, R. T. Bakker, Z. Zhou, and J. H. Ostrom. 2000. Remarkable new birdlike dinosaur (Theropoda: Maniraptora) from the Upper Cretaceous of Montana. University of Kansas Paleontological Contributions New Series 13:1–14.

Carpenter, K., C. Miles, and K. Cloward. 2005. New small theropod from the Upper Jurassic Morrison Formation of Wyoming; pp. 23–48 in K. Carpenter (ed.), The Carnivorous Dinosaurs. Indiana University Press, Bloomington, IN.

Carrano, M. T. 1998. The evolution of dinosaur locomotion: functional morphology, biomechanics and modern analogs. Doctoral thesis/dissertation, Chicago, IL.

Chen, P.-j., Z.-m. Dong, and S.-n. Zhen. 1998. An exceptionally well-preserved theropod dinosaur from the Yixian Formation of China. Nature 391:147–152.

Choiniere, J. N., C. A. Forster, and W. J. de Klerk. 2012. New information of *Nqwebasaurus thwazi*, a coelurosaurian theropod from the Early Cretaceous Kirkwood Formation in South Africa. Journal of African Earth Sciences 71–72:1–17.

Choiniere, J. N., J. M. Clark, C. A. Forster, and X. Xu. 2010. A basal coelurosaur (Dinosauria: Theropoda) from the Late Jurassic (Oxfordian) of the Shishugou Formation in Wucaiwan, People's Republic of China. Journal of Vertebrate Paleontology 30:1773–1796.

Colbert, E. H. 1989. The Triassic dinosaur *Coelophysis*. Bulletin of the Museum of Northern Arizona 57:1–160.

Currie, P. J., and X. Zhao. 1993. A new carnosaur (Dinosauria, Theropoda) from the Jurassic of Xinjiang, People's Republic of China. Canadian Journal of Earth Sciences 30:2037–2081.

Currie, P. J., and K. Carpenter. 2000. A new specimen of *Acrocanthosaurus atokensis* (Theropoda, Dinosauria) from the Lower Cretaceous Antlers Formation (Lower Cretaceous, Aptian) of Oklahoma, USA. Geodiversitas 22:207–246.

Dececchi, T. A., and H. C. E. Larsson. 2013. Body and limb size dissociation at the origin of birds: uncoupling allometric constraints across a macroevolutionary transition. Evolution doi:10.1111/evo.12150.

Dong, Z.-m. 1984. A new theropod dinosaur from the Middle Jurassic of Sichuan Basin. Vertebrata PalAsiatica 22:213–218.

Gao, Y. 1993. A new species of *Szechuanosaurus* from the Middle Jurassic of Dashanpu, Zigong, Sichuan. Vertebrata PalAsiatica 31:308–314.

Gilmore, C. W. 1920. Osteology of the carnivorous Dinosauria in the United States National Museum, with special reference to the genera *Antrodemus* (*Allosaurus*) and *Ceratosaurus*. Bulletin of the United States National Museum 110:1–159.

Hwang, S. H., M. A. Norell, Q. Ji, and K. Gao. 2002. New specimens of *Microraptor zhaoianus* (Theropoda: Dromaeosauridae) from northeastern China. American Museum Novitates: 1–44.

Janensch, W. 1925. Die Coelurosaurier und Theropoden der Tendaguru-Schichten Deutsch-Ostafrikas. Palaeontographica Supplement VIII:1–100.

Lambe, L. M. 1917. The Cretaceous theropodous dinosaur *Gorgosaurus*. Memoirs of the Geological Survey of Canada 100:1–84.

Larson, N. L. 2008. One hundred years of *Tyrannosaurus rex*: the skeletons; pp. 1–56 in P. Larson and K. Carpenter (eds.), *Tyrannosaurus rex*: The Tyrant King. Indiana University Press, Bloomington, IN.

Madsen, J. H., and S. P. Welles. 2000. *Ceratosaurus* (Dinosauria, Theropoda): a revised osteology. Utah Geological Survey Miscellaneous Publications 2:1–80.

Makovicky, P. J., S. Apesteguía, and F. L. Agnolin. 2005. The earliest dromaeosaurid theropod from South America. Nature 437:1007–1011.

Maleev, E. A. 1974. Mesozoic and Cenozoic faunas and biostratigraphy. Transactions of the Joint Soviet-Mongolian Palaeontogical Expedition 1:132–191.

Matthew, W. D., and B. Brown. 1923. Preliminary notices of skeletons and skulls of Deinodontidae from the Cretaceous of Alberta. American Museum Novitates 89:1–10.

Novas, F. E., D. Pol, J. I. Canale, J. D. Porfiri, and J. O. Calvo. 2009. A bizarre Cretaceous theropod dinosaur from Patagonia and the evolution of Gondwanan dromaeosaurids. Proceedings of the Royal Society of London Series B 276:1101–1107.

Ortega, F., F. Escaso, and J. L. Sanz. 2010. A bizarre, humped Carcharodontosauria (Theropoda) from the Lower Cretaceous of Spain. Nature 467:203–206.

Osborn, H. F. 1903. *Ornitholestes hermanni*, a new compsognathoid dinosaur from the Upper Jurassic. Bulletin of the American Museum of Natural History 19:459–464.

Ostrom, J. H. 1969. Osteology of *Deinonychus antirrhopus*, an unusual theropod from the Lower Cretaceous of Montana. Bulletin of the Peabody Museum of Natural History 30:1–165.

Ostrom, J. H. 1976. On a new specimen of the Lower Cretaceous theropod dinosaur *Deinonychus antirrhopus*. Breviora 439:1–21.

Parks, W. A. 1928. *Albertosaurus arctunguis*, a new species of theropodous dinosaur from the Edmonton Formation of Alberta. University of Toronto Studies 26:1–19.

Peyer, K. 2006. A reconsideration of *Compsognathus* from the Upper Tithonian of Canjuers, southeastern France. Journal of Vertebrate Paleontology 26:879–896.

Pol, D., and O. W. M. Rauhut. 2012. A Middle Jurassic abelisaurid from Patagonia and the early diversification of theropod dinosaurs. Proceedings of the Royal Society B 279:3170–3175.

Raath, M. A. 1969. A new coelurosaurian dinosaur from the Forest Sandstone of Rhodesia. Arnoldia Series of Miscellaneous Publicatons 4:1–25.

Reig, O. A. 1963. La presencia de dinosaurios saurisquios en los "Estratos de Ischigualasto" (Mesotriásico superior) de las provincias de San Juan y La Rioja (República Argentina). Ameghiniana 3:3–20.

Russell, D. A. 1970. Tyrannosaurs from the Late Cretaceous of Western Canada. National Museum of Natural Sciences Publications in Paleontology 1:1–32.

Sadlier, R. W., P. M. Barrett, and H. P. Powell. 2008. The anatomy and systematics of *Eustreptospondylus oxoniensis*, a theropod dinosaur from the Middle Jurassic of Oxfordshire, England. Monograph of the Palaeontographical Society, London 106:1–82.

Sereno, P. C., C. A. Forster, H. C. E. Larsson, D. B. Dutheil, and H.-D. Sues. 1994. Early Cretaceous dinosaurs from the Sahara. Science 266:267–271.

Sereno, P. C., A. L. Beck, D. B. Dutheil, B. Gado, H. C. E. Larsson, G. H. Lyon, J. D. Marcot, O. W. M. Rauhut, R. W. Sadlier, C. A. Sidor, D. J. Varricchio, G. P. Wilson, and J. A. Wilson.

1998. A long-snouted predatory dinosaur from Africa and the evolution of spinosaurids. Science 282:1298–1302.

Turner, A. H., D. Pol, J. A. Clarke, G. M. Erickson, and M. A. Norell. 2007. A basal dromaeosaurid and size evolution preceding avian flight. Science 317:1378–1380.

White, M. A., A. G. Cook, S. A. Hocknull, T. Sloan, G. H. K. Sinapius, and D. A. Elliot. 2012. New forearm elements discovered of holotype specimen *Australovenator wintonensis* from Winton, Queensland, Australia. PLoS ONE 7:e39364.

Zheng, X.-T., X. Xu, H.-L. You, Q. Zhao, and Z.-m. Dong. 2009. A short-armed dromaeosaurid from the Jehol Group of China with implications for early dromaeosaurid evolution. Proceedings of the Royal Society B 277:211–217.

Chapter VIII: Conclusions

The primary objective of this dissertation was to provide new insights into the evolution and function of reduced forelimbs in nonavian theropod dinosaurs through analysis of osteology, myology, and scaling trends. To meet this goal, studies were undertaken to establish the plesiomorphic conformation of the osteology and myology in an early theropod, to assess major changes in the forelimbs of abelisaurs and tyrannosaurs, and to reveal the overarching allometric and evolutionary trends within the clade as a whole. Taken together, these analyses have made substantial progress in answering the question, "What, if anything, did reduced-limbed theropods do with their tiny arms?"

The first step in any study of the evolution of a specialized morphology is to gain a thorough understanding of the plesiomorphic form. Complete forelimbs are known for many early theropod taxa, but this dissertation provides the first detailed documentation and description of the forelimb and pectoral girdle of a species that is unambiguously a member of Theropoda, *Tawa hallae*. Comparisons with the forelimbs of other early theropods allowed me to evaluate the distribution of commonly used phylogenetic characters and assess their bearing on the positions of the controversial saurischians *Herrerasaurus* and *Eoraptor* (e.g., Martinez et al., 2011). Results of this study solidify *Tawa*'s position as a transitional taxon among early theropods by revealing its mosaic morphology of derived and plesiomorphic features. In particular, *Tawa* links *Herrerasaurus* with early theropods through characters such as an elongate scapular blade, the shape of the humeral articular surfaces, and the presence of a specialized lateralmost distal carpal that is currently restricted to only three early theropod taxa. Despite this valuable new information, the early evolution of the saurischian carpus remains mysterious due to the relatively distinct morphology of the carpus in each taxon; future discoveries will help to clarify the sequence of carpal fusion and loss toward the relatively reduced carpus of neotheropods. Evaluation of the joint surface morphology of the forelimb of *Tawa* presented here helps to establish the types of movements that early theropods would have been capable of, providing a starting point for assessment of the limitations imposed by subsequent modification of the forelimb in more derived neotheropods.

The bizarre morphology of the forelimb of abelisaurids was previously recognized but not clearly documented. This study provides a detailed description of the first known elements of

the *Majungasaurus* forelimb distal to the humerus and further description of the complete pectoral girdle and forelimb, together with a comparative analysis of forelimb evolution in Ceratosauria. The extremely shortened antebrachium and manus of abelisaurids exhibit a highly specialized morphology unlike that of any other tetrapod, raising many questions as to the driving factors behind such a unique form. Furthermore, despite the overall extremely reduced morphology of the limb, the morphology of the articular surfaces indicates that each joint likely allowed an extensive range of motion, one extreme of which is preserved in the forelimb of *Aucasaurus*. Unfortunately, a large morphological gap exists between derived abelisaurids and the most basal members of Ceratosauria, providing little clue as to the intervening stages in the evolution of the forelimb. Further materials of basal abelisaurid and noasaurid forelimbs will no doubt allow more detailed analysis of forelimb evolution in Ceratosauria.

This dissertation establishes the plesiomorphic conformation of the forelimb musculature in a theropod, providing the basis for many future functional studies. Furthermore, the reconstruction of the antebrachial and manual musculature of *Tawa* represents the first analysis of these muscles in any dinosaur. The inclusion of a phylogenetically broad sample of extant taxa and an ancestral state reconstruction in this analysis allowed for the unequivocal reconstruction of many distal forelimb muscles that have been previously deemed too uncertain to reconstruct. Although these muscles have been dismissed as secondary in investigations of locomotor function (e.g., Maidment and Barrett, 2011), they have great importance when considering function of the forelimbs in bipedal theropods, including hypotheses of grasping and predatory behavior. Additionally, some antebrachial muscles have an important role in the automating musculoskeletal mechanism of avian flight (Vazquez, 1994), and an analysis of the changes in their distal attachments may elucidate when this mechanism evolved in the avian lineage. Not only did this research provide the necessary starting point for the subsequent studies of other theropod taxa in this dissertation, it will also serve as the basis for future investigations of forelimb function across the entire clade, from the robust forelimbs of allosauroids to the evolution of flight. As studies of functional morphology in extinct animals move toward advanced analytical techniques such as three-dimensional computer modeling of muscle moment arms and simulation of biomechanically relevant scenarios (e.g., Hutchinson et al., 2005b), a

complete muscular reconstruction is essential for continued advancement in the study of theropod forelimb function.

Reconstructing the musculature of the forelimb in *Majungasaurus* allowed me to identify some of the hallmarks of forelimb reduction and loss within this taxon. The low deltopectoral crest provides smaller attachment areas for several brachial muscles, and unossified carpals and a highly reduced manus likely limited the intrinsic manual musculature to a single layer. Despite the extreme reduction in length of the distal elements, sizeable muscle scars on the radius and ulna indicate that well developed antebrachial muscles were present in these taxa, and tubercles on the phalanges suggest that digital flexion was a possible action for at least some digits of the manus. Abelisaurids also exhibit an odd form of manual reduction that involves substantial foreshortening of all digits, which is not typical of most extant tetrapods. The shoulder musculature appears to have been substantial, but modified for pulling the arm through a large excursion instead of muscles optimized for strong actions. Taken together, the osteology and reconstructed musculature suggest that the forelimbs of abelisaurids were not truly vestigial, but instead maintained a myology that was adapted for large excursion of the forelimb. The unusual morphology of the abelisaurid forelimb makes straightforward functional hypotheses difficult, but this reconstruction provides the first step in future analyses of the functional capabilities of such a limb. Although it is hard to imagine abelisaurids using their forelimbs to interact with their environment due to their extremely short length, possible uses for these limbs may have included intraspecific displays and a role in mating to stimulate the female, as in the pelvic spurs of some snakes. The effects of limb reduction and the changing osteology on the myology of the limb is not well understood, but the musculature of *Majungasaurus* provides an example of the results of extreme reduction and will be an important comparative model for future analyses of the musculature of reduced limbs in other extant and extinct species.

In comparison, the forelimb musculature of tyrannosaurids is relatively straightforward, with no distinct forelimb morphology characterizing the entire clade. Although abelisaurids and tyrannosaurids are often lumped together as reduced-forelimbed taxa, their forelimb morphology is highly distinct, and this is reflected in the musculature as well. Whereas the muscles crossing the glenohumeral joint in abelisaurids are well-suited for pulling the forelimb through a large

excursion, those of tyrannosaurids display features that appear to have provided substantial torque for certain actions. The majority of these changes were rapidly acquired at the node Tyrannosauridae or just before it, and appear to be correlated with dramatic reduction of the forelimb relative to body size. They are not necessarily correlated with an increase in body size itself, however, as many of these characters are present in the small-bodied *Raptorex kreigsteini*, reinforcing the idea that the tyrannosaurid body plan was present at small body sizes (Sereno et al., 2009). Instead, the development of these characters is likely related to functional shifts in the forelimb concurrent with reduction in overall proportions of the limb. This analysis allows the first tests of several established hypotheses of forelimb function in tyrannosaurids, indicating that although the muscle groups required for supporting the body when rising from the ground show evidence of reduction, the development of other groups is consistent with the functional demands of close-quarters grappling with struggling prey and potential mates. Additionally, the forelimb musculature and arthrology also supports the potential use of the forelimbs in intraspecific display, a common use of reduced forelimbs in modern birds. Nevertheless, more rigorous tests of these hypotheses using biologically realistic forces and three-dimensional models are necessary before more definitive statements can be made on the forelimb function of *Tyrannosaurus*.

Finally, the research presented here shows that there is no evidence of negative allometric scaling of the forelimb elements across the entire clade when phylogeny is taken into account, despite long-standing hypotheses that variations in forelimb length of nonavian theropods, whether reduction in Tyrannosauridae or elongation in Paraves, are directly dependent on overall body size (Vargas, 1999; Bybee et al., 2006; Dececchi and Larsson, 2013). Furthermore, although a negative allometric trend may be present within the clade Tyrannosauroidea, models of forelimb size evolution show that it is not a passive process, but instead undergoing active selection. Trends of scapular elongation in these taxa further support the results from the analysis of the musculature that these limbs retained function even at a reduced size. Additionally, although this study confirms previous results that there is no trend of forelimb elongation across the entire clade Maniraptoriformes, forelimb elongation within Paraves is not a result of negative allometry and is also undergoing active selection toward forelimb proportions that characterize

early avians. These results establish a baseline pattern of forelimb length evolution within the clade as a whole, making it possible for future tests to identify deviations that may represent unique adaptive evolutionary scenarios.

There have been a wide range of forelimb functions proposed for nonavian theropods, including prey apprehension mechanisms of grasping, raking, and clasping (Sereno, 1993; Carpenter, 2002), as well as clamping or hooking of foliage among herbivorous clades (Nicholls and Russell, 1985; Russell and Russell, 1993). Despite the differences in these actions, they may share common biomechanical requirements; unfortunately, few if any studies have created full biomechanical models of these activities to assess the functional demands on the forelimb and how they vary. The myological reconstructions produced by this dissertation will provide vital input data for future work using three-dimensional models to estimate realistic muscle moment arms and assess the response of different muscle conformations to various external forces acting on the limb. Furthermore, the allometric relationships of extant flightless bipedal animals remain essentially unknown, so it is unclear whether the forelimb conservatism shown by nonavian theropods is typical of flightless bipeds or a unique characteristic of the clade. Future work in these areas will greatly enhance our understanding of the factors affecting forelimb size and shape of bipedal animals.

LITERATURE CITED

Bybee, P. J., A. H. Lee, and E.-T. Lamm. 2006. Sizing the Jurassic theropod dinosaur *Allosaurus:* assessing growth strategy and evolution of ontogenetic scaling of limbs. Journal of Morphology 267:347–359.

Carpenter, K. 2002. Forelimb biomechanics of nonavian theropod dinosaurs in predation. Senckenbergiana Lethaea 82:59–76.

Dececchi, T. A., and H. C. E. Larsson. 2013. Body and limb size dissociation at the origin of birds: uncoupling allometric constraints across a macroevolutionary transition. Evolution doi:10.1111/evo.12150.

Hutchinson, J. R., F. C. Anderson, S. S. Blemker, and S. L. Delp. 2005. Analysis of hindlimb muscle moment arms in *Tyrannosaurus rex* using a three-dimensional musculoskeletal computer model: implications for stance, gait, and speed. Paleobiology 31:676–701.

Maidment, S. C. R., and P. M. Barrett. 2011. The locomotor musculature of basal ornithischian dinosaurs. Journal of Vertebrate Paleontology 31:1265–1291.

Martinez, R. N., P. C. Sereno, O. A. Alcober, C. E. Colombi, P. R. Renne, I. P. Montañez, and B. S. Currie. 2011. A basal dinosaur from the dawn of the dinosaur era in southwestern Pangaea. Science 331:206–210.

Nicholls, E. L., and A. P. Russell. 1985. Structure and function of the pectoral girdle and forelimb of *Struthiomimus altus* (Theropoda: Ornithomimidae). Palaeontology 28:643–677.

Russell, D. A., and D. E. Russell. 1993. Mammal-dinosaur convergence. National Geographic Research & Exploration 9:70–79.

Sereno, P. C. 1993. The pectoral girdle and forelimb of the basal theropod *Herrerasaurus ischigualastensis*. Journal of Vertebrate Paleontology 13:425–450.

Sereno, P. C., L. Tan, S. L. Brusatte, H. J. Kriegstein, X. Zhao, and K. Cloward. 2009. Tyrannosaurid skeletal design first evolved at small body size. Science 326:418–422.

Vargas, A. O. 1999. Evolution of arm size in theropod dinosaurs: a developmental hypothesis. Noticiario Mensual 338:16–19.

Vazquez, R. J. 1994. The automating skeletal and muscular mechanisms of the avian wing (Aves). Zoomorphology 114:59–71.

Complete Bibliography

Abdala, V., A. S. Manzano, and A. Herrel. 2008. The distal forelimb musculature in aquatic and terrestrial turtles: phylogeny or environmental constraints? Journal of Anatomy 213:159–172.

Abdala, V., and S. Moro. 2006. Comparative myology of the forelimb of *Liolaemus* sand lizards (Liolaemidae). Acta Zoologica 87:1–12.

Alberch, P., and E. A. Gale. 1985. A developmental analysis of an evolutionary trend: digital reduction in amphibians. Evolution 39:8–23.

Alexander, R. M. 1981. Allometry of the leg muscles of mammals. Journal of Zoology 194:539–552.

Baier, D. B., S. M. Gatesy, and F. A. Jenkins Jr. 2007. A critical ligamentous mechanism in the evolution of avian flight. Nature 445:307–310.

Barker, D. G., J. B. Murphy, and K. W. Smith. 1979. Social behavior in a captive group of Indian pythons, *Python molurus* (Serpentes, Boidae) with formation of a linear social hierarchy. Copeia 1979:466–471.

Barrett, P. M. 2000. Prosauropods and iguanas: speculation on the diets of extinct reptiles; pp. 42–78 in H.-D. Sues (ed.), Evolution of Herbivory in Terrestrial Vertebrates: Perspectives from the Fossil Record. Cambridge University Press, Cambridge, UK.

Barrett, P. M., R. J. Butler, and S. J. Nesbitt. 2011. The roles of herbivory and omnivory in early dinosaur evolution. Earth and Environmental Science Transactions of the Royal Society of Edinburgh 101:383–396.

Barrett, P. M., and E. J. Rayfield. 2006. Ecological and evolutionary implications of dinosaur feeding behaviour. Trends in Ecology and Evolution 21:217–224.

Bates, K. T., P. L. Manning, D. Hodgetts, and W. I. Sellers. 2009. Estimating mass properties of dinosaurs using laser imaging and 3D computer modeling. PLoS ONE 4:e4532.

Baumel, J. J., A. S. King, A. M. Lucas, J. E. Breazile, and H. E. Evans eds. 1979. Nomina Anatomica Avium. Academic Press, New York, 637 pp.

Beddard, F. E. 1898. The Structure and Classification of Birds. Longmans, Green, and Co., London.

Beddard, F. E. 1889. Contributions to the anatomy of the Hoatzin (*Opisthocomus cristatus*), with particular reference to the structure of the wing in the young. Ibis 31:283–293.

Bejder, L., and B. K. Hall. 2002. Limbs in whales and limblessness in other vertebrates: mechanisms of evolutionary and developmental transformation and loss. Evolution and Development 4:445–458.

Berger, A. J. 1954. The myology of the pectoral appendage of three genera of American cuckoos. Miscellaneous Publications Museum of Zoology, University of Michigan 85:1–35.

Berger, A. J. 1956. On the anatomy of the Red Bird of Paradise, with comparative remarks on the Corvidae. The Auk 73:427–446.

Berger-Dell'mour. 1983. Der übergang von echse zu schleiche in der gattung *Tetradactylus* Merrem. Zoologische Jahrbücher. Abteilung für Anatomie und Ontogenie der Tiere 110:1–152.

Bever, G. S., J. A. Gauthier, and G. P. Wagner. 2011. Finding the frame shift: digit loss, developmental variability, and the origin of the avian hand. Evolution & Development 13:269–279.

Bonaparte, J. F., F. E. Novas, and R. A. Coria. 1990. *Carnotaurus sastrei* Bonaparte, the horned, lightly built carnosaur from the Middle Cretaceous of Patagonia. Natural History Museum of Los Angeles County Contributions in Science 416:1–41.

Boyer, D. M., E. R. Seiffert, J. T. Gladman, and J. I. Bloch. 2013. Evolution and allometry of calcaneal elongation in living and extinct primates. PLoS ONE 8:e67792.

Brandley, M. C., J. P. Huelsenbeck, and J. J. Wiens. 2008. Rates and patterns in the evolution of snake-like body form in squamate reptiles: Evidence for repeated re-evolution of lost digits and long-term persistence of intermediate bodyforms. Evolution 62:2042–2064.

Brochu, C. A. 2003. Osteology of *Tyrannosaurus rex*: Insights from a nearly complete skeleton and high-resolution computed tomographic analysis of the skull. Journal of Vertebrate Paleontology 22:1–138.

Brown, B. 1915. *Tyrannosaurus*, the largest flesh-eating animal that ever lived. The American Museum Journal 15:271–274.

Brusatte, S. L., M. J. Benton, D. G. Lloyd, M. Ruta, and S. C. Wang. 2011. Macroevolutionary patterns in the evolutionary radiation of archosaurs (Tetrapoda: Diapsida). Earth and Environmental Science Transactions of the Royal Society of Edinburgh 101:367–382.

Bryant, H. N., and A. P. Russell. 1992. The role of phylogenetic analysis in the inference of unpreserved attributes of extinct taxa. Philosophical Transactions: Biological Sciences 337:405–418.

Bryant, H. N., and K. L. Seymour. 1990. Observations and comments on the reliability of muscle reconstruction in fossil vertebrates. Journal of Morphology 206:109–117.

Burch, S. H., and M. T. Carrano. 2012. An articulated pectoral girdle and forelimb of the abelisaurid theropod *Majungasaurus crenatissimus* from the Late Cretaceous of Madagascar. Journal of Vertebrate Paleontology 32:1–16.

Burnham, K. P., and D. R. Anderson. 2004. Multimodal inference: understanding AIC and BIC in model selection. Sociological Methods Research 33:261–304.

Buscalioni, A. D., F. Ortega, D. Rasskin-Gutman, and B. P. Pérez-Moreno. 1997. Loss of carpal elements in crocodilian limb evolution: morphogenetic model corroborated by palaeobiological data. Biological Journal of the Linnean Society 62:133–144.

Butler, M. A., and A. S. King. 2004. Phylogenetic comparative analysis: a modeling approach for adaptive evolution. The American Naturalist 164:683–695.

Butler, R. J., and A. Goswami. 2008. Body size evolution in Mesozoic birds: little evidence for Cope's rule. Journal of Evolutionary Biology 21:1673–1682.

Bybee, P. J., A. H. Lee, and E.-T. Lamm. 2006. Sizing the Jurassic theropod dinosaur *Allosaurus:* assessing growth strategy and evolution of ontogenetic scaling of limbs. Journal of Morphology 267:347–359.

Caputo, V., B. Lanza, and R. Palmieri. 1995. Body elongation and limb reduction in the genus *Chalcides* Laurenti 1768 (Squamata Scincidae): a comparative study. Tropical Zoology 8:95–152.

Carpenter, C. C., J. B. Murphy, and L. A. Mitchell. 1978. Combat bouts with spur use in the Madagascan boa (*Sanzinia madagascariensis*). Herpetologica 34:207–212.

Carpenter, K. 2002. Forelimb biomechanics of nonavian theropod dinosaurs in predation. Senckenbergiana Lethaea 82:59–76.

Carpenter, K., and M. Smith. 2001. Forelimb osteology and biomechanics of *Tyrannosaurus rex*; pp. 90–116 in D. Tanke and K. Carpenter (eds.), Mesozoic Vertebrate Life. Indiana University Press, Bloomington, IN.

Carrano, M. T. 2001. Implications of limb bone scaling, curvature and eccentricity in mammals and non-avian dinosaurs. Journal of Zoology 254:41–55.

Carrano, M. T., R. B. J. Benson, and S. D. Sampson. 2012. The phylogeny of Tetanurae (Dinosauria: Theropoda). Journal of Systematic Palaeontology 10:211–300.

Carrano, M. T., and J. R. Hutchinson. 2002. Pelvic and hindlimb musculature of *Tyrannosaurus rex* (Dinosauria: Theropoda). Journal of Morphology 253:207–228.

Carrano, M. T., and S. D. Sampson. 2008. The phylogeny of Ceratosauria (Dinosauria: Theropoda). Journal of Systematic Palaeontology 6:183–236.

Chiappe, L. M. 2002. The Cretaceous, short-armed Alvarezsauridae, *Mononykus* and its kin; pp. 87–120 in L. M. Chiappe and L. M. Witmer (eds.), Mesozoic Birds: Above the Heads of Dinosaurs. University of California Press.

Choiniere, J. N., J. M. Clark, C. A. Forster, and X. Xu. 2010. A basal coelurosaur (Dinosauria: Theropoda) from the Late Jurassic (Oxfordian) of the Shishugou Formation in Wucaiwan, People's Republic of China. Journal of Vertebrate Paleontology 30:1773–1796.

Choiniere, J. N., C. A. Forster, and W. J. de Klerk. 2012. New information of *Nqwebasaurus thwazi*, a coelurosaurian theropod from the Early Cretaceous Kirkwood Formation in South Africa. Journal of African Earth Sciences 71–72:1–17.

Christiansen, P., and R. A. Fariña. 2004. Mass prediction in theropod dinosaurs. Historical Biology 16:85–92.

Claessens, L. P. A. M. 2004. Dinosaur gastralia: origin, morphology, and function. Journal of Vertebrate Paleontology 24:89–106.

Codd, J. R., D. F. Boggs, S. F. Perry, and D. R. Carrier. 2005. Activity of three muscles associated with the uncinate processes of the giant Canada Goose *Branta canadensis maximus*. Journal of Experimental Biology 208:849–857.

Colbert, E. H. 1989. The Triassic dinosaur *Coelophysis*. Bulletin of the Museum of Northern Arizona 57:1–160.

Cong, L., L. Hou, X.-C. Wu, and J. Hou. 1998. The Gross Anatomy of *Alligator sinensis* Fauvel. Science Press, Beijing, 388 pp.

Conrad, J. L. 2008. Phylogeny and systematics of Squamata (Reptilia) based on morphology. Bulletin of the American Museum of Natural History 310:1–182.

Coombs, W. P. 1978. Theoretical aspects of cursorial adaptations in dinosaurs. The Quarterly Review of Biology 53:393–418.

Coria, R. A., L. M. Chiappe, and L. Dingus. 2002. A new close relative of *Carnotaurus sastrei* Bonaparte 1985 (Theropoda: Abelisauridae) from the Late Cretaceous of Patagonia. Journal of Vertebrate Paleontology 22:460–465.

Davies, S. J. J. F. 2002. Ratites and Tinamous, Bird Families of the World, Volume 9. Oxford University Press, Oxford, UK, 310 pp.

Dececchi, T. A., and H. C. E. Larsson. 2013. Body and limb size dissociation at the origin of birds: uncoupling allometric constraints across a macroevolutionary transition. Evolution doi:10.1111/evo.12150.

Dececchi, T. A., and H. C. E. Larsson. 2009. Patristic evolutionary rates suggest a punctuated pattern in forelimb evolution before and after the origin of birds. Paleobiology 35:1–12.

Dececchi, T. A., H. C. E. Larsson, and D. W. E. Hone. 2012. *Yixianosaurus longimanus* (Theropoda: Dinosauria) and its bearing on the evolution of Maniraptora and ecology of the Jehol fauna. Vertebrata PalAsiatica 50:111–139.

Dial, K. P. 1992a. Activity patterns of the wing muscles of the pigeon (*Columba livia*) during different modes of flight. Journal of Experimental Zoology 262:357–373.

Dial, K. P. 1992b. Avian forelimb muscles and nonsteady flight: can birds fly without using the muscles in their wings? The Auk 109:874–885.

Dilkes, D. W. 2000. Appendicular myology of the hadrosaurian dinosaur *Maiasaura peeblesorum* from the Late Cretaceous (Campanian) of Montana. Transactions of the Royal Society of Edinburgh: Earth Sciences 90:87–125.

Diogo, R., and V. Abdala. 2010. Muscles of Vertebrates: Comparative Anatomy, Evolution, Homologies and Development. Science Publishers, Enfield, NH, 482 pp.

Ezcurra, M. D. 2010. A new early dinosaur (Saurischia: Sauropodomorpha) from the Late Triassic of Argentina: a reassessment of dinosaur origin and phylogeny. Journal of Systematic Palaeontology 8:371–425.

Ezcurra, M. D., and F. Novas. 2007. New dinosaur remains (Saurischia: Herrerasauridae) from the Ischigualasto Formation (Carnian) of NW Argentina. Ameghiniana 44:17R.

Farlow, J. O., S. M. Gatesy, T. R. Holtz, J. R. Hutchinson, and J. M. Robinson. 2000. Theropod locomotion. American Zoologist 40:640–663.

Fastovsky, D. E., and D. B. Weishampel. 2005. The Evolution and Extinction of the Dinosaurs. Cambridge University Press, Cambridge, UK, 485 pp.

Felsenstein, J. 1985. Phylogenies and the comparative method. The American Naturalist 125:1–15.

Fisher, H. I. 1946. Adaptation and comparative anatomy of the locomotor apparatus of New World vultures. American Midland Naturalist 35:545–727.

Fisher, H. I., and D. C. Goodman. 1955. The myology of the Whooping Crane, *Grus americana*. Illinois Biological Monograph 24:1–127.

Fitzgerald, T. C. 1969. The Coturnix Quail: Anatomy and Histology. The Iowa State University Press, Des Moines, IA, 306 pp.

Fong, D. W., T. C. Kane, and D. C. Culver. 1995. Vestigialization and loss of nonfunctional characters. Annual Review of Ecology and Systematics 26:249–268.

Fürbringer, M. 1870. Die Knochen und Muskeln der Extremitäten bei den Schlangenähnlichen Sauriern. Vergleichend-anatomische Abhandlung. W. Engelmann, Leipzig, 135 pp.

Gans, C. 1975. Tetrapod limblessness: evolution and functional corollaries. American Zoologist 15:455–467.

Gans, C., and M. Fusari. 1994. Locomotor analysis of surface propulsion by three species of reduced-limbed fossorial lizards (*Lerista*: Scincidae) from Western Australia. Journal of Morphology 222:309–326.

Gatesy, S. M. 1991. Hind limb scaling in birds and other theropods: implications for terrestrial locomotion. Journal of Morphology 209:83–96.

Gatesy, S. M. 1990. Caudofemoral musculature and the evolution of theropod locomotion. Paleobiology 16:170–186.

Gatesy, S. M., and K. P. Dial. 1996. Locomotor modules and the evolution of avian flight. Evolution 50:331–340.

Gatesy, S. M., and K. M. Middleton. 1997a. Bipedalism, flight and the evolution of theropod locomotor diversity. Journal of Vertebrate Paleontology 17:308–329.

Gatesy, S. M., and K. M. Middleton. 1997b. Bipedalism, flight, and the evolution of theropod locomotor diversity. Journal of Vertebrate Paleontology 17:308–329.

George, J. C., and A. J. Berger. 1966. Avian Myology. Academic Press, New York, NY, 500 pp.

Giffin, E. B. 1995. Postcranial paleoneurology of the Diapsida. Journal of Zoology 235:389–410.

Gillingham, J. C., and J. A. Chambers. 1982. Courtship and pelvic spur use in the Burmese python, *Python molurus bivittatus*. Copeia 1982:193–196.

Gilmore, C. W. 1920. Osteology of the carnivorous Dinosauria in the United States National Museum, with special reference to the genera *Antrodemus* (*Allosaurus*) and *Ceratosaurus*. Bulletin of the United States National Museum 110:1–159.

Gilmore, C. W. 1909. Osteology of the Jurassic reptile *Camptosaurus*, with a revision of the species of the the genus, and descriptions of two new species. Proceedings of the United States National Museum 36:197–332.

Gishlick, A. D. 2001. The function of the manus and forelimb of *Deinonychus antirrhopus* and its importance for the origin of avian flight; pp. 301–318 in J. A. Gauthier and L. F. Gall (eds.), New Perspectives on the Origin and Early Evolution of Birds: Proceedings. Peabody Museum of Natural History, Yale University, New Haven, CT.

Greer, A. E. 1987. Limb reduction in the lizard genus *Lerista*. 1. Variation in the number of phalanges and presacral vertebrae. Journal of Herpetology 21:267–276.

Greer, A. E., V. Caputo, B. Lanza, and R. Palmieri. 1998. Observations on limb reduction in the scincid lizard genus *Chalcides*. Journal of Herpetology 32:244–252.

Günther, A. 1867. Contribution to the anatomy of *Hatteria* (*Rhynchocephalus*, Owen). Philosophical Transactions of the Royal Society of London 157:595–629.

Haines, R. W. 1950. The flexor muscles of the forearm and hand in lizards and mammals. Journal of Anatomy 84:13–29.

Haines, R. W. 1939. A revision of the extensor muscles of the forearm in tetrapods. Journal of Anatomy 73:211–233.

Hall, A. R., and N. Colegrave. 2008. Decay of unused characters by selection and drift. Journal of Evolutionary Biology 21:610–617.

Hamrick, M. W. 2002. Developmental mechanisms of digit reduction. Evolution and Development 4:247–248.

Hansen, T. F. 1997. Stabilizing selection and the comparative analysis of adaptation. Evolution 51:1341–1351.

Harmon, L., J. Weir, C. Brock, R. Glor, W. Challenger, G. Hunt, R. FitzJohn, M. Pennell, G. Slater, J. Brown, J. Uyed, and J. Eastman. 2013. geiger: Analysis of evolutionary diversification. 1.99-3.

Harvey, P. H., and M. D. Pagel. 1991. The Comparative Method in Evolutionary Biology. Oxford University Press, Oxford, UK, 239 pp.

Holmes, R. 1977. The osteology and musculature of the pectoral limb of small captorhinids. Journal of Morphology 152:101–140.

Holtz, T. R. 2004. Tyrannosauroidea; pp. 111–136 in D. B. Weishampel, P. Dodson, and H. Osmolska (eds.), The Dinosauria (Second Edition). University of California Press, Berkeley, CA.

Horner, J. R., and D. Lessem. 1993. The Complete *T. rex*. Simon & Schuster, New York, 239 pp.

Howell, A. B. 1936. Phylogeny of the distal musculature of the pectoral appendage. Journal of Morphology 60:287–315.

Howell, A. B. 1937. Morphogenesis of the shoulder architecture: Aves. The Auk 54:364–375.

Hudson, G. E., and P. J. Lanzillotti. 1955. Gross anatomy of the wing muscles in the Family Corvidae. American Midland Naturalist 53:1–44.

Hudson, G. E., and P. J. Lanzillotti. 1964. Muscles of the pectoral limb in galliform birds. American Midland Naturalist 71:1–113.

Hudson, G. E., D. O. Schreiweis, S. Y. C. Wang, and D. A. Lancaster. 1972. A numerical study of the wing and leg muscles of Tinamous (Tinamidae). Northwest Science 46:207–255.

Hutchinson, J. R. 2001a. The evolution of pelvic osteology and soft tissues on the line to extant birds (Neornithes). Zoological Journal of the Linnean Society 131:123–168.

Hutchinson, J. R. 2001b. The evolution of femoral osteology and soft tissues on the line to extant birds (Neornithes). Zoological Journal of the Linnean Society 131:169–197.

Hutchinson, J. R. 2006. The evolution of locomotion in archosaurs. Comptes Rendus Palevol 5:519–530.

Hutchinson, J. R., F. C. Anderson, S. S. Blemker, and S. L. Delp. 2005a. Analysis of hindlimb muscle moment arms in *Tyrannosaurus rex* using a three-dimensional musculoskeletal computer model: implications for stance, gait and speed. Paleobiology 31:676–701.

Hutchinson, J. R., F. C. Anderson, S. S. Blemker, and S. L. Delp. 2005b. Analysis of hindlimb muscle moment arms in *Tyrannosaurus rex* using a three-dimensional musculoskeletal computer model: implications for stance, gait, and speed. Paleobiology 31:676–701.

Hutchinson, J. R., F. C. Anderson, S. S. Blemker, and S. L. Delp. 2005c. Analysis of hindlimb muscle moment arms in *Tyrannosaurus rex* using a three-dimensional musculoskeletal computer model: implications for stance, gait and speed. Paleobiology 31:676–701.

Hutchinson, J. R., and S. M. Gatesy. 2000. Adductors, abductors, and the evolution of archosaur locomotion. Paleobiology 26:734–751.

Hutchinson, J. R., V. Ng-Thow-Hing, and F. C. Anderson. 2007. A 3D interactive method for estimating body segmental parameters in animals: application to the turning and running performance of *Tyrannosaurus rex*. Journal of Theoretical Biology 246:660–680.

Hutson, J. D., and K. N. Hutson. 2012. A test of the validity of range of motion studies in fossil archosaur elbow mobility using repeated-measures analysis and the extant phylogenetic bracket. Journal of Experimental Biology 215:2030–2038.

Irmis, R. B., R. Mundil, J. W. Martz, and R. A. Parker. 2011. High resolution U–Pb ages from the Upper Triassic Chinle Formation (New Mexico, USA) support a diachronous rise of dinosaurs. Earth and Planetary Science Letters 309:258–267.

Irmis, R. B., S. J. Nesbitt, K. Padian, N. D. Smith, A. H. Turner, D. Woody, and A. Downs. 2007. A Late Triassic dinosauromorph assemblage from New Mexico and the rise of dinosaurs. Science 317:358–361.

Jasinoski, S. C., A. P. Russell, and P. J. Currie. 2006. An integrative phylogenetic and extrapolatory approach to the reconstruction of dromaeosaur (Theropoda: Eumaniraptora) shoulder musculature. Zoological Journal of the Linnean Society 146:301–344.

Jetz, W., G. H. Thomas, J. B. Joy, K. Hartmann, and A. O. Mooers. 2012. The global diversity of birds in space and time. Nature 491:444–448.

Kilbourne, B. M., and P. J. Makovicky. 2010. Limb bone allometry during postnatal ontogeny in non-avian dinosaurs. Journal of Anatomy 217:135–152.

King, A. S., and M. A. Butler. 2012. ouch: Ornstein-Uhlenbeck models for phylogenetic comparative hypotheses. 2.8-2.

Koehl, M. A. R., D. Evangelista, and K. Yang. 2011. Using physical models to study the gliding performance of extinct animals. Integrative and Comparative Biology 51:1002–1018.

Kuijper, S., A. Beverdam, C. Kroon, A. Brouwer, S. Candille, G. Barsh, and F. Meijlink. 2005. Genetics of shoulder girdle formation: roles of Tbx15 and aristaless-like genes. Development 132:1601–1610.

Kundrát, M. 2009. Primary chondrification foci in the wing basipodium of *Struthio camelus* with comments on interpretation of autopodial elements in Crocodilia and Aves. Journal of Experimental Zoology 312B:30–41.

Lambe, L. M. 1917. The Cretaceous theropodous dinosaur *Gorgosaurus*. Memoirs of the Geological Survey of Canada 100:1–84.

Lande, R. 1978. Evolutionary mechanisms of limb loss in tetrapods. Evolution 32:73–92.

Landsmeer, J. M. F. 1983. Mechanism of forearm rotation in *Varanus exanthematicus*. Journal of Morphology 175:119–130.

Langer, M. C., and M. J. Benton. 2006. Early dinosaurs: a phylogenetic study. Journal of Systematic Palaeontology 4:309–358.

Langer, M. C., M. A. G. Franca, and S. Gabriel. 2007. The pectoral girdle and forelimb anatomy of the stem-sauropodomorph *Saturnalia tupiniquim* (Upper Triassic, Brazil). Special Papers in Palaeontology 77:113–137.

Lauder, G. V. 1995. On the inference of function from structure; pp. 1–9 in J. J. Thomason (ed.), Functional Morphology in Vertebrate Paleontology. Cambridge University Press, Cambridge, UK.

Laurin, M. 2004. The evolution of body size, Cope's Rule and the origin of amniotes. Systematic Biology 53:594–622.

Legendre, P. 2013. lmodel2: Model II Regression. R package version 1.7-1.

Lipkin, C., and K. Carpenter. 2009. Looking again at the forelimb of *Tyrannosaurus rex*; pp. 167–190 in P. Larson and K. Carpenter (eds.), *Tyrannosaurus rex*: the Tyrant King. Indiana University Press, Bloomington, IN.

Livezey, B. C. 2003. Evolution of flightlessness in rails (Gruiformes: Rallidae): phylogenetic, ecomorphological, and ontogenetic perspectives. Ornithological Monographs 53:1–654.

Livezey, B. C. 1989. Flightlessness in Grebes (Aves, Podicipedidae): its independent evolution in three genera. Evolution 43:29–54.

Livezey, B. C. 1992a. Morphological corollaries and ecological implications of flightlessness in the Kakapo (Psittaciformes: Strigops habroptilus. Journal of Morphology 213:105–145.

Livezey, B. C. 1992b. Flightlessness in the Galápagos cormorant (*Compsohalieus* [*Nannopterum*] *harrisi*): heterochrony, giantism and specialization. Zoological Journal of the Linnean Society 105:155–224.

Livezey, B. C. 1990. Evolutionary morphology of flightlessness in the Aukland Islands Teal. The Condor 92:693–673.

Livezey, B. C., and R. L. Zusi. 2007. Higher-order phylogeny of modern birds (Theropoda, Aves: Neornithes) based on comparative anatomy. II. Analysis and discussion. Zoological Journal of the Linnean Society 149:1–95.

Lockley, M., R. Kukihara, and L. Mitchell. 2009. Why *Tyrannosaurus rex* had puny arms: an integral morphodynamic solution to a simple puzzle in theropod paleobiology; pp. 131–164 in P. Larson and K. Carpenter (eds.), *Tyrannosaurus rex*: the Tyrant King. Indiana University Press, Bloomington, IN.

Longrich, N., and P. Currie. 2009. *Albertonykus borealis*, a new alvarezsaur (Dinosauria: Theropoda) from the Early Maastrichtian of Alberta, Canada: implications for the systematics and ecology of the Alvarezsauridae. Cretaceous Research 30:239–252.

Losos, J. B. 1999. Commentaries — Uncertainty in the reconstruction of ancestral character states and limitations on the use of phylogenetic comparative methods. Animal Behavior 58:1319–1324.

Maddison, W. P., and D. R. Maddison. 2010. Mesquite: a modular system for evolutionary analysis. 2.73. http://mesquiteproject.org.

Madsen, J. H. 1976. *Allosaurus fragilis*: a revised osteology. Utah Geological Survey Bulletin 109:1–163.

Maidment, S. C. R., and P. M. Barrett. 2011. The locomotor musculature of basal ornithischian dinosaurs. Journal of Vertebrate Paleontology 31:1265–1291.

Maidment, S. C. R., and P. M. Barrett. 2012. Does morphological convergence imply functional similarity? A test using the evolution of quadrupedalism in ornithischian dinosaurs. Proceedings of the Royal Society B 279:3765–3771.

Martinez, R. N., P. C. Sereno, O. A. Alcober, C. E. Colombi, P. R. Renne, I. P. Montañez, and B. S. Currie. 2011. A basal dinosaur from the dawn of the dinosaur era in southwestern Pangaea. Science 331:206–210.

Martins, E. P. 1999. Estimation of ancestral states of continuous characters: a computer simulation study. Systematic Biology 48:642–650.

Martins, E. P., and T. F. Hansen. 1997. Phylogenies and the comparative method: a general approach to incorporating phylogenetic information into the analysis of interspecific data. The American Naturalist 149:646–667.

Maxwell, E. E., and H. C. E. Larsson. 2007a. Osteology and myology of the wing of the Emu (*Dromaius novaehollandiae*), and its bearing onf the evolution of vestigial structures. Journal of Morphology 268:423–441.

Maxwell, E. E., and H. C. E. Larsson. 2007b. Osteology and myology of the wing of the Emu (*Dromaius novaehollandiae*), and its bearing on the evolution of vestigial structures. Journal of Morphology 268:423–441.

McGowan, C. 1979. The hind limb musculature of the Brown Kiwi, *Apteryx australis mantelli*. Journal of Morphology 160:33-74.

McGowan, C. 1982. The wing musculature of the Brown kiwi *Apteryx australis mantelli* and its bearing on ratite affinities. Journal of Zoology 197:173–219.

McKitrick, M. C. 1985. Myology of the pectoral appendage in kingbirds (*Tyrannus*) and their allies. The Condor 87:402–417.

McMahon, T. A. 1975. Using body size to understand the structural design of animals: quadrupedal locomotion. Journal of Applied Physiology 39:619–627.

Meers, M. B. 2003. Crocodylian forelimb musculature and its relevance to Archosauria. The Anatomical Record Part A 274A:891–916.

Middleton, K. M., and S. M. Gatesy. 2000. Theropod forelimb design and evolution. Zoological Journal of the Linnean Society 128:149–187.

Miner, R. W. 1925. The pectoral limb of *Eryops* and other primitive tetrapods. Bulletin of the American Museum of Natural History 51:145–312.

Müller, G. B., and P. Alberch. 1990. Ontogeny of the limb skeleton in *Alligator mississippiensis*: developmental invariance and change in the evolution of archosaur limbs. Journal of Morphology 203:151–164.

Munns, S. L., T. Owerkowicz, S. J. Andrewartha, and P. B. Frappell. 2012. The accessory role of the diaphragmaticus muscle in lung ventilation in the estuarine crocodile *Crocodylus porosus*. Journal of Experimental Biology 15:845–852.

Murphy, J. B., D. G. Barker, and B. W. Tryon. 1978. Miscellaneous notes on the reproductive biology of reptiles. II. Eleven species of the family Boidae, genera *Candoia*, *Corallus*, *Epicrates* and *Python*. Journal of Herpetology 12:385–390.

Nesbitt, S. J. 2011. The early evolution of archosaurs: relationships and the origin of major clades. Bulletin of the American Museum of Natural History 352:1–292.

Nesbitt, S. J., N. D. Smith, R. B. Irmis, A. H. Turner, A. Downs, and M. A. Norell. 2009a. A complete skeleton of a Late Triassic saurischian and the early evolution of dinosaurs. Science 326:1530–1533.

Nesbitt, S. J., A. H. Turner, M. Spaulding, J. L. Conrad, and M. A. Norell. 2009b. The theropod furcula. Journal of Morphology 270:856–879.

Newman, B. H. 1970. Stance and gait in the flesh-eating dinosaur *Tyrannosaurus*. Biological Journal of the Linnean Society 2:119–123.

Nicholls, E. L., and A. P. Russell. 1985. Structure and function of the pectoral girdle and forelimb of *Struthiomimus altus* (Theropoda: Ornithomimidae). Palaeontology 28:643–677.

Novas, F. E., D. Pol, J. I. Canale, J. D. Porfiri, and J. O. Calvo. 2009. A bizarre Cretaceous theropod dinosaur from Patagonia and the evolution of Gondwanan dromaeosaurids. Proceedings of the Royal Society of London Series B 276:1101–1107.

Nudds, R. L. 2007. Wing-bone length allometry in birds. Journal of Avian Biology 38:515–519.

Nunn, C. L. 2011. The Comparative Approach in Evolutionary Anthropology and Biology. University of Chicago Press, Chicago, 392 pp.

O'Connor, P. M., and L. P. A. M. Claessens. 2005. Basic avian pulmonary design and flow-through ventilation in non-avian theropod dinosaurs. Nature 436:253–256.

Olmos, M., A. Casinos, and J. Cubo. 1996. Limb allometry in birds. Annales Des Sciences Naturelles, Zoologie 17:39–49.

Orme, D., R. Freckleton, G. H. Thomas, T. Petzoldt, S. Fritz, N. Isaac, and W. Pearse. 2012. caper: Comparative Analyses of Phylogenetics and Evolution in R. 0.5.

Ortega, F., F. Escaso, and J. L. Sanz. 2010. A bizarre, humped Carcharodontosauria (Theropoda) from the Lower Cretaceous of Spain. Nature 467:203–206.

Osborn, H. F. 1906. *Tyrannosaurus*, Upper Cretaceous carnivorous dinosaur (second communication). Bulletin of the American Museum of Natural History 22:281–296.

Padian, K. 2004. Basal Avialae; pp. 210–231 in D. B. Weishampel, P. Dodson, and H. Osmolska (eds.), The Dinosauria, Second Edition. University of California Press, Berkeley, CA.

Padian, K., and L. M. Chiappe. 1998a. The origin and early evolution of birds. Biological Review 73:1-42.

Padian, K., and L. M. Chiappe. 1998b. The origin and early evolution of birds. Biological Reviews 73:1–42.

Pagel, M. 1999. Inferring the historical patterns of biological evolution. Nature 401:877–884.

Pagel, M., and A. Meade. 2013. BayesTraits. V 2.0 (Beta).

Parker, T. J. 1891. Observations on the anatomy and development of *Apteryx*. Philosophical Transactions of the Royal Society B 182:25–134.

Perle, A., M. A. Norell, L. M. Chiappe, and J. M. Clark. 1993. Flightless bird from the Cretaceous of Mongolia. Nature 362:623–626.

Peterson, J. A. 1984. The locomotion of *Chamaeleo* (Reptilia: Sauria) with particular reference to the forelimb. Journal of Zoology 202:1–42.

Peterson, J. A. 1973. Adaptation for arboreal locomotion in the shoulder region of lizards. Doctoral thesis/dissertation, Anatomy, University of Chicago, Chicago, IL, 603 pp.

Pol, D., and O. W. M. Rauhut. 2012. A Middle Jurassic abelisaurid from Patagonia and the early diversification of theropod dinosaurs. Proceedings of the Royal Society B 279:3170–3175.

Poore, S. O., A. Sanchez-Haiman, and G. E. Goslow. 1997. Wing upstroke and the evolution of flapping flight. Nature 387:799–802.

Prange, H. D., J. F. Anderson, and H. Rahn. 1979. Scaling of skeletal mass to body mass in birds and mammals. The American Naturalist 113:103–122.

Presch, W. 1975. The evolution of limb reduction in the teiid lizard genus *Bachia*. Bulletin of the Southern California Academy of Sciences 74:113–121.

R Development Core Team. 2013. R: A language and environment for statistical computing. 3.0.1. R Foundation for Statistical Computing, Vienna, Austria.

Raath, M. A. 1969. A new coelurosaurian dinosaur from the Forest Sandstone of Rhodesia. Arnoldia Series of Miscellaneous Publicatons 4:1–25.

Raath, M. A. 1990. Morphological variation in small theropods and its meaning in systematics: evidence from *Syntarsus rhodesiensis*; pp. 91–105 in K. Carpenter and P. J. Currie (eds.), Dinosaur Systematics. Cambridge University Press, Cambridge, UK.

Raikow, R. J. 1977. Pectoral appendage myology of the Hawaiian honeycreepers (Drepanididae). The Auk 94:331–342.

Rambaut, A., and A. Drummond. 2009. Tracer. V 1.5.

Rayner, J. M. V. 1985. Linear relationships in biomechanics: the statistics of scaling functions. Journal of Zoology 206:415–439.

Reese, A. M. 1915. The Alligator and Its Allies. The Knickerbocker Press, New York, NY, 358 pp.

Ribbing, L. 1907. Die distale armmuskulatur der Amphibien, Reptilien und Säugetiere. Zoologische Jahrbücher 23:587–682.

Rinehart, L. F., S. G. Lucas, and A. P. Hunt. 2007. Furculae in the Late Triassic theropod dinosaur *Coelophysis bauri*. Paläontologische Zeitschrift 81:174–180.

Romer, A. S. 1944. The development of tetrapod limb musculature — the shoulder region of *Lacerta*. Journal of Morphology 74:1–41.

Rowe, T. A. 1989. A new species of the theropod dinosaur *Syntarsus* from the Early Jurassic Kayenta Formation of Arizona. Journal of Vertebrate Paleontology 9:125–136.

Russell, A. P., and A. M. Bauer. 2008. The appendicular locomotor apparatus of *Sphenodon* and normal-limbed squamates; pp. 1–466 in C. Gans, A. S. Gaunt, and K. Adler (eds.), Biology of the Reptilia 24, Morphology 1. Society for the Study of Amphibians and Reptiles, Ithaca, NY.

Russell, D. A., and D. E. Russell. 1993. Mammal-dinosaur convergence. National Geographic Research & Exploration 9:70–79.

Santa Luca, A. P. 1980. The postcranial skeleton of *Heterodontosaurus tucki* (Reptilia, Ornithischia) from the Stormberg of South Africa. Annals of the South African Museum 79:159–211.

Schmidt-Nielsen, K. 1984. Scaling: Why is Animal Size so Important? Cambridge University Press, Cambridge, UK, 256 pp.

Senter, P. 2005. Function in the stunted forelimbs of *Mononykus olecranus* (Theropoda), a dinosaurian anteater. Paleobiology 31:373–381.

Senter, P. 2006. Forelimb function in *Ornitholestes hermanni* Osborn (Dinosauria, Theropoda). Palaeontology 49:1029–1034.

Senter, P., and J. M. Parrish. 2006. Forelimb function in the theropod dinosaur *Carnotaurus sastrei*, and its behavioral implications. PaleoBios 26:7–17.

Senter, P., and J. H. Robins. 2005. Range of motion in the forelimb of the theropod dinosaur *Acrocanthosaurus atokensis*, and implications for predatory behavior. Journal of Zoology 266:307–318.

Sereno, P. C. 1993. The pectoral girdle and forelimb of the basal theropod *Herrerasaurus ischigualastensis*. Journal of Vertebrate Paleontology 13:425–450.

Sereno, P. C. 1999. The evolution of dinosaurs. Science 284:2137-2147.

Sereno, P. C., A. L. Beck, D. B. Dutheil, B. Gado, H. C. E. Larsson, G. H. Lyon, J. D. Marcot, O. W. M. Rauhut, R. W. Sadlier, C. A. Sidor, D. J. Varricchio, G. P. Wilson, and J. A. Wilson. 1998. A long-snouted predatory dinosaur from Africa and the evolution of spinosaurids. Science 282:1298–1302.

Sereno, P. C., L. Tan, S. L. Brusatte, H. J. Kriegstein, X. Zhao, and K. Cloward. 2009. Tyrannosaurid skeletal design first evolved at small body size. Science 326:418–422.

Shah, R. V., and V. B. Patel. 1964. Myology of the chelonian pectoral appendage. Journal of Animal Morphology and Physiology 11:58–84.

Shapiro, M. D. 2002. Developmental morphology of limb reduction in *Hemiergis* (Squamata: Scincidae): chondrogenesis, osteogenesis, and heterochrony. Journal of Morphology 254:211–231.

Shapiro, M. D., N. H. Shubin, and J. P. Downs. 2007. Limb diversity and digit reduction in reptilian evolution; pp. 225–244 in B. K. Hall (ed.), Fins into Limbs. University of Chicago Press, Chicago.

Shufeldt, R. W. 1918. Notes on the osteology of the young of the Hoatzin (*Opisthocomus cristatus*) and other points on its morphology. Journal of Morphology 31:599–606.

Snively, E., and A. P. Russell. 2007a. Craniocervical feeding dynamics of *Tyrannosaurus rex*. Paleobiology 33:610–638.

Snively, E., and A. P. Russell. 2007b. Functional morphology of neck musculature in the Tyrannosauridae (Dinosauria, Theropoda) as determined via a hierarchical inferential approach. Zoological Journal of the Linnean Society 151:759–808.

Snively, E., and A. P. Russell. 2007c. Functional variation of neck muscles and their relation to feeding style in Tyrannosauridae and other large theropod dinosaurs. The Anatomical Record 290:934–957.

Sookias, R. B., R. J. Butler, and R. B. J. Benson. 2012. Rise of dinosaurs reveals major body-size transitions are driven by passive processes of trait evolution. Proceedings of the Royal Society B doi:10.1098/rspb.2011.2441.

Sterli, J. 2010. Phylogenetic relationships among extinct and extant turtles: the position of Pleurodira and the effects of fossils on rooting crown-group turtles. Contributions to Zoology 79:93–106.

Stevens, K. A., P. Larson, E. D. Wills, and A. Anderson. 2009. Rex, sit: digital modeling of *Tyrannosaurus rex* at rest; pp. 192–203 in P. Larson and K. Carpenter (eds.), *Tyrannosaurus rex*: the Tyrant King. Indiana University Press, Bloomington, IN.

Stickel, W. H., and L. F. Stickel. 1946. Sexual dimorphism in the pelvic spurs of *Enygrus*. Copeia 1946:10–12.

Straus, W. L. 1942. The homologies of the forearm flexors: urodeles, lizards, mammals. American Journal of Anatomy 70:281–316.

Sullivan, C., D. W. E. Hone, X. Xu, and F. Zhang. 2010. The asymmetry of the carpal joint and the evolution of wing folding in maniraptoran theropod dinosaurs. Proceedings of the Royal Society B doi:10.1098.

Sullivan, G. E. 1962. Anatomy and embryology of the wing musculature of the domestic fowl (*Gallus*). Australian Journal of Zoology 10:458–518.

Swinebroad, J. 1954. A comparative study of the wing myology of certain passerines. American Midland Naturalist 51:488–514.

Thewissen, J. G. M., M. J. Cohn, L. S. Stevens, S. Bajpai, J. Heyning, and W. E. Horton. 2006. Developmental basis for hind-limb loss in dolphins and origin of the cetacean bodyplan. Proceedings of the National Academy of Sciences 103:8414–8418.

Tickle, P. G., M. A. Norell, and J. R. Codd. 2012. Ventilatory mechanics from maniraptoran theropods to extant birds. Journal of Evolutionary Biology 25:740–747.

Tsuihiji, T. 2010. Reconstructions of the axial muscle insertions in the occipital region of dinosaurs: evaluation of past hypotheses on Marginocephalia and Tyrannosauridae using the Extant Phylogenetic Bracket approach. The Anatomical Record 293:1360–1386.

Turner, A. H., P. J. Makovicky, and M. A. Norell. 2012. A review of dromaeosaurid systematics and paravian phylogeny. Bulletin of the American Museum of Natural History 371:1–206.

Turner, A. H., and S. J. Nesbitt. 2013. Body size evolution during the Triassic archosauriform radiation. Geological Society, London, Special Publications 379:doi 10.1144/SP379.15.

Turner, A. H., D. Pol, J. A. Clarke, G. M. Erickson, and M. A. Norell. 2007. A basal dromaeosaurid and size evolution preceding avian flight. Science 317:1378–1380.

Valasek, P., S. Theis, A. DeLaurier, Y. Hinits, G. N. Luke, A. M. Otto, J. Minchin, L. He, B. Christ, G. Brooks, H. Sang, D. J. Evans, M. Logan, R. Huang, and K. Patel. 2011. Cellular and molecular investigations into the development of the pectoral girdle. Developmental Biology 357:108–116.

Vanden Berge, J. C. 1970. A comparative study of the appendicular musculature of the Order Ciconiiformes. American Midland Naturalist 84:289–364.

Vanden Berge, J. C., and G. A. Zweers. 1993. Myologia; pp. 189–247 in J. J. Baumel, A. S. King, J. E. Breazile, H. E. Evans, and J. C. Vanden Berge (eds.), Handbook of Avian Anatomy: Nomina Anatomica Avium. Nuttall Ornithological Club, Cambridge, UK.

Vargas, A. O. 1999. Evolution of arm size in theropod dinosaurs: a developmental hypothesis. Noticiario Mensual 338:16–19.

Vazquez, R. J. 1994. The automating skeletal and muscular mechanisms of the avian wing (Aves). Zoomorphology 114:59–71.

Walker, J. W. F. 1973. The locomotor apparatus of testudines; pp. 1–100 in C. Gans and T. S. Parsons (eds.), Biology of the Reptilia 4. Academic Press, New York.

Wang, X., R. L. Nudds, and G. J. Dyke. 2011. The primary feather lengths of early birds with respect to avian wing shape evolution. Journal of Evolutionary Biology 24:1226–1231.

Wang, Z., R. L. Young, H. Xue, and G. P. Wagner. 2011. Transcriptomic analysis of avian digits reveals conserved and derived digit identities in birds. Nature 477:583–587.

Wiens, J. J. 2004. Development and evolution of body form and limb reduction in squamates: a response to Sanger and Gibson-Brown. Evolution 58:2107–2108.

Witmer, L. M. 1995. The extant phylogenetic bracket and the importance of reconstructing soft tissues in fossils; pp. 9–33 in J. J. Thomason (ed.), Functional Morphology in Vertebrate Paleontology. Cambridge University Press, Cambridge, UK.

Xu, X., J. M. Clark, J. Mo, J. Choiniere, C. A. Forster, G. M. Erickson, D. W. E. Hone, C. Sullivan, D. A. Eberth, S. J. Nesbitt, Q. Zhao, R. Hernandez, C. Jia, F.-l. Han, and Y. Guo. 2009. A Jurassic ceratosaur from China helps clarify avian digital homologies. Nature 459:940–944.

Xu, X., M. A. Norell, X. Kuang, X.-L. Wang, Q. Zhao, and C. Jia. 2004. Basal tyrannosauroids from China and evidence for protofeathers in tyrannosauroids. Nature 431:680–684.

Xu, X., K. Wang, K. Zhang, Q. Ma, L. Xing, C. Sullivan, D. Hu, S. Cheng, and S. Wang. 2012. A gigantic feathered dinosaur from the Lower Cretaceous of China. Nature 484:92–95.

Xu, X., Z. Zhou, and X.-L. Wang. 2000. The smallest known non-avian theropod dinosaur. Nature 408:705–708.

Young, C. G. 1888. On the habits and anatomy of *Opisthocomus cristatus*, Illig. Notes from the Leyden Museum 10:169–175.

Zanno, L. E., and P. J. Makovicky. 2011. Herbivorous ecomorphology and specialization patterns in theropod dinosaur evolution. Proceedings of the National Academy of Sciences 108:232–237.

Zanno, L. E., and P. J. Makovicky. 2012. No evidence for directional evolution of body mass in herbivorous theropod dinosaurs. Proceedings of the Royal Society B 280:20122526.